Regulation of neurotrophin receptors by receptor-type protein tyrosine phosphatases

Viktoria Tchetchelnitski

University College London

Institute of Child Health

A thesis submitted for the degree of Doctor of Philosophy

2011

Declaration

I, Viktoria Tchetchelnitski, confirm that the work presented in this thesis is my own. Where information has been derived from other sources, I confirm that this has been indicated in the thesis.

Abstract

Reversible protein phosphorylation plays a key role in cell signalling during neural development and thus controls cell proliferation, survival, differentiation and function. Kinases and their counter-partners the phosphatases tightly regulate protein phosphorylation. In the developing nervous system the neurotrophin receptor family of protein tyrosine kinases (TrkA, B and C) are major players in this signalling network during normal neuron development and also in several diseases such as neuropathies, degenerative disorders and cancers. Recently, receptor-type protein tyrosine phosphatases (RPTPs) were suggested to be possible regulators of Trks. Thus understanding the relationships between RPTPs and Trks may help to develop new therapeutics to control aberrant neurotrophin signalling in disease. In this study I investigated the relationship between RPTPs and Trks in murine embryonic sensory neurons from dorsal root ganglia (DRGs), a primary cell model. The expression and coexpression of RPTPs and Trks was extensively studied during critical stages of DRG maturation using qPCR arrays at Merck-Serono, Geneva, and fluorescent *in-situ* hybridization and immunohistochemical techniques. This revealed a relatively high expression of several candidate RPTPs, which were expressed in particular $TrkA^+$, $TrkB^+$ and/or $TrkC^+$ subpopulations of sensory neurons, indicating a potential relationship in their signalling functions. To further analyze a potential direct interaction between candidate RPTPs with Trk proteins, a bimolecular-fluorescent complementation assay (BiFc) was tested. However, this particular assay, when used with type I transmembrane proteins, suffered from high, unspecific protein interactions. In the main experimental approach, a lentiviral-mediated shRNAi-induced knockdown system in primary cell cultures was set-up and the effects of the knockdowns of *Ptprf, Ptprs* and *Ptpro* on endogenous Trk gene expression and Trk phosphorylation and activation were analysed. These results suggest a potential role of the encoded proteins LAR and RPTPσ in Trk function and of RPTP-BK in the differentiation and specification of Trk^+ neurons.

Acknowledgements

Firstly, I would like to thank my supervisor Dr. Andrew Stoker for his guidance, support and motivation throughout my PhD and for giving me the freedom to work independently. I am especially thankful for his help in the last stage of my writing. My thanks also go to Dr. JP Martinez-Barbera, my secondary supervisor, for his valuable advice, help and support in the last few years.

Secondly, I would like to thank all members of the PTPNET. It was an absolute honour to be part of this network and I am very grateful for the experience and the great atmosphere during our meetings. I've certainly grown scientifically and personally on this experience. My thanks go to all PIs in our network and associates Dr. Jörg Mueller, Prof. Frank Böhmer, Dr. Sheilla Harroch and Dr. Radu Aricescu, Prof. Arne Östman, Prof. Dr. Stefan Szedlacsek, Prof. Jeroen den Hertog, Prof. Ari Elson, Dr. Lydia Tabernero, Dr. Wiljan Hendriks, Prof. Yvonne Jones, and Dr. Rafael Pulido, who have provided me with invaluable materials, protocols and advice and for the organisation of the great meetings and the cultural experiences. I'd like to thank especially Dr. Rob Hooft van Huijsduijnen for giving me the opportunity to visit Merck-Serono for a while. My special thanks go to all the trainees in PTPNET: Barbara, Caroline, Deepanker, Deepika, Fanny, Irene, Jeroen, Leo, Monique, Thomas, Sujay, Vasu and Vincent for our scientific and not so scientific discussions and the adventures and great times we've had all around Europe. These were certainly some of the best times during my PhD. I am especially thankful to Dr. Monique van den Eijnden, who helped me during my stay at Merck-Serono in Geneva and also showed me the beauty of Switzerland.

I would also like to thank the European Commission for my funding through the FP6 Marie Curie Actions (MRTN-CT-2006-35830).

My thanks also go to previous and current members of NDU and ICH for the help and advice on my work. My thanks go especially to Dr. Natalie Ward for the help with the viruses in the beginning and to the Western lab staff for making my life much easier. I am especially thankful to Sandra for all the help, encouragement, support and advice. And I am very thankful to Ellen for being "my PostDoc", and someone who knows what Trks and DRGs are. Thank you for your help and support and for bringing a bit of Germany into this lab. My thanks also go to Aya for feeding me with cookies at

midnight and keeping me company on looong working days and on the weekends. Weerapong, Aya and Sandra, thank you for rescuing the lab with me one of those weekends. I am also very thankful to Pascal, Bruno, Michael, Simon, Rachel, Steffi, Muhamed, Sigrun, Lucy, Adam, Marco, Yannis, Ezat, Nabila, Selda, Pachy, Rita and everyone else whom I've met during this long journey and who has given me a helping hand, advice, support and shared the fun times with me as well.

My deepest thanks go to my parents, my sister and my entire family. Vielen Dank, dass Ihr immer an mich glaubt, für Eure grenzenlose Liebe, Unterstützung und Hilfe mein ganzes Leben lang und vor allem während meines Studiums. Ohne Euch, wäre ich nicht, wo ich jetzt bin.

I am also deeply thankful to all my friends; especially the ones far away back home. Thank you for your friendship, your endless support, help and belief in me especially during some of the toughest times of my life and for not forgetting about me and your understanding, when I had no time to call on you. I am so glad for having shared some of the best times of my life with you. I would not be where I am now without all of you, guys; you know, who you are. Thank you so much.

And last but definitely not least I'd like to thank Alex. I cannot put my gratitude in words for you. You've done so much for me over all these years. Thank you for always being there to support me, for cheering me up, for the much-needed distraction and for keeping me sane and especially for reminding me of the more important things in life. And a huge thank you for your patience, understanding, support and help during the last period of my writing. Merci beaucoup, cheri.

For my parents:

Thank you for your endless support and belief in me.

Abbreviations

5'LTR	5' long terminal repeat
aa	Amino acid
AAV	Adeno-associated-virus
Actb	β-actin gene
AJ	Adherens junction
AP	Alkaline phosphatase
APS	Amonium persulfate
ARMS	Ankyrin Rich Membrane Spanning (ARMS) protein
ATP	Adenosine triphosphate
BCA	Bicistronic acid
BCC	Boundary cap cells
BDNF	Brain-derived neurotrophic factor
BF	Bright field
BiFc	Bimolecular Fluorescent Complementation Assay
bHLH	Basic helix-loop-helix
bp	Base pair
BSA	Bovine serum albumin
CAH	Carbonic anhydrase-like domain
CAM	Cell adhesion molecule
CaMPK	Calcium calmodulin-regulated protein kinase
$CaPO_4$	Calcium phosphate
CD34	Cluster of differentiation 34
CD45	Cluster of differentiation 45 (PTPRC)
CDC	Cell division control
cDNA	Complementary deoxyribonucleic acid
CMV	Cytomegalo virus
CNS	Central nervous system
Co-IP	Co-immunoprecipitation
cppt	Central polypurine tract
CR	Cysteine-rich motif
CREB	cAMP response element binding protein
CRYP-1/2	Chick Receptor tYrosine Phosphatase alpha/beta (RPTPσ/RPTP-BK)
CSPG	Chondroitin sulfate proteoglycan
C_T	Threshold cycle
ctrl	Control
Cys	Cysteine
D1	Catalytically active phosphatase domain
D2	Pseudo-phosphatase domain
DAG	Diacylglycerol
DAPI	4',6-diamidino-2-phenylindole
DEP-1	Density enhanced phosphatase 1 (PTPRJ)
DEPC	Diethyl-pyrocarbonate
DFISH	Double fluorescent in situ hybridisation
DIG	Digoxigenin
DMEM	Dulbecco´s Modified Eagle Medium
DMSO	Dimethyl sulfoxide

DNA	Deoxyribonucleic acid
DNase	Deoxyribonuclease
dNTPs	Deoxynucleotid triphosphate
DREZ	Dorsal root entry zone
DRG	Dorsal root ganglion
DSP	Dual specificity phosphatase
dsRNA	Double-stranded RNA
DTT	1.4-dithiothreitol
E	Embryonic day
E.*coli*	*Escherichia coli*
EboZ	Ebola Zaire virus
ECD	Extracellular domain
EDTA	Ethylenediamine tetraacetic acid
EGF	Epidermal growth factor
eGFP	Enhanced green fluorescent protein
EGFR	EGF receptor
ENV	Envelope
Eph	Ephrin
EphR	Eph receptor
Erk	Ras/extracellular signal regulated kinase (MEK, MAPK)
EtBr	Ethidium bromide
EYFP	Enhanced yellow fluorescent protein
F	Forward
FACS	Fluorescence activated cell sorting
FAK	Focal adhesion kinase
FBS	Fetal bovine serum
FCS	Fetal calf serum
FGF	Fibroblast growth factor
FGFR	FGF receptor
FISH	Fluorescent *in situ* hybridisation
FITC	Fluorescein isothiocyanate
FL	Full-length
FN III	Fibronectin type III
FP	Fluorescent protein
FRET	Förster resonance energy transfer
Frs2	Fibroblast growth factor receptor substrate 2
Gab-1/2	Grb2-associated binder-1/2
GAG	Viral structural proteins
GAPDH	Glyceraldehyde-3-phosphate dehydrogenase
gDNA	Genomic DNA
GDNF	Glial derived neurotrophic factor
GEF	Guanine nucleotide exchange factor
GITC	Guanidine isothiocyanate
GLEPP1	Glomerular ephithelial protein 1 (PTPRO)
GOI	Gene of interest
gp64	Baculovirus gp64
GPCR	G-Protein-Coupled-Receptor
Gps1	G-protein pathway suppressor 1 gene
Grb2	Growth receptor-bound protein 2
GSK-3	Glycogen synthase kinase 3

h	Hours
HAD	Haloacid dehalogenase
HBSS	Hanks balanced salt solution
HEK293T	Immortalised human embronic kidney cell line 293T
HGF	Hepatocyte growth factor
HGFR/Met	HGF receptor/Met
HIV	Human Immunodeficiency Virus
HKG	Housekeeping gene
hPGK	Human phosphoglycerate kinase promoter
Hprt1	Hypoxanthine-guanine phosphoribosyl transferase 1 gene
HRP	Horseradish peroxidase
HSPG	Heparan sulphate proteoglycan
ICC	Immunocytochemistry
ICD	Intracellular domain
IF	Immunofluorescence
Ig	Immunoglobulin
IHC	Immunohistochemistry
IP3	Inositol-trisphosphate
ISH	*In situ* hybridization
IU	Infectious units
JNK	C-Jun amino-terminal kinases (MAPK)
Kan	Kanamycin
kb	Kilobase
kd	knockdown
kDa	Kilodalton
KIM	Kinase-interaction motif
LAR	Leukocyte common antigen-related (PTPRF)
LMPTP	Low molecular weight protein tyrosine phosphatase
LN	Laminin
LRR	Leucine-rich repeats
LTP	Long term potentiation
MAM	Mephrin/5A/PTPμ domain
MAPK	Mitogen-activated protein kinase
mg	Milligram
min	Minute(s)
MKP	MAPK phosphatase
ml	Milliliter
MLV-A	Amphotropic Murine Leukaemia Virus
MLV-E	Ecotropic Murine Leukaemia Virus
MOI	Multiplicity of infection
mRNA	Messenger ribonucleic acid
MTM	Myotubularin
N-CAM	Neural cell adhesion molecule
NC	Neural crest
NCC	Neural crest cell
NGF	Nerver Growth Factor
Ngn1/2	TF neurogenin 2
NGL-3	Netrin-G-ligand-3
NMJ	Neuromuscular junction
NPTP	Non-transmembrane protein tyrosine phosphatase

NT	Neurotrophin
NTRK	Neurotrophin protein tyrosine kinases
ON	Overnight
P/S	Penicillin/streptomycin
PAGE	Polyacrylamide gel electrophoresis
PBS	Phosphate-buffered saline
PC12	Rat pheochromocytoma cell line
PCA	Protein fragment complementation assay
PCR	Polymerase chain reaction
PDGF	Platelet-derived growth factor
PDGFR	PDGFR
PDK-1	Phosphoinositide-dependent protein kinase
PI3K	Phosphatidylinositol-3-kinase
PIP2	Phosphatidylinositol 4,5-bisphosphate or PtdIns(4,5)P
PKA/C	Protein kinase A/C
PLCγ	Phospholipase Cγ
PLL	Poly L-lysine
PMSF	Phenylmethylsulfonyl floride
PNS	Peripheral nervous system
POL	Reverse transcriptase/integrase
PPI	Protein-protein interaction
PRL	Phosphatase of regenerating liver
Psmb2	proteasome subunit beta type 2 gene
PTEN	Phosphatase and tensin homolog
PTP	Protein tyrosine phosphatase
PVDF	Polyvinylidene difluoride
qPCR	Quantitative reverse transcription real-time polymerase chain reaction
R	Reverse
RE	Restriction enzymes
RGC	Retinal ganglion cell
RISC	RNA-inducing silencing complex
RNA	Ribonucleic acid
RNAi	RNA interference
ROS	Reactive oxygen species
rpm	Rounds per minute
RPTK	Receptor-like protein tyrosine kinase
RPTP	Receptor-like protein tyrosine phosphatase
RRE	Rev response element
rRNA	Ribosomal RNA
RRV	Ross River Virus
RSV	Rous Sarcoma Virus
RT-PCR	Reverse transcription-polymerase chain reaction
RTK	Receptor tyrosine kinases
Runx1/3	Runt-related transcription factor 1/3
SGCs	Satellite glial cells
Ser	Serine
SD	Standard deviation
SDS	Sodium dodecyl sulphate
SE	Stadard error
SFKs	Src family of tyrosine kinases

SH	Small hairpin
SH2	Src homology 2
Shc	Src homologous and collagen-like (Shc) adaptor protein
shRNA	small-hairpin RNA
SIN/3'LTR	self-inactivating long terminal repeat
siRNA	small interfering RNA
SNP	Single nucleotide polymorphism
Sos	Son of sevenless
SSC	Saline sodium citrate
SSH	Slingshot
SVZ	Subventricular zone
TBS	Tris-buffered saline
TE	Tris-EDTA
TEMED	N,N,N',N'-tetramethylethylene-diamine
TF	Transcription factor
TG	Trigeminal ganglia
Thr	Threonin
Tm	Melting temperature
TMD	Transmembrane domain
TNF	Tumour necrosis factor
TNFR	TNF receptor
Tris	Tris[hydroxymethyl]-amino-methane
TRITC	Tetramethyl Rhodamine Iso-Thiocyanate
Trk	**T**ropomosin **r**eceptor **k**inase
TrkA	Neurotrophin receptor A for NGF
TrkB	Neurotrophin receptor B for BDNF and NT-4
TrkC	Neurotrophin receptor C for NT-3
TU	Transducing units
Tyr	Tyrosine
U	Units
Ubc	Ubiquitin C gene
UV	Ultraviolet
V	Volt
v/v	Volume/volume
VEGF	Vascular endothelial cell growth factor
VEGFR	VEGF receptor
VSVg	Vesicular stomatitis virus glycoprotein
VZ	Ventricular zone
w/v	Weight/volume
WB	Western blotting/immuno blotting
WPRE	Woodchuck hepatitis virus posttranscriptional regulatory element
wt	Wild type
Y	Tyrosine (Tyr)
Y2H	Yeast-2-hybrid
YFP	Yellow fluorescent protein

Table of Contents

List of Figures and Tables

Chapter 1

Chapter 2

Chapter 3

Chapter 4

Chapter 5

Chapter 6

Chapter 7

Appendix

Chapter 1

General introduction

1.1. Introduction

The nervous system is the most complex system in the animal kingdom. It consists of the central and peripheral nervous systems (CNS and PNS), which are built up by many different types of neurons and glia cells. The developmental processes that create this elaborate structure are even more complex. Like in any other tissue each individual cell decides throughout its lifespan upon the fundamental processes survival or death, proliferation, differentiation, function and aging, and reacts to environmental signals and interacts with other cells. All of these processes are governed on the molecular level by a complex and highly coordinated network of signalling cascades that finally result in the down- or upregulation of specific genes and cellular changes. These signalling cascades are interactions of biochemical molecules such as lipids, carbohydrates and above all proteins. The interactions between these molecules are especially governed by their post-translational modification such as glycosylation, methylation, ubiquitination, acetylation and reversible phosphorylation. These transient protein modifications create new recognition motifs for interactions with other molecules, direct their cellular localisation, affect the stability and thus lifespan of the proteins and regulate enzyme activity, by altering their conformation and electrical charge.

But what controls these transient protein modifications such as reversible protein phosphorylation? In the 1950's Krebs and Fischer described for the first time that two specific enzymes, the kinases and phosphatases, regulate the phosphorylation state of a crucial enzyme in the initial step of glycogenolysis in muscle and thus control its function (Krebs et al., 1959, Graves et al., 1960). Nowadays it is known that kinases, which phosphorylate proteins, and their counter partners the phosphatases, which dephosphorylate them, tightly control and balance the phosphorylation state of proteins in virtually any type of tissue and system. It is also clear that a misbalance in the phosphorylation state consequently leads to cell malfunction or even death and results in the onset of many severe diseases. Whereas much is already known about protein kinases, phosphatases remain more mysterious as their study has been technically much more challenging.

In my thesis I was investigating the reversible protein phosphorylation in the developing PNS of the mouse. In this respect I have analysed the expression and function of receptor protein tyrosine phosphatases (RPTPs) and neurotrophin tyrosine

kinase receptors (Trks) in the cell model of sensory neurons from murine embryonic dorsal root ganglia (DRGs). The main focus of this thesis was to decipher a potential regulation of Trks by RPTPs.

1.2. Protein tyrosine kinase (PTK) family

Protein kinases are a family of enzymes, which transfer a phosphate group from high-energy donor molecules such as ATP mostly to the amino acid residues threonine (Thr), serine (Ser) or tyrosine (Tyr). This biochemical process is called reversible protein phosphorylation.

Whereas threonine and serine phosphorylation of proteins was known for over 40 years, tyrosine phosphorylation was discovered later in the 1980s. Tony Hunter demonstrated that v-Src, a retroviral proto-oncogene, phosphorylates tyrosine residues and not threonines as previously falsely assumed (Hunter and Sefton, 1980). This break-through discovery was followed by the demonstration that epidermal growth factor receptor (EGFR) is as well a tyrosine kinase (Ushiro and Cohen, 1980) and many more followed. Protein tyrosine phosphorylation is a relatively rare post-translational modification (1% of total phosphoamino acids) in comparison to serine or threonine phosphorylation. Nevertheless, it is of immense importance in the context of signal transduction especially via growth factor receptors.

Among the 522 known protein kinases in the human and mouse genome, 90 are protein tyrosine kinases (PTKs) of which 58 are transmembrane receptor kinases (RPTKs) and 32 are non-receptor or cytoplasmic (NRPTKs) protein tyrosine kinases. RPTKs have been categorized into 20 subfamilies based on their extracellular structure. Some of the most famous subfamilies and essential kinases are the previously mentioned EGFRs, insulin receptors, platelet-derived growth factor (PDGF) receptors, vascular endothelial cell growth factor (VEGF) receptor, fibroblast growth factor (FGF) receptors, hepatocyte growth factor (HGF) receptors, ephrin (EPH) receptors, the Ret receptor and the family of nerve growth factor (NGF) receptors (Robinson et al., 2000, Blume-Jensen and Hunter, 2001). The latter are of major importance in the nervous system and were the focus of this thesis.

1.2.1. Neurotrophin protein tyrosine kinases (Trks)

The family of nerve growth factor (NGF) receptors consists of three neurotrophin protein tyrosine kinases (Trks), TrkA, B and C. These single-pass type I membrane proteins are high-affinity receptors for their ligands the neurotrophins. Upon ligand binding Trk receptors become activated and trigger a plethora of downstream signal transduction mechanisms (described in section 1.2.3). The first Trk receptor identified was TrkA. In the late 1980's *trk* (later referred to as TrkA) was discovered as a proto-oncogene in a colon carcinoma biopsy of a patient. Generated by a somatic rearrangement it consisted of the first seven out of eight exons of non-muscle tropomyosin fused to the transmembrane and cytoplasmic domains of a tyrosine kinase, which is reflected in its name tropomyosin (t)-receptor(r)-kinase (k), *trk* (Martin-Zanca et al., 1986). Several years later the putative form of TrkA was identified and characterised as a cell surface receptor with a kinase activity specific for tyrosine residues (Martin-Zanca et al., 1989). Subsequently TrkB (Klein et al., 1989, Middlemas et al., 1991) and TrkC (Lamballe et al., 1991) were discovered due to their 66-68% sequence homology with TrkA. However, their role as neurotrophin receptors was not recognized until Kaplan *et al*. (Kaplan et al., 1991a, Kaplan et al., 1991b) and Klein *et al*. (Klein et al., 1991a) have convincingly demonstrated in several binding studies using different cell types, that TrkA is a specific high-affinity receptor for NGF. Following these discoveries, TrkB and TrkC were also recognized as high-affinity neurotrophin receptors (Klein et al., 1991b, Lamballe et al., 1991).

Trks like all other members of the RTK family show a rather uniform pattern of structural motifs (Figure 1.1). They contain a signal peptide, which is required for trafficking to the cell surface, an extracellular domain (ECD), a transmembrane domain (TMD) consisting of 25-38 amino acids and an intracellular domain (ICD) and regulatory sequences, which are located near the COOH end. The ECD is involved in ligand recognition, whereas the ICD contains the catalytic kinase domain (Huang and Reichardt, 2003). The ECD of all three Trks show high homology, but their ICD have the greatest sequence similarity. The ECD consists of leucine-rich repeats (LRR) flanked by one cysteine cluster on each side. Its juxtamembrane region contains two immunoglobulin-like (Ig-like) domains, which represent the actual binding sites for the neurotrophin ligands (Urfer et al., 1995). Additionally to the mature highly glycosylated Trk receptors unglycosylated forms exist. However, only the fully glycosylated mature

form is targeted to the plasma membrane and interacts with the neurotrophins (Watson et al., 1999). Importantly, each Trk receptor has several different isoforms due to alternative splicing and alternative promoters and also protein cleavage. Most of these isoforms show different expression patterns, signalling properties and substrate specificity, as I will describe later in more detail.

In addition to the high-affinity Trk receptors, a low-affinity pan-neurotrophin receptor, the **p75^{NTR}** receptor, exists. In fact it was the first neurotrophin receptor discovered, but unlike Trks it binds all NTs with much lower affinity (Johnson et al., 1986). This 80kDa glycoprotein is a member of the tumour necrosis factor (TNF) receptor superfamily. It contains four highly glycosylated and cysteine-rich motifs in its ECD, a single transmembrane domain and a short cytoplasmic domain, which instead of a catalytic domain like in Trk receptors contains a "death" domain (Liepinsh et al., 1997) (Figure 1.1).

1.2.2. Neurotrophins (NTs)

Neurotrophins (NTs) are a family of polypeptide growth factors, which exert their function upon binding and activation of Trk receptors. NTs were discovered and their function was analyzed decades before their receptors were identified. In the early 1950s Rita Levi-Montalcini and Viktor Hamburger showed for the first time that growth, development and survival of peripheral neurons is controlled by specific target-derived survival factors. They demonstrated, that neurons are produced in a surplus and that limiting quantities of NTs in the target-tissues of these neurons control their survival and thus establish a specific innervation density of the target tissue, known as the "neurotrophic hypothesis" (Hamburger and Levi-Montalcini, 1949, Davies, 1996). Further, Rita Levi-Montalcini together with Stanley Cohen identified a diffusible nerve growth factor (NGF) from sarcoma tissue and showed that it promotes the survival and neurite outgrowth of sympathetic and neural crest-derived sensory neurons. They produced an antibody against NGF and demonstrated that it inhibits the survival of these neurons during the time of target innervation (Levi-Montalcini, 1952, Levi-Montalcini et al., 1954, Cohen and Levi-Montalcini, 1956, Levi-Montalcini and Cohen, 1956, Cohen and Levi-Montalcini, 1957, Marx, 1986). Decades later in the 1980s a further NT, the brain-derived neurotrophic factor (BDNF), was isolated from porcine brain (Barde et al., 1982, Leibrock et al., 1989) and homology cloning using NGF and

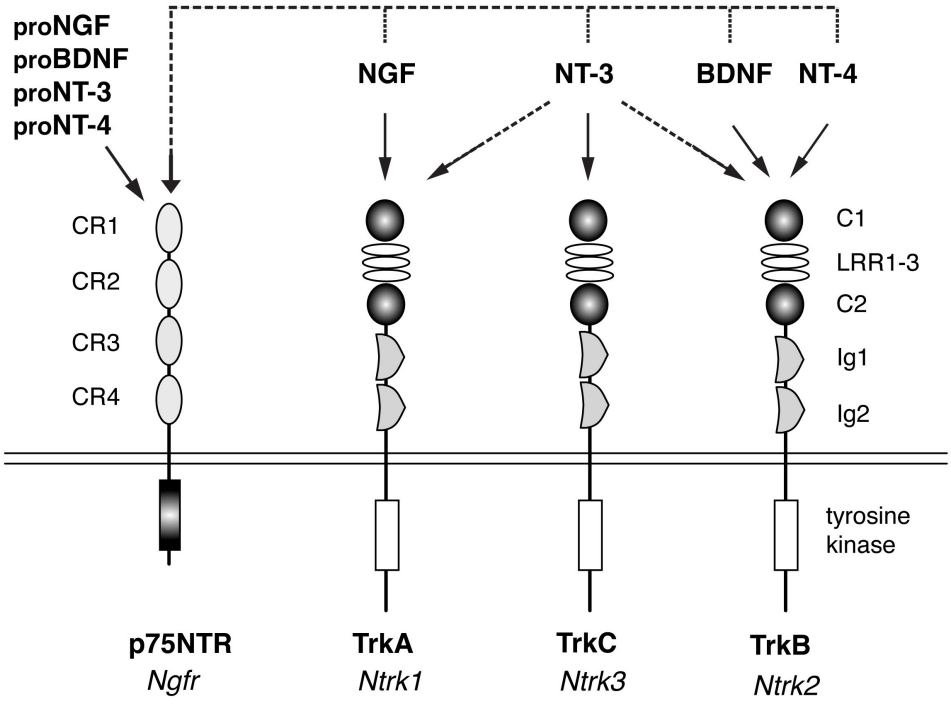

Figure 1.1. Schematic representation of Trks and NTs.
Neurotrophins interact with highest affinity with specific Trk receptors, whereby NGF binds to TrkA, BDNF and NT-4 bind to TrkB and NT-3 binds to TrkC and with lower affinity to TrkA and TrkB. All neurotrophins bind with lower affinity (dashed lines) to p75NTR, which binds with highest affinity the proneurotrophins. Displayed are only the full-length isoforms of the neurotrophin receptors. Gene names are displayed in italic, protein names in bold letters. CR1-CR4, cysteine-rich motifs; C1/C2, cysteine-rich clusters; LRR1-3, leucine-rich repeats; Ig1/Ig2, immunoglobulin-like domains (adapted after (Reichardt, 2006)).

BDNF sequences lead to the discovery of the remaining members of the NT family neurotrophin 3 (NT-3) (Hohn et al., 1990, Maisonpierre et al., 1990b) and neurotrophin 4 (NT-4) also known as NT-4/5 or NT-5 (Hallbook et al., 1991) and the fish-specific neurotrophin-6 (NT-6) (Gotz et al., 1994) and neurotrophin-7 (NT-7) (Lai et al., 1998).

NTs are homodimers, which are generated from immature precursor proteins, the proneurotrophins, by proteolytic cleavage. However, not only mature NTs but also proneurotrophins are biologically active (Teng et al., 2010). All NTs share approximately 50-60% amino acid identity and have similar structures. However, they differ in their expression patterns and the affinities to specific Trk receptors and hence perform distinct biological activities. NGF binds exclusively to TrkA (Cordon-Cardo et al., 1991, Kaplan et al., 1991b, Klein et al., 1991a, Loeb et al., 1991, Bibel and Barde,

2000), BDNF and NT-4 bind to TrkB (Klein et al., 1991b) and NT-3 binds with highest affinity to TrkC (Lamballe et al., 1991) and with lower affinity also to TrkA and TrkB (Squinto et al., 1991, Tsoulfas et al., 1993). The pan-neurotrophin receptor $p75^{NTR}$ binds any of the neurotrophins but with a 1000-fold lower affinity than Trk receptors (Raffioni et al., 1993). Instead, $p75^{NTR}$ binds proneurotrophins, the precursor NTs, with highest affinity (Lee et al., 2001).

1.2.3. Expression and function of Trks and NTs in the nervous system

NTs were first described as neurotrophic factors, but nowadays it is also known that they have additional immunotrophic and metabotrophic effects and thus play a role in cardiac development, neovascularisation and the immune system (Lin et al., 2000, Vega et al., 2003, Nockher and Renz, 2006, Caporali and Emanueli, 2009). In this review I will focus, however, primarily on their expression and function in the nervous system.

Expression patterns of all Trk receptors and NTs are dynamic and show distinct but also overlapping patterns during development and in adult organisms. Some neurons also switch from the expression of one Trk receptor to the other. Whereas TrkA and TrkC and their ligands are primarily expressed in the PNS, TrkB and BDNF are mostly found in the CNS. In the PNS, TrkB and TrkC are expressed in almost all sensory ganglia, but TrkA expression is limited only to neural crest-derived ganglia (Lindsay, 1996). NTs can be found in the nervous system in a variety of specific target organs of Trk^{+} neurons during development and in adult organisms. Within the organs they are primarily produced and secreted by neurons but also by glia cells and different types of cells of the connective tissue. The picture of Trk expression is further complicated by the presence of different splice variants and isoforms, which all have specific expression patterns and functions. For instance apart from full-length catalytically active isoforms, truncated isoforms of TrkB and TrkC receptors lacking the catalytic kinase domain also exist. Different functions were attributed to the catalytically inactive splice variants such as inhibition of dimerization and hence inactivation of full-length Trks and even active but different roles in signalling than their full-length counterparts such as an implication in synaptogenesis (Barbacid, 1995a, Barbacid, 1995b, Eide et al., 1996, Baxter et al., 1997, Haapasalo et al., 2001, Takahashi et al., 2011). Interestingly, the expression of the non-catalytic relative to kinase-active Trk isoforms is increased during the peak period of synaptogenesis in the second and third postnatal weeks (Valenzuela

et al., 1993). Importantly some transcript variants appear to be also species-specific. In this review I will mostly concentrate on transcript variants found in rodents.

The importance of Trk receptors or NTs became evident, when it was realized that mice lacking either of these proteins die postnatally, whereas mice with reduced levels are viable but show impaired brain function, behaviour and sensory deficits (Lindsay, 1996, Chao, 2003). In general in the developing PNS Trks are especially important for neuronal survival upon ligand binding. Limiting quantities of NTs secreted from peripheral non-neuronal target tissues of neurons control the numbers of these neurons to achieve a specific innervation density of their target tissues. This is known as the classical "neurotrophic hypothesis" as mentioned earlier (Hamburger and Levi-Montalcini, 1949, Davies, 1996). However, it was realized early on that this hypothesis might be specific for the developing PNS but not the CNS, as unlike neurons of the PNS, most neurons from the CNS do not depend solely on one NT. This was supported by reports that mice lacking a specific NT do not display any loss of a particular cell population in the CNS (Tessarollo, 1998). In a more elaborate study it was also shown that TrkB and TrkC promote together but not alone the survival of hippocampal and cerebellar granule neurons (Minichiello and Klein, 1996). Another interesting insight into Trk signalling has disproven former assumptions that in the absence of NTs Trks are inactive and promote apoptosis by not activating survival pathways. As of late many studies have provided evidence that Trk receptors are so-called "dependence receptors" and can actively induce apoptosis by "negative signal transduction" in the absence of their ligands (Harel et al., 2010). For instance Nikoletopoulou *et al.* used engineered mouse embryonic stem cells and embryos to demonstrate that TrkA and TrkC but not TrkB can induce apoptosis in the absence of their ligands. In addition they suggested that cell death was not mediated by the activity of the kinase itself but partially through initiation of $p75^{NTR}$ cleavage (Nikoletopoulou et al., 2010). They also provided further evidence for the differences in NT dependence in PNS and CNS neurons. Based on their recent findings and the knowledge that TrkB is the evolutionary ancestor of TrkA and TrkC, these scientists hypothesized that the expansion of the Trk gene family accompanied by the separation of CNS and PNS during evolution generated new mechanisms to control neuronal numbers. This is supported by the predominant expression of TrkB in the CNS, but TrkA and TrkC in the PNS. This study is also well in agreement with the previously mentioned hypothesis,

that NTs have different effects on neuronal survival in PNS and CNS as described above.

In addition to cell survival Trk receptors and NTs are responsible for precursor proliferation, commitment, and axon and dendrite growth and guidance of neurons in the developing PNS and CNS. Moreover they play an important role in synapse formation, function and plasticity (Thoenen, 1995, Chao, 2003, Huang and Reichardt, 2003, Lu et al., 2005, Takahashi et al., 2011). Finally in the adult organism Trks regulate the expression of ion channels and neurotransmitters and thus direct the differentiation, maturation and function of neurons (Bibel and Barde, 2000).

1.2.3.1. TrkA and NGF

The TrkA gene *Ntrk1* is transcribed into a single 3.2 kb transcript, which encodes two different isoforms. Both isoforms are catalytically active but one of them (TrkA-II) contains an 18 bp insert (exon 9) in the extracellular domain, which enhances its responsiveness to NT-3 (Clary and Reichardt, 1994). The two isoforms are expressed in a tissue-specific manner. Neuronal cells express predominantly the isoform TrkA-II, whereas non-neuronal tissues such as kidney express both isoforms (Barker et al., 1993). Further, TrkA shedding produces a soluble ECD and an active membrane-bound ICD (Diaz-Rodriguez et al., 1999). In the PNS, TrkA receptors are preferentially expressed in sympathoadrenal neurons, such as sympathetic neurons, chromaffin cells etc. and peptidergic nociceptive, thermoceptive and puriceptive sensory neurons in DRGs and the TG (Martin-Zanca et al., 1990). The TrkA ligand NGF is produced by non-neuronal tissues such as skin, vascular and smooth muscle cells, and various endocrine tissues, such as the testis and ovary, pituitary, thyroid and parathyroid glands (Davies, 1987, Sofroniew et al., 2001). In addition PNS glia such as immature Schwann cells and SGCs produce NGF (Mirsky and Jessen, 1999). In the CNS TrkA receptors and NGF can be found in cholinergic neurons of many structures of the basal forebrain such as the cerebral cortex, cerebellum, hippocampus and hypothalamus and additionally in the corpus striatum, which are degenerated in Alzheimer's and Huntington's Diseases respectively. Interestingly, TrkA expression is absent in the spinal cord (Martin-Zanca et al., 1990, Fagan et al., 1997), whereas NGF was detected in the spinal cord, pons and medulla (Shelton and Reichardt, 1984). Transgenic mice with reduced levels of NGF suffer from a loss of nociceptors in DRGs by increased

apoptosis at around E13.5 in mouse embryos and NGF- or TrkA-null mutants lose more than 70-90% of their sensory neurons embryonically. Additionally these mice suffer from decreased cholinergic innervation of the hippocampus, deficiency in memory acquisition and retention at postnatal stages (Lindsay, 1996).

1.2.3.2. TrkB, BDNF and NT-4

The expression of *Ntrk2* gene, which encodes TrkB, is more complex. Seven TrkB mRNA transcripts of different sizes ranging from 0.7-9 kb were detected in rodent brain as early as E 9.5 (Klein et al., 1989, Klein et al., 1990b). However, only four transcripts are translated into a full-length isoform and the three truncated isoforms T1, the rodent specific T2, and T4, also called T-Shc, which all lack the catalytic domain. The transcripts T1 and T2 differ from each other solely in their C-terminus that, however, lacks homology to any known protein motif (Klein et al., 1990a, Middlemas et al., 1991, Baxter et al., 1997, Haapasalo et al., 2001). The T-Shc isoform contains an Shc-binding site in the juxtamembrane domain similar to the full-length form but lacks the catalytic domain (Forooghian et al., 2001, Stoilov et al., 2002). The full-length and truncated isoforms differ not only in their function but also in their expression patterns. During development the full-length isoform is the most abundant form. Transcripts were found as early as E9.5 in the neuroepithelium and in the neural crest and later on in their derivatives the neurons of the CNS and PNS (Klein et al., 1990a). In the CNS it was detected for example in the cerebral cortex, thalamus, hippocampus, in the Purkinje cells, granular layer caudal peduncle of the cerebellum, brain stem and the mantle zone and ventral horn of the spinal cord, where motor neurons reside (Armanini et al., 1995). In the PNS its expression was observed during development in cranial ganglia, the ophthalmic nerve, the vestibular system, in facial structures, the sub maxillary glands, and in large proprioceptive neurons in DRGs (Klein et al., 1989). Interestingly, in the mature nervous system the amount of the truncated TrkB isoforms is tenfold higher than of the full-length forms (Lindsay, 1996). The non-catalytic transcripts were found in the developing and adult NS mostly in non-neuronal cells, but also colocalized with full-length TrkB in neurons including motor neurons and hippocampal cells (Tessarollo, 1998). In the PNS they were detected in SGCs in DRGs and TG and in the CNS in the cerebellar granule cell layer, where astrocytes reside, in the ventricular zone (VZ) and the medial mantle zone of midbrain and the spinal cord and the roof plate of the spinal

cord, where neural crest cells (NCCs) are generated at earlier stages (Valenzuela et al., 1993, Armanini et al., 1995, Ninkina et al., 1996, Kumanogoh et al., 2008).

The TrkB and its ligands BDNF and NT-4/5 are known to participate in axon growth and targeting and synaptic plasticity (Bibel and Barde, 2000). BDNF and NT-4/5 mRNA and protein are expressed in many different neural structures of the CNS and PNS, which also contain TrkB transcripts, and their expression levels peak upon maturity (Leibrock et al., 1989, Hofer et al., 1990, Maisonpierre et al., 1990a, Katoh-Semba et al., 1997). BDNF expression is highest in the CNS, where it can be found next to NT-4/5 for example in the spinal cord, and in septal cholinergic and dopaminergic neurons in the brain that are known to degenerate in Alzheimer's Disease and Parkinson's Disease (Alderson et al., 1990, Hyman et al., 1991). Further it was identified in granule cells and retinal glia cells (RGCs) (Hyman et al., 1994, Gao et al., 1995, Studer et al., 1995). Although the expression and function of BDNF and NT-4/5 are mostly overlapping, they differ in their concentrations and some structures do not express both neurotrophins. For instance BDNF but not NT-4 was detected in the thalamus and hypothalamus and in certain areas of the pons, and NT-4 but not BDNF is present in the putamen (Zhang et al., 2007a). In the PNS, BDNF is expressed in neurons and glia cells in cranial and dorsal root ganglia and also in non-neuronal tissues such as the trunk epidermis, spleen and heart (Wetmore and Olson, 1995, Yamamoto et al., 1996). NT-4/5 is additionally expressed in all of these tissues apart from the heart (Hiltunen et al., 1996).

The phenotype of TrkB knockout mice is similar to BDNF deficient animals. Both transgenic mice are three times smaller than their wild type littermates due to disturbed feeding behaviour, they show impaired movement, coordination and balance due to cell loss in vestibular ganglia, breathing difficulties and impaired development of rod photoreceptors and die shortly after birth (Klein et al., 1993, Jones et al., 1994). TrkB conditional knockout mice with ablated TrkB expression in the brain lose specific populations of CNS neurons such as in the cerebellum and show inhibited synapse formation and plasticity (Lei and Parada, 2007). Mice with BDNF deficiency in the CNS show enhanced aggressiveness, hyperactivity and hyperphagia and have impaired memory, which can be reversed by local administration of BDNF (Erickson et al., 1996, Lyons et al., 1999, Rios et al., 2001). Reduced levels of BDNF in the PNS lead to a loss of mechanosensitivity (Ernfors et al., 1994a). Interestingly, although NT-4 and BDNF

show similar effects *in vitro*, knockout mice do not have the same phenotypes. In contrast to BDNF- and TrkB-deficient mice NT-$4^{-/-}$ animals do not die postnatally and show only mild sensory deficits (Liu et al., 1995, Conover et al., 1995, Erickson et al., 1996, Roosen et al., 2001). A knock-in study of NT-4 into the BDNF gene has demonstrated that differences in NT-4 and BDNF action might be probably due to the differences in their expression patterns, but also functions. For instance NT-4 has a higher potency in promoting survival of sensory neurons and formation of hippocampal synapses due to the different activation of TrkB downstream pathways (Fan et al., 2000). Accordingly, mice carrying a point mutation in the Shc binding site of the TrkB receptor lose most of their NT-4 dependent neurons, whereas BDNF-dependent neurons remain mostly unaffected (Minichiello et al., 1998). BDNF$^{-/-}$ but not NT-$4^{-/-}$ mice showed also altered nociceptive reflexes and reflex plasticity in the spinal cord (Heppenstall and Lewin, 2001).

1.2.3.3. TrkC and NT-3

TrkC mRNA can be already detected together with its ligand NT-3 in the neuroepithelium of E7.5 mouse embryos (Maisonpierre et al., 1990a, Lamballe et al., 1991, Tessarollo et al., 1993). The expression of the TrkC encoding gene *Ntrk3* is highly complex. Due to alternative splicing six different isoforms exist in the nervous system and in non-neural tissues, of which four are full-length forms and two are truncated isoforms lacking a tyrosine kinase domain. In addition to the "normal" full-length isoform, the three isoforms Ki14, Ki25 and Ki39 contain an insert of 14, 25 or 39 amino acids respectively in their catalytic domain. The two truncated isoforms T1 and T2 differ solely in the length of their cytoplasmic part. Interestingly, all of these isoforms are mostly expressed in the same neuronal tissues. However, similar to truncated TrkB isoforms, the truncated TrkC isoforms were mostly found in non-neuronal tissues and their expression increased during development. All isoforms have different biochemical and biological properties such as substrate specificity and thus activate different TrkC downstream signalling pathways (Merlio et al., 1992, Tsoulfas et al., 1993, Valenzuela et al., 1993, Lamballe et al., 1994, McMahon et al., 1994, Guiton et al., 1995, Menn et al., 1998, Palko et al., 1999, Funfschilling et al., 2004). In the embryonic and adult CNS, TrkC and NT-3 are abundant with most expression in the hippocampus, in several thalamic nuclei, and in the cerebral cortex

and the granular cell layer of the cerebellum and in the spinal cord (Jones and Reichardt, 1990, Maisonpierre et al., 1990a, Rosenthal et al., 1990, Tessarollo et al., 1993). Truncated forms were additionally found in glia cells such as oligodendrocytes and astrocytes (Lamballe et al., 1993, Valenzuela et al., 1993, Cohen et al., 1996). In the PNS during development TrkC and NT-3 are expressed in neurons derived from neural crest and ectodermal placodes such as DRGs, nodose and early TG and support the survival and proliferation (Hallbook et al., 1995, Huang et al., 1999) and the formation of peripheral and central connections of these neurons (Phillips et al., 1990, Ernfors and Persson, 1991). Both TrkC and NT-3 are additionally found in SGCs at early stages, but this expression disappears later on (Funfschilling et al., 2004). Further expression was detected throughout the enteric nervous system, and mostly truncated isoforms were additionally found in the sciatic nerve and in non-neuronal tissues such as spleen, heart, connective tissue, muscles, and major blood vessels (Lamballe et al., 1993, Tessarollo et al., 1993, Funfschilling et al., 2004). The different functions of truncated and full-length isoforms of TrkC receptors were demonstrated by their overexpression in DRGs *in vitro.* Their different effects on axon-outgrowth were revealed, when it was shown that the full-length form of TrkC initiates primary process formation, whereas truncated TrkC reduced the amount of primary processes but instead enhances branching. Recently, the truncated TrkC isoform was also implicated in synaptogenesis (Takahashi et al., 2011).

Many different mouse models were developed to elucidate the function of TrkC and NT-3. For instance NT-3 haploinsufficiency in mice causes movement disorders as well as deficient amygdala activity, which is involved in epilepsy, and also cardiovascular defects (Ernfors et al., 1994b). This phenotype was obviously more severe in NT-$3^{-/-}$ mice, which displayed severe movement defects of the limbs due to loss of the majority of peripheral sensory and sympathetic neurons but not motor neurons, and most homozygotes died shortly after birth in contrast to heterozygotes (Farinas et al., 1996, Wilkinson et al., 1996, Tessarollo et al., 1997). Interestingly, mice overexpressing a truncated TrkC receptor showed a similar phenotype to NT-3 deficient animals, as they died perinatally, because of severe cardiac defects and PNS abnormalities, suggesting a sequestering role of this TrkC isoform (Palko et al., 1999). On the other hand the phenotype of $TrkC^{-/-}$ mice lacking the full-length isoform was not as severe as the NT-$3^{-/-}$ phenotype. Both show impaired movement, but $TrkC^{-/-}$ mice

have no obvious cardiac defects and survive up to 3 weeks (Ernfors et al., 1994b, Farinas et al., 1994, Klein et al., 1994).

Unlike animals with mutations in other NTs and their corresponding Trk receptors, loss of neurons in NT-$3^{-/-}$ mutants exceeds the numbers lost in mutants lacking all TrkC receptors (Tessarollo et al., 1997). This indicates that NT-3 is not only required for the survival of proprioceptors but that it can also signal through TrkA and TrkB receptors. This result was further supported by the fact that TrkA and TrkB neurons were also lost in NT-3 null mutants (Liebl et al., 1997) and that NT-3 promoted survival of $TrkC^{-/-}$ sensory neurons *in vitro* (Davies et al., 1995). The importance of NT-3 and TrkC in many other neuronal functions, which are impaired in pathological human conditions such as mood disorders, was demonstrated in an interesting mouse model that overexpressed full-length TrkC. These mice exhibited a phenotype of an anxiety and panic disorder due to increased numbers of catecholaminergic neurons and increased hippocampal potentiation, thus providing a good model to study this disease (Dierssen et al., 2006).

1.2.3.4. $p75^{NTR}$

The low-affinity neurotrophin receptor $p75^{NTR}$ triggers a diverse repertoire of biological functions through protein-protein interactions, because of its ability to act as a coreceptor for a diversity of ligands (Teng et al., 2010). For instance it can induce apoptosis during development and injury, inhibit axonal growth, modulate synaptic plasticity and promote myelination of axons from sensory neurons. It was already earlier suggested that in DRG neurons $p75^{NTR}$ is closely related to Trk receptors. Interestingly, whereas most $TrkA^{+}$ or $TrkB^{+}$ neurons coexpressed $p75^{NTR}$, half of $TrkC^{+}$ neurons did not (Wright and Snider, 1995). Moreover it is well established that $p75^{NTR}$ can regulate Trk function through direct interaction or crosstalk with Trk signalling pathways (Reichardt, 2006). For instance $p75^{NTR}$ increases specificity and affinity of Trk receptors for their ligands (Lee et al., 1994, Brennan et al., 1999). Further, $p75^{NTR}$ can delay destruction of TrkA and TrkB proteins (Makkerh et al., 2005). Its most important function in Trk signalling, however, is to facilitate endocytosis and retrograde transport of Trk-ligand complexes resulting in enhanced axon growth and cell survival and differentiation (Curtis et al., 1995). $p75^{NTR}$ acts especially as a proneurotrophin

receptor and promotes apoptosis (Lee et al., 2001). But for now it is still not completely understood how $p75^{NTR}$ functions and interactions are brought about.

1.2.4. Trk and NT signalling pathways in the nervous system

Binding of NTs to appropriate Trk receptors leads to a rapid activation of downstream signalling pathways. In neurons this has a local effect on growth cone motility, neurite outgrowth and synapse function. The NT-Trk complex is then internalized via endocytosis and ultimately degraded in lysosomes. Alternatively the complex is transported in membranous vesicles, the endosomes, in a retrograde manner from distal axons to the nucleus, which leads to the expression of genes that promote cell survival, proliferation and differentiation (Ginty and Segal, 2002, Zweifel et al., 2005).

On the molecular level binding of NTs to Trk receptors leads to their homodimerization and activation of their catalytic domains through autotrans-phosphorylation of ten evolutionary conserved intracellular Tyr residues situated inside and outside the catalytic domain. Initially three of these tyrosines (Y670, Y674 and Y675 according to human TrkA nomenclature), which lie within the activation loop of the kinase domain, are phosphorylated. This event potentiates the tyrosine kinase activity leading to the phosphorylation of the remaining seven Tyr residues (Segal et al., 1996). The phosphorylated tyrosines represent docking sites for a plethora of Src homology 2 (SH2) and phosphotyrosine binding (PTB) domain-containing proteins, which mediate the major signalling pathways phosphatidylinositol-3-kinase (PI3K)/Akt, the phospholipase C-γ (PLCγ)-Ca^{2+}, and the Ras/MAPK pathways (Ullrich and Schlessinger, 1990, Kaplan and Miller, 2000). The three phospho-Tyr Y490, Y751 and Y785 initiate the mentioned signalling pathways via interactions with adaptor proteins and enzymes. Phosphorylated Y490 situated in the juxtamembrane domain interacts with adaptor proteins, which consequently activate the Ras/MAPK and PI3K/Akt pathways. Phosphorylated Y785 interacts directly with PLCγ-1 and Y751 with PI3K. Upon binding to the phosphotyrosines these proteins become also Trk kinase substrates and are activated. These mechanisms are, however, still poorly understood. Here I will summarize the role of Trk receptors in the major signalling pathways Ras-MAPK, PI3K and PLCγ-1 (Figure 1.2).

1.2.4.1. Ras-MAPK pathway

The mitogen activated protein kinase (MAPK) pathways control proliferation and differentiation including neurite outgrowth, and prolonged survival of neurons. At least five MAPK signalling cascades exist in mammalian cells, which are grouped according to their MAPKs including the extracellular signal-related kinases Erk1/2 (also known as p44/42), Erk3/4, and Erk5, the c-Jun amino-terminal kinases (JNKs) and the p38 MAPK. These pathways are sequential phosphorylation cascades of kinases, which are initiated by growth factors, mitogens, cytokines, G-Protein-Coupled-Receptors (GPCRs) and stress signals ultimately leading to the phosphorylation and activation of transcription factors (TFs), which control gene expression (Schlessinger, 2000). MAPKs can be activated either transiently or prolonged, which determines the biological response. For instance in PC12 cells prolonged activation mediates differentiation, whereas transient activation results in proliferation (Qiu and Green, 1991, Traverse et al., 1992, Yaka et al., 1998). Activated Trk receptors stimulate MAPK pathways via at least three phosphorylated tyrosines. The major player in this pathway is Y490. For a transient response it recruits the Src homologous and collagen-like (Shc) adaptor protein. Upon binding Shc is phosphorylated by Trk and binds to the adaptor protein complex growth receptor-bound protein 2 (Grb2)-Son of sevenless (Sos). The nucleotide exchange factor Sos catalyses the exchange of GTP to GDP in Ras, which leads to the activation of this GTPase. Ras activates the MAPKKK c-Raf (Raf-1). In the classical MAPK pathway c-Raf then turns on the MAPKKs MEK1 or MEK2 by phosphorylation of a Ser in the activation loop. MEK1/2 phosphorylates the MAPK Erk1 or Erk2 on Tyr and Thr residues, which leads to their activation. Activated Erk1/2 then turns on several TFs such as Elk-1 and Egr-1 leading for instance to axonal growth in neurons. Erk1/2 can additionally be directly translocated to the nucleus and thus activate the TF cyclic AMP-response element binding (CREB) (Segal and Greenberg, 1996). CREB initiates for instance cell survival, neurite outgrowth and plasticity in neurons (Finkbeiner, 2000). The other MAPK pathways are activated in a similar manner and have overlapping but also distinct targets. For instance Erk5 but not Erk1/2 is involved in retrograde signalling events during Trk trafficking towards the nucleus (Watson et al., 2001). The prolonged Erk activation is mediated through the fibroblast growth factor receptor substrate 2 (Frs2), which also binds to the phosphorylated Y490 of Trk receptors. Frs2 is phosphorylated and binds to the adaptor protein and

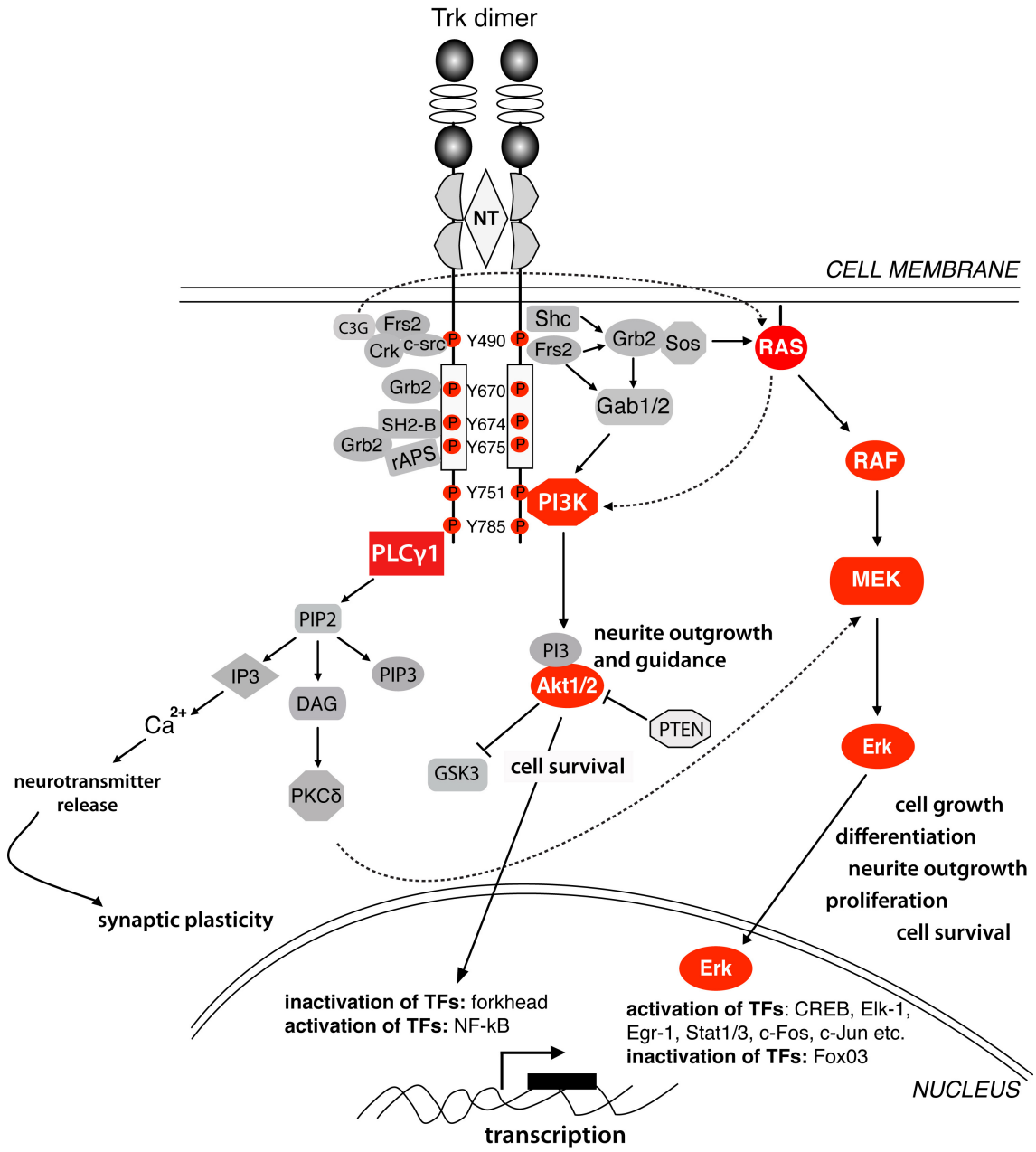

Figure 1.2. Trk receptor signalling pathways.

Schematic representation of the major intracellular Trk signalling pathways Ras/MAPK, PI3K/Akt and PLCγ pathways, which all result in the regulation of gene expression. Upon NT-binding the Trk receptors dimerize. This initiates transphosphorylation of the tyrosine residues and activates the kinase. For simplicity only five of the ten identified tyrosine residues are shown. Binding of adaptor proteins and enzymes to the phosphotyrosines results in the activation of the signalling pathways. The Ras/MAPK pathway is initiated by Tyr 490 phosphorylation and leads to neuronal survival, differentiation, proliferation and growth including neurite outgrowth. Only the classical Erk1/2 pathway is displayed for simplicity. The PI3K/Akt pathway is activated by phosphorylated Tyr 751 or through Ras and Gab-1/2 and promotes survival and growth of neurons. The PLCγ-1 pathway is initiated by Tyr 785 phosphorylation and results in the regulation of Ca^{2+}-dependent synaptic plasticity and is cross-linked to the MAPK pathway.

proto-oncogene c-Crk (p38), which initiates the interaction of the guanine nucleotide exchange factor (GEF) C3G, the small G protein Rap1, and B-Raf and thus initiates the Erk cascade (Kao et al., 2001). Additionally, Frs2 provides binding sites for the Grb2-Sos complex and thus activates the Ras/MAPK pathway. Another adaptor protein, Ankyrin Rich Membrane Spanning (ARMS) protein also interacts with Trk in some cells in a similar manner to Frs2 through Crk and B-Raf to activate the MAPK pathways (Arevalo et al., 2004) (Figure 1.2).

1.2.4.2. PI3K/Akt pathway

The class IA phospholipid kinase (PI3K) pathway is the major regulator of the survival of neurons. It can be activated via a Ras-dependent or -independent pathway, which are both initiated by the phosphorylation of Y490 in the activated Trk receptor. Ras, which is activated as described above for the MAPK pathway, subsequently turns on PI3K. This is the major survival pathway in most, but not all neurons. The Ras-independent PI3K activation is mediated through Y490-Shc-Grb2 interaction and activation of the Grb2-associated binder-1/2 (Gab-1/2), which binds and stimulates PI3K. PI3K also binds directly to phosphorylated Y751 in the catalytic kinase domain of Trk receptors and is phosphorylated and thus activated by Trk. PI3K then generates P3-phosphorylated phosphoinositides, which stimulate the phosphoinositide-dependent protein kinase (PDK-1) and subsequently the protein kinase Akt also known as protein kinase B (PKB). Akt phosphorylates and inhibits proteins such as Bad, a Bcl2-family member of proapoptotic proteins. Additionally Akt regulates the activity of several transcription factors such as forkhead, which results in the inhibition of apoptosis or activation of NF-κB-promoted neuronal survival. Finally, Akt phosphorylates and inactivates the proapoptotic glycogen synthase kinase 3 (GSK-3) thus enhancing cell survival (Pap and Cooper, 1998). The PI3K pathway additionally regulates axon growth and guidance and neuronal differentiation. For instance the 3-phosphoinositides recruit the Rho family of GTPases such as Cdc42 and Rac, which control cell motility, growth cone behaviour and the organization of the cytoskeleton and so regulate neurite outgrowth and growth cone guidance (Yuan et al., 2003) (Figure 1.2).

1.2.4.3. PLCγ pathway

The enzyme phospholipase C isoform PLCγ-1 binds directly to phosphorylated Y785 in the N-terminus of the Trk receptor and is activated through phosphorylation by Trk (Patapoutian and Reichardt, 2001). PLCγ-1 hydrolyzes phosphatidylinositides (PIP2) into diacylglycerol (DAG) and inositol trisphosphate (IP3). DAG activates DAG-regulated protein kinase C (PKC) isoforms such as PKCδ in neurons, which activates the Erk1/2 MAPK pathway and controls for instance NGF-induced neurite outgrowth in PC12 cells (Corbit et al., 1999). IP3 promotes the release of Ca^{2+} ions, which activates Ca^{2+}-dependent protein kinase A (PKA) and the synaptic Ca^{2+}-calmodulin-regulated protein kinases (CaMPK). An increase in intracellular Ca^{2+} additionally enhances neurotransmitter release and thus implicates the PLCγ-1 in synaptic plasticity (Lessmann, 1998). In fact mice with a mutation in the TrkB Y816 (corresponding to Y785 in human TrkA), the PLCγ-1 binding site, show impaired hippocampal long-term potentiation (LTP) similar to TrkB and BDNF null mice (Minichiello et al., 2002) and structural abnormality of synapses in vestibular neurons (Sciarretta et al., 2010) (Figure 1.2).

The current Trk signalling pathway models mostly include just the major components of Trk downstream signalling pathways, which are primarily mediated through the phosphorylated Y490, Y751 and Y785 residues and the adaptor proteins Frs-2 and Shc. However, Trk signalling is more complex and it is clear that the other seven tyrosines also play important roles. In fact many responses are mediated by several tyrosines together. For instance the three phosphotyrosines Y643, Y704 and Y760 in rat TrkA in addition to Y499 and Y794 (correspond to Y490 and Y785 in human TrkA respectively) together mediate NGF-induced neurite outgrowth in PC12 cells (Inagaki et al., 1995). Furthermore, two additional adaptor proteins rAPS and SH2-B were identified. They are recruited by phosphotyrosines in the activation loop (Y670, Y674 and Y675) and associate with Grb2 and might thus link to the Ras/MAPK and PI3K pathways (Huang and Reichardt, 2003).

All of these pathways compete with each other for several proteins and are thus also cross-linked. Additionally Trk receptors interact with many other intracellular and receptor proteins such as $p75^{NTR}$ and ion channels, which complicates the picture of Trk signalling even more (Huang and Reichardt, 2001, Huang and Reichardt, 2003,

Reichardt, 2006). The role of Trk receptor function is also not limited to the described pathways. Trks can also bind to adapters and enzymes such as c-Abl independently of the phosphorylated tyrosine residues and mediate cellular responses such as differentiation (Yano et al., 2000). In addition, Trk receptors can be activated ligand-independently by interaction with GPCRs, leading to a transactivation of Trk receptors similar to other TKR. However, this is a slow and rare event. The two GPCR ligands adenosine and pituitary adenylate cyclase-activating polypeptide (PACAP) were shown to mediate this transactivation, which selectively results in the activation of the PI3K/Akt pathway and thus in cell survival (Lee and Chao, 2001). The cytosolic Src family of tyrosine kinases (SFKs) such as FYN, SYK, and ICK etc. can also associate with and activate Trk receptors in the absence of NTs. Src phosphorylates the Y490 residue on Trk receptors and thus promotes neuronal survival and neurite outgrowth through activation of the MAPK and/or the PI3K/Akt pathways (Lee and Chao, 2001, Encinas et al., 2001).

Not all of these pathways are stimulated simultaneously upon Trk activation. Which pathway is active depends mainly on the cell type and developmental stage of the cell, which influence the presence of specific pathway components and different isoforms. But many other control mechanisms exist such as the compartmentalization and transport of Trk receptors. As previously mentioned Trk-NT complexes are internalised and either degraded or retrogradely transported in endosomes to the nucleus or other compartments. These compartments contain specific signalling intermediates and thus also determine which pathways are activated. Additionally, it was suggested that different types of signalling endosomes exist, which also influence the repertoire of Trk signalling (Zweifel et al., 2005).

Finally, a regulatory role of several protein tyrosine phosphatases in these pathways has also been described. For instance the phosphatase and tensin homolog deleted on chromosome 10 (PTEN) is a major negative regulator of the PI3 kinase/Akt signaling pathway (Cantley and Neel, 1999). Additionally the Src homology 2 domain-containing protein tyrosine phosphatase 2 (Shp2), another cytosolic PTP, together with its substrate signal-regulatory protein (SIRP) was shown to positively regulates BDNF-induced PI3K and MAPK pathway activation and thus survival of cortical neurons (Takai et al., 2002). Shp2 is also activated through binding to Gab1/2 or Frs2. It was suggested to act as an adaptor protein between growth factor receptors and Grb2

and so to activate MAPK signalling. Shp2 phosphatase activity in this scenario is also essential, but not understood yet (Li et al., 1994). In contrast Shp1 directly associates with TrkA in PC12 cells and in sympathetic neurons and dephosphorylates and inactivates this growth factor (Marsh et al., 2003). Further, MAPK phosphatases (MKP) dephosphorylate MAPK and terminate MAPK signalling (Barr and Knapp, 2006). A role of several RPTPs in the regulation of Trk signalling has also been suggested for instance as regulators of the SFKs (Bixby, 2001, Johnson and Van Vactor, 2003) or directly through Trk dephosphorylation and will be described later in more detail.

1.2.5. Implication of Trk receptors and NTs in diseases

Trk receptors and their ligands play essential roles during development and in adult organisms. Thus it is not surprising that they are also implicated in the manifestation of several human genetic, neurodegenerative, and inflammatory, cardiovascular or metabolic diseases. For instance they play a role in diabetes, psychiatric disorders, asthma and allergy, and neuropathic pain just to mention a few. Although the molecular mechanisms remain mostly unknown, the implication of Trk receptors is supported by the correlation of the disease phenotypes with the phenotype of NT and/or Trk deficient mouse models.

Mutations in the human TrkA gene have been identified in several sensory neuropathies such as congenital insensitivity to pain with anhydrosis (CIPA), which is characterized by absence of reaction to noxious stimuli, sweating and mental retardation and results in self-mutilating behaviour. A cause of CIPA might be the death of NGF-dependent neurons during embryogenesis (Indo, 2001). In addition, TrkA function is impaired in Leprous, Diabetic and traumatic neuropathies and pain (Anand, 2004). TrkA was also linked to neurodegenerative diseases such as Alzheimer's Disease and the psychiatric disorders depression, schizophrenia, autism and eating disorders (Ginsberg et al., 2006, Buckley et al., 2007). Aberrant TrkB and BDNF signalling due to mutations in their genes have been associated with many neurodegenerative and psychiatric disorders in humans, which are often characterized by abnormal synaptic plasticity such as sensory impairment, learning and memory deficits, Alzheimer's, Parkinson's and Huntington's Disease, eating disorders including obesity, depression, bipolar disorders, schizophrenia and obsessive compulsive disorder (OCD) (Sklar et al., 2002, Alberch et al., 2004, Yeo et al., 2004, Ribases et al., 2005, Buckley et al., 2007,

Chen et al., 2008, Pillai, 2008, Dwivedi, 2009, Xiu et al., 2009, Maina et al., 2010). Interestingly, a single nucleotide polymorphism (SNP) Val66Met in the BDNF prodomain, which results in abnormal BDNF trafficking and distribution, was also shown to increase the susceptibility towards several of these disorders (Neves-Pereira et al., 2002, Egan et al., 2003, Ribases et al., 2003, Sen et al., 2003). A reduced level of TrkC was linked to mood disorders, schizophrenia and neuropathies (Schramm et al., 1998) and specific loss of NT-3 responsive proprioceptive neurons is also a consequence of chemotherapy using cisplatin, diabetes or vitamin B6 (pyridoxine) intoxication, resulting in the loss of sense in limb position (Lindsay, 1996).

PTKs represent 70% of all known oncogenes and proto-oncogenes as they control growth and proliferation. Thus it is not surprising that all three Trk receptors and their ligands are also implicated in the formation and progression of several tumours and cancers (Nakagawara, 2001). Whereas Trks and NTs are found in neoplastic tissues, they are not always expressed in the corresponding normal tissues. Additionally, oncogenes with constitutive activation have all been found in non-neuronal tumours, whereas proto-oncogenes are also aberrantly expressed in neuronal neoplasms. Mutations in the TrkA, TrkB or TrkC genes have been identified in several cancer types (Martin-Zanca et al., 1989, Schneider et al., 2001). For example all three Trks are associated with two of the most common paediatric neoplasms, the medulloblastoma, a malignant tumour of the CNS, and neuroblastoma, a paediatric neuroendocrine tumour, which arises from the neural crest-derived sympathetic nervous system and mostly originates in the adrenal glands. Trks may play a role in growth control of NBL cells and their expression correlates with the outcome. Whereas TrkA and TrkC expression correlates with a good prognosis, TrkB and BDNF expression is correlated with a bad prognosis (Brodeur, 2003, Schramm et al., 2005). In medulloblastoma TrkC expression was correlated with a positive outcome (Segal et al., 1994).

Since the 1980's recombinant NTs were welcomed as "miracle drugs" and enthusiastically used in clinical trials for treatment of neurodegenerative diseases such as Amyotrophic Lateral Sclerosis (ALS), Alzheimer's, Parkinson's and Huntington's Diseases and peripheral neuropathies. Although animal models were promising, first clinical trials by local administration of NTs failed due to lack of effects or severe off-site effects as NTs promote a diverse spectrum of mechanisms. Future attempts are thus aimed at specific expression of NTs and Trks in target neurons via genetically

modified cells or viral transfer. Interference with Trk downstream pathways or alternative activation routes of Trks such as transactivation by GPCRs or modulation of the $p75^{NTR}$ receptor action are also promising therapeutic goals. Additionally, small molecule mimetics of NTs are currently being investigated (Thoenen and Sendtner, 2002, Price et al., 2007, Skaper, 2008). PTPs, which are recently emerging as regulatory molecules of Trk receptors, also become a focus of particular attention. Thus understanding the implication of PTPs in these signalling pathways may lead to new therapeutic approaches to control aberrant Trk function.

1.3. Protein tyrosine phosphatase (PTP) family

The counter partners of PTKs are protein tyrosine phosphatases (PTPs). These enzymes maintain a determined balance of the phosphorylation state in the cell by removing phosphate groups from phosphorylated tyrosine residues in proteins. In the past PTPs have been dismissed as passive housekeeping enzymes, which only terminate kinase signalling. These assumptions were based on their overall low endogenous expression levels, relatively high enzymatic activity and promiscuity and lack of substrate specificity *in vitro,* or lack of knowledge about their regulation. Additionally in the beginning the progress in this research field was relatively slow in comparison to the analysis of kinases due to several mostly technical limitations such as the poor availability of protein tyrosine phosphate substrates for studies. But with the production of artificial phosphotyrosine substrates and the development of more advanced technical and computational tools, a plethora of studies has been conducted ever since. The *in vivo* function of these enzymes was first analysed in lower organisms such as *Drosophila melanogaster* and *Caenorhabditis elegans*, and more recently also in zebrafish, chick and in mammals. This extensive research led to the understanding that PTPs are not just passive actors but that they actively modify RTK signalling either negatively or positively (Ostman and Bohmer, 2001). For instance the two receptor-type phosphatases RPTPα and CD45 do not inhibit kinase activity as expected but in contrary activate it (den Hertog et al., 1993, Mustelin et al., 1989).

Nowadays it is known that PTPs play crucial roles in all biological processes such as cell survival, growth and differentiation, mitosis, insulin signalling, integrin mediated cell-cell or cell-substrate adhesion, the immune system, osteogenesis,

angiogenesis, metabolism and many different processes in the developing and adult nervous system (Stoker, 2005). It is therefore not surprising that they are also implicated in many different diseases such as metabolic, immune, neurological and developmental disorders, and some were found to be essential tumour suppressor genes such as the popular phosphatase PTEN (Irshad et al., 2004, Ostman et al., 2006, Hendriks et al., 2008).

To date 106 murine and 107 human PTP genes are known (Alonso et al., 2004). And most of these PTPs have homologs and orthologs both in vertebrates and invertebrates. PTPs are defined by their active-site signature motive HCX5R, in which the cysteine (Cys) residue is crucial for catalysis, and they share a common catalytic mechanism and a similar structure (Tonks, 2006). PTPs are classified into four families according to the primary structure of their catalytic domains, and are then grouped into subfamilies based on their substrate specificities. The class I cysteine-based PTPs represent the largest family and constitute of 38 classical PTPs and 60 structurally more diverse dual specificity (DSPs) phosphatases. The classical PTPs are further sub-categorized into 17 non-transmembrane (NPTPs) and 21 receptor-like PTPs (RPTPs) (Figure 1.3). However, this classification is complicated by the fact that due to alternative splicing or alternative promoters, several transmembrane and cytoplasmic forms can be generated from the same gene. DSPs can dephosphorylate phospho-Tyr, phospho-Ser, phospho-Thr residues and non-proteinaceous substrates such as lipids and complex carbohydrates and are subdivided according to their substrate specificity into seven subfamilies. The Thr- and Tyr-specific MAPK phosphatases (MKPs) include eleven PTPs, which are specific for the MAP kinases Erk, Jnk and p38. The group of 19 atypical DSPs has instead a function unrelated to MAP kinase with DUSP11 even dephosphorylating mRNA by interacting with the RNA–ribonucleoprotein complex 1 (PIR1). Three further groups consist of the three poorly characterized phosphatases of regenerating liver (PRLs), the three slingshots (SSHs), which play a role in actin dynamics, and the four cell cycle regulating CDC14 phosphatases. The myotubularins (MTMs) comprise 16 genes and the PTEN-related phosphatases five genes and both groups specifically dephosphorylate the D3-phosphate of inositol phospholipids. The single class II cysteine-based PTP is the Tyr-specific low molecular weight phosphatase (LMPTP) encoded by *Acp1*. The class III cysteine-based PTPs are specific for Tyr and Thr and comprise the three CDC25 cell cycle regulators. The fourth and last family

contains the four Tyr-, or Ser- and Tyr-specific aspartic acid-based haloacid dehalogenases (HADs) Eyes absent (EyAs) (Tonks, 2006, Pulido and Hooft van Huijsduijnen, 2008, Patterson et al., 2009).

1.3.1. Receptor-type protein tyrosine phosphatases (RPTPs)

The RPTP family is part of the classical PTPs and consists of 21 members grouped into eight distinct subfamilies based on the similarity of their ECD. The structure of RPTPs consists of an ECD, which potentially allows ligand binding, followed by a TMD and an ICD with catalytic activity (Figure 1.3). The ECD is very complex in its structure and contains several domains. The FN type III repeats are present in most of the RPTPs (PTPR1/6, 2A, 2B, 3 and 5) and possibly promote interaction with integrins (Montgomery et al., 1996). The Ig-like domains, present only in the PTPR2A and 2B subgroups, have intra-molecular disulfide bonds and have a homophilic binding site that is mostly seen in cell-cell adhesion molecules, such as the neural cell adhesion molecule (N-CAM) (Frei et al., 1992). Other protein domains present in RPTPs are the Mephrin/5A/(PTP)μ (MAM) domain, carbonic anhydrase-like domain (CAH) (PTPR5), RDGS-adhesion recognition motif (PTPR8) and the heavily glycosylated domain (PTPR4). The PTPR7 subgroup is characterized by the absence of any extracellular protein domain (Tonks, 2006). The ECD structures of many RPTPs display characteristics of cell-adhesion molecules and their interaction with the extracellular matrix and other cells has been shown (Aricescu et al., 2007).

The ICDs of all RPTPs show more similarities than their ECDs. Twelve of the RPTPs have two tandem PTP domains in their ICD, while the remaining nine RPTPs contain a single PTP domain. The PTP domain (D1), which is adjacent to the membrane, is catalytically active, whereas the other PTP pseudo-phosphatase domain (D2) is catalytically inactive. However, the latter appears to be important for activity, specificity, stability and dimerization of the phosphatase (Streuli et al., 1990, Jiang et al., 2000, Blanchetot et al., 2002b). An exception to this ICD structure is found in RPTPα from the PTPR4 subgroup, with two catalytically active domains and also in the two RPTPs IA-2 (PTPRN) and IA-2β (PTPRN2) from the PTPR8 subgroup, which contain only the inactive PTP pseudo-phosphatase domain and thus lack catalytic activity altogether (Magistrelli et al., 1996, Jiang et al., 1998). Further, RPTPR is the

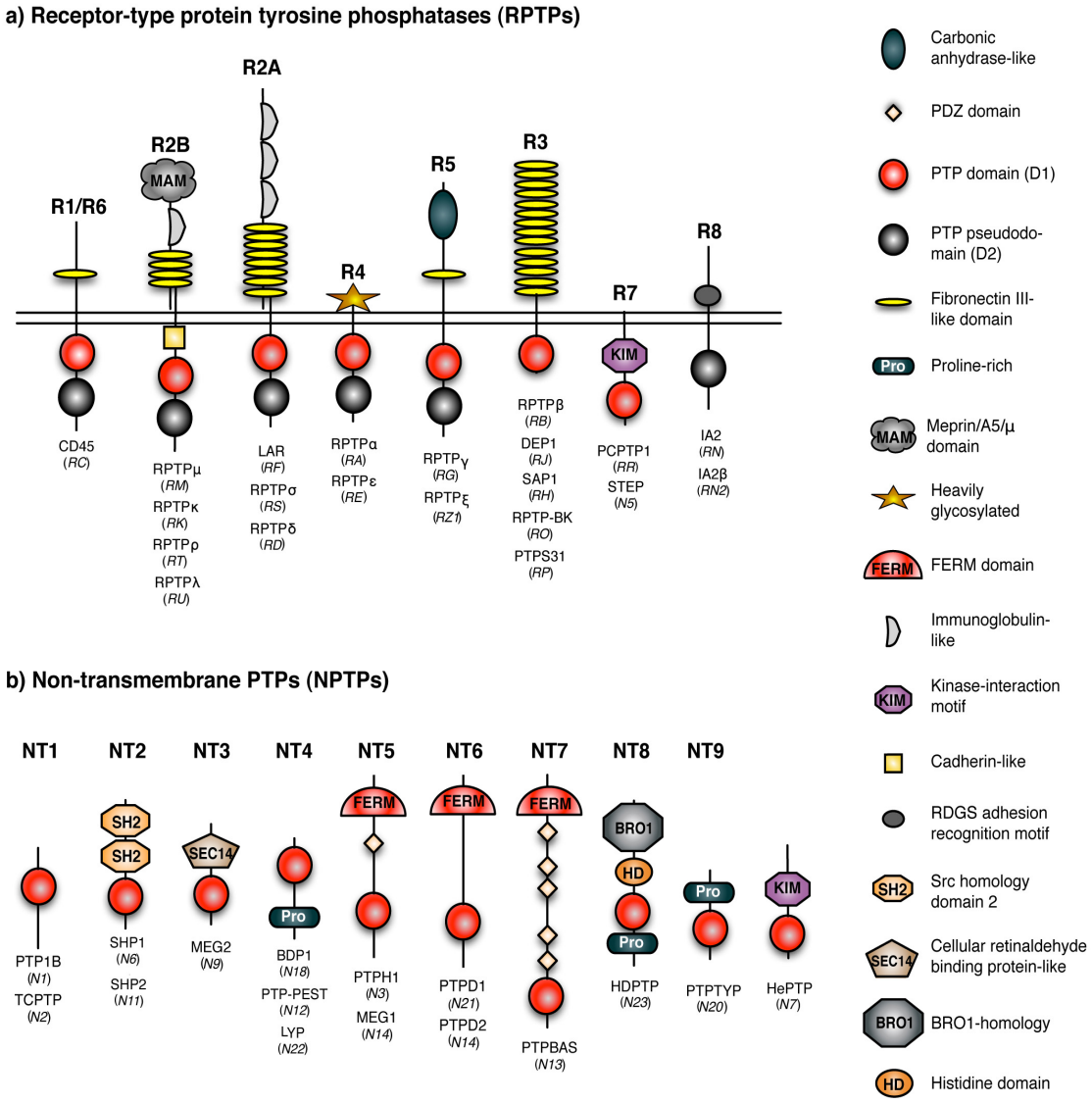

Figure 1.3. The classical PTP family.

a) 21 receptor-like PTPs (RPTPs) and **b**) 17 non-transmembrane PTPs (NPTPs) are known in mammals, but due to alternative splicing or alternative promoters several transmembrane and cytoplasmic forms can be generated from the same gene. The RPTPs are subcategorized into 8 different subgroups based on their extracellular domain similarities. The names represent protein names with gene symbols in brackets (adapted and modified from (Tonks, 2006)).

	GENE SYMBOL	PROTEIN NAME
Trk receptors	Ntrk1	TrkA
	Ntrk2	TrkB
	Ntrk3	TrkC
RPTPs	Ptpra	RPTPα
	Ptprb	VE-PTP
	Ptprc	CD45
	Ptprd	RPTPδ
	Ptpre	RPTPε
	Ptprf	LAR
	Ptprg	RPTPγ
	Ptprh	SAP1
	Ptprj	DEP-1
	Ptprk	RPTPκ
	Ptprm	RPTPμ
	Ptprn	IA-2
	Ptprn2	IA2β
	Ptpro	PTP-BK
	Ptprq	PTPS31
	Ptprr	PTPRR
	Ptprs	RPTPσ
	Ptprt	RPTPρ
	Ptpru	RPTPλ
	Ptprv	OST-PTP
	Ptprz1	RPTPζ

Table 1.1. Gene and protein names of Trk receptors and RPTPs.

only RPTP enzyme that additionally contains in its ICD a membrane proximal kinase-interaction motif (KIM), which is normally found in cytoplasmic PTPs and mediates interaction with MAP kinases, predominantly Erk1 and Erk2 (Pulido et al., 1998). Finally, the PTPR2B subgroup contains a cadherin-like motif adjacent to the plasma membrane, which is required for catenin binding (Tabernero et al., 2008).

1.3.2. Regulation of RPTP function

RPTP function and specificity towards their substrates is highly regulated *in vivo* at different levels. First, differential expression of PTPs in organisms, tissues and cells, which is regulated by developmental or cellular processes such as differentiation and proliferation, but also for instance by cell density, determines their presence and thus function. Additionally, the specific subcellular location of RPTPs such as lipid rafts in the plasma membrane determines their interaction partners and function (den Hertog et al., 2008). Similar to the previously described Trk kinases, RPTPs also have several different isoforms with specific expression patterns and functions due to alternative splicing and promoters and also proteolytic cleavage and shedding. This complicates even the classification of RPTPs as some of them have intracellular isoforms such as in the case of RPTPε (Gil-Henn et al., 2000) and RPTPR (Van Den Maagdenberg et al., 1999) or secreted extracellular forms such as phosphacan in the case of RPTPζ (Garwood et al., 2003). On the molecular level RPTP function is regulated by many different mechanisms such as dimerization, ligand binding, and post-translational modifications of specific domains like reversible oxidation, glycosylation and also phosphorylation.

Dimerization is an essential control mechanism of RPTPs and can either activate or inhibit RPTP function. Ligand-binding and post-translational modifications affect the conformation of the enzyme and thus its dimerization state. Some phosphatases such as RPTPα, RPTPδ, RPTPμ, RPTPσ, the leukocyte antigen-related protein (LAR) and CD45 (PTPRC) also contain a helix-loop-helix (HLH) wedge-shaped domain between the membrane proximal region and the D1 domain, which plays a regulatory role (Bilwes et al., 1996). Several studies including crystal structure analysis, biochemical studies and yeast two-hybrid screens have suggested an “inhibitory wedge model”, in which this domain provides dimerization and inhibition of the phosphatase (Majeti and

Weiss, 2001, Blanchetot et al., 2002b, Tonks, 2006). However, in a recent structural screen, evidence was provided that such a "wedge"-mediated dimerization is not possible for RPTPs other than RPTPα due to conformational hindrance under physiological conditions (Barr et al., 2009). Nevertheless, the "wedge" domain plays a very important role in the regulation of RPTP function as has been demonstrated by Xie *et al.*, who have shown that a LAR wedge Tat peptide inhibits LAR function and thus increases proliferation and neurite outgrowth and decreases cell death (Xie et al., 2006). Whether the "wedge" domain is involved in substrate interaction or has another effect on RPTP function remains to be determined.

As receptors, RPTPs can either undergo homophilic interactions and build adhesion junctions such as in the case of RPTPμ, RPTPκ, RPTPλ and RPTPδ, or interact with heterologous ligands. Binding of ligands can cause, prevent or disrupt dimerization of the receptors, which subsequently negatively or positively affects their function. For instance ligand binding promotes dimerization and inhibits the function of RPTPs such as LAR and RPTPζ (Majeti et al., 1998, Jiang et al., 1999, van der Wijk et al., 2005) or it disrupts dimerization and activates the phosphatase in case of RPTPα (Bilwes et al., 1996, Jiang et al., 2000, Tertoolen et al., 2001a). However, only few such ligands have been identified and their function remains mostly uncertain. For instance known ligands for RPTPζ are contactin, tenascin and pleiotrophin but only the latter has been shown to modulate the activity of this phosphatase (Meng et al., 2000, Perez-Pinera et al., 2007). Furthermore, DLAR in *Drosophila* binds to the heparan sulphate proteoglycans (HSPG) syndecan and Dallylike and controls the presynaptic development of the neuromuscular junction (Fox and Zinn, 2005, Johnson et al., 2006). A specific isoform of mammalian LAR, which can be found in non-neuronal cells, was also shown to bind the extracellular matrix laminin-nidogen complex (O'Grady et al., 1998). Moreover, nucleolin and the HSPG agrin and collagen XVIII, and chondroitin sulfate proteoglycans (CSPG) such as neurocan and aggrecan, which can be found in the nervous system and in skeletal muscles, bind to specific isoforms of RPTPσ (Aricescu et al., 2002, Sajnani-Perez et al., 2003, Alete et al., 2006, Shen et al., 2009). Interestingly, RPTPσ-dimers can bind their ligands only in a specific conformation (Lee et al., 2007). Recently, trans-synaptic adhesion between netrin-G-ligand-3 (NGL-3) and the three mammalian phosphatases LAR, RPTPσ and RPTPδ, was shown

and the regulation of excitatory synapse formation mediated by these complexes was demonstrated (Woo et al., 2009, Kwon et al., 2010).

Post-translational modifications such as phosphorylation of specific domains and reversible oxidation of the catalytic Cys residue by reactive oxygen species (ROS) additionally regulate RPTP function (Ostman and Bohmer, 2001). In the case of RPTPα reversible oxidation of Cys in the active site of the D2 domains of two RPTPs upon treatment with H_2O_2 causes a conformational change in the D2 domain. This leads to the formation of a Cys–Cys disulfide bond between the D2 domains and thus results in the stabilisation of the dimers and thus inactivation of RPTPα (Blanchetot et al., 2002a, Persson et al., 2004, den Hertog et al., 2005). The phosphorylation of Ser and Tyr residues in the RPTPs also controls their function, but the actual mechanisms remain unknown. For instance RPTPα is phosphorylated on two Ser residues in its juxtamembrane domain, which regulates its activity. It was suggested that the phosphorylation of these residues prevents the dimerization and thus inactivation of this phosphatase (Tracy et al., 1995, Zheng et al., 2002). Further, RPTPα is phosphorylated on a C-terminal Tyr, which creates a binding site for Grb2 and activates downstream signalling pathways (den Hertog et al., 1994). Interestingly, RPTPα is dephosphorylated by CD45 in T cells, which reveals a cross talk between RPTPs (Maksumova et al., 2007). These modifications occur mostly in the C-terminus of the ICD and lead consequently to conformational changes, which can be transmitted to the ligand-binding ECD and the catalytic D1 domain and thus reveal a possibility of a ligand-independent "inside-out" signalling mechanism in RPTPs.

All these regulatory mechanisms of RPTPs not only complicate the overall picture of RPTP function but they also represent potential targets for drugs. Small peptides have been developed and already tested as inhibitors or mimetics of the catalytic and ligand binding site as well as the wedge domain. But before we proceed with the interference with RPTP function more knowledge has to be acquired about their function. A first hint towards their possible function is the analysis of their expression.

1.3.3. RPTP expression and function in the nervous system

RPTP expression as well as their function is very diverse and also species-specific. RPTPs promote ligand-controlled protein tyrosine dephosphorylation of specific protein substrates in almost any known signalling pathway in the developing and adult organism such as insulin signalling, bone homeostasis, angiogenesis, the immune system and the nervous system. RPTPs have also been associated with many human diseases due to the alteration of their expression and function under pathological conditions (Tonks, 2006). However, the analysis of RPTP function is complicated since neither ligands nor substrates are known for most of these phosphatases to date. Additionally, *in vitro* analysis leads to false conclusions due to the promiscuity of RPTPs under non-endogenous conditions. Therefore the most reliable analysis of their function are loss-of-function studies in animal models such as *Drosophila*, *Xenopus laevis*, *C. elegans*, chick, zebrafish and mice. At the current stage mice with RPTP gene deletions of all RPTPs with the exception of RPTPλ were generated and provide valuable insights into RPTP function (Paul and Lombroso, 2003, Hendriks et al., 2008).

The majority of the initially discovered RPTPs from different species were found at high levels and often exclusively in the CNS and PNS during axon guidance and synapse formation (Sommer et al., 1997, Stoker and Dutta, 1998, Chilton and Stoker, 2000). Thus from the beginning the function of RPTPs was extensively studied in the nervous system, first in *Drosophila* and later also in vertebrates. RPTPs were shown to play many different roles in the regulation of axon guidance by promoting target recognition, as inhibitory guidance cues and in synapse formation in motor neurons and within the visual system (Burden-Gulley and Brady-Kalnay, 1999, Wang and Bixby, 1999, Sun et al., 2000b, Stepanek et al., 2001, Johnson and Van Vactor, 2003, Ensslen-Craig and Brady-Kalnay, 2004). RPTPs are also implicated in neural tissue histogenesis during development whereby they control the formation of several brain areas such as the visual system, cerebellum and hypothalamus and neuromuscular development (Ledig et al., 1999b, Sun et al., 2000a, Rashid-Doubell et al., 2002, Ensslen-Craig and Brady-Kalnay, 2004). Additionally several knockout mice also show neurological and behavioural abnormalities (Hendriks et al., 2008). Together, the RPTPs LAR, RPTPσ, RPTPδ, RPTP-BK (an RPTPO form in rodents), RPTPα, RPTPγ, RPTPζ, RPTPR, RPTPμ and RPTPκ are all expressed in the nervous system of different species, where they play an important role. Strikingly, whereas the expression

of some of these RPTPs is similar across species, other RPTPs show completely different expression patterns and functions.

One of the first cloned RPTPs was LAR, a founding member of the PTPR2A subgroup that also includes RPTPδ and RPTPσ. All three mammalian RPTPs are expressed in the nervous system and homologues have been found in chick (CRYPα), leech (HmLAR1 and 2), *Drosophila* (DLAR and PTP69D) and *C. elegans* (CLAR) (Van Vactor, 1998), which also play crucial roles in the nervous system. For instance in *Drosophila* DLAR and PTP69D are exclusively expressed in the nervous system, where they control axon guidance of motor neurons (Desai et al., 1996, Krueger et al., 1996, Sun et al., 2000b) and retinal cells (Garrity et al., 1999, Clandinin et al., 2001, Maurel-Zaffran et al., 2001). Additionally, DLAR was shown to regulate synapse morphogenesis of cultured hippocampal neurons by positively regulating the formation of neuromuscular junction (NMJ) synapses (Kaufmann et al., 2002). The expression of all three mammalian RPTPs, LAR, RPTPδ and RPTPσ, is very dynamic, partly overlapping but mostly distinct during development and persistent into adulthood in many neural tissues. Based on the structure of their ECD a role of these RPTPs in cell adhesion or cell surface recognition was suggested (Streuli et al., 1989, Harrington et al., 2002). However, despite their similar structure and expression patterns these RPTPs exhibit different and sometimes contrary functions.

LAR, which is encoded by *Ptprf,* is one of the strongest expressed RPTPs in the developing nervous system, but the least specific to neural tissues among the PTPR2A members. LAR was indentified during development in the CNS in neurons of the cerebellum, cortex, and brain stem. In the PNS it is expressed in neurons in the DRGs and the geniculate ganglia. Additionally, LAR was also found in astrocytes and pheochromacytoma cells (PC12). LAR expression is mostly restricted to the subventricular zone (SVZ) and is rather low in differentiated neuronal cells within the CNS but remains high in PNS nuclei (Schaapveld et al., 1998, Van Vactor, 1998). LAR is also present in RGCs, where it modulates neuritogenesis and cell survival and its expression is elevated during regeneration (Lorber et al., 2004, Lorber et al., 2005). LAR was found along neurites and in growth cones and is involved in the proliferation and maturation of neurons and regulates axon guidance, growth and regeneration, whereby LAR can play both augmenting and inhibiting roles depending on the context (Zhang et al., 1998). For instance inhibition of HmLAR2, a leech ortholog of LAR,

causes shortened and aberrant neuronal projections, growth cone collapse and navigational crossover errors (Gershon et al., 1998, Baker et al., 2000, Baker and Macagno, 2000, Baker and Macagno, 2010). An upregulation of LAR in DRGs causes enhanced neurite outgrowth (Xie et al., 2001). And an increase of LAR activation through peptide mimetics, which bind to the fifth LAR FNIII region in its ectodomain and probably prevent homodimerization of LAR and so its inhibition, also resulted in increased neurite outgrowth in DRG explants (Yang et al., 2005a, Yang et al., 2005b). The absence of LAR in a mixed sensory and motor nerve delayed axonal regeneration *in vivo* following injury (Xie et al., 2001). On the other hand LAR downregulation in PC12 cells resulted in an increase in NGF-mediated neurite outgrowth and decreased apoptosis (Moshnyakov et al., 1996, Tisi et al., 2000). LAR also regulates excitatory synapse formation as LAR downregulation in hippocampal neurons leads to a loss of excitatory synapses and dendritic spines (Ip et al., 1993, Marsh et al., 1993, Culmsee et al., 2002, Dunah et al., 2005). Interestingly, postsynaptic LAR regulates synapse morphogenesis partly through its association with AMPA receptors in cultured hippocampal neurons (Dunah et al., 2005), whereas presynaptic LAR regulates synapse formation through a trans-synaptic adhesion with NGL-3 regulation (Woo et al., 2009, Kwon et al., 2010). $LAR^{-/-}$ mice present a delay in sciatic nerve regeneration and a decrease in collateral nerve sprouting after injury (Van der Zee et al., 2000, Xie et al., 2001) as well as a decrease in innervation of the hippocampus, reduced size of basal forebrain cholinergic neurons and impaired spatial learning (Yeo et al., 1997, Van Lieshout et al., 2001, Van Der Zee et al., 2003, Kolkman et al., 2004). However, $LAR^{-/-}$ mice grow normally and their abnormalities are rather mild. But this could be attributed to traces of full-length LAR and a truncated LAR isoform being still present in these mouse models (Yeo et al., 1997, Yang et al., 2003). A better $LAR^{-/-}$ mouse model is currently not available.

RPTPσ is strongly expressed in the PNS, CNS and the endocrine system in tissues such as DRGs, the sciatic nerve and cranial nerve ganglia, in the VZ and SVZ of the spinal cord and in the developing brain in the cortex, hippocampus, cerebellum, brain stem, olfactory bulb, the retinotectal system and the pituitary gland (Yan et al., 1993, Stoker et al., 1995, Van Vactor, 1998, Elchebly et al., 1999, Wallace et al., 1999, Meathrel et al., 2002, Johnson and Van Vactor, 2003). Its expression is strongest during embryonic development and was predominantly detected in proliferating and

differentiated cells (Sahin et al., 1995, Wang et al., 1995). RPTPσ is expressed in neurons but its expression in the VZ and SVZ additionally suggested an expression in glia cells. This was supported by detection of a specific shorter RPTPσ isoform in cultured primary glia cells and Schwann cells in the adult mouse sciatic nerve (Wang et al., 1995, McLean et al., 2002). RPTPσ was the first vertebrate RPTP, whose function in axon outgrowth and guidance was demonstrated in the developing chick retina and the tectum (Ledig et al., 1999a, Rashid-Doubell et al., 2002). Moreover mammalian RPTPσ was recently implicated in glutaminergic pre- and postsynaptic differentiation in co-culture experiments with hippocampal neurons (Takahashi et al., 2011). Using knockout mice it was also shown that RPTPσ inhibits axon regeneration after peripheral nerve injury of sciatic nerve axons and that a loss of RPTPσ enhances the rate of facial motor neuron regeneration, which is however accompanied by directional errors (Thompson et al., 2001, Thompson et al., 2003). RPTPσ loss also increases axon regrowth of RGCs after optic nerve lesion (Sapieha et al., 2005). Interestingly, whereas in RGCs and in facial motor neurons RPTPσ gene expression did not change after injury (Thompson et al., 2003, Sapieha et al., 2005), in adult DRGs and sciatic nerves RPTPσ mRNA increased during regeneration (Haworth et al., 1998, McLean et al., 2002). This illustrates that RPTPσ gene expression is differently regulated in the CNS and PNS, which also differ in their regenerative capacities. Recently, one mechanism for the implication of RPTPσ in nerve regeneration was deciphered, when CSPGs, which represent a barrier for axon regeneration and are secreted by astroglia at injury sites, were identified as ligands for RPTPσ. In culture experiments of RPTPσ$^{-/-}$ DRG neurons the inhibitory effect of CSPGs on neurite outgrowth was indeed reduced compared to wild type cells. And in an *in vivo* spinal cord injury model in adult RPTPσ$^{-/-}$ mice increased neurite outgrowth was observed through the CSPG-rich lesion area (Shen et al., 2009). Furthermore, mice lacking RPTPσ show severe growth retardation and semi-lethality after birth and the most obvious neurological defects among RPTP knockout mice with developmental abnormalities in the pituitary gland, hypothalamus, corpus callosum and cerebral cortex. Additionally, RPTPσ-deficient mice suffer from hypomyelination of peripheral nerves and defects in proprioception, as well as abnormalities in motor coordination and ataxia (Elchebly et al., 1999, Wallace et al., 1999, Batt et al., 2002, Meathrel et al., 2002). The proprioceptive defects might be caused by aberrant RPTPσ expression in DRGs or the cerebellum.

RPTPδ is predominantly expressed in the CNS in the spinal cord, the cortex, diencephalon, forebrain and hindbrain and in the retina during early rodent development (Van Vactor, 1998, Johnson and Holt, 2000). It is not expressed in the proliferating neuroepithelium but instead can be found in differentiated neurons and in connective tissues and muscular compartments (Sommer et al., 1997, Schaapveld et al., 1998). RPTPδ is a homophilic cell-adhesion molecule (CAM) and promotes neuronal adhesion and regulates neurite outgrowth of CNS neurons in chick embryos (Wang and Bixby, 1999). A soluble ECD of RPTPδ is possibly an attractive guidance cue for retinal and forebrain neurons (Sun et al., 2000b), whereas a transmembrane form is a repulsive guidance cue in cortical neurons in culture (Tuttle et al., 1999). Interestingly, in contrast to rodents and *Drosophila*, RPTPδ expression was not detected in MNs in chick E4-8 embryos. RPTPδ knockout mice exhibit growth retardation and neonatal mortality caused by insufficient food intake due to motor defects such as abnormal positioning of hind limbs and abnormal flexion of limbs. Additionally, they have memory deficits and suffer from hypomyelination and hyperpotentiation of hippocampal synapses demonstrating that RPTPδ is involved in synapse formation (Uetani et al., 2000).

Ptpro encodes a phosphatase of the PTPR3 subgroup, which also contains DEP-1, RPTPβ, SAP-1 and PTPS31. In rodents this phosphatase is known as RPTP-BK, in humans as PTP-U2, in rabbits as GLEPP-1, in chick as CRYP-2 and in *Drosophila* as PTP10D. Interestingly, the ECD of RPTP-BK is not particularly conserved in these species indicating that the physiological function of this domain such as ligand binding might be divergent, but probably not their substrate specificity (Tomemori et al., 2000). The murine RPTP-BK has five isoforms due to alternative splicing; two transmembrane isoforms, of which the smaller one is found in podocytes of renal glomeruli and the larger form in the CNS and PNS and three truncated isoforms, which lack the ECD and can be found in macrophages, B cells and osteoclasts (Tomemori et al., 2000). The mammalian neuronal isoform is expressed in the developing brain in postmitotic maturing neuronal cells in the cerebral cortex, olfactory bulb and nucleus, thalamus, hippocampus and midbrain, and also motor neurons, the midline of the spinal cord and in dorsal root, cranial, and sympathetic ganglia, where it is involved in the differentiation and axonogenesis of neurons (Tomemori et al., 2000, Beltran et al., 2003). An increase in expression throughout development from E12 on and a peak between E16 until P3, the time of highest axonogenesis, was detected

(Van Vactor, 1998). It was also suggested that RPTP-BK exerts its activity in undifferentiated progenitor cells in the telencephalon and hindbrain (Sommer et al., 1997). In chick CRYP-2 is also strongly expressed in the developing brain for instance in RGCs and their target the optic tectum during periods of axon outgrowth and guidance (Ledig et al., 1999b). CRYP-2 acts as a chemorepulsive guidance cue for RGC axons *in vitro*, induces growth cone collapse and inhibits retinal neurite outgrowth. Recently Shintani *et al.* have elucidated the molecular mechanisms behind these observations. They have shown that CRYP-2 regulates the sensitivity of retinal axons to ephrins by dephosphorylating Tyr residues in the juxtamembrane region of EphA and B receptors, and thus plays a key role in the establishment of retinotectal projections in the chick (Shintani et al., 2006). In addition a knockdown of CRYP-2 lead to aberrant axon guidance in developing motor neurons (Stepanek et al., 2001). And in *Drosophila* DPTP10D was also shown to control axon guidance of motor neurons (Desai et al., 1996, Krueger et al., 1996, Sun et al., 2000b). RPTP-BK knockout mice show defects in the differentiation but not survival of peptidergic nociceptive and proprioceptive neurons in the DRGs, resulting in abnormal projections and behavioural abnormalities such as a loss of response to thermal stimuli. Thus it was suggested that RPTP-BK is required for differentiation and neurite guidance of sensory neurons and mature sensory function (Gonzalez-Brito and Bixby, 2009).

Ptprr encodes four different PTPR7-type protein isoforms, the two receptor-type isoforms PTPBR7 and the shorter PTP-SL and the two cytosolic isoforms PTPPBSγ-37 and -47 (Hendriks et al., 1995, Ogata et al., 1995, Chirivi et al., 2004). PTPBR7 is expressed in DRGs, and in different brain tissues such as hippocampus and Purkinje cells in the cerebellum during early embryonic development. Interestingly, whereas PTPBR7 levels decrease postnatally in cerebellar Purkinje cells, PTP-SL transcripts arise, which are additionally expressed in most of the other brain tissues (Van Den Maagdenberg et al., 1999, Augustine et al., 2000). PTPPBSγ expression is very low in the brain, and is instead mostly found in non-neuronal tissues. RPTPR knockout mice suffer from impaired motor coordination and balance skills and a mild form of ataxia. However, no morphological changes could be observed in the brain of these mice compared to their wild type littermates. Since RPTPR interacts and dephosphorylates several MAPK, Erk1/2 phosphorylation was significantly elevated in the brain in RPTPR-deficient animals (Chirivi et al., 2007).

The expression of RPTPα, a member of the PTPR4 subgroup, is dynamic and abundant in the entire developing nervous system and persists into adulthood (den Hertog et al., 1996, Ledig et al., 1999b). It is highly expressed in NC derivatives such as adrenal gland, and cranial and spinal sensory ganglia, in retina and tectum and additionally in radial glia, Bergmann glia and Mueller glia and their extended fibres (Van Vactor, 1998, Ledig et al., 1999b). RPTPα was implicated in the differentiation and migration of NCCs and neurons (den Hertog et al., 1993, den Hertog et al., 1996, Fang et al., 1996). Morpholino studies in Zebrafish embryos revealed its role in retinal lamination (van der Sar et al., 2002) and convergence and extension cell movements during gastrulation (van Eekelen et al., 2010). RPTPα is expressed in RGCs, where it modulates neuritogenesis and cell survival and its expression is elevated after lesion (Lorber et al., 2004, Lorber et al., 2005). RPTPα knockout mice do not have an obvious phenotype but show some aberrant neurological functions such as impaired neuronal migration in the hippocampus (Petrone et al., 2003) and NCAM-mediated neurite elongation, affected synaptic plasticity and locomotor activity as well as decreased anxiety (Skelton et al., 2003, Bodrikov et al., 2005).

RPTPγ is a PTPR5 phosphatase and its expression was documented in the CNS and PNS in mice and chick. It was detected in the spinal cord of chick embryos first in interneurons and later also in the motor neuron progenitor (pMN) domain (Chilton and Stoker, 2000, Gustafson and Mason, 2000, Jessell, 2000). Recently in our lab a role of this phosphatase in proliferation, survival and adhesion of progenitor cells was demonstrated in gain- and loss-of-function studies in the chick spinal cord. And RPTPγ was implicated in the canonical Wnt/β-catenin pathway (Hashemi et al., 2010). Surprisingly, in the mouse RPTPγ is not expressed in the early spinal cord but was detected predominantly in sensory and pyramidal neurons (Lamprianou et al., 2006). RPTPγ immunoreactive protein was also found in neuronal and some glia cells in the human brain including Purkinje cells and in Schwann cells of human sensory ganglia (Vezzalini et al., 2007). RPTPγ$^{-/-}$ mice are viable and display only moderate behavioural changes in comparison to wild type animals such as abnormal motor coordination. Lack of RPTPγ expression in proliferating areas of the adult brain also indicated that it is not necessary for adult neurogenesis (Lamprianou et al., 2006).

RPTPζ (formerly known as RPTPβ), which is also a member of the PTPR5 subgroup, is predominantly expressed in the CNS and PNS during early and late

development in centres of neural proliferation such as the SVZ (Canoll et al., 1996a). Its expression was identified in a subset of neurons but predominantly in radial glia cells, which give rise to astrocytes and neurons, oligodendrocyte progenitors, and in Schwann cells and SGCs surrounding large neurons in rat embryonic and adult DRGs (Canoll et al., 1993, Haworth et al., 1998, Shintani et al., 1998, Van Vactor, 1998, Harroch et al., 2000). The *Rptpz1* gene encodes three isoforms. The two transmembrane isoforms are found throughout the developing rat brain at earlier developmental stages, and later with highest abundance in astroglia (Van Vactor, 1998). The soluble isoform phosphacan is a chondroitin sulfate proteoglycan (CSPG), which is released from glia cells. The transmembrane isoforms are most abundant during development, whereas phosphacan is predominantly expressed during postnatal stages (Canoll et al., 1996a). *In vitro* assays have shown that RPTPζ controls axon outgrowth and cell adhesion (Canoll et al., 1993), proliferation and differentiation of radial glia cells and neurogenesis in neural stem cells (Lamprianou and Harroch, 2006). Moreover, it is implicated in cell migration, synaptogenesis, synaptic function, myelination and neuron–glial interaction (Maeda and Noda, 1998, Murai et al., 2002). Phosphacan acts as a ligand for a variety of axonal cell-adhesion receptors such as N-CAM and contactin (Milev et al., 1994, Grumet et al., 1996, Milev et al., 1996, Margolis and Margolis, 1997) and can influence tyrosine phosphorylation in cortical neurons (Maeda and Noda, 1996). Despite the many different roles RPTPζ plays in the nervous system, knockout mice show only mild neuronal defects such as impaired working memory, aberrant motor coordination, and reduced responses to moderate but not high nociceptive stimuli (Lafont et al., 2009). These mice have also an impaired ability in the recovery from demyelination (Harroch et al., 2000, Harroch et al., 2002).

RPTPμ is a member of the PTPR2B subgroup and a homophilic CAM, which promotes neurite outgrowth. In the chick RPTPμ is expressed in axons and growth cones of RGCs and in the tectum (Ledig et al., 1999b, Burden-Gulley et al., 2002), where it mediates cell-cell aggregation via trans-homophilic binding and is additionally a key regulator of cadherin-dependent neurite outgrowth. Interestingly, RPTPμ appears to be both an inhibitory and permissive guidance cue within the visual system at specific embryonic developmental stages depending on its concentration and is involved in the formation of retinal lamination (Brady-Kalnay et al., 1993, Burden-Gulley and Brady-Kalnay, 1999, Ensslen et al., 2003, Ensslen-Craig and Brady-Kalnay, 2004,

Major and Brady-Kalnay, 2007, Oblander et al., 2007). Further RPTPμ gene expression was found in other CNS areas in non-neural cells, for instance in blood vessels in the spinal cord of chick and rat E13.5 embryos (Longo et al., 1993, Van Vactor, 1998, Chilton and Stoker, 2000). In mice RPTPμ expression was predominantly found in the cardiovascular system but was also detected in Purkinje cells and other neurons in the brain. However, RPTPμ mice have no neuronal phenotype (Koop et al., 2003).

RPTPκ is similar to RPTPμ a homophilic PTPR2B CAM. Its gene expression was documented in the rat CNS in actively developing areas in the hippocampus and cerebral cortex, cerebellum, brain stem and spinal cord, and in the adult, in areas capable of plasticity such as the cortex, olfactory bulb and the hippocampal formation with generally higher expression levels in the developing CNS (Jiang et al., 1993). RPTPκ expression suggests an involvement in axon growth and guidance and in fact a soluble form of RPTPκ stimulated neurite outgrowth in cultured cerebellar neurons (Drosopoulos et al., 1999, Leighton et al., 2001). RPTPκ was also detected in specific neurons in murine E14 DRGs (Hantman and Perl, 2005) and in radial processes of retinal progenitor cells during murine development. It was suggested to play a role in the migration of neurons, possibly mediated through its substrate β-catenin (Horvat-Brocker et al., 2008). However, like RPTPμ, RPTPκ-deficient mice do not show abnormalities in neural development (Shen et al., 1999).

Since many transgenic animals with RPTP deficiency lack an obvious neurological phenotype and appear mostly normal and healthy, a compensatory effect of different phosphatases, possibly from the same subgroup, as a safety mechanism was suggested. In this respect studies in *Drosophila* have revealed that RPTPs compensate for each other's loss in motor neurons as only double, triple or quadruple knockouts achieved defects (Desai et al., 1997, Sun et al., 2001). However, RPTPs also display antagonistic and complementing roles *in vivo* (Ensslen-Craig and Brady-Kalnay, 2004). For instance lack of either LAR or RPTPσ in mice affected the regenerative capacity of their neurons in opposite ways. Whereas LAR-deficient animals showed a delay in sciatic nerve regeneration and decreased collateral nerve sprouting after injury, RPTPσ-deficient animals exhibited enhanced nerve regeneration (Xie et al., 2001, Van Der Zee et al., 2003). Deficiency in either RPTPδ or RPTPσ in mice results in viable animals with mostly neuronal abnormalities. However, an RPTPδ/RPTPσ double knockout in mice

resulted in paralysed animals, which could not breathe and died shortly after birth. Since these mice showed loss in spinal cord motor neurons and extensive muscle dysgenesis, their functional redundancy in motor neuron survival and axon targeting in mammals could be demonstrated (Uetani et al., 2006). Nevertheless, a non-redundant function between structurally similar RPTPs exists as well and was demonstrated in RPTPα/RPTPε double knockout mice (Tiran et al., 2006), which both specifically regulate the activity of voltage-gated potassium channels and Src kinase in Schwann cells (Tsai et al., 1999, Peretz et al., 2000).

1.3.4. RPTP substrates and signalling pathways

RPTPs are implicated in a plethora of physiological processes such as cell-cell and cell-matrix adhesions and migration, metabolism, cell survival, growth and death. However, we do not only lack knowledge about their ligands but also about their actual physiological substrates and thus signalling mechanisms.

RPTP function was particularly studied in cell-cell and cell-matrix adhesions and migration, which are of immense importance in embryogenesis, angiogenesis, and tissue repair and in nerve growth (Larsen et al., 2003). This is due to two main reasons. First, it is known that phosphorylation plays a crucial role in these fundamental processes and second several RPTPs resemble CAMs and are involved in neural outgrowth as described above. It is now appreciated that some RPTPs regulate cell-cell and cell-matrix adhesions via association with cadherins and catenins, which are a major component of adherens junctions (AJ). For example RPTPμ mediates cell-cell adhesion via homophilic trans interactions and binding of its ICD to cadherins and is thus implicated in the formation of AJ. Interestingly, RPTPμ has several functions in this respect. It dephosphorylates cadherins and catenins, and works as a scaffold for additional regulatory proteins. The RPTPs LAR, RPTPκ, RPTPλ, DEP-1, VE-PTP and RPTPζ also interact directly with cadherins and/or catenins and dephosphorylate them, and so control cell-cell adhesion and some of them also control neurite outgrowth (Stoker, 2005, Sallee et al., 2006, Aricescu et al., 2007, Oblander et al., 2007). Moreover RPTPs regulate cell-cell and cell-matrix adhesions via interaction with the integrin signalling. Integrins are a major component of cell-matrix adhesions as they control the formation of so-called focal adhesions (FAs), and thus link the extracellular

matrix (ECM) with the actin cytoskeleton of the cell. Integrins are part of a multi-molecular complex and are responsible for the activation of FA kinases (FAK) and the downstream signalling cascades leading to actin cytoskeleton remodelling, which is important for instance at the growth cones during axon guidance and extension. The involvement of RPTPs in this process was demonstrated for example for LAR. It binds with its D2 domain to α-liprins, which act in this case as scaffold proteins and translocate LAR to FAs, where LAR also docks to the Rho/Rac GEF factor TRIO and dephosphorylates it (Debant et al., 1996, Serra-Pages et al., 1998, Burridge et al., 2006). TRIO was demonstrated to control axon guidance in *Drosophila* (Bateman et al., 2000) and TRIO is a substrate of FAK and itself activates FAK in a bi-directional mechanism (Medley et al., 2003). Interestingly, LAR not only dephosphorylates TRIO but also FAK (Cheung et al., 2000) and thus might counteract the formation and function of FAs.

Furthermore RPTPs can dephosphorylate other receptors such as ion channels. As an example RPTPα and RPTPε both regulate the activity of potassium channels (Tsai et al., 1999, Peretz et al., 2000), whereas RPTPζ influences the activity of sodium channels (Ratcliffe et al., 2000, Salter and Wang, 2000).

Many NRTKs and RTKs are also direct physiological substrates of RPTPs and can be deactivated or activated upon dephosphorylation (Ostman and Bohmer, 2001). For instance RPTPα controls the activity of several members of the cytoplasmic SFKs, since RPTPα-knockout mice have reduced Src and Fyn activities in the brain (Ponniah et al., 1999, Su et al., 1999). SFKs are implicated in many different signalling pathways such as cell migration and adhesion, differentiation, proliferation and mitosis, and so is RPTPα. This regulatory mechanism has been well described. RPTPα itself is constitutively phosphorylated on its D2 domain, and is thus associated with the SH2-containing adaptor protein Grb2. Additional phosphorylation of RPTPα releases Grb2 and RPTPα binds and dephosphorylates the autoregulatory Y527 in the C-terminus of c-Src leading to its activation (Den Hertog and Hunter, 1996). LAR is also known to activate the SFKs LCK and FYN via dephosphorylation of their Y529 residues (Tsujikawa et al., 2002). Similarly, CD45 dephosphorylates the inhibitory but also the stimulatory Tyr of the SKFs Lck in T cells and Lyn in B cells (Li and Dixon, 2000). CD45 can also bind and directly dephosphorylate the Janus family kinases (JAKs) and thus for instance negatively regulate cytokine-induced cell proliferation

(Irie-Sasaki et al., 2001). Further, several RTKs were also shown to be substrates of RPTPs *in vitro*. For example RPTPσ can dephosphorylate EGFRs (Suarez Pestana et al., 1999). LAR dephosphorylates the HGFR/Met tyrosine kinase (Kulas et al., 1996) and Ret (Qiao et al., 2001) and inhibits FGF-induced MAPK activation (Wang et al., 2000). The insulin receptor can be dephosphorylated by LAR, RPTPα and RPTPε (Kulas et al., 1995, Moller et al., 1995). DEP-1 also dephosphorylates HGFR/Met (Palka et al., 2003) and additionally controls the function of VEGFRs (Grazia Lampugnani et al., 2003) and PDGFRs (Kovalenko et al., 2000). Additionally, DEP-1 dephosphorylates EGFRs and limits endocytosis of active EGFRs and thus their ability to generate intracellular signals (Tarcic et al., 2009). RPTP-BK negatively regulates EphRs and so inhibits neurite outgrowth in RGCs (Shintani et al., 2006). Recently RPTP-BK phosphorylation on its C-terminus by FYN and its subsequent association with FYN and Grb2, a scaffold protein in many growth factor signalling pathways, was described. Thus it was suggested that RPTP-BK could also dephosphorylate and activate SFKs (Murata et al., 2010).

Together, a plethora of different RTKs appear to be physiological substrates of RPTPs, and so it is not surprising that some RPTPs can directly bind and dephosphorylate Trk receptors as well.

1.4. RPTP and Trk interaction and function - previous findings

First evidence for an implication of specific RPTPs in Trk signalling arose, when it was realized that mRNA expression of some RPTPs and Trks overlaps in specific tissues in the nervous system. And both protein types are also localized to neurites and growth cones. A role of PTPs in the regulation of neurite outgrowth and specifically in Trk signalling was also suggested, when non-specific PTP inhibitors, including vanadate and orthovanadate (Rogers et al., 1994, Fujiwara et al., 1997), stimulated neurite outgrowth in PC12 cells, a well-characterized model of neural precursor cells, and activated Trk signalling and prevented cell death in hippocampal neurons (Gerling et al., 2004).

LAR was the first RPTP that was suggested to regulate TrkA signalling, as LAR mRNA expression increased upon NGF-treatment in PC12 cells, which highly express TrkA receptors (Aparicio et al., 1992, Longo et al., 1993). Much evidence has since

been provided for a regulation of TrkA and also TrkB by LAR. Interestingly, depending on the context, LAR may up- or downregulate NT signalling. Its inhibitory role was shown, when an antisense induced downregulation of LAR decreased apoptosis and augmented NGF-induced neurite outgrowth in PC12 cells (Moshnyakov et al., 1996, Tisi et al., 2000). Further, a specific wedge peptide, which inhibits LAR function, caused an augmented NGF-induced activation of TrkA and its downstream pathway components Erk and Akt in PC12 cells. Their activation even in the absence of NGF lead to the differentiation and survival of PC12 cells and thus suggests a possible effect of LAR on the transactivation of Trk receptors (Xie et al., 2006). An augmenting role of LAR on TrkB signalling was demonstrated in hippocampal neurons, which predominantly express TrkB receptors, lower amounts of TrkC and traces of TrkA receptors. This augmenting effect of LAR on Trk signalling was suggested to occur indirectly through its interaction with Src and subsequent activation of this kinase, which is known to activate Trk receptors (Tsuruda et al., 2004). This hypothesis was supported by abolishing the ability of LAR to augment TrkB signalling in hippocampal neurons by administration of the Src inhibitor PP2 to the cells (Yang et al., 2006). When LAR function was augmented through peptide mimetics an increase in neurite outgrowth in DRG explants and hippocampal neurons was observed. On the molecular level increased TrkB Y515 phosphorylation and activation of downstream pathway components such as Akt, Erk and CREB were detected (Yang et al., 2005a, Yang et al., 2005b). Additionally LAR co-immunoprecipitates with TrkA and TrkB either via direct interaction or in a complex for instance with Src, as Src knockdown prevented TrkB-LAR co-immunoprecipitation (Xie et al., 2006, Yang et al., 2006). Finally, $LAR^{-/-}$ mice showed impaired neurite outgrowth of CNS (Yeo et al., 1997) and PNS neurons (Xie et al., 2001), which express both LAR and Trk receptors, thus supporting an augmenting effect of LAR possibly on Trk signalling. Although many insights hint towards an implication of LAR in Trk signalling, its function through modulation of non-Trk-related mechanisms such as through FAK and EGFR signalling cannot be excluded at this point. In fact both of these RTKs are also known to be involved in neurite outgrowth and cell proliferation and were shown to interact with LAR (Kulas et al., 1996).

RPTPσ, another member of the PTPR2A subgroup such as LAR, is expressed in overlapping patterns with TrkA, B and C mRNA within the developing nervous system

and has been implicated in the regulation of neurite outgrowth; hence an interaction with Trks appears to be very likely. In our laboratory Faux *et al.* investigated the role of RPTPσ and demonstrated selective and strong binding to TrkA and C, but only weak binding to TrkB in co-IPs. However, a binding to a Trk-complex instead of a direct interaction with the receptor cannot be excluded. An indication for this is the ability of RPTPσ to dephosphorylate all three Trks despite the differing strengths of their interactions. Additionally, the over-expression of RPTPσ in embryonic chick sensory neurons resulted in the suppression of NGF-dependent neurite outgrowth but without affecting cell survival (Faux et al., 2007). Recently, in a binding assay in COS cells RPTPσ, unlike LAR or RPTPδ, was shown to bind a non-catalytic form of TrkC through an interaction of their ECDs but not TrkA or TrkB. Additionally a trans-synaptic, neurotrophin-independent interaction between axonal RPTPσ and dendritic non-catalytic TrkC in co-cultures with hippocampal neurons triggered glutaminergic pre- and postsynaptic differentiation (Takahashi et al., 2011). Interestingly, RPTPσ-deficient mice suffer from defects in proprioception, thus supporting the hypothesis of a possible interaction of RPTPσ with TrkC (Elchebly et al., 1999, Wallace et al., 1999, Batt et al., 2002, Meathrel et al., 2002).

First expression studies of another RPTP, RPTP-BK, during mouse development showed specific and almost exclusive gene expression in neurons of the CNS and PNS such as in DRGs and TG. Most of these neurons also expressed TrkC, to some extent TrkA and fewer neurons also expressed TrkB. Thus a possible role of RPTP-BK in the differentiation and axonogenesis of NT-3 and NGF-dependent neurons in the CNS and PNS was suggested (Beltran and Bixby, 2003, Chen and Bixby, 2005). In a recent overexpression study Hower *et al.* have shown that an over-expression of RPTP-BK in stably TrkC-expressing cell lines decreased NT-3 induced TrkC phosphorylation (Hower et al., 2009). Further, RPTP-BK$^{-/-}$ mice show deficits in the development of sensory neurons, particularly of peptidergic nociceptors, and abnormalities in neuronal guidance of proprioceptors and nociceptors within the spinal cord accompanied by behavioural abnormalities such as loss of response to thermal pain (Gonzalez-Brito and Bixby, 2009).

Recent coexpression studies in HEK293T cells showed that RPTPζ but not RPTPγ dephosphorylates Tyr residues in the activation loop of TrkA and that an

over-expression of RPTPζ in PC12 cells inhibited NGF-dependent neurite outgrowth (Shintani and Noda, 2008). This study contradicts previous findings, where it was suggested that RPTPγ and not RPTPζ inhibits NGF-mediated neurite outgrowth in PC12 cells (Shintani et al., 2001). It was suggested that whereas RPTPγ probably interacts with Trk downstream pathways, RPTPζ directly dephosphorylates Y674 and/or Y675 in the catalytic domain of TrkA and thus controls its kinase activity (Shintani et al., 2001, Shintani and Noda, 2008). The more recent findings are consistent with the elevated TrkA-phosphorylation state in RPTPζ-deficient mice (Shintani and Noda, 2008) and reduced responses to moderate nociceptive stimuli (Lafont et al., 2009). Whereas RPTPγ-deficient mice did not show any abnormalities in NGF-induced neurite outgrowth (Lamprianou et al., 2006). An interaction of RPTPζ with Trks was suggested early on as RPTPζ is coexpressed mostly with the truncated TrkB-isoform in the CNS especially in areas where glia cells reside (Snyder et al., 1996).

Implication of RPTPR in Trk signalling became apparent when RPTPR mRNA was twelvefold upregulated in PC12 cells following NGF-treatment (Sharma and Lombroso, 1995). Recent studies on RPTP-BR7 and TrkA in an over-expression system in COS-1 cells have also demonstrated their binding, as well as dephosphorylation of TrkA but not TrkB by RPTPR and possible effects of RPTPR action on TrkA maturation (Noordman *et al.*, unpublished data).

Taken together, all of these studies provide strong evidence for a possible interaction of RPTPs in Trk signalling either directly or in a complex of proteins. Thereby they can play either augmenting or inhibitory roles depending on the context. But many questions remain unanswered and the actual regulatory mechanisms remain mostly in the dark. Shining some light on this interaction will not only expand our knowledge about the functional mechanisms of these essential enzymes but also provide possible tools to regulate abnormal Trk signalling in diseases. Thus in this PhD project I have focused on the analysis of a possible regulation of Trk signalling by RPTPs.

1.5. DRGs, a model system to study Trk and RPTP function

Dorsal root ganglia (DRGs) are a very well established primary neuronal cell system to study growth factor signalling pathways. They are especially suitable for the study of Trk receptors, which are endogenously expressed and play crucial roles in these ganglia. Therefore this cell model system was chosen for the study of RPTPs in Trk signalling.

DRGs are spinal ganglia, which contain mainly cell bodies of sensory neurons. They are part of the somatic nervous system (SNS), which belongs to the PNS. The PNS transmits information from the interior and the environment of the organism to the CNS. It contains sensory and motor neurons and consists on the one hand of the autonomic nervous system (ANS) including the sympathetic, parasympathetic and enteric nervous system, which transmits information from the interior of the body, and on the other hand of the mentioned SNS, which conveys information from the external environment. The SNS consists of cranial and spinal nerves and ganglia such as TG and DRGs, which transmit sensations such as position, touch, pressure, vibration, temperature, pain and itching from skin, bones and muscles of the head and face directly, and at spinal levels mostly from the limbs through the spinal cord to designated areas of the brain.

DRGs are situated bilaterally and dorsally along the spinal cord. In most mouse strains there are in total 60 DRGs, of which 8 pairs are located at cervical (C1-8), 13 pairs at thoracic (T1-13), 5 pairs at lumbar (L1-5) and 4 pairs at sacral (S1-4) vertebrate levels (Malin et al., 2007). In addition to cell bodies of sensory neurons, DRGs contain SGCs (Figure 1.4). The postmitotic bipolar sensory neurons project two axonal processes in opposite directions, one towards specific peripheral targets and the other towards designated central targets in the spinal cord (Le Douarin and Kalcheim, 1999). The sensory neurons in DRGs are an extremely heterogeneous population of at least 20 different subclasses of neurons. They show variations in sensory modality, the content of neurotransmitters, the sites of innervation of central and peripheral targets, morphology, growth factor dependencies and neurochemical properties (Scott, 1992). The majority of these different classes of neurons express specific Trk receptors. Upon peripheral target innervation the ganglia composition changes immensely as the majority of neurons undergoes cell death due to limited amounts of NTs at the targets (“neurotrophic hypothesis”) (Hamburger and Levi-Montalcini, 1949).

DRGs are derivates of multipotent trunk neural crest cells (NCCs), which commit to a sensory fate instructed by BMP and Sox10 from the neural tube, the latter being a Wnt/β-catenin pathway mediator. The NCCs migrate, proliferate, and aggregate into DRGs, where they differentiate into sensory neurons and SGCs (Le Douarin and Kalcheim, 1999). Sensory neurogenesis occurs in three partly overlapping waves orchestrated by genetic cascades of specific TFs (Marmigere and Ernfors, 2007). The first wave of neurogenesis takes place during the migration of multipotent NCCs at around E8.5 and E10 in the mouse. It is initiated in one third of migrating multipotent trunk NCCs by the basic helix-loop-helix (bHLH) TF neurogenin 2 (Ngn2). These cells express subsequently the forkhead TF Foxs1, terminate migration and express the POU homeodomain TF Brn3a, which drives the expression of runt-related transcription factor 3 (Runx3) (Dykes et al., 2010). Consequently the cells differentiate into large $TrkC^+$ neurons (Kramer et al., 2006), which are proprioceptive and allow limb position and movement sensations. Down regulation of Runx3 in these cells leads to the generation of $TrkB^+$ neurons, which are medium sized cutaneous mechanoreceptive neurons and are responsible for touch, pressure and vibration sensations (Huang and Reichardt, 2003). The expression of $TrkC^+$ and/or $TrkB^+$ neurons shows a peak at E11.5 in lumbar sensory neurons of mouse embryos (Phillips and Armanini, 1996, White et al., 1996). Neurogenin 1 (Ngn1) drives the second wave of neurogenesis. Multipotent cells within the DRGs express Ngn1, Foxs1 and Brn3a, which initiate the expression of Runx3 or Runx1 (Dykes et al., 2010) and this drives the production of $TrkC^+$ or $TrkA^+$ neurons, respectively. The majority of generated cells in this wave are small $TrkA^+$ nociceptive, thermoceptive and pruriceptive neurons responsible for pain, temperature and itching sensations, respectively (Liu and Ma, 2010). TrkA expression increases gradually between E10 and E13 in DRGs (Lawson and Biscoe, 1979, Phillips and Armanini, 1996, Farinas, 1999). In the third wave beginning at E10.75 in the mouse boundary cap cells (BCC) from the dorsal root entry zone (DREZ) of the spinal cord, which express the zinc finger TF Krox20, also known as Egfr2, and proliferate and migrate into the DRG. They generate almost exclusively $TrkA^+$ neurons and glia cells. However, the genetic cascade controlling this wave remains still unknown (Maro et al., 2004). Recently the implication of Islet1 as a pan-sensory TF in these events was described. It terminates the expression of neurogenic bHLH TFs Ngn1 and Ngn2 and thus initiates the terminal differentiation and specification of $TrkA^+$ and $TrkB^+$ but not $TrkC^+$ neurons in DRGs (Sun et al., 2008). An additional subtype of sensory neurons expresses the

receptor tyrosine kinase Ret, a co-receptor for the glia cell line derived neurotrophic factor (GDNF) family of ligands (Molliver et al., 1997). These neurons are mostly mechanoreceptors at embryonic stages and some of them also coexpress TrkB. At postnatal stages Ret^+ neurons are proprioceptors and to some extent coexpress TrkA. The different subtypes of specific Trk^+ or Trk^- neurons differ further by expression of specific ion channels and other receptors, whose expression is partly controlled by Trk receptors. The cells generated in the first wave of neurogenesis account finally for 4%, in the second wave for 91%, and in the third wave for 5% of the final total neural population in DRGs (Marmigere and Ernfors, 2007). However, when Maro *et al*. ablated the BCCs they have detected a much higher decrease in $TrkA^+$ cells than estimated and therefore the contribution of neurons from the BCCs could be well underestimated and in fact be even as high as 35% (Maro et al., 2004).

Some subsets of sensory neurons also coexpress TrkA, TrkB and/or TrkC receptors and Ret at early stages or switch expression from one to the other receptor (Buchman and Davies, 1993, Liebl et al., 1997, Enokido et al., 1999). First evidence for a possible coexpression of Trk receptors in DRG cells was observed in transgenic mice with gene deletions of a Trk receptor or NT, as unexpected amounts of surviving cells were detected. For example the loss of neurons in double-mutant mice lacking two Trk receptors was not additive and therefore indicated a coexpression of these receptors in the same cells (Minichiello et al., 1995). A further hint towards coexpression in DRG neurons was the observation that Trk receptors were expressed by neurons of many different sizes at earlier developmental stages, but that their expression was confined mainly to neurons of a specific size at later stages, i.e. TrkA was mostly expressed in small neurons, TrkB in medium-sized neurons, and TrkC in large neurons (Mu et al., 1993, McMahon et al., 1994). Further analysis showed that for instance TrkC and TrkB genes are coexpressed at early developmental stages in many regions of the embryo such as the pyramidal cell layer of the hippocampus, in the postmitotic mantle of the ventral horn of the spinal cord, where motor neurons reside, and in several non-neuronal tissues such as mesenchyme and tongue (Tessarollo et al., 1993). TrkA and TrkC expression shows remarkable similarities in gene expression patterns during development in sympathetic ganglia and DRGs (Ernsberger, 2009). These coexpression patterns and switch of Trk expression can be mainly explained by the two major waves of neurogenesis in which neurons first express TrkC or TrkB as described above.

Although neurogenesis in DRGs has been extensively studied, our knowledge is not complete by far and even less is known about gliogenesis such as of SGCs and Schwann cells, which ensheath peripheral nerves. However, these glia cells play crucial roles for instance in the control of the neuronal microenvironment and clearing of apoptotic cells, and are also involved in chronic pain (Hanani, 2005, Wu et al., 2009, Hanani, 2010a, Hanani, 2010b). Interestingly, unlike autonomic SGCs, sensory SGCs do not have any synapses (Hanani, 2005). SGCs are mostly generated during the second and third waves of neurogenesis and their formation is instructed by Notch signalling (Carr and Simpson, 1978, Lawson and Biscoe, 1979, Morrison, 2001, Taylor et al., 2007). However, details about the genetic cascades, which control these events, remain mostly unknown (Wakamatsu, 2004).

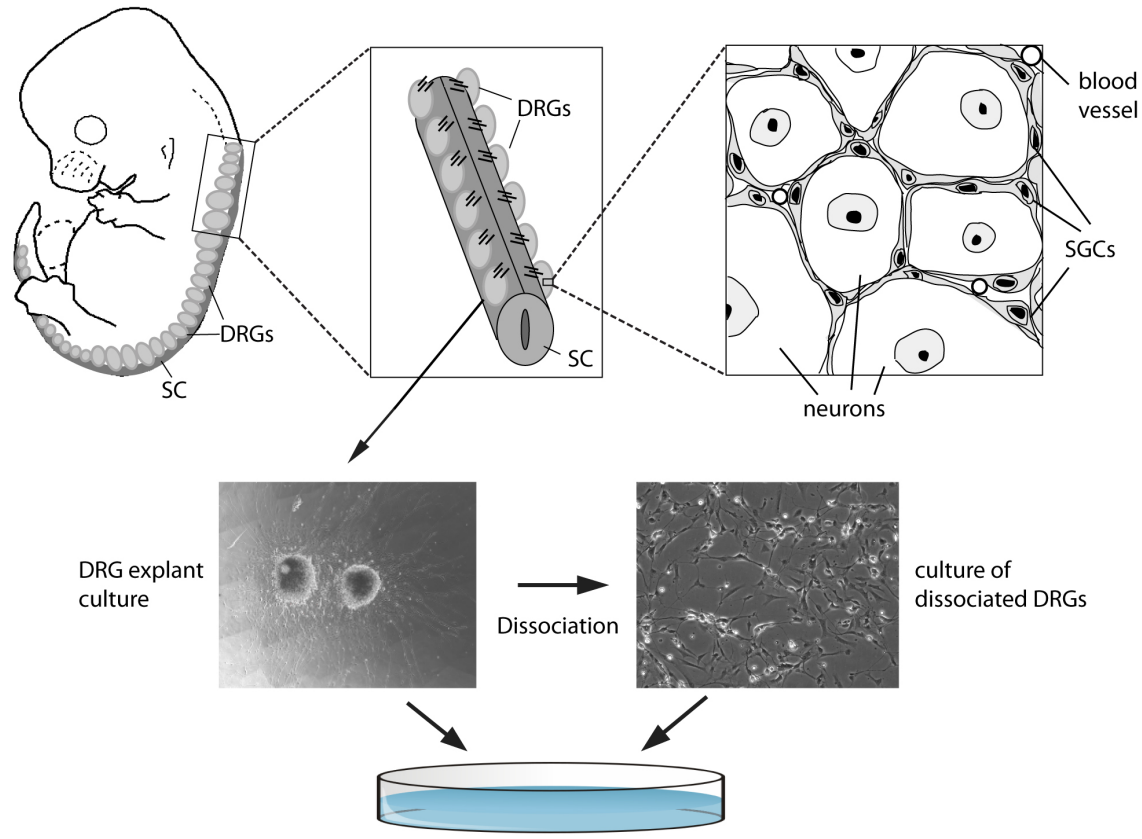

Figure 1.4. Schematic presentation of DRGs in mouse embryos and their cell cultures.
Upper panel: Schematic presentation of DRGs in a mouse embryo, which are situated in 30 pairs along the spinal cord (SC). Each soma of a neuron is surrounded by several satellite glia cells (SGCs). Lower panel: Embryonic DRGs can be cultured in a medium containing neurotrophins either as explant cultures (left) or they can be dissociated and cultured (right).

DRGs are a good cell model to study neurotrophin signalling

DRGs offer many advantages as a cell model system. First, DRG composition and development have been extensively studied and are well characterized as described above. Furthermore the ganglion composition is stereotyped in each mouse and hence several DRGs and animals can be pooled and thus supply enough material for many different applications. DRGs can be used as whole explant cultures or in a dissociated form (Malin et al., 2007) (Figures 1.4 and 1.5). Since DRG sensory neurons are a mixture of neurons with different growth factor responsiveness, target tissue innervations etc., they allow the analysis of a diverse spectrum of neurons. Additionally it is possible to tightly control the extracellular environment, such as by addition of specific growth factors, which regulate neuronal phenotype, survival and function *in vivo.* Importantly, these neurons maintain the ability to respond to chemical, thermal and mechanical stimuli in culture.

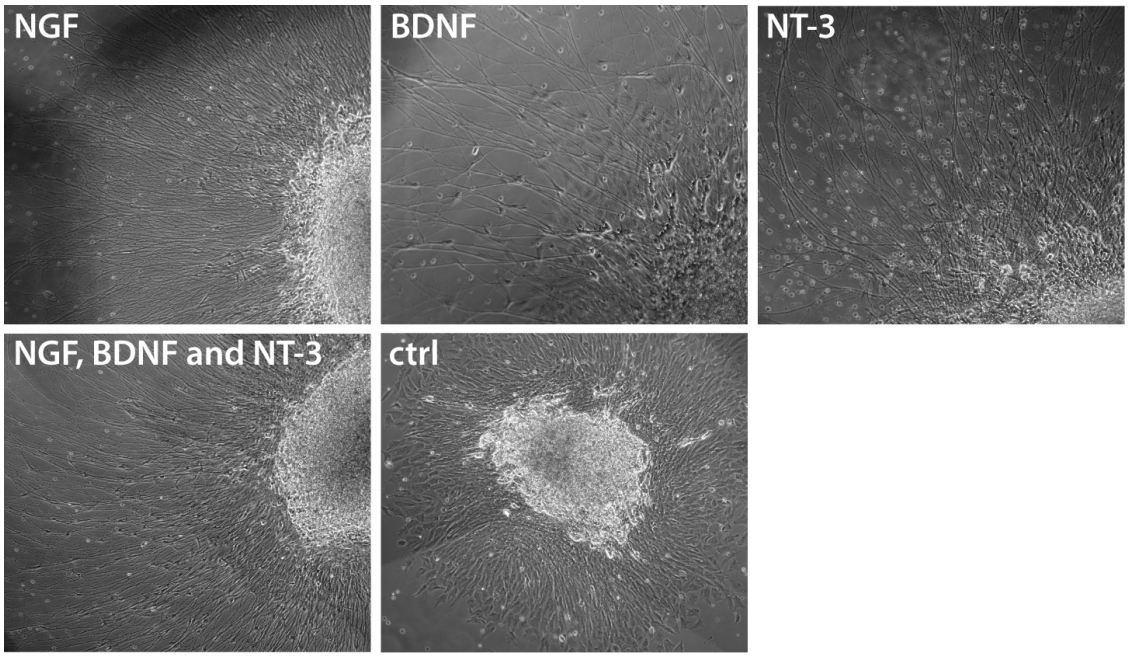

Figure 1.5. Effects of NTs on neurite outgrowth in chick E7 DRG explant cultures.
Embryonic chick DRGs were cultured for 48h either in the presence of NGF, BDNF, NT-3, or all three NTs (50ng/ml), or without any growth factors. All three neurotrophins caused visible neurite outgrowth compared to the untreated control (ctrl). Differences in the amounts, length and branching of axons are visible between explant cultures with different neurotrophins (unpublished data, Viktoria Tchetchelnitski).

1.6. Outline of this thesis

One of the main goals in the NT field remains to understand the different signalling pathways activated by Trk receptors. Recently it has been shown that one component of this signalling cascade might be the RPTPs (section 1.4). However, the research of phosphatases is technically quite challenging and thus the progress in understanding their role in Trk signalling is slow. But with new remarkable technological tools being developed we are coming step by step closer to deciphering the role of these important enzymes. Understanding how to control Trk activity in diseases can possibly help to develop therapeutics in future.

Previous studies have suggested a role of RPTPs in regulating Trk signalling and therefore the control of important neuronal mechanisms such as differentiation, neurite outgrowth and cell survival (section 1.4). However, most of these experiments have been performed in over-expression systems and the physiological relevance of the interaction of these RPTPs and Trks remains to be demonstrated. Additionally, several RPTPs have been implicated and therefore a certain degree of redundancy is possible, which was not experimentally assessed yet. Also a certain specificity of RPTPs towards certain Trk subtypes was suggested, but remains to be shown *in vivo*. Furthermore, the mechanisms by which RPTPs control Trk receptor phosphorylation remain poorly understood. In this study I have addressed these questions.

One hint towards a possible interaction of RPTPs and Trks is their temporal and spatial coexpression *in vivo*. Although the expression of RPTPs and Trks has previously been described (section 1.2 and 1.3), none of these studies analysed the expression of RPTPs and Trks in the same tissue at the same time. Therefore, the first aim of this study was to identify which RPTPs are present in murine embryonic DRGs, which also highly express Trk receptors (Chapter 3). For this purpose an extensive analysis of the gene expression patterns of PTPs with a focus on RPTPs was performed in developing murine embryonic DRGs at three time points (E12.5, 13.5 and 14.5) during organogenesis. This analysis allowed us to select the highest expressed RPTPs for a comparative analysis of their gene expression patterns with Trks (Chapter 4). Furthermore, a detailed coexpression analysis of the selected RPTPs and Trks in the same sensory neurons was performed. This analysis allowed us to clearly show which

RPTPs are coexpressed with Trk receptors at the same time in sensory neurons making their interaction with each other likely.

In previous studies the mechanisms of the regulation of Trk phosphorylation and function were analysed mostly in over-expression systems apart from LAR and TrkB in hippocampal neurons (section 1.4). Therefore, the physiological relevance of these interactions needs to be assessed. It is a challenging task to investigate the function of proteins under physiological conditions and usually knockdown studies are a good choice for the analysis. For this purpose transgenic animals are generated or knockdown strategies are employed. The latter is a more straightforward approach and was used in this study to elucidate the role of RPTPs in Trk signalling. I have therefore established a shRNA-mediated knockdown system using lentiviruses (Chapter 5) and analysed the effects of the reduction of the three promising candidate RPTPs in Trk signalling, LAR, RPTPσ or RPTP-BK, on the direct phosphorylation state of Trk receptors and their downstream signalling pathways using immunoblotting, and on the gene expression using qPCR (Chapter 6).

The (direct) interaction of RPTPs with Trks was previously assessed using co-immunoprecipitation, which have shown an interaction of Trks with LAR, RPTPσ or RPTP-BK (section 1.4). However, the limitation of this technique is that protein interactions are assessed not under physiological conditions. Therefore I have also tested an *in vivo* assay, the Bimolecular Fluorescent Complementation Assay (BiFc), for its feasibility to analyse the (direct) interaction of RPTPs with TrkA (Chapter 7).

Chapter 2

Materials and methods

The described protocols are modified versions taken from (Sambrook et al., 1989) or instructions from manufacturers if not otherwise stated. General chemicals were obtained from BDH, Invitrogen, Sigma or VWR unless otherwise stated. Basic techniques were described in this chapter whereas more specific techniques can be found in the individual result chapters

2.1. DNA methods

2.1.1. Growth and maintenance of E.coli

Escherichia coli (*E.coli*) were cultured in flasks with sterile LB broth (1% bacto-tryptone, 0.5% bacto-yeast extract, 1% NaCl, pH 7.0) supplemented with a selective antibiotic (ampicilin, carbanecillin or kanamycin) at a concentration of 50 µg/ml in a shaker at 250 rpm and 37ºC overnight (< 16 h). Alternatively they were streaked and grown on LB agar (1% bacto-tryptone, 0.5% bacto-yeast extract, 1% NaCl, pH 7, 1.5% agar) plates supplemented with a selective antibiotic at a concentration of 100 µg/ml at 37ºC overnight. *E.coli* LB cultures carrying the plasmid of interest were preserved with 15% glycerol in a sterile Eppendorf tube at -80°C.

2.1.2. Transformation of chemically competent E.*coli*

An aliquot of 30-50 µl of chemically competent *E.coli* (DH5α; Invitrogen) were thawed on ice and added to 1-10 ng of plasmid DNA and gently mixed. Following incubation on wet ice for 30 min the bacteria were heat shocked for 20 sec in a 42°C water bath and immediately transferred back on wet ice for 2 min. The transformed bacteria were resuspended in 1 ml SOC agar (2% bacto-tryptone, 0.5% bacto-yeast extract, 10 mM NaCl, 2.5 mM KCl, 10 mM $MgCl_2$, 10 mM $MgSO_4$, 20 mM glucose, pH 7.0) and shaken at 250 rpm and 37ºC for 1 h. An aliquot of 100-500 µl was spread on an LB agar plate supplemented with a selective antibiotic (100 µg/ml) and grown overnight at 37ºC.

2.1.3. Plasmid preparations: Mini preps

The QIAprep® Spin Mini Kit (Qiagen) was used to extract high quality plasmid DNA (< 10 kb) from bacterial cultures with an approximate yield of 10 µg. It is based on a modified alkaline lysis method of Birnboim and Doly and utilizes binding properties of silica-membranes to purify the DNA. Briefly, bacteria are lysed under alkaline conditions, neutralized and bound in the presence of high salt (chaotropic agents) and appropriate pH to a silica-gel-membrane in a spin column, while impurities (cell debris, gDNA, RNA, proteins etc.) are removed. Following several washes with medium salt buffers the plasmid DNA is finally eluted from the membrane in low-salt buffer or ddH_2O.

For plasmid preparation transformed *E.coli* (DH5α; Invitrogen) containing the plasmid of interest were cultured in 1-10 ml LB broth supplemented with a selective antibiotic for 12-16 h. The bacteria were pelleted by centrifugation for 10 min. All centrifugation steps were carried out at 13,000 rpm in a microcentrifuge at room temperature. The bacterial pellet was resuspended in 250 µl buffer P1 (50 mM Tris-Cl, pH 8.0, 10 mM EDTA) including 100 µg/ml RNAse A, 250 µl buffer P2 (200 mM NaOH, 1% w/v SDS) were added and the solution thoroughly mixed by inversion. 350 µl buffer N3 (25-50% guanidinium chloride, 10-25% acetic acid) were added and the mix centrifuged for 10 min. The supernatant was applied onto a QIAprep® spin column and centrifuged for 1 min. The flow-through was discarded and the column washed with 500 µl PB buffer (25-50% guanidinium chloride, 25-50% propanol) to remove endonucleases and endotoxins (depending on bacterial strain optional) and then with 750 µl ethanol-containing PE buffer. The column was dried by centrifugation for 1 min. To elute the plasmid DNA from the column 50 µl of EB buffer (10 mM Tris-HCl, pH 8.5), TE buffer (10 mM Tris-HCl, 1 mM EDTA, pH 8.0) or ddH_2O were applied onto the column, let stand for 1 min and centrifuged.

2.1.4. Plasmid preparations: Midi/Maxi preps

QIAprep® Spin Midi or Maxi Kits (Qiagen) were used to extract larger amounts of high quality plasmid DNA from bacterial cultures with approximate yields of up to 100 µg or 500 µg DNA. It is based on the same modified alkaline lysis method of Birnboim and Doly as described for the mini preps (see section 2.1.3) and Anion-Exchange Resin tips

with appropriate buffers are used to bind and purify the DNA, which is finally concentrated and desalted by isopropanol precipitation.

A starter culture of 2-5 ml LB medium supplemented with a selective antibiotic containing *E.coli* (DH5α; Invitrogen) carrying the plasmid of interest was cultured for approximately 8 h. 1/1000 of the starter culture were inoculated in 50 ml/100 ml or 100 ml/500 ml (midi or maxi) LB broth for high or low copy-number plasmids respectively and cultured overnight (< 16 h). The bacterial cells were harvested by centrifugation at 4600 rpm for 20 min at 4ºC. The pellet was resuspended in 4 ml/10 ml buffer P1 (50 mM Tris-Cl, pH 8.0, 10 mM EDTA) including 100 µg/ml RNAse A, mixed with 4 ml/10 ml lysis buffer P2 (200 mM NaOH, 1% w/v SDS), inverted vigorously and incubated at room temperature for 5 min. It was mixed with 4 ml/10 ml chilled neutralization buffer P3 (3 M potassium acetate, pH 5.5) and incubated on ice for 15 min/20 min followed by centrifugation at 4600 rpm at 4ºC for 30 min and for 15 min. The cleared lysate was applied onto QIAGEN tip-100 or -500 equilibrated with 4 ml/10 ml buffer QBT (50 mM MOPS, pH 7.0, 750 mM NaCl, 15% volume per volume (v/v) isopropanol, 0.15% v/v Triton® X-100) and allowed to enter the resin by gravity flow. The tip was washed twice with 10 ml/30 ml buffer QC (50 mM MOPS, pH 7.0, 1 M NaCl, 15% v/v isopropanol) and the DNA was eluted with 5 ml/15 ml buffer QF (50 mM Tris-HCl, pH 8.5, 1.25 M NaCl, 15% v/v isopropanol). To precipitate the DNA 0.7 volumes of isopropanol were added and the mix centrifuged at 12.000 rpm for 30 min at 4ºC. The DNA pellet was washed with 2 ml of 70% ethanol and centrifuged at 20.000 rpm for 10 min. The supernatant was discarded; the DNA pellet was air-dried for 10 min and resuspended in 100-1000 µl EB buffer (10 mM Tris-HCl, pH 8.5), TE buffer (10 mM Tris-HCl, 1 mM EDTA, pH 8.0) or ddH_2O.

2.1.5. Quantification of nucleic acids

A NanoDrop® ND-1000 spectrophotometer (NanoDrop Technologies) was used to determine the amount of DNA or RNA. This method is based on the measurement of the absorbance of nucleic acids at 260 nm (A260). Additionally, the ratio of absorbance of 260 to 280 nm (A260/A280) between nucleic acids and for instance proteins gives an estimation of the purity of the solution, and should ideally lie between 1.8 and 2.0 (neutral pH).

2.1.6. Analytical agarose gel electrophoresis

DNA or RNA was visualized via agarose gel electrophoresis. To prepare an agarose gel of an appropriate concentration (w/v) agarose was boiled in 1x TAE buffer (0.4 M Tris acetate, 10 mM EDTA, pH 8.3), chilled to room temperature, ethidium bromide (EtBr; 0.5 µg/ml) was added and the mixture was poured into a gel cast with a comb to polymerize. An aliquot of DNA was mixed 1:5 with a 5x gel loading dye (2.5% glycerol or Ficoll 400, 11 mM EDTA, 3.3 mM Tris-HCl, 0.017% SDS, 0.015% Bromophenol Blue, pH 8.0; Bioline) to facilitate sample loading and to monitor the migration rate of DNA fragments and electrophoresed on the gel next to a 1 kb or 100 bp DNA-ladder (HyperLadder™ I or V; Bioline) at 50-150 V for 0.5-1 h. A UV transilluminator (Uvitec) was used to excite and visualize EtBr, which intercalates into double-stranded DNA and fluoresces at 260 nm.

2.1.7. Restriction enzyme digest

Restriction enzymes (RE) are endo-deoxyribonucleases that recognize specific DNA sequences, and digest double-stranded DNA by cleaving two phosphodiester bonds and producing cohesive or blunt ends. This produces a characteristic pattern of DNA fragments of different sizes and can be used to create diagnostic plasmid maps or for cloning purposes. Each RE requires appropriate conditions such as temperature and buffers containing following chemicals at specific concentrations Tris-HCL, NaCl, $MgCl_2$, magnesium acetate, potassium acetate, 2-β-mercaptoethanol, 1.4-dithiothreitol (DTT), 1.4-dithioerythritol (DTE) at a specific pH. Enzymes used in this project were mostly obtained from Promega, New England Biolabs or Gibco BRL.

For digestion DNA was mixed with 2 µl of 10x buffer, 2 µl of BSA, and 1 unit of enzyme per µg DNA in a final volume of 20 µl of ddH_2O. The mixture was quickly spun in a table centrifuge and incubated at an appropriate temperature (for most enzymes 37°C) for a minimum of 2 h. Enzymes were heat-inactivated if possible or removed via phenol-chloroform extraction or another purification method (see below). The digest was examined via agarose gel electrophoresis.

2.1.8. Polymerase chain reaction (PCR)

To amplify specific DNA sequences for diagnostic purposes or cloning PCR was performed using BIOTAQ™ (Bioline) reagents for most reactions (unless otherwise stated). A master mix of a PCR reaction was prepared per primer pair or DNA, if several samples were amplified. Each sample contained 1.5-5 mM $MgCl_2$, 1x NH_4 PCR buffer (160 mM $(NH_4)_2SO_4$, 670 mM Tris-HCl pH 8.8, 0.1% stabilizer), 200 µM dNTPs, 25 nmol primers (Operon), 2.5 units DNA polymerase and 50-100 ng DNA templates in a final volume of 25 µl ddH_2O. Positive and negative controls were included in the experiment. The samples were vortexed, spun and the reaction was run in a PCR thermo cycler under conditions summarized in table 2.1. The PCR products were analyzed via agarose gel electrophoresis.

	BIOTAQ™ (Bioline)		**GoTaq® (Promega)**	
STEP	**TEMPERATURE**	**TIME**	**TEMPERATURE**	**TIME**
Heated lid	104°C		104°C	
Initial template denaturation (and polymerase activation)	94°C	3 min	94°C	5 min
3-step cycling				
Denaturation	94°C	0.5-1 min	94°C	0.5-1 min
Annealing	50-70°C*	0.5-1 min	50-70°C*	0.5-1 min
Extension	72°C	1-4 min**	72°C	1-4 min**
Number of cycles	29-40		29-40	
Final extension	72°C	10 min	72°C	5 min

Table 2.1. PCR conditions.
* Annealing temperature was selected 5ºC below the melting temperature (Tm) of the primers;
** Extension time was set to 1 min/1 kb.

2.1.9. Purification of PCR products and RE digests

The QIAquick® PCR purification Kit (Qiagen) was used to quickly purify PCR reactions and RE digests on column following the manufacturer's instructions. It is based on the same principle as the mini prep (see section 2.1.3) utilizing a silica-membrane to bind and purify nucleic acids. All centrifugation steps were carried out at 13,000 rpm for 1 min at room temperature.

The DNA solution was mixed with 5 volumes of binding buffer PBI (guanidine hydrochloride and isopropanol) and bound on a silica-gel membrane of the spin-column by centrifugation. The column was washed with 750 µl of ethanol-containing buffer PE and dried in an additional spin. To elute the DNA 30 µl EB buffer (10 mM Tris-HCl, pH 8.5) or ddH_2O were applied onto the column, incubated for 1 min at room temperature and centrifuged.

2.1.10. Gel extraction of DNA fragments

Plasmid fragments of specific size derived from digests or PCR reactions were isolated via gel extraction using the QIAquick® Gel Extraction Kit (Qiagen) following the manufacturer's instructions. It is based on the same principle as the mini prep (see section 2.1.3) utilizing a silica-membrane to bind and purify nucleic acids. All centrifugation steps were carried out at 13,000 rpm for 1 min at room temperature.

DNA was electrophoretically separated on an agarose gel. The band of correct size was cut out from the gel under UV-light using a sterile scalpel. To extract the DNA from the agarose gel band it was dissolved in 3 volumes per weight (v/w) of the provided buffer QG (containing guanidine isothiocyanate) for approximately 10 min at 65°C. The DNA was then bound to a silica-gel membrane in a spin-column by centrifugation. The column was washed with 750 µl buffer PE and the concentrated purified DNA was eluted with EB buffer (10 mM Tris-HCl, pH 8.5) or ddH_2O by centrifugation after an incubation of 1 min at room temperature.

2.1.11. Ethanol precipitation of nucleic acids

To purify and sterilize DNA I used the sodium acetate method. The DNA solution was mixed with 1/10 of its volume with 3 M NaOAc (sodium acetate), pH 5.2 and incubated for at least 1 h at -20ºC. The salt-DNA mixture was spun at 13,000 rpm for 15 min at 4°C. The pellet was washed twice with 1 ml 70% ethanol to remove the salts. The pellet was air dried and resuspended in an appropriate volume of sterile Tris-EDTA (TE) buffer or ddH_2O and stored at -20°C.

2.1.12. Phenol-chloroform extraction

In order to purify DNA from other organic substances such as lipids and proteins for instance after a RE digest phenol-chloroform extraction was performed. It is based on the properties of phenol to dissolve lipids and proteins, whereas DNA solubilises in an aqueous solution and so can be separated.

The DNA solution was mixed with an equal volume of phenol:chloroform: isoamylalcohol-solution pH 7.0 (25:24:1; Sigma) in a fume hood. The mixture was centrifuged at 13,000 rpm for 3 min at room temperature. The upper aqueous layer containing the DNA was transferred into a new tube and the lower phase was discarded. This step was repeated twice and subsequently ethanol precipitation (as described above) was performed.

2.1.13. Alkaline phosphatase treatment

In order to prevent re-circularisation of the plasmid after linearization with RE it was treated with Shrimp Alkaline phosphatase (AP). This enzyme removes the phosphate groups from the 5'-end and thus prevents plasmid re-circulation. 4 µl AP buffer, 1 µl AP (1 unit/ 1 µg DNA, Roche) and 5 µl ddH_2O were added to the purified digest (30 µl) and incubated for 1 h at 37ºC. The AP was irreversibly deactivated by incubation for 15 min at 65°C.

2.1.14. Plasmid ligation

100-200 ng linearized and AP-treated plasmid backbone were mixed with insert DNA in a molar ratio of 1:1, 1:2 or 1:3 (estimated by agarose gel electrophoresis), 2 µl (2U) T4 DNA ligase (Roche) and 4 µl ligation buffer (660 mM Tris-HCl, pH 7.8, 50 mM $MgCl_2$, 10mM DTT and 10 mM ATP; Roche) in a total volume of 20 µl. The mixture was incubated overnight at 15°C. An aliquot of the ligation mixture was used for the transformation of competent *E. coli.*

2.1.15. Blue-white screen of recombinant bacterial colonies

The blue-white screen allows the detection of successful ligations transformed into bacteria through the colour of the bacterial colony. It is based on the principle that the

β-galactosidase (β-gal) enzyme encoded by the LacZ gene can be split into two non-functional peptides the α and Ω subunits. Most *E.coli* strains used in the lab encode only the Ω subunits and the vectors used in this screen contain the α subunit with an internal multiple cloning site (MCS), into which the insert is ligated. The colourless modified galactose sugar X-gal, which is metabolized into the characteristic insoluble blue product 5-bromo-4 chloroindole, is used as an indicator. Additionally isopropyl β-D-1-thiogalactopyranoside (IPTG), an inducer of the transcription of the Ω subunit from the Lac operon in the bacterial chromosome, is used as an enhancer. When the ligated vector contains an insert in the MCS, the α subunit is not correctly expressed, no functional β-gal enzyme can be assembled, X-gal is not metabolized and hence the bacterial colonies remain white. If the vector is empty the colonies turn blue.

E.coli were transformed with the ligation mixture and grown on LB agar plates coated with 2 mg X-gal and 100 µM of IPTG overnight at 37ºC, and the colour development was examined on the following day.

2.1.16. Micropreps

Micropreps were used for rapid screening of a large number of bacterial colonies for the presence of recombinant plasmids containing inserts (protocol modified after (Sambrook et al., 1989)). In principle bacterial colonies are lysed in an alkaline solution and directly electrophoresed on a denaturing agarose gel.

Bacterial colonies were picked from the agar plate and incubated in 3 ml LB medium containing a selective antibiotic overnight at 37ºC in a shaker at 250 rpm. 10 µl of the bacterial culture were mixed with 5 µl of protoplaster buffer (30 mM Tris-Cl pH 8.0, 5 mM Na_2EDTA, 50 mM NaCl, 20% sucrose, 50 µg/µl RNAse A and 50 µg/µl lysozyme), vortexed and incubated for 10 min at room temperature. 5 µl of lysis solution (1x TAE buffer, 2% SDS, 5% sucrose, bromophenol blue) were loaded into each slot of a 1% agarose gel containing 0.05% SDS and the bacterial lysate was added. As a control (preferably a bacterial colony containing) an empty uncut non-recombinant plasmid was used. The gel was initially electrophoresed for 15 min at 40 V and then for approximately 90 min at 100 V and examined under a UV transilluminator.

2.1.17. Sequencing

DNA sequencing was delegated to the Scientific Support Service at the Wolfson Institute for Biomedical Research at UCL. Samples were prepared with a concentration of 0.1 µg/1 µl of template plasmid DNA per sequencing reaction in a total volume of 10 µl ddH_2O. Standard primers were provided by the Sequencing Service (summarized in Table 2.2). Custom primers were provided at a concentration of 5 pmoles/ 1 µl.

The sequencing results were analysed using the 4 Peaks software 1.5 (Mek&Tosj), DNASTAR Lasergene 7.2.1 software and the BLAST search against whole mouse genome option on NCBI/BLAST (http://blast.ncbi.nlm.nih.gov/Blast.cgi).

STANDARD PRIMERS	SEQUENCE (5' → 3')	TM (ºC)
T3	AAT TAA CCC TCA CTA AAG GG	56.23
T7	GTA ATA CGA CTC ACT ATA GGG C	56.02
Sp6	ATT TAG GTG ACA CTA TAG	42.58
M13-40	GTT TTC CCA GTC ACG AC	56.14
M13 Reverse	GGA AAC AGC TAT GAC CAT G	58.01
Universal T7	TAA TAC GAC TCA CTA TAG GG	50.83

Table 2.2. Standard sequencing primers.
Primers were provided by the Scientific Support Service at the Wolfson Institute for Biomedical Research at UCL.

2.1.18. Genomic DNA extraction

Cultured cells were rinsed three times with PBS and PK lysis buffer (10 mM Tris pH 8, 10 mM NaCl, 10 mM EDTA pH 8, 1% SDS) was added. After incubation for 5 min on wet ice the cells were scraped off the plate using a cell scraper and the cell suspension was transferred into an Eppendorf tube. Proteinase K was added at a final concentration of 0.5 mg/ml and the digests were incubated overnight at 55ºC until the solution was clear. The gDNA was then extracted using the phenol:chloroform procedure (as described in section 2.1.12).

2.2. RNA methods

2.2.1. Isolation of RNA from tissue and cell samples

2.2.1.1. Isolation of RNA with the RNeasy® Plus Mini Kit (Qiagen)

The RNeasy® Plus Mini Kit (Qiagen) was used to extract RNA and proteins in parallel from animal tissues and cells following manufacturer's instructions. In principle, guanidine isothiocyanate (GITC)-containing lysis buffer and ethanol are added to the sample to create conditions that promote selective binding of RNA to the RNeasy® silica-gel membrane, contaminants are efficiently washed away, and high quality RNA is eluted in water. In parallel proteins may be recovered using acetone precipitation. All steps were carried out quickly at room temperature under RNAse-free conditions unless otherwise stated. All centrifugation steps were performed at 13,000 rpm in a micro-centrifuge at room temperature (20-25ºC).

For sample preparation DRGs were collected, washed with phosphate-buffered saline (PBS; 137 mM NaCl, 2.7 mM KCl, 4.3 mM Na_2HPO_4, 1.47 mM KH_2PO_4, pH 7.4) and either snap frozen on dry ice and stored at -80ºC or directly used for RNA extraction. Cultured cells were washed with PBS and directly lysed on the plate with 350 µl RLT buffer (contains GITC and 10 µl/1 ml 14.3 M β-mercaptoethanol (β-ME)) collected in Eppendorf tubes and stored at -20ºC or used directly for RNA extraction. The lysed tissue or cell samples were homogenized by passing the lysate at least 10 times through a 20-gauge needle fitted onto an RNAse-free syringe. The sample lysate was spun for 3 min and the cleared lysate was transferred to a gDNA Eliminator spin column and centrifuged for 30 sec. The flow-through was mixed with 1 volume of 70% ethanol and applied to a silica-gel-membrane containing RNeasy® spin column and centrifuged for 15 sec. The flow-through was kept for protein extraction (see below). The spin column was first washed with 1 volume of buffer RW1 (containing GITC and ethanol) and then with 500 µl buffer RPE by centrifugation for 15 sec each. To dry the silica-gel membrane it was spun for 2 min. RNA was eluted 2 times by centrifugation for 15 sec with 15 µl RNAse-free ddH_2O. One µl of RNAse inhibitor (RNAsin, Promega) was added and the riboprobe was stored at -20ºC.

Acetone precipitation of protein from buffer RLT lysates

Four volumes of ice-cold acetone were added to the flow-through of the RNeasy spin column, incubated for 30 min on ice and centrifuged for 10 min at 4ºC. The pellet was air-dried and resuspended in SDS-PAGE loading buffer, heated for 10 min at 100ºC and stored at -20ºC.

2.2.1.2. Isolation of RNA with the RNeasy® Lipid Tissue Kit (Qiagen)

At Merck Serono in Geneva the RNeasy® Lipid Tissue Kit (Qiagen) was used to extract RNA from murine embryonic DRGs. All centrifugation steps were performed at 8000 x g at room temperature unless stated otherwise. Briefly, the DRG samples were unfrozen on wet ice and 1 ml QIAzol Lysis Reagent was added immediately. The tissue was disrupted with the Precellys®24 homogenizer and the samples were incubated for 5 min at room temperature. 200 µl chloroform were added and the samples were vigorously shaken for 15 sec before another incubation at room temperature for 2-3 min followed by a centrifugation at 12.000 x g for 15 min at 4ºC. The upper, aqueous phase was transferred to a new tube, 1 volume of 70% ethanol was added and the sample was mixed. The solution was applied onto a spin column, centrifuged for 15 sec and the flow through discarded. In order to avoid genomic DNA contamination a DNAse I digest was performed using an RNAse-free DNAse Set (Qiagen). 350 µl supplied buffer RW1 were added to the spin column, which was centrifuged for 15 sec. 10 µl DNAse I stock solution were mixed with 70 µl buffer RDD and directly added onto the spin column membrane and incubated for 15 min at room temperature. The column was washed sequentially with 350 µl buffer RW1 and 500 µl buffer RPE and the membrane was dried by centrifugation for 1 min. For RNA elution 30 µl of RNAse-free water were added onto the column and centrifuged for 15 sec. The elution was repeated with the eluted 30 µl to concentrate the RNA. mRNA purity (260/280 ratio) and concentration were measured using the NanoDrop. The RNA was stored at –80ºC for further use.

2.2.2. Test of RNA integrity

The integrity of ribosomal RNA (rRNA) was measured using the RNA 6000 Nano LabChip® Kit (Agilent) on an Agilent 2100 BioAnalyzer® (Agilent Biotechnologies) as an indicator for total RNA integrity in the samples. To prepare the multi-well chip 65 µl

of filtered gel matrix and 1 µl of dye were mixed and centrifuged at 13,000 x g for 10 min. Nine µl of this matrix-dye solution were added to each well of the chip and pressed through with a 1 ml-piston for 30 sec. Then 5 µl of Nano Marker were added in all wells of the chip. Finally 2 µl of the RNA samples were heated for 2 min at 70°C and added to the wells as well as 1 µl of the ladder. The chip was then vortexed for 1 min at 2400 rpm and placed into the BioAnalyzer to start the analysis. The integrity of the RNA is indicated by the RIN values of the rRNA (18S and 28S rRNA) and the electropherogram, which should reveal two distinctive peaks or bands of the rRNA. Only RIN values between 4-10 are acceptable.

2.2.3. Reverse transcription (RT) of mRNA into cDNA

2.2.3.1. RT using the QuantiTect® RT Kit (Qiagen)

The QuantiTect® RT Kit (Qiagen) was used to transcribe mRNA into cDNA following manufacturer's instructions. It utilizes a transcriptase mix of Omniscript™ and Sensiscript™ Reverse Transcriptases and an optimized blend of oligo-dT and random primers, which allows highly efficient cDNA transcription from all regions of RNA transcripts and even 5' regions. All reactions were assembled on ice. To eliminate residual genomic DNA in the RNA sample, 1 µg of RNA and 2 µl of the 7x gDNA wipe-out buffer were mixed in a total volume of 14 µl RNAse-free ddH_2O, incubated for 2 min at 42ºC and then cooled on ice. For the reverse transcription reaction the entire genomic elimination reaction was mixed with 1 µl transcriptase, 4 µl 5x RT buffer and 1 µl RT primer mix and incubated for 20 min at 42ºC in a PCR cycler. The transcriptase was inactivated by heating at 95ºC for 3 min. The total cDNA concentration was adjusted to 10 ng/µl with RNAse-free ddH_2O and stored at -20ºC.

2.2.3.2. RT using the iScript™ cDNA Synthesis Kit (BioRad)

At Merck Serono, Geneva, the mRNA was reverse transcribed into cDNA using the iScript™cDNA Synthesis Kit (BioRad). iScript™ is a modified MMLV-derived reverse transcriptase. Briefly, 1x reaction mix containing RNAse inhibitor and a blend of oligo (dT) and random hexamer primers, 2 µl reverse transcriptase and 1 µg mRNA were mixed in a total volume of 30 µl ddH_2O. The mix was incubated for 5 min at 25ºC, 30 min at 42ºC, and 5 min at 85ºC in a PCR thermo cycler. The reaction was

adjusted with RNAse-free ddH_2O to a concentration of 1 µg/100 µl total cDNA and stored at -20ºC.

2.2.4. Quantitative RT real-time PCR (qPCR) with SYBR Green

For gene expression analysis the QuantiFast® SYBR Green PCR Kit (Qiagen) was used. It contains a master mix of HotStarTaq Plus DNA Polymerase, SYBR Green I, ROX as a passive reference dye, dNTPs and an optimized QIAGEN PCR buffer system, which provides stringent primer annealing conditions and hence increased PCR specificity. It also contains Q-Bond, which increases the affinity of Taq DNA polymerases for short single-stranded DNA and reduces the time required for primer annealing.

A master mix was prepared per primer pair and combined with the cDNA on a 96-well-plate at room temperature. Each reaction contained 6.25 µl 2x SYBR Green PCR Master mix, 1.25 µl 10x QuantiTect® Primer Assay mix, 1.5 µl (~15 ng) template cDNA and 3.5 µl ddH_2O in a total volume of 12.5 µl.

All primers were obtained as QuantiTect® Primer Assays (Qiagen) unless otherwise stated. A proprietary algorithm was used to design these primers, which only amplify RNA sequences (overlap a splice site). The primers were all bioinformatically validated and also randomly tested in qRT-PCR experiments. They were only selected, when the criteria of high sensitivity, efficiency and specificity such as a single peak in the melting curve analysis and no primer dimers in the no-template control (NTC) etc. were met.

The qPCR was run in duplicates in the 7500 Fast Real-Time PCR System (Applied Biosystems) under following PCR conditions: stage 1 (initial activation step): 95ºC for 5 min, stage 2: 40 cycles (10 sec at 95ºC (denaturation) and 30 sec at 60ºC (annealing and extension)), stage 3 (dissociation curves): 15 sec at 95ºC, 15 sec at 60ºC, 15 sec at 95ºC with a heated lid at 105ºC. Data acquisition was performed during the combined annealing and extension step. PCR products were examined by agarose gel electrophoresis.

For data analysis the 7500 software SDS v 2.0.1 (Applied Biosystems) was used to adjust the baseline measured between cycles 3 and 15 and to set the threshold to ΔRn 0.1. Dissociation curves of each reaction were examined for a single product peak and no primer dimer formation otherwise data were omitted from the analysis. In

ambiguous cases products were examined for specificity of the reaction (single product band) via gel electrophoresis. In ideal cases no amplification was observed in the non-targeting control (NTC) samples containing ddH_2O instead of template DNA or in some cases the shift in the C_T value or in the melting curve between experimental and control sample was sufficient to distinguish between specific and non-specific signals. C_T values were then extracted and analysed with Microsoft® Excel®. Data were normalized to an endogenous reference gene (ΔC_T) and compared to an untreated or mock treated control sample ($\Delta\Delta C_T$) (Livak and Schmittgen, 2001). The results were displayed as percentage of expression relative to the control sample. Statistical analysis was performed using Prism 4 (GraphPad Software) as described in section 2.7.

2.3. Protein methods

2.3.1. Cell lysis

Cultured cells (5-10 x 10^6) were washed twice with ice-cold PBS. Depending on the cell amount they were either collected via trypsinization or directly scraped from the plate in PBS and collected in a 15 ml falcon tube. The cell suspension was centrifuged for 4 min at 1500 rpm and the supernatant was aspirated. The cell pellet was dissolved in 1-2 ml of lysis buffer (50 mM Tris pH 7.5, 150 mM $NaCl_2$, 1% Triton x-100, 200 µl 50x serine and cysteine proteinase inhibitor cocktail (Complete EDTA-free tablets; Roche), 2 mM of the PTP inhibitor Sodium Orthovanadate (BioLabs) and incubated on ice for 30 min. The lysate was centrifuged at 13,000 rpm for 30 min at 4ºC and the supernatant was saved and frozen at -20ºC.

2.3.2. Protein quantification

To measure the protein amount in lysates the Bradford assay (Bio-Rad) was used. It is a colorimetric method based on the Coomassie dye, which binds through ionic interactions and non-covalent bonds to non-polar amino acids in the polypeptides. Upon binding of Coomassie dye to proteins in an acidic medium its absorption maximum shifts from 465 to 595 nm causing a colour change from brown to blue. Relative protein concentrations are estimated by comparison of the absorbance of the sample to the absorbance obtained from a series of standard protein dilutions (Bradford, 1976).

A protein standard consisting of 5 serial dilutions of bovine serum albumin (BSA) ranging from 1.5 to 0.1 mg/ml in lysis buffer including a blank (no protein) was prepared. Experimental protein samples were diluted 1:2 or 1:5 in lysis buffer. 10 µl of sample or standard were mixed with 200 µl of Bradford reagent (Coomassie® Brilliant Blue G-250, methanol, phosphoric acid) in a well of a 96-well-plate in duplicates. During incubation at 37ºC for 10 min the reagent changed colour from brown to blue. The absorbance was read at 595 nm on a micro-plate-reader (Dynex Revelation 4.21, Dynex Technology). For data analysis all measurements were corrected for blank and a plot of standard vs. concentration prepared. The slope was used to estimate the protein concentration of the unknown samples.

2.3.3. Western blotting/ Immunoblotting

In principle the denaturing one dimensional (1-D) polyacrylamide gel electrophoresis (PAGE) separates proteins according to their molecular weight. The proteins are subsequently electrophoretically eluted from the gel onto a membrane and the proteins of interest are detected with specific antibodies in an immuno assay. A denaturing Tris-Glycine system and a semi-dry blotting system from Bio-Rad Laboratories were used.

2.3.3.1. Sample preparation

Protein lysates were mixed in a 1:1 ratio with 2x Laemmli buffer (4% sodium-dodecyl-sulphate (SDS), 20% glycerol, 10% β-ME, 0.004% bromophenol blue, 0.125 M Tris-HCl, pH 6.8; Sigma), heated at 100ºC for 5 min to denature the proteins and stored on ice to be loaded on the gel.

2.3.3.2. SDS-polyacrylamide gel electrophoresis (PAGE)

Eight and 10% polyacrylamide gels consisting of a stacking and a resolving gel were used. To prepare the separating gel 3.3 ml of 30% acrylamide/bis-acrylamide (29:1) solution (Bio-Rad) were mixed with 2.5 ml gel buffer (1.5 M Tris-HCL, pH of 8.8), 4.1 ml ddH_2O, 100 µl 10%-SDS and finally 50 µl 10%-amonium persulfate (APS, Sigma) and 5 µl TEMED (N,N,N',N'-Tetrame-thylethylene-diamine, Sigma). The mix was poured into a vertical gel mould, covered with isobutanol and left to polymerize for 30 min. When set, the isobutanol was poured off and the mould was washed with

ddH_2O. A 1% stacking gel consisting of 650 µl 30% acrylamide/bis-acrylamide solution (Bio-Rad), 1.25 ml gel buffer (0.5 M Tris-HCL, pH of 8.8), 3 ml ddH_2O, 50 µl 10% SDS, 25 µl 10% APS and 2.5 µl TEMED was poured onto the resolving gel, a multi-well-comb was inserted and the gel left to polymerize for 20 min. 15 µl protein ladder (Precision Plus Protein™, BioRad) and protein samples were then loaded onto the gel. It was placed into a running chamber filled with running buffer (25 mM Tris-base, 192 mM glycine, 10% SDS, ddH_2O) and electrophoresed first at 70 V until the samples reached the resolving gel and then at 100-200 V for 1-1 ½ h.

2.3.3.3. Transfer of proteins onto PVDF membranes

After electrophoreses the gel was equilibrated for 15-30 min in transfer buffer (39 mM glycine, 48 mM Tris-Base, 0.13 mM SDS, ddH_2O, 20% methanol). Meanwhile the polyvinylidene difluoride (PVDF) membrane (Immobilon Transfer Membrane; Millipore) was activated in methanol for 1 min, washed in ddH_2O for 2 min and equilibrated in transfer buffer for 10 min. 2 Whatman filter papers were soaked in transfer buffer and a transfer sandwich was assembled by placing the gel onto the membrane between the two Whatman filter papers. The transfer occurred at 22 V for 1 h towards the positive electrode in a semi-dry electroblotting apparatus (TransBlot SD Semi Dry transfer cell, Bio-Rad).

2.3.3.4. Immunoblotting

Following the transfer the membrane was incubated in methanol for 10 sec and dried for 15 min at room temperature to enhance the adsorption of the proteins to the PVDF polymer. The membrane was again wet in methanol for 5 min and incubated in blocking solution (5% Milk Powder (Waitrose or Tesco), TBST buffer (50 mM Tris, 150 mM NaCl, 0.2% Tween® 20, Sigma) for 1h with gentle agitation on a shaker at room temperature to block non-specific binding sites. The membrane was washed 2 times 5 min in TBST and incubated for 1 h at room temperature or overnight on a roller at 4ºC in 5%-milk-TBST solution containing monoclonal primary antibodies or in 5%-BSA fraction V-TBST solution containing polyclonal primary antibodies (Table 2.3).

2.3.3.5. Detection of antibodies

The membrane was washed 3 times each 10 min in TBST and incubated in 5%-milk-TBST solution containing the secondary IgG horseradish peroxidase (HRP) conjugated antibody (Table 2.4) with gentle agitation for 1-2 h at room temperature. The membrane was washed once again and the antibodies were detected with ECL Plus Western Blotting Detection System (Amersham Biosciences), an Enhanced Chemiluminescence (ECL) method. In principle chemiluminescence is the emission of light resulting from the release of energy from a substance in an excited state caused by a chemical reaction. The chemical reaction is an HRP/Hydrogen Peroxide catalyzed oxidation of luminol, a cyclic Diacylhydrazides, in alkaline conditions, resulting in light emission in the presence of chemical enhancers such as phenols. The membrane was incubated for 5 min with ECL reagent and wrapped in saran foil followed by exposure of a light sensitive autoradiography film (Chemiluminescence BioMax Light Film, KODAK) placed into an x-ray film cassette in the dark. The films were developed in the Compact X4 Automatic X-ray Film Processor (Xograph Healthcare Ltd).

2.3.3.6. Stripping membranes for reprobing

In order to apply a further primary antibody on the same blot, the membrane was stripped after detection. For this the membrane was wet in methanol for 10 sec and incubated in stripping buffer (100 mM β-ME, 2% SDS, 62.5 mM Tris-HCl pH 6.7) with occasional agitation for 30-45 min at 50-60ºC. It was washed 4 times each 5 min with TBST and used for further immunoblotting as described above beginning with the blocking step.

2.3.3.7. Quantitative densitometry analysis

Quantitative western blotting analysis was performed on technical replicates of blots from two or three independent experiments. Briefly, developed films were scanned with the GS-800 Calibrated Densitometer (Bio-Rad) using Quantity One® Software (version 4.6.3, Bio-Rad). For analysis of protein signals the Volume Rectangle Tool of the Quantity One® Software with equal space areas were used to quantify signal intensity of specific protein bands. The volume values, reduced by global background, are the sum of the intensities of the pixels inside the volume boundary multiplied by the area of a

single pixel (in mm^2). The data were exported to Microsoft® Excel® and protein expression was normalized to the expression of the HKG β-tubulin or to the total unphosphorylated protein. Ratios of normalized volumes were calculated in respect to the mock treated or wild type control (= 1) and standard errors (SE) were determined.

2.3.4. Coomassie Brilliant Blue staining of PAGE gels

Polypeptides separated by SDS-PAGE gels can be stained with Coomassie Brilliant Blue R250, a dye that binds through ionic interactions and non-covalent bonds to non-polar amino acids and thus visualizes the polypeptides. This procedure was used to analyse gels for complete electrophoretic transfer onto membranes and also to estimate total protein amounts in the samples.

After electrophoreses the SDS-PAGE gel was submerged in a Coomassie-staining and fixation solution (0.25% Coomassie Brilliant Blue R250 (Invitrogen), 40% methanol, 10% acetic acid) with gentle agitation for 30 min at room temperature. To remove background it was incubated in coomassie-destaining solution (40% methanol, 10% acetic acid) with gentle agitation and frequent changes of solution for up to 24 h. The destained gel was scanned with the GS-800 Calibrated Densitometer (Bio-Rad) and stored in ddH_2O.

2.3.5. Primary and secondary antibodies

Primary and secondary antibodies were commercially obtained or kindly provided by collaborators as listed in tables 2.3 and 2.4. Primary Trk and pTrk antibodies were tested in WB experiments for their specificity (Appendix, Figures 1 and 2).

PRIMARY ANTIBODY	SPECIES	SUPPLIER (Cat. No.)	EPITOPE and REFERENCES	DILUTION IHC/ WB
TrkA	Rabbit, polyclonal	Upstate (# 06-574)	ECD of TrkA protein (Clary et al., 1994, Kramer et al., 2006)	1:500/ 1:5000
TrkB	Goat, polyclonal	R&D (AF1494)	ECD of TrkB protein (Komori et al., 2008)	1:75/ 1:3000
TrkC	Goat, polyclonal	R&D (AF1404)	ECD of TrkC protein (Nakamura et al., 2008, Zhang et al., 2010)	1:75/ 1:3000
panTrk (C-14)	Rabbit, polyclonal	SC (sc-139)	ICD of all Trk proteins (Lo et al., 2005, Nikoletopoulou et al., 2010)	1:125/ 1:1000
pTrkA (Y496) (E-6)	Mouse, monoclonal	SC (sc-8058)	Phosphorylated Y496 of all TrkA proteins (Jullien et al., 2003)	1:1000 (WB)
pTrkA (Y674/Y675)/ TrkB (Y706/Y707)	Rabbit, monoclonal	CS (# 4621)	Phosphorylated Y674/675 of TrkA and Y706/707 of TrkB and TrkC (Lo et al., 2005)	1:1000 (WB)
pTrkA (Y490)	Rabbit, polyclonal	CS (# 9141)	Phosphorylated Y490 of all Trk proteins (Lo et al., 2005, Yang et al., 2006)	1:1000 (WB)
pTrkA (Y794) (= pTrk*)	Rabbit, polyclonal	M. Chao/ S.Harroch	Phosphorylated Y794 of all Trk proteins, (Rajagopal et al., 2004)	1:1000 (WB)
pTrkB (Y816) (= pTrk)**	Rabbit, polyclonal	M. Chao/ S.Harroch	Phosphorylated Y816 of all Trk proteins, (Arevalo et al., 2006).	1:1000 (WB)
pAkt (S473) (D9E) XP™	Rabbit, monoclonal	CS (# 4060)	Phosphorylated S473 of Akt protein (Lo et al., 2005, Mandai et al., 2009)	1:2000 (WB)
p44/42 MAPK	Rabbit, polyclonal	CS (# 9102)	Total p44/42 MAP kinase (Erk1/Erk2) protein (Lo et al., 2005, Mandai et al., 2009)	1:1000 (WB)
p44/42 MAPK (T202/Y204) (E10)	Mouse, monoclonal	CS (# 4060)	p44/42 MAPK (Erk1/Erk2) when dually phosphorylated at T202 and Y204/T815 and Y187 (Lo et al., 2005, Mandai et al., 2009)	1:2000 (WB)
Stat3 (124H6)	Mouse, monoclonal	CS (# 9139)	Total Stat3 protein (Zhang et al., 2007b, Miranda et al., 2010)	1:1000 (WB)
pStat3 (Y705) (M6C6)	Mouse, monoclonal	CS (# 4113)	Phosphorylated Y705 of Stat3 protein (Zhang et al., 2007b, Miranda et al., 2010)	1:2000 (WB)
TU-20 (Tuj1)	Mouse, monoclonal	CI (MAB1637)	C-terminus of β III tubulin in neuronal processes (Vaegter et al., 2011)	1:150 (IHC)
β tubulin (H-235)	Rabbit, polyclonal	SC (sc-9104)	Amino acids 210-444 of β tubulin protein (Sacco et al., 2009)	1:5000 (WB)

Table 2.3. Primary antibodies used for ICC, IHC and WB.

CI stands for Chemicon® International, R&D for R&D Systems, SC for Santa Cruz Biotechnology, INC., CS for Cell Signaling Technology®, SA for Sigma-Aldrich®.

SECONDARY ANTIBODY	SPECIES	SUPPLIER (Cat. No.)	EPITOPE	DILUTION IHC/ WB
anti-mouse/goat/rabbit Immunoglobulins/ Biotinylated	Goat/rabbit, polyclonal	Dako Cytomation Denmark A/S	Mouse/rabbit or goat immunoglobulins of all classes	1:200/ 1:10000
anti-mouse/ goat/rabbit Immunoglobulins/HRP	Goat/rabbit, polyclonal	Dako Cytomation Denmark A/S	Mouse/rabbit or goat immunoglobulins of all classes	1:200/ 1:10000
anti-goat Alexa Fluor® 488	Donkey, polyclonal	Invitrogen® (A-11055)	goat immunoglobulins of all classes	1:100 (IHC)
FluoroLink™Cy™3 labelled streptavidin		Amersham Biosciences (PA43001)	Biotinylated antibodies	1:400 (IHC)

Table 2.4. Secondary antibodies and dyes used for ICC, IHC and WB.

2.4. Histology and cytology methods

2.4.1. Collection of mouse embryos

Wild type CD-1 mice were maintained and matings set up by the Western Laboratory at the Institute of Child Health. Detection of vaginal plugs was considered 0.5 days of gestation (E0.5). The mice and embryos were sacrificed at midday of E12.5, E13.5 and E14.5. Uteri were dissected and the embryos were immediately placed into Dulbecco's Modified Eagle Medium (DMEM, Sigma). Extra-embryonic tissue was removed and the embryos were either washed in PBS and fixed (section 2.4.2) or used for DRG dissections (section 2.5.3).

2.4.2. Sample tissue preparation and cryosectioning

For sample preparation the mouse embryos (E12.5-14.5) were fixed in 4%-paraform-aldehyde (PFA)-PBS solution overnight at 4ºC and cryoprotected by equilibration in an RNAse-free 20%-sucrose-PBS solution for 4-5 hours at room temperature. The embryos were embedded either in Cryo-M-bed O.C.T. embedding compound (Bright Instrument Co.), a formulation of water-soluble glycerols and resins, or in gelatine.

For embedding in O.C.T. embryos were briefly washed in PBS after cryoprotection and submerged in O.C.T. in a polystyrene beaker (cryomold), which was cooled in a pentane - dry ice-bath until fully frozen, which was indicated by its opaque colour, and stored at –80ºC.

For embedding in gelatin embryos were incubated in sucrose–gelatine solution (15% sucrose, 7.5% gelatine (from bovine skin, type B; Sigma), diethyl-pyrocarbonate (DEPC)-treated PBS) for 1 hour at 37ºC. They were placed into a fresh sucrose-gelatine solution in a petri dish and cooled until set. The embryos were cut out into appropriate blocks, placed onto thin cork pieces with a drop of O.C.T., immersed in isopentane pre-cooled to -80ºC (with liquid nitrogen) for 1 min and stored at -80ºC.

For sectioning the embryos were equilibrated to -20ºC and sectioned (11 μm) with a cryostat (Leica CM 1900 UV). Sections were thaw-mounted onto charged SuperFrost® Plus microscope slides (VWR) and stored at -20ºC.

2.4.3. *In situ* hybridization

In situ hybridization (ISH) is a technique used to visualize the location of DNA or RNA in cells. Probes, which are reverse complimentary or "anti-sense" to the nucleic acid sequence of interest, are labelled with chemical groups, which can be recognized by specific antibodies linked to reporter enzymes. The probes are hybridized under stringent conditions to the specimen and excess probes are removed with several washes. Antibodies linked to reporter enzymes recognize the label on the probes and can be detected by addition of substrates of the reporter enzymes such as chromophores or fluorophores.

The used protocol in this study is a modified version of published protocols (Alonso et al., 2004, Schaeren-Wiemers and Gerfin-Moser, 1993, Wilkinson and Nieto, 1993, Pringle et al., 1996). All materials were RNAse-free, solutions were prepared with RNAse-free chemicals and DEPC-treated reagents, which were all obtained from Roche unless otherwise stated.

2.4.3.1. Generation of template DNA

A transcription plasmid containing the cDNA of the gene to be analyzed was linearized with appropriate RE in order to obtain RNA probes (sense and anti-sense) of defined length. 10-20 μg of template DNA were digested in a total volume of 100 μl for 1-2 h at 37ºC and an aliquot was examined on an agarose gel. The digested template DNA was cleaned using the QIAquick® PCR purification Kit (Qiagen).

2.4.3.2. In vitro transcription of in situ riboprobes

The RNA-probe was transcribed using a specific phage RNA-polymerase, which anneals to and transcribes from promoters such as T3, T7 or SP6. For chromogenic ISH probes were labelled with digoxigenin (DIG) and for fluorescent ISH one of the probes was also labelled with fluorescein isothiocyanate (FITC).

The *in vitro* transcription reaction containing 2.5 µl of linearized template DNA (approx. 1 µg), 2 µl of 10x transcription buffer, 6 µl of 100 mM DTT, 2 µl of 10x DIG or FITC RNA labelling mix (10 mM each of dATP, dCTP, dGTP, 6.5 mM dUTP, 3.5 mM DIG-11-UTP or 3.5 mM FITC-12-UTP), 1 µl (20 U) RNAse Inhibitor (Bioline), 2 µl (20 U) of the appropriate RNA polymerase (SP6, T3 or T7) and ddH_2O in a final volume of 20 µl was set up at room temperature. The mixture was gently mixed and incubated for 2 h at 37ºC. An aliquot was examined by agarose gel electrophoresis using DEPC-treated gel-loading dye (50% glycerol, 1 mM EDTA pH 8.0, 0.25% bromphenol blue, 0.25% xylene cyanol FF).

The probe was cleaned from unincorporated nucleotides, which might increase background, by size exclusion chromatography using a resin-containing spin column (CHROMA SPIN™-1000 DEPC-H_2O Columns, BD Biosciences). The spin column was prepared by re-suspending the resin by inverting and drying via centrifugation in a 15 ml-falcon tube at 700 g for 5 min at 4°C. 40 µl DEPC-treated H_2O were added to 20 µl of the transcription reaction and the mix was loaded in the centre of the column, spun at 700 g for 5 min at 4°C and eluted into a centrifuge tube. 40 µl of 100 mM DTT and 1 µl RNase inhibitor were added to the probe, which was stored at -20°C. An aliquot was examined by agarose gel electrophoresis using a formaldehyde-loading dye.

2.4.3.3. Single chromogenic and fluorescent ISH

Single chromogenic and fluorescent ISH was performed on O.C.T. or gelatine sections. Frozen slides with O.C.T. sections were dried at room temperature, whereas slides with gelatine sections were washed in DEPC-treated PBS at 37ºC for 30 min before hybridization.

RNA probes were diluted 1:100 in pre-warmed (65ºC) hybridization buffer (1x "salts" (0.2 M NaCl, 5 mM EDTA, 10 mM Tris-HCl pH 7.5, 5 mM $NaH_2PO_4.2H_2O$, 5 mM Na_2HPO_4), 50% deionized formamide, 0.1 mg/ml yeast tRNA, 10% dextran

sulphate, 1x Denhardt's solution (1% Ficoll 400, 1% Polyvinylpyrrolidone (PVP), 1% BSA). Slides were incubated with 300 µl of this solution covered with a coverslip and incubated in a sealed humidified chamber filled with wash buffer (1x sodium citrate chloride (SSC) buffer (0.3 M sodium citrate, 3 M NaCl), 50% formamide, 0.1% Tween-20) at 65ºC overnight. After hybridisation the coverslips were removed and the slides were washed twice for 5 min at room temperature in MABT (100 mM maleic acid, 150 mM NaCl, 0.1% Tween-20, pH 7.5), followed by 2 stringency washes for 30 min at 65ºC in wash buffer in order to remove non-specifically bound probes. After a second round of washes in MABT the slides were incubated in blocking solution (2% blocking reagent (Roche), 10% heat inactivated sheep serum, MABT) in a humidified chamber for 1 h at room temperature.

For chromogenic detection of the probe alkaline phosphatase (AP)-conjugated-anti-DIG/FITC Fab fragments (Roche) were diluted 1:1500 or for fluorescent detection horseradish peroxidase (HRP)-conjugated anti-DIG/FITC Fab fragments (Roche) at a dilution of 1:500 in blocking solution were used. 500 µl of the antibody-solution were added per slide and incubated in a humidified chamber filled with water overnight at 4ºC. The excess antibodies were washed off with MABT for chromogenic detection or PBS-T (PBS with 0.1% Triton x 100) for fluorescent detection 3 times each for 10 min.

For chromogenic detection the slides were washed for 2 min at room temperature in developing buffer (100 mM Tris pH 9.8, 100 mM NaCl, 50 mM $MgCl_2$) and incubated with 500 µl per slide of developing buffer containing 5% polyvenylalcohol (PVA) and the AP substrates 0.12 mM NBT (Nitro-Blue Tetrazolium Chloride) and 0.11 mM BCIP (5-Bromo-4-Chloro-3'-Indolyphosphate p-Toluidine Salt). The purple colour was developed for at least 1 h to overnight. Reactions were stopped using tap water.

For fluorescent detection the Tyramide Signal Amplification (TSA) plus fluorescent system kit (PerkinElmer Life Sciences) was used. Briefly, HRP-conjugated antibodies against DIG or FITC-labelled probes are used to catalyze the deposition of a fluorophore-labelled tyramide amplification reagent, FITC or Tetramethylrhodamine, onto tissues. The fluorophore-labelled tyramide dissolved in dimethyl sulphoxide (DMSO, Sigma) was mixed 1:150 with amplification buffer (100 mM borate buffer pH 8.0 (borax and boric acid), 0.004% H_2O_2) prior to detection. 200 µl of this reagent mix were added per slide covered with a coverslip and incubated in the dark for 10 min

at room temperature. After a wash in PBS-T for 10 min the slides were examined under a fluorescent microscope.

The stained slides were finally washed with ddH_2O and dried. Chromogenically stained slides were mounted in VectaMount™ medium (Vector Laboratories), allowed to dry and stored at room temperature. Fluorescent slides were mounted in Vectashield® medium (Vector Laboratories) containing 4',6-diamidino-2-phenylindole (DAPI), a fluorescent stain that binds strongly to DNA and hence stains cell nuclei. The coverslip was sealed with nail polish and the slides were stored in the dark at cold temperatures.

2.4.3.4. Double fluorescent ISH on O.C.T. sections

In principal double fluorescent *in situ* hybridization (DFISH) was performed in the same way as single ISH, but instead of one probe two differently labelled (DIG and FITC) probes were hybridized to the specimen in the same step. After the first colour reaction the reporter enzyme was deactivated by incubation for 30 min in 3% H_2O_2-PBS solution before proceeding with the second colour reaction starting with the blocking step.

2.4.3. Fluorescent ICC and IHC/ Immunofluorescence

Immunocytochemistry (ICC) and immunohistochemistry (IHC) are techniques used to detect antigens on cells or in tissue sections respectively using specific antibodies. Fluorescent ICC and IHC are also referred to as immunofluorescence (IF). Primary and secondary antibodies and fluorophores used in the present study are summarized in tables 2.3 and 2.4.

For ICC the cells were fixed onto coverslips or directly on the plate with 4% PFA–PBS for 15 min, washed twice with PBS and stored in PBS containing 0.2% sodium azide at 4ºC. For IHC tissue sections were obtained and prepared as described in section 2.4.2. To prevent non-specific binding, the samples (cells or sections) were pre-blocked with 1% BSA/PBS/0.05% Triton X-100 for 15 min at room temperature. The primary antibody was diluted in 3% BSA/PBS/0.05% Triton and added to the section or coverslip. After incubation in a humidified chamber for 30-60 min, depending on the antibody, the slides or coverslips were washed 3 times each for 5 min with 0.1% BSA/PBS/0.05% Triton. The secondary biotin-conjugated antibody was diluted in 3%

BSA/PBS/0.25% Triton and added for 1h, followed by washes as above. The streptavidine-conjugated fluorophore was diluted in 3% BSA/PBS/0.25% Triton and incubated in the dark for 1 h at room temperature followed by washes as above. For double immunostaining the section or coverslip was blocked once again and the same procedure was carried out with a second primary antibody of an other species than the first primary antibody as described above. Slides or coverslips were mounted with Vectashield® medium containing DAPI. Pictures were taken and processed as described in section 2.6.

2.5. Cell culture methods

2.5.1. Maintenance of adherent cell lines

In this project two different cell lines were used, HEK 293T cells and 3T3 cells. HEK 293T cells are human embryonic kidney cells, which were transformed with an adenovirus. This particular variant contains the SV40 Large T-antigen, which allows the replication of plasmids containing the SV40 origin of replication (Graham et al., 1977). The 3T3 cell line is a standard fibroblast cell line originally obtained by Todaro and Green from Swiss mouse embryo tissue, that spontaneously immortalized during cultivation (Todaro and Green, 1963).

2.5.1.1. Culture of adherent cell lines

HEK 293T and NIH 3T3 cells were cultured in growth medium containing DMEM, 10% heat-inactivated fetal bovine serum (FBS; Sigma) and 1% penicillin (100 U/ml) and streptamycin (100 µg/ml) mixture (Sigma) in a tissue culture incubator in the presence of 5% CO_2 at 37ºC. Cells were fed 2 to 3 times a week.

For subculturing of the adherent cells they were washed with pre-warmed PBS, harvested with a trypsin-EDTA solution (0.05% trypsin and 0.5 mM EDTA; Sigma) and pelleted at 1000 rpm for 4 min. The cell pellet was resuspended in an appropriate amount of growth medium containing serum, which inhibits trypsin. 10 µl of cell suspension were mixed 1:1 with 0.4% trypan blue (Sigma), which stains dead cells, incubated for 5-10 min at room temperature, and cells were counted using a haemocytometer (Neubauer improved, Superior Marienfeld Laboratory Glassware). An

appropriate amount of cells was plated on dishes or in flasks in growth medium and incubated in a 5% CO_2-incubator at 37ºC.

2.5.1.2. Freezing and thawing of cell lines

Cell lines can be frozen and preserved indefinitely in liquid nitrogen (N_2, -196ºC). A cryoprotective agent such as glycerol or dimethyl sulfoxide (DMSO, Sigma) has to be used as it lowers the freezing point and hence prevents crystal formation inside the cells and hence lethal rupture of the cells. Storage of cells below -130ºC further retards crystal formation.

The cells were harvested and resuspended at a concentration of 10^6-10^7 cells/ml in ice-cold freezing medium containing 90% FBS and 10% DMSO. 1 ml aliquots were transferred into cryo vials on ice and placed in the "Mr. Frosty" (Nalgene® labware), a Cryo Freezing Container, which contains isopropanol and decreases its temperature at a rate of 1º/min, and stored at -80ºC overnight. Finally the cells were transferred into liquid nitrogen.

To thaw frozen cells, vials were recovered from liquid nitrogen and transferred into a water bath at 37ºC for 1 min. The cells were seeded on dishes with pre-warmed growth medium and cultured overnight. Dead floating cells were removed during washes with PBS and cells were grown for one week to recover before their use in experiments.

2.5.1.3. Transient transfection with calcium phosphate

Cells were cultured until they reached a confluence of 70-80% and before transfection the medium was replaced with fresh growth medium. Per transfection of a 10 cm^2 dish/12-well-plate 10/1-2 μg of sterile high quality DNA in 450/90μl ddH_2O were mixed with 50/10 μl of 2.5 M $CaCl_2$. 500/100 μl of 2x HeBS (280 mM NaCl, 50 mM HEPES, 1.5 mM Na_2HPO_4, pH 7.05 adjusted with 5 M NaOH) were preloaded in a sterile 15 ml conical tube and the DNA/$CaCl_2$ mixture was added drop-wise, whilst bubbling air up with an automatic pipette pump. The DNA/$CaCl_2$/2x HeBS solution was incubated for 20 min at room temperature and then pipetted drop-wise onto the cells. After an incubation time of 6-16 h the cells were washed with PBS and fresh complete medium was added. 48 h after transfection the cells were examined for transgene

expression as described in section 2.6, if a GFP-expressing vector was used, and/or else harvested for western blotting analysis.

2.5.2. Primary murine embryonic DRG cultures

2.5.2.1. Dissociation of murine embryonic DRGs with papain, collagenase and dispase

The protocol used for dissociation of murine DRG cells in the current study was a modified version of the protocol published by Malin et al. (Malin et al., 2007).

CD-1 wild type mouse embryos (E12.5 - 14.5) were harvested as described in 2.4.1. and kept in DMEM (Sigma) at room temperature. Dissection was carried out in DMEM under sterile conditions (i.e. sterile tools, EtOH-desinfected surfaces etc.). DRGs were dissected from the intervertebral foramen along the spinal cord of the embryos, collected in a centrifuge tube and spun down at 1000 rpm for 2 min. Under laminar flow the medium was replaced with 750 µl Hank's balanced salts (HBSS) medium (Invitrogen) and 750 µl papain dissociation solution (40 U/ml papain (Worthington), 2 µl/ml saturated $NaHCO_3$, 0.7 mg/ml L-Cysteine (Sigma), 0.2 mg/ml DNaseI (Sigma), HBSS) and the cells were incubated for 10 min at 37ºC. The tubes were spun for 2 min at 1000 rpm, the medium was replaced with 1.5 ml dispase and collagenase II (CLS2) dissociation medium (6 mg CLS2 (Sigma), 7 mg dispase type II (Sigma), HBSS) and the cells were incubated for 10 min at 37ºC. The tubes were spun for 2 min at 1000 rpm and the medium was replaced with 1 ml fresh complete DRG medium (fresh DMEM, 1% Pen/Strep, 10% FCS, 50 ng/ml murine NGF (Promega), 25 ng/ml human recombinant BDNF (Insights Biotechnology Ltd.) and 25 ng/ml human recombinant NT-3 (Sigma)). The DRGs were mechanically dissociated by trituration with a 23- and 21-gauge needle attached to a sterile 1 ml-syringe sequentially. The cells were pre-plated on a petri dish (bacterial) and incubated for 1 h in a tissue culture incubator. During this time the fibroblasts and glia cells attached to the petri dish, whereas the neurons floated in the medium. The neurons containing cell suspension was collected and cells were counted using a haemocytometer. An appropriate amount of cells was seeded in fresh complete DRG medium on coated plates with poly-L-lysine and fibronectin (as described in section 2.5.4). One day after plating, mitotic inhibitors (50 mM Floxuridine (FdUrd; Calbiochem®) and 150 mM Uridine (Sigma) in ddH_2O)

were added to the cells to eliminate non-neural cells such as glia cells and fibroblasts. Pictures and estimations of the composition of the cell cultures are displayed in the appendix (Appendix, Figure 5).

2.5.2.2. Dissociation of embryonic chick DRG cells with trypsin

Fertilized eggs from brown Leghorn chickens (Henry Stewart & Co. Ltd.) were kept in an incubator at 38.5ºC. At a specific developmental stage eggs were opened, embryos removed and rinsed in PBS. DRGs were dissected from the embryos in DMEM, aspirated into an Eppendorf tube and incubated in DMEM containing 0.1% trypsin (Sigma) and 0.2 mg/ml DNAseI (Sigma) for 30 minutes at 37ºC. The tube was centrifuged at 4000 rpm for 2 minutes, the supernatant was aspirated and 1 ml of pre-warmed fresh complete DRG medium (fresh DMEM, 1% Pen/Strep, 10% FCS, 50 ng/ml murine NGF (Promega), 25 ng/ml human recombinant BDNF (Insights Biotechnology Ltd.) and 25 ng/ml human recombinant NT-3 (Sigma)) was added. The DRGs were sequentially gently triturated with a 23-gauge and 21-gauge needle connected to a 1 ml-syringe. The cell suspension was pre-plated on a petri dish (bacterial) for 1-1.5 hours in a tissue culture incubator. The neurons containing cell suspension was collected and cells were counted using a haemocytometer. An appropriate amount of cells was seeded in fresh complete DRG medium on plates or coverslips coated with poly-L-lysine and fibronectin (as described in section 2.5.4).

2.5.2.3. Embryonic chick and mouse DRG explants

Murine or chick DRGs were dissected out as described above. The DRGs were crushed with forceps and a couple of DRGs was placed on a pre-coated culture dish or plate in a drop of medium for 30 min in the tissue culture incubator to allow attachment. The wells were then filled with complete DRG medium (DMEM, 1% Pen/Strep, 10% FCS, 50 ng/ml murine NGF (Promega), human recombinant BDNF (Insights Biotechnology Ltd.) and human recombinant NT-3 (Sigma)) and cultured in a tissue culture incubator.

2.5.3. Preparation of coverslips

Coverslips (Agar Scientific) were rinsed for 30 min in concentrated nitric acid on a shaker at room temperature. They were first rinsed for 30 min with distilled water and

then with absolute methanol for another 30 min. Coverslips were finally air dried and baked in a conventional oven for 4 h (or overnight) at 150ºC.

2.5.4. Coating of plates and coverslips with PLL and FN for DRG cultures

Unlike most cell lines primary cells only attach and grow on specific substrates and not on untreated culture dishes. Therefore plastic ware and coverslips were coated with reagents such as poly-L or D-lysine (PLL, PDL), fibronectin (FN), laminin (LN) etc. Poly-lysine (PLL and PDL) enhances electrostatic interactions by increasing the number of positively charged sites available for cell binding. And fibronectin, an adhesive glycoprotein, which is found both as cell surface protein and in plasma, contains active domains for collagen binding, cell adhesion, heparin binding and neurite outgrowth.

For DRG cultures plates and activated coverslips (section 2.5.3) were coated first with PLL and subsequently with FN. The whole procedure was carried out under sterile conditions in a laminar flow tissue culture hood. PLL (Sigma) was diluted at a final concentration of 0.02 mg/ml in sterile ddH_2O and added onto the culture ware or coverslip and incubated for at least 30 min at room temperature. The PLL-solution was removed and the culture ware or coverslip was washed with PBS and dried for at least 30 min at room temperature. FN (Sigma) was diluted at a final concentration of 0.02 mg/ml in PBS and added to the culture ware or coverslip and incubated for at least 30 min at room temperature. The FN solution was removed; the culture ware or coverslips were dried at room temperature and used for cell culture immediately or stored for up to 4 weeks at 4ºC.

2.6. Photography of cells and tissue sections

Pictures of cultured cells were taken with the Zeiss Axiovert-135 and the Hamamatsu ORCA-ER digital camera using Openlab 5.5.1 or Volocity 5.3.1 software (both Improvision). Pictures of the *in situ* hybridized and/or immuno-stained sections were taken with the Zeiss Axiophot and Leica DC 500 camera and with the Zeiss Imager.Z1 ApoTome using the AxioVision40 V 4.8.0.0 software. Images were processed using Adobe Photoshop and Illustrator CS4.

2.7. Statistical analysis

Statistical analysis was performed with Prism 4 (GraphPad Software). One-way analysis of variance (ANOVA) with the Tukey's Multiple Comparison post-test was used to analyse data for significant changes. Data were categorized according to their p values as non-significant (ns) with $p > 0.05$, significant (∗) with $0.01 < p < 0.05$, very significant (∗∗) with $0.001 < p < 0.01$ and extremely significant (∗∗∗) with $p < 0.001$.

Chapter 3

Gene expression analysis of PTPs and Trk receptors in murine embryonic DRGs

3.1. Introduction

Several RPTPs play important roles in neurons by controlling for instance their differentiation, neurite outgrowth and synapse formation and plasticity similar to Trk receptors (sections 1.2 and 1.3). Some of these RPTPs were therefore previously analysed for their role in regulating Trk signalling. However, most of these studies were undertaken in over-expression experiments (section 1.4), while the physiological relevance of the RPTP and Trk interaction has yet to be shown.

First valuable hints towards a possible biological function of proteins are provided by their expression patterns. Similarities in temporal and spatial expression patterns of several proteins might also be indicative of a possible interaction of these proteins with each other. Therefore a detailed analysis of the gene expression patterns of RPTPs and Trks was performed in this study on DRGs from wild type mouse embryos, which is a widely accepted cell model to study Trk signalling (reviewed in 1.5.). The aim of this chapter was to select candidate RPTP genes based on their relatively high temporal gene expression levels for further in-depth analysis of their spatial expression patterns in comparison to Trk expression and the coexpression of these enzymes in the same sensory neurons (chapter 4).

The expression of all three Trk genes was previously analysed in different species during development in a variety of tissues including DRGs (described in section 1.2.3). Also he expression of several RPTP genes has been previously studied during development, implicating some of these RPTPs in the development and function of neurons. In particular, the genes *Ptpra* (encoding RPTPα), *Ptprf* (LAR), *Ptprg* (RPTPγ), *Ptpro* (RPTP-BK), *Ptprr* (RPTPR), *Ptprs* (RPTPσ), *Ptprz1* (RPTPζ), *Ptprn* (IA2) and *Ptprk* (RPTPκ) were found to be expressed in DRGs at different developmental stages in mice and other species (described in section 1.3.3). Due to some similarities to the expression of Trk enzymes specific RPTPs were suggested to be implicated in Trk signalling. However, so far no gene expression study has been performed for Trks and most RPTPs in parallel in the same tissue and at the same time points, which has the advantage of a direct and accurate comparison of the gene expression patterns with each other. Therefore, we have analysed almost the entire PTP

family and assessed whether RPTPs are among the highest expressed PTPs in DRGs, which also naturally and highly express Trk receptors.

This study was carried out on DRGs from murine embryos at the developmental stages E12.5, 13.5 and 14.5 (Theiler stages 20, 21 and 22 respectively). Such a three-time-point analysis allowed us to create a characteristic expression profile of each analysed gene throughout development and to compare it to other genes, and in particular to Trks. These specific developmental stages cover the time window, when sensory neurogenesis in DRGs is almost complete but the neurites did not yet innervate their targets. Once the targets are reached at around E15.5 in hind limb innervating DRGs (White et al., 1996), target-mediated apoptosis occurs and this is accompanied by changes in many signalling mechanisms and in ganglia composition (Hamburger and Levi-Montalcini, 1949, Carr and Simpson, 1978). Most mouse strains have 60 DRGs grouped into cervical, thoracic, lumbar and sacral DRG pairs according to their position relative to the spinal cord. In this study the analysis was mainly performed on cervical/thoracic and lumbar DRGs from fore and hind limb regions, since limb-innervating ganglia are much larger and contain more cells compared to other ganglia due to lower cell death (Hamburger and Levi-Montalcini, 1949).

Most of the previous studies were carried out using *in situ* hybridization (ISH) and in some cases RT-PCR. In our study gene expression was analysed using three different techniques. First, recently designed qPCR arrays, which allow the analysis of the entire PTP family in parallel, were used on whole DRG tissue and additionally an exon microarray was tested. Usually both techniques are used to compare samples under different conditions with each other such as treated or untreated with chemicals. However, in this study I have unconventionally used them to create a gene expression profile similar to at least one reported study (Lakics et al., 2010). Both techniques provided us convincingly with the same outcome. Furthermore, I have confirmed these results for selected highly expressed RPTP genes using chromogenic ISH on mouse embryo sections, which additionally provided spatial information of the expression of these genes in DRGs. This analysis was then further expanded in order to assess the coexpression of selected RPTPs and Trks in the same neurons in Chapter 4, which further supports the hypothesis of a possible interaction of RPTPs with Trk receptors.

3.2. Experimental procedures

3.2.1. qPCR arrays - semi-automated high-throughput qPCR analysis

Semi-automated qPCR arrays developed by the laboratory of Dr. Rob Hooft van Huijsduijnen at Merck-Serono Pharmaceuticals AG in Geneva, Switzerland, were used with the assistance of Dr. Monique van den Eijnden to screen samples from murine embryonic DRGs (E12.5, 13.5 and 14.5) for PTP and Trk gene expression.

QPCR arrays are 384-well-plates, robotically pre-filled with primers for 92 PTPs and four different housekeeping genes (HKG): *Psmb2* (proteasome subunit beta type2), *Hprt1* (hypoxanthine-guanine phosphoribosyltransferase 1), *Ubc* (ubiquitin C) and *Gps1* (G protein pathway suppressor 1). Additionally, a screen with PTP primers for *Dusp27* (FMDSP) and *Ptpru* (PTPλ) and primers for *Ntrk1* (TrkA), *Ntrk2* (TrkB) and *Ntrk3* (TrkC) and four HKGs was performed using manually pre-filled 384-well-plates. Primers were obtained as QuantiTect® Primer Assays (Qiagen) (Table 3.1 and Appendix, Table 1) and tested for primer dimer formation and specificity by Dr. M. van den Eijnden. The primers for *Dusp9* (MKP4), *Dusp13a* (MDSP), *Dusp13b* (TMDP), *Dusp21* (LMW DSP21), *Tpte* (TPIP), *Dusp24* (STYXL1), the four Asp-based HADs and *Mtmr14* (MTMR14) and *Mtmr15* (MTMR15) were excluded from the final analysis, as these genes were either not expressed in our samples (provided undetermined C_T values) or (good) primers were unavailable. Details of the general techniques were described in section 2.2.

3.2.1.1. Sample preparation

DRGs from limb regions of E12.5 (44, 65, 65 DRGs from 8 embryos of the same litter), 13.5 (55, 65, 65 DRGs from 8 embryos of the same litter) and 14.5 (65, 65, 65 DRGs from 11 embryos of the same litter) mouse embryos were dissected, snap frozen and shipped on dry ice to Merck-Serono, Geneva, Switzerland. There Monique and I extracted RNA from all samples in parallel using the RNeasy® Lipid Tissue Kit (Qiagen). RNA purity (260/280 ratio) and concentration were measured using the NanoDrop ND-1000 Spectrophotometer and the integrity of the mRNA was tested with the Agilent Bioanalyzer using the RNA 6000 Nano LabChip Kit according to manufacturer's instructions. The RIN values of all RNA samples were high quality with

values above 8.6. mRNA was reverse transcribed into cDNA using the iScript™cDNA Synthesis Kit (BioRad) for all samples in the same reaction to minimise variability. A qPCR test with primers spanning intron regions of *Gapdh* and *Actb* was carried out to control for gDNA contamination, which was neglectable in the samples.

3.2.1.2. qPCR reactions

Each qPCR reaction contained 1.25 ng of cDNA, 2.5 µl primer pair and 5 µl of 2x QuantiTect® SYBR Green PCR Master mix (Qiagen) including HotStart Taq DNA polymerase, QuantiTect® SYBR Green PCR buffer (Tris·HCl, KCl, $(NH_4)_2SO_4$, 5 mM $MgCl_2$, pH 8.7), dNTP mix, SYBR Green I, ROX passive reference dye and RNase-free H_2O. The experiments were performed in technical duplicates with three biological replicates for each embryonic stage. The 384-well-plates containing qPCR reactions were run in a LightCycler (ABI 7900HT Fast Real-Time PCR System) under the following PCR conditions: stage 1: 95ºC for 5 min, stage 2: 40x (10 sec at 95ºC, 30 sec at 60ºC), stage 3 (dissociation curves): 15 sec at 95ºC, 15 sec at 60ºC, 15 sec at 95ºC with a heated lid at 105ºC.

3.2.1.3. Data analysis

C_T values were extracted with the Fast 7900 SDS 2.2.2 software (Applied Biosystems) after adjustment of the baseline between cycles 3 and 15 and the threshold at ΔRn 0.1, and analysed using a Microsoft® Excel® analysis. Dissociation curves of each reaction were examined and only data with a single product peak and no primer dimer formation were used for analysis. Amplification plots of each reaction were analysed and omitted, if they were not parallel to the HKGs (~ similar PCR amplification efficiency). For relative global gene expression analysis, $2^{-\Delta CT}$ values were calculated with ΔC_T representing the expression of the gene of interest (GOI) normalized to the mean of three HKGs (*Psmb2, Hrpt1* and *Gps1,* see below). The results were displayed as percentage of expression compared to the set of HKGs (% $2^{-\Delta CT}$). For instance, a value of 100% means that the expression of the HKGs equals the expression of the GOI ($\Delta C_T = 0$). 300% gene expression means that the expression of the GOI is 3x higher than the expression of the HKGs and 5% means that the expression of the GOI is

	GENE NAME	AMPLICON SIZE (bp)	COVERED EXONS	DETECTED TRANSCRIPTS	OLIGO ID
$RPTP_S$	***Ptpra***	87	3/4	1 and 2	QT00141610
	Ptprb	106	16/17	1	QT00197981
	Ptprc	96	7/8/9	1 and 2	QT00139405
	Ptprd	125	4/5/6	2 but not 1	QT01167180
	Ptpre	99	17/18	1	QT00101941
	Ptprf	115	33	1	PPM05105E
	Ptprg	73	9/10	1	QT00160832
	Ptprh	104	9/10/11	1	QT01059415
	Ptprj	111	5/6	1 and 2	QT00169785
	Ptprk	147	30/31	1	QT01063615
	Ptprm	81	17/18	1	QT00167545
	Ptprn	79	4/5	1	QT01748971
	Ptprn2	139	9/10	1	QT01057868
	Ptpro	119	15/16/17	1 and 2, not 3 and 4	QT00134540
	Ptprq	123	8/9	1	QT01077237
	Ptprr	105	2/3	1, not 3, 4 or 5	QT00173530
	Ptprs	107	7/8	1	QT00150416
	Ptprt	71	14/15	1	QT01063594
	Ptpru	71	14/15	2 but not 1	QT00101430
	Ptprv	110	19/20/21	1	QT01070930
	Ptprz1	125	9/10/11	1	QT01057854
$NTRK_S$	***Ntrk1***	137	2/3/4	1	QT01046143
	Ntrk2	67	6/7	1 and 2	QT00132111
	Ntrk3	135	8/9/10	1 and 2	QT00146153
HKG_S	***Psmb2***	67	4/5	1	QT00113701
	Hprt1	168	3/4/5	1	QT00166768
	Ubc	75	/	1	QT00245189
	Gps1	79	3/4	1 and 2	QT00120113
	Gapdh	144	2/3	1	QT01658692
	Actb	149	1/2	1	QT01136772

Table 3.1. Primers used in the qPCR arrays.

All primers to detect RPTP, Trk and HKG gene expression were obtained as QuantiTect primer assays from Qiagen. The information of the detected transcript variants is based on the information from EntrezGene/NCBI with 1 meaning only one transcript variant exists. (For a full list of primers see Appendix, Table 1.)

1/20 of the expression of the HKGs. For comparison and evaluation of global gene expression, the mean of all three stages was calculated. Statistical analysis was performed with Prism 4 (GraphPad Software) as described in section 2.7.

3.2.1.4. Expression stability analyses of HKGs

3.2.1.4.1. Comparison of CT values

To assess the variation in gene expression of the four HKGs (*Psmb2, Hrpt1, Ubc* and *Gps1*) during development, 2^{-CT} values were calculated for each embryonic stage and compared with each other and with *Gapdh* and *Actb* (Schmittgen and Livak, 2008).

3.2.1.4.2. GeNorm software

GeNorm V 3.5, a publicly available Microsoft® Excel® Visual Basic Application (Vandesompele et al., 2002), was used to determine the most stabile reference genes in the analysed samples among a set of candidate genes using data from the qPCR analysis. It is based on the principle that the expression ratio between two ideal reference genes is identical in all analysed samples. It calculates the standard deviation of the logarithmically transformed expression ratios between analysed genes and calculates the gene expression stability measure *M* as the average pairwise variation *V* for that gene with all other tested reference genes and provides a ranking based on *M*. The lower the *M* value, the higher the gene stability. For the calculations of *M* C_T values of the HKGs were transformed into quantities by using a comparative ΔC_T method. For each gene the lowest C_T value (highest relative quantity) was subtracted from its C_T value and this ΔC_T value was converted to a relative abundance value ($E^{\Delta CT}$) due to the exponential nature of PCR with E representing the amplification efficiency (2 for 100%). The C_T value with the highest relative quantity was set to 1. These raw (not normalized) reference gene quantities were the input data for geNorm analysis (Vandesompele et al., 2007).

3.2.1.4.3. NormFinder software

NormFinder, a publicly available Microsoft® Excel® Visual Basic Application (Andersen et al., 2004), is used to identify the optimal reference gene among a set of candidate genes using data from any quantitative analysis such as qPCR and

microarrays. It estimates the overall expression variation of the reference genes and the variation between sample subgroups. The calculated stability value is a direct measure for the estimated expression variation. The input data are the same as used for geNorm (see above). The log transformation and extended analysis options were used. Intergroup variances were plotted for all candidate genes with the average of the intragroup variances as error bars. The higher the stability of the candidate gene, the closer the intergroup variance to zero and the smaller the error bars.

3.2.2. Microarray analysis

Microarray analysis is a fast high throughput technique for global gene expression analysis and other applications. The basic concept is to hybridize labelled cDNA samples onto chips containing many thousands or millions of different oligonucleotide sequences corresponding to specific genes and detect their binding. The pilot microarray experiment in this study was performed by the Institute of Child Health Microarray Facility (UCL Genomics, http://www.genomics.ucl.ac.uk/platforms/affymetrix.htm) using a GeneChip® Mouse Exon 1.0 ST array (Affymetrix). The high-density mouse chip contains 1.2 million probe sets, which target approximately one million exons. A probe set consists of four probes, which are categorized into "core probes", "extended probes" or "full probes" according to the underlying mRNA evidence. "Core probes" detect fully annotated exons for instance from RefSeq and are regarded as the most confident. "Extended probes" target exons with partial mRNA evidence such as ESTs. And "full probes" target exons, which are only supported by computational predictions. The detected exons are grouped into transcript clusters (genes) (Affymetrix, 2005).

3.2.2.1. Sample preparation

60 DRGs from fore and hind limb regions were dissected from E12.5 mouse embryos and snap frozen on dry ice and stored at -80°C. RNA was extracted using the RNAeasy® Mini Kit (Qiagen) following manufacturer's instructions (see chapter 2.2.1). RNA was quantified with the NanoDrop® ND-1000 Spectrophotometer (NanoDrop Technologies) and its quality was verified with the Agilent 2100 BioAnalyzer® (Agilent Technologies). Samples were labelled for hybridisation to the array according to the

GeneChip® Whole Transcript (WT) Sense Target Labelling Assay. Briefly, cDNA was synthesized with random hexamers incorporating a T7 promoter sequence using the GeneChip® WT cDNA Synthesis and Amplification Kit (Affymetrix). The recommended rRNA reduction step to minimize possible non-specific hybridisation on the array was omitted since not enough RNA was available. The generated double stranded cDNA was used to generate cRNA with random priming from the T7 promoters, which was then used to generate single stranded cDNA in the sense direction for hybridisation to the array. After fragmenting and end labelling of the cDNA with the GeneChip® Terminal Labelling Kit (Affymetrix), the cDNA fragments were hybridized to the GeneChip® Mouse Exon 1.0 ST array (Affymetrix) at 45°C for 16 h, followed by washing and staining on the automated Fluidics station 450 (Affymetrix) using the Hybridization Wash and Stain Kit (Affymetrix). The chip was finally scanned on the GeneChip® Scanner 3000.

3.2.2.2. Data analysis

The Affymetrix® GeneChip® Command Console® 3.1.1 and Expression Console™ V 1.0 software products were used to perform qualitative and quantitative analysis for each probe set by subtracting the background and annotation of the probe sets to obtain gene-level and exon-level signal estimates. Additionally the Detection Above Background (DABG)-*P*-values were calculated by comparing the probe signals with the signals of the background probes with the same GC-content and using the Wilcoxon's Signed Rank Test. Further analysis was performed with Microsoft® Excel® using additional information retrieved from the web-based Affymetrix® NetAffx™ Analysis Centre. The analysis was restricted to RPTPs, Trks and the two HKGs *Psmb2* and *Ubc*. First, data from probe sets of the Expression Console™ "exon report" were selected with DABG-*P*-values < 0.01 and unique hybridization to a single target (cross-hybridisation = 1) and for most analyzed genes only data from "core probes" were used. For *Ptprh, Ptprq, Ptprz1* and *Ntrk1* no "core probes" were available and therefore data from the "extended probes" were used. To estimate overall gene expression from the selected data the signal intensity values ($\log_2$) of all selected probe sets for a transcript cluster (= gene) were displayed in "box plots" to visualize overall abundance, whereby the signal intensity values represent a quantitative measure of the relative abundance of a transcript or exon. For calculations of the medians and quantiles

all intensity values were used except outliers with $\log_2 < 5$. These data were compared to the results from the "gene report", in which the expression of transcript clusters based on the expression profile of "core probes" was calculated by the Expression Console® software. The cut-off for reliable exon and transcript detection was set to the signal intensity value of $\log_2$ 7 based on previous experiences of the Bloomsbury Centre for Bioinformatics, UCL (http://www.bcb.lon.ac.uk/). The NetAffx™ analysis centre was used to retrieve additional information about the transcript clusters and probe sets (http://www.affymetrix.com/analysis/index.affx).

3.2.3. Chromogenic *in situ* hybridisation

Chromogenic *in situ* hybridisation (ISH) was performed on transverse O.C.T. cryosections of wild type CD-1 mouse embryos at the developmental stages E12.5, 13.5 and 14.5 and on E13.5 sagittal gelatine mouse embryo sections as described in 2.4.2. Hybridisation of all available sense probes did not provide any specific signal (Appendix, Figure 1) compared to corresponding antisense probes.

3.2.3.1. In situ riboprobes

Antisense and sense probes were generated by *in vitro* transcription from DNA templates using T3-, T7- or Sp6 RNA polymerases as described in 2.4.2.2. DNA templates such as transcription plasmids or cDNAs were obtained from collaborators from within PTPNET or elsewhere, or from the I.M.A.G.E. Consortium (LLNL) cDNA Clones (Lennon et al., 1996) (Geneservice, Cambridge, UK). If necessary they were modified by cloning. All plasmids were verified by restriction enzyme digests and sequencing.

The riboprobe for ***Ptpra*** was a gift of Prof. Jeroen den Hertog and was previously described (den Hertog et al., 1992, den Hertog et al., 1993). A fragment bp 342-1799 of NM_008980 was subcloned between the *Bam*HI restriction sites of pT7/T3α-19 (Gibco BRL). The antisense RNA probe was transcribed with T3 polymerase from the plasmid linearized with *Hind*III, and the sense probe with T7 polymerase from the plasmid linearized with *Asp*718. Both sense and antisense riboprobes were approx. 1.4kb in size and covered the entire ECD and TM and almost the entire D1 domain. The antisense probe matches bp 342-1799 of transcript 1

(NM_008980) and bp 342-1089 and bp 1090-1691 of transcript 2 (NM_001163688). Transcript 2 lacks 100 bp corresponding to an alternate in-frame exon in the 5' coding region, to which the probe aligns. Still since this part is flanked by around 600 bp on each side, this transcript is likely to be detected by the antisense probe.

The riboprobe for ***Ptprd*** was a gift of Dr. Wiljan Hendriks and was previously described (Mizuno et al., 1993, Schaapveld et al., 1998). The cDNA fragment matches bp 2544-3956 of transcript 1 (NM_001014288) and bp 3226-4638 of transcript 2 (NM_011211), which covers most of the ICD. The 1.7 kb antisense probe was transcribed with T7 RNA polymerase from the plasmid linearized with *Not*I. The sense probe was transcribed with T3 polymerase from the plasmid linearized with *Xho*I.

Ptprf riboprobe was a gift of Dr. Wiljan Hendriks (Schaapveld et al., 1995). The antisense probe was transcribed with T3 polymerase from the plasmid linearized with *Not*I and the sense probe with T7 polymerase from the plasmid linearized with *Hind*III. Both probes cover bp 4712-6881 of NM_011213, which includes the whole D2 and a part of the D1 domain and the 3' UTR.

The riboprobe for ***Ptprg*** was a gift of Dr. Sheilla Harroch (Lamprianou et al., 2006). It was transcribed by T3 polymerase from the plasmid linearized with *Kpn*I and is coding for the N-terminus of the carbonic anhydrase domain of RPTPγ (amino acids 1-832) and hence recognizes all isoforms. It corresponds to bp 460-1291 of NM_008981.

A cDNA encoding **RPTPJ** was PCR amplified with the primers: forward 5'-GGTCTAGACAGATCCAGGGAATCTCCAA-3' and reverse 5'-GGTCTAGAATT CCTCTGCAAACCCACAG-3') from total cDNA isolated from DRGs of E13.5 CD-1 mouse embryos. Both primers contained an *Xba*I site (TCTAGA) for cloning into pT7T3α-18 (Gibco BRL). The antisense RNA probe was transcribed using Sp6 RNA polymerase from the plasmid linearized with *Nco*I and the sense probe by T7 polymerase from the plasmid linearized with *Hind*II. Both probes were approximately 1.3 kb in size. The antisense probe corresponds to bp 1889-3182 of transcript variant 1 (NM_08982) and bp 1655-2948 of transcript variant 2 (NM_001135657) spanning the entire ECD, TM domain and part of the ICD until D1.

Ptprk cDNA was a gift of Prof. Jan Sap (Jiang et al., 1993). To obtain a smaller riboprobe the plasmid was digested with *Hind*III and religated, thus deleting the entire

ICD and TM domains and part of the ECD. The remaining fragment of 2 kb corresponds to bp 262-2040 of NM_008983. The 1.9 kb antisense probe was generated from the T3 promoter of the plasmid linearized with *Xho*I. The 1.8 kb sense probe was transcribed with T7 RNA polymerase from the plasmid linearized with *Hind*III.

The riboprobe for ***Ptprm*** was a gift of Dr. Claire Faux (Faux et al., 2010). Both sense and antisense probes were 1.6 kb in size and detect bp 471-1448 in the ECD of NM_008984. The antisense RNA probe was generated from the T3 promoter and the sense probe from the T7 promoter of the plasmid linearized with *Sal*I or *Not*I respectively.

The ***Ptpro*** cDNA was a gift of Dr. Takahiko Shimizu (Tomemori et al., 2000). A fragment covering bp 522-2409 in the ECD of NM_011216 and also transcript variant 2 (NM_001164401) was subcloned into pT7T3α-19 (Gibco BRL) between *Xba*I and *Hind*III. The antisense probe was transcribed with T3 polymerase from the linearized plasmid with *Hind*III and the sense probe with T7 polymerase from the plasmid linearized with *Xba*I. Both probes are 1.7 kb in size. The antisense probe detected both known transcript variants 1 and 2, but not 3 and 4. The latter lack the ECD and are known as PTPϕ or PTPROt and are not expressed in neurons (Tomemori et al., 2000).

The cDNA for ***Ptprr*** was a gift of Dr. Wiljan Hendriks and Irene Chisini and was previously described (Van Den Maagdenberg et al., 1999). A fragment corresponding to bp 301-1580 of transcript variant 1 (NM_011217) covering the ECD, TM domain and part of the ICD until D1 was subcloned between the *BamH*I and *EcoR*I sites of pT7T3α-19 (Gibco BRL). The 1.9 kb antisense RNA probe was transcribed with T3 RNA polymerase from the plasmid linearized with *Xho*I. The 1.8 kb sense probe was transcribed with T7 polymerase from the plasmid linearized with *Hind*III. The antisense riboprobe corresponds to bp 301-1580 of transcript variant 1 (NM_011217), bp 369-931 of variant 3 (NM_001161838), bp 60-622 of variant 4 (NM_001161839) and bp 252-814 of variant 5 (NM_001161840).

Ptprs cDNA was a gift of Dr. Masato Ogata (Osaka University Medical School, Japan) and was previously described (Ogata et al., 1994). A fragment corresponding to bp 400-2142 (only ECD) of NM_011218 was subcloned between *Hind*III and *BamH*I of pT7T3α-19 (Gibco BRL). The 1.2 kb antisense riboprobe was transcribed with T7 polymerase from the plasmid linearized with *Xba*I and corresponds to bp 977-1142

of NM_011218. The 0.8 kb sense probe was transcribed with T3 polymerase from the plasmid linearized with *Bgl*II.

The transcription plasmids containing mPtprz1-CAH-pBS-KS2 and mPtprz1-385mD2-pTOPOII containing fragments of ***Ptprz1*** cDNA were gifts of Dr. Sheilla Harroch and were previously described (Harroch et al., 2002). The 500 bp antisense riboprobe *Ptprz1*-CAH was transcribed with Sp6 polymerase of the plasmid linearized with *EcoR*I and detected all known isoforms of *Ptprz1*. The 1 kb antisense riboprobe *Ptprz1*-385mD2 was transcribed with T7 polymerase from the corresponding plasmid linearized with *BamH*I, and detected only the transmembrane isoform.

Ntrk1 cDNA was obtained from the I.M.A.G.E. Consortium as clone ID: 5256438, which contains a 960 bp fragment from lung tissue of the mouse in pT7T3D-PacI between *EcoR*I and *Not*I. It corresponds to bp 1321-2280 of NM_001033124. The 900bp antisense riboprobe was transcribed with T3 polymerase from the linearized plasmid with *Xho*I. The 900bp sense probe was generated with T7 polymerase from the plasmid linearized with *Not*I.

Ntrk2 cDNA was obtained from the I.M.A.G.E. Consortium as clone ID: 5707891. It contains a cDNA fragment corresponding to bp 869-2424 of transcript variant 2 NM_008745 with an additional poly-A tail in pYX-Asc between *EcoR*I and *Not*I. The 1.6kb antisense riboprobe was transcribed with T3 polymerase from the plasmid linearized with *Hind*III. It corresponds to bp 793-1920 of transcript variant 1 (NM_001025074) and bp 869-2422 of transcript variant 2 (NM_008745) covering most of the ECD and the TM domain. The 1.5 kb sense probe was transcribed with T7 polymerase from the plasmid linearized with *Bgl*II.

Ntrk3 cDNA was obtained from the I.M.A.G.E. Consortium as clone ID: 40110345. A cDNA fragment corresponding to bp 16-1898 of transcript variant 2 (NM_182809) was subcloned between the *Xba*I and *Hind*III sites of pT7T3α-19 (Gibco BRL). The 1.2kb antisense riboprobe was transcribed with T3 polymerase from the plasmid linearized with *Hind*II. It is complementary to bp 707-1878 of transcript variant 2 (NM_182809) and bp 707-1640 of transcript variant 1 (NM_008746) covering most of the ECD, The TM and part of the ICD in transcript 1 until the kinase domain and in transcript 2 the entire protein encoding region. The 1.9 kb sense probe was transcribed with T7 polymerase from the linearized plasmid with *BamH*I.

3.3. Results

3.3.1. QPCR arrays for PTP and Trk gene expression analysis

QPCR is a very sensitive quantitative gene expression analysis technique, but it is mostly used to analyse the expression of just a few genes at a time. Recently, high-throughput qPCR arrays have been developed, which allow the analysis of hundreds of genes in parallel in one sample and additionally save reagents, template cDNA amounts, and experimental time. This is most suitable for the analysis of gene families with 100-400 members and is more accurate and sensitive than microarray analysis. For instance Schmittgen *et al.* (Schmittgen et al., 2008) have profiled the expression of microRNA using 384-well-plate qPCR arrays. And in a similar approach Lakics *et al.* have recently compared the expression of cyclic nucleotide-specific phospho-diesterases mRNA across 24 different tissues (Lakics et al., 2010). Additionally commercial qPCR arrays from different companies became available recently, such as the RT^2 Profiler™ PCR Array from SABiosciences, Qiagen, (http://www.sabiosciences.com/PCRArray Plate.php). For this study I had the opportunity to use a semi-automated high-throughput qPCR array tailor-made for the analysis of almost the entire murine PTP gene family. This was made available to us by the laboratory of Dr. Rob van Huijsduijnen at Merck-Serono Geneva, Switzerland, a member of PTPNET. I used this array to profile the gene expression of PTPs in parallel with Trk receptors in murine embryonic DRGs across the developmental stages E12.5, 13.5 and 14.5.

3.3.1.1. Selection of HKGs

The PTP qPCR array can be used to analyse gene expression of 94 of the 106 known PTP genes in murine tissues. A relative quantification (ΔC_T) method is utilized for data analysis similar to the one described by Lakics *et al.* (Lakics et al., 2010), which requires reference genes as an endogenous control to normalize differences in template cDNA amounts in the samples due to possible variations in mRNA quantity and quality, efficiency of cDNA synthesis, pipetting errors etc. The choice of reference genes is crucial for optimal relative expression results in order to identify real gene-specific differences and is a challenging task especially for samples from developing organisms. A good reference gene is constitutively expressed in the samples and does not change

under the experimental conditions. As there is no universal reference gene, each candidate gene has to be tested in the experimental set-up for suitability.

The PTP qPCR array contains four different HKGs *Psmb2*, *Hprt1*, *Ubc* and *Gps1*, which were selected due to their stable expression in several neuronal mouse tissues (personal communication with Dr. M. van den Eijnden). *Psmb2* encodes the proteasome subunit beta type 2, which is involved in the cleavage of proteins and is highly expressed in eukaryotic cells. *Hprt1* encodes the hypoxanthine-guanine phosphoribosyl transferase 1, an essential enzyme for purine recycling. The protein product of *Ubc* is ubiquitin C, a small regulatory protein, which binds to proteins and directs them towards recycling or other functions. *Gps1* encodes the G-protein pathway suppressor 1, which suppresses the expression of G-protein and mitogen-activated genes in mammalian cells. All four are frequently used as reference genes in relative quantification analyses of different tissue types.

To identify the most suitable reference genes for this study among these four HKGs, I have analysed the robustness of their expression in the murine embryonic DRG tissue. Additionally I have compared these data with the expression of two of the most frequently used reference genes in qPCR experiments, *Gapdh* (glyceraldehyde-3-phosphate dehydrogenase) and *Actb* (β-actin). First, I examined the variations in gene expression between samples of different embryonic stages using 2^{-CT} values from all qPCR experiments (Schmittgen and Livak, 2008) (Figure 3.1A). *Psmb2* expression values varied least among all HKGs at the three developmental stages, followed by *Hprt1* and *Gps1,* whereas *Ubc* showed least stable expression during development due to increased expression at E14.5. Therefore it was not surprising that the mean of the expression values of *Psmb2, Hprt1* and *Gps1* was more stable compared to the mean of all four HKGs. In comparison *Actb* showed a very strong decrease in expression at E14.5 and *Gapdh* showed a peak at E13.5 and high variation between samples of the same stage. Although both genes were previously seen as universal reference genes, their regulation was subsequently proven in many different experiments (Schmittgen and Zakrajsek, 2000). Overall the mean of the expression values of *Psmb2, Hprt1* and *Gps1* was more stable than the expression of any individual gene.

In addition, I have used two publicly available Microsoft® Excel® Visual Basic applications geNorm V 3.5 (Vandesompele et al., 2002) and NormFinder (Andersen et al., 2004) to assess the expression stability of the reference genes. Both methods are

widely recognized and used to determine gene expression stability among a set of reference genes, which is reflected in hundreds of citations of both methods. GeNorm is based on the principle that the expression ratio between two ideal reference genes is identical in all analysed samples. This program identified *Actb* as the least robust gene (Figure 3.1B) in agreement with the described analysis of individual data points (see above). However, *Ubc*, which showed highest variation in C_T values between samples across different embryonic stages (Figure 3.1A), together with *Hprt1* were chosen by this program to be the most stable among the four HKGs in contrast to the individual data point analysis. This is due to the nature of the algorithm, which identifies similarity in expression among genes. Thus geNorm falsely identifies co-regulated genes as best reference genes, and does not reflect variation between different subgroups (developmental stages) (Jung et al., 2007). The second application NormFinder is a model based estimation method, which uses analysis of variance on all log-transformed values simultaneously to calculate gene stability values for the most stable gene or the best combination of two genes. In contrast to geNorm this program estimates not only the variation among candidates but also the variation between sample subgroups (embryonic stages in this case) and was reported to be more robust towards co-regulated genes. Due to the nature of its algorithm it was possible to additionally include two averages of HKGs into the calculations, all four genes *Psmb2*, *Hprt1*, *Ubc* and *Gps1* together and an average lacking *Ubc*. Unlike the first tested application NormFinder has confirmed the analysis of the differences in C_T values during development for the tested HKGs. It has ranked the genes according to their robustness in gene expression with *Actb* as the least stable gene and the average of the HKGs *Psmb2, Hprt1* and *Gps1* as most stable (Figure 3.1C). The intergroup variance, which reflects the log differences between embryonic stages (Figure 3.1D), agreed with the analysis of the C_T values for each gene as described above. Additionally the intragroup variance displayed in the graph as error bars highlighted for instance in case of *Gapdh* the big differences among samples from the same embryonic stage, which makes this gene a less good candidate reference gene. Overall the average of the HKGs *Psmb2, Hprt1* and *Gps1* was evaluated as the most robust among tested candidates. Similar to *Psmb2* this set of HKGs shows a small stability value and also small intergroup variance, but additionally a slightly smaller intragroup variance than *Psmb2*.

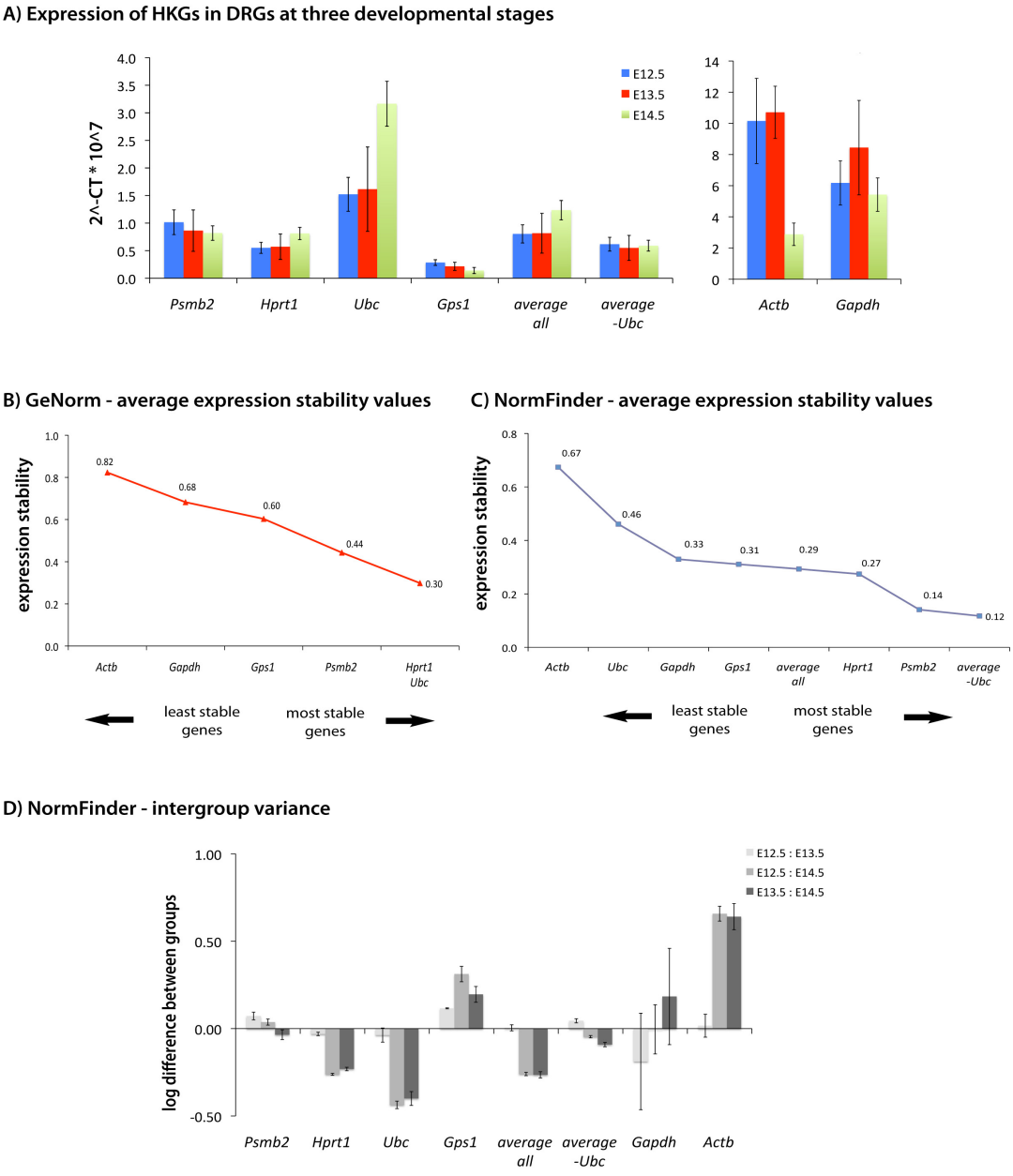

Figure 3.1. Assessment of the stability of HKG expression during DRG development.

A) Mean expression is represented as $2^{-CT} * 10^7$ for each HKG (*Psmb2*, *Hprt1*, *Ubc*, *Gps1*, *Actb* and *Gapdh*) and two averages (*Psmb2*, *Hprt1*, *Ubc* and *Gps1*) or (*Psmb2*, *Hprt1*, *Gps1*) across three developmental stages. Error bars represent standard deviations (SD). **B)** Average gene expression stability values (M) of remaining reference genes during stepwise exclusion of the least stable gene were calculated with geNorm software. **C)** Average expression stability values of reference genes were obtained with NormFinder software. **D)** Intergroup variance displayed as log differences between groups (embryonic stages) were calculated with NormFinder software. Error bars represent averages of intragroup variances.

Taken together, the individual data point and NormFinder analyses agree with each other on the set of HKGs *Psmb2, Hprt1* and *Gps1* as the most suitable reference genes for the qPCR analysis among the six tested genes. GeNorm has proven to be an unsuitable tool for our purposes due to the nature of its algorithm as it suggests regulated genes with similar expression as best reference genes. As it was pointed out in many studies and reviews, it is preferable and of more advantage to use several reference genes. And thus finally a set of the three HKGs *Psmb2, Hprt1* and *Gps1* was used for normalization of the qPCR data generated with the qPCR array.

3.3.1.2. Trk gene expression in murine embryonic DRGs

Using the described qPCR array we could show that all three Trk genes were highly expressed in murine embryonic DRGs at the three analyzed developmental stages with a dynamic expression pattern (Figure 3.2). It has to be noted that all given expression values refer to the expression of the HKGs (see 3.2. for more details). *Ntrk1* gene encoding TrkA was as expected the most abundant of all three Trk genes with a mean expression of 183% relative to the set of HKGs, followed by *Ntrk3* encoding TrkC with 79% and finally *Ntrk2* encoding TrkB with 24%. The expression levels of *Ntrk2* and *Ntrk3* decreased significantly during development, whereas the expression of *Ntrk1* showed a peak in expression at E13.5 but without statistical significance (Figure 3.2A). It is important to keep in mind that these described gene expression dynamics refer to samples containing whole DRGs with many different subpopulations of sensory neurons and also SGCs. Possible residual axons encircled by Schwann cells and some fibroblasts surrounding the DRGs and endothelial cells might be present in the samples as well. Therefore an observed decrease or increase in gene expression can reflect a change in gene expression in the subpopulation of cells *per se* or a change in the proportion of cells in the DRGs expressing this particular gene. Thus the observed decrease in TrkB and TrkC gene expression in this study can be interpreted in several ways. First, as described by the "three wave-theory of neurogenesis in DRGs" (see Introduction section 1.3) the proportion of $TrkB^+$ and $TrkC^+$ neurons in DRGs at the analysed stages decreased due to higher expansion of other neuronal subpopulations such as $TrkA^+$ neurons and glia cells. Into the bargain, there is evidence of early pre-target-mediated cell death of neuronal populations, which results in a decrease in cell numbers of TrkB and TrkC neurons but not TrkA neurons at this time-point (White

et al., 1996). In the case of TrkC a termination of its expression in specific cells, which switch to TrkB and/or Ret expression at around E14.5 in mouse embryos (Marmigere and Ernfors, 2007), is also responsible for the observed decrease in gene expression.

Overall these results are in strong agreement with numerous IHC and ISH studies, which analysed Trk expression in rodent embryonic and postnatal DRGs, although the numbers in these reports vary between studies due to different techniques (White et al., 1996, Molliver and Snider, 1997, Farinas et al., 1998, Ernsberger, 2009). Previously it was reported that TrkC expression begins at around E10 in thoracolumbar DRGs in mouse embryos and that the proportion of $TrkC^+$ cells at E11 increases to 70% of all cells. At E11.5 the majority of lumbar DRG cells are $TrkC^+$ and their proportion drops to less than 10% at E13 (Phillips and Armanini, 1996, White et al., 1996, Farinas et al., 1998). The generation of $TrkB^+$ neurons was first observed at E10.5. At E11 these neurons account for 40% of all L1 sensory neurons with a peak of expression at E11.5 (Phillips and Armanini, 1996, White et al., 1996). Their proportion drops to around 8% at E13 and remains constant into adulthood (Farinas et al., 1998).

The changes in *Ntrk1* expression in this analysis were a bit trickier to interpret, as they were not statistically significant due to a high variation in expression in different biological samples at E13.5 (Figure 3.2B). A technical cause such as an inhibitory effect on reverse transcription or on PCR amplification efficiency in this particular sample cannot be ruled out but is unlikely, for all samples were processed simultaneously using the same reagents. A biological explanation concerning differences in developmental stages of the mouse embryos used for the analysis is also unlikely since a pool of embryos from one litter was used for all three samples per stage. Thus the reason for this observation remains unknown. Nevertheless, in two out of three samples the expression of *Ntrk1* at E13.5 was well above the expression levels at the other stages, thus pointing to a possible peak in mRNA expression of TrkA at this stage. Previous IHC and ISH studies have shown that the amount of $TrkA^+$ neurons increases constantly during development until it reaches a peak of expression at early postnatal stages in mice. It was reported that $TrkA^+$ cells could be detected as early as E10.5 in mouse DRGs. At E11 20% of L1 DRG cells were $TrkA^+$ and at E11.5 50% of the cells were positive for TrkA mRNA (White et al., 1996). At E13 and E15 80% of cells are $TrkA^+$ and in neonatal mice TrkA mRNA expression was detected in around 80-90% of cells. Their proportion drops to 60% at P7 and 40% in adult mice (Molliver and Snider, 1997,

Farinas et al., 1998, Ernsberger, 2009). In this study we observed a possible peak in *Ntrk1* expression at E13.5 and a decrease in expression at E14.5, back to the E12.5 levels. This is in contrast to previous studies. The discrepancies between the present results and previous findings might stem from the nature of the used techniques. Whereas this study accurately quantifies mRNA present in total DRGs, previous studies are merely based on cell counts and not intensity of the staining. Therefore a peak in expression might be caused by higher amounts of mRNA in individual neurons at E13.5, which would have not been picked up by cell counts alone. The possible drop back at E14.5 would be likely due to a down regulation of mRNA expression in individual cells and increased proliferation of non-neuronal cells such as SGCs in DRGs. In fact in birthdates studies Lawson *et al.,* have demonstrated that the generation of non-neuronal cells in the mouse DRGs begins at around E10-11 and that it shows a peak in proliferation at around E13 (Lawson and Biscoe, 1979).

Our results for TrkB and TrkC strongly agree with documented Trk gene expression in rodent embryonic DRGs and confirm the validity of the qPCR array. Especially the differences in expression levels not only between developmental stages, but also between the genes agree with previously reported studies. The differences between the present data and reported findings for TrkA might be due to the differences in the nature of the used techniques as described above. Nevertheless, as reported, the gene expression levels of TrkA were well above both TrkB and TrkC genes at all three developmental stages as expected. This unique Trk expression profile was further used for a comparison to RPTP gene expression as an indication of possible coexpression and hence potential interaction of the encoded proteins (chapter 4).

3.3.1.3. PTP gene expression in murine embryonic DRGs

The qPCR arrays were used to create a quantitative gene expression profile of 96 of 106 known PTPs (Alonso et al., 2004) in E12.5, 13.5 and 14.5 murine DRGs. We have analysed the gene expression of all known classical PTPs comprising 21 RPTPs and 17 NPTPs (Figure 3.4) and 52 of the 60 known DSPs. The latter group consists of the class I Cys-based DSPs comprising MKPs the atypical DSPs, PRLs, SSHs, CDC14s, PTENs and MTMs (Figures 3.3A and B), the class III Cys-based CDC25 subfamily and the single class II Cys-based LMPTP *Acp1* (Figure 3.3C). The expression levels of different RPTP genes cannot be strictly speaking compared with each other directly due

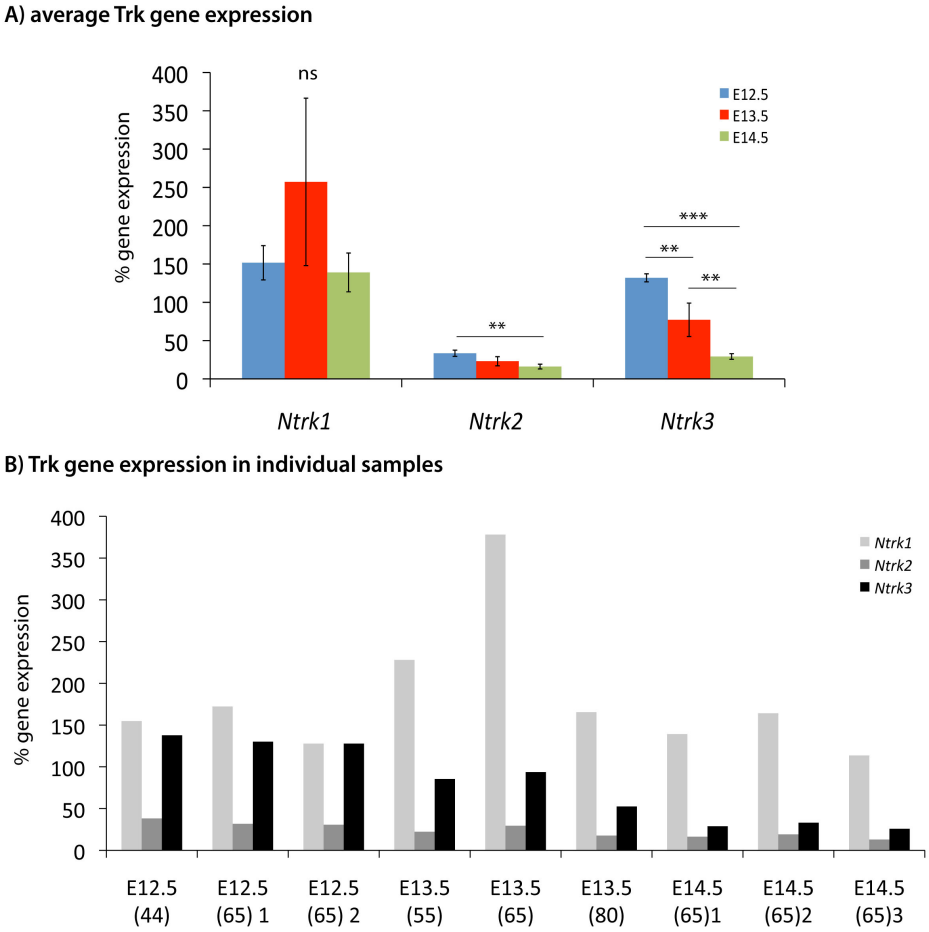

Figure 3.2. qPCR analysis of Trk gene expression during DRG development.

Expression of *Ntrk1*, *Ntrk2* and *Ntrk3* encoding TrkA, B and C respectively was measured in murine embryonic DRGs at the developmental stages E12.5, 13.5 and 14.5 using qPCR arrays. Results of the relative quantification analysis are displayed as $2^{-\Delta CT}$ % gene expression relative to the HKG set. **A)** Average Trk gene expression in E12.5 (blue), 13.5 (red) and 14.5 (green) murine DRGs. SD and statistical analysis (ANOVA) included in the graph with $p > 0.05$ non-significant (ns), $0.01 < p < 0.05$ significant (∗), $0.001 < p < 0.01$ very significant (∗∗) and $p < 0.001$ extremely significant (∗∗∗). **B)** Trk gene expression in individual DRG samples. The approximate amounts of used DRGs in the samples are included behind the sample names in brackets.

to possible differences in the efficiencies of the PCR reactions. However, our results from the previously described Trk expression analysis have demonstrated that the different levels in Trk gene expression in fact mostly agree with previous findings and thus allow at least a careful inter-gene analysis. Therefore to create a broad expression profile of the PTPs in DRGs I have divided the different expression levels into five categories: "extremely high" gene expression relative to the HKGs for values above 60%, "very high" levels for values between 30 and 60%, "high" levels for values between 15 to 30%, "moderate" levels for values between 5 and 15%. Values below the set threshold of 5% were seen as too low to be of much interest for this study, since any *in situ* analysis would likely be impractical. The actual means of gene expression were included in brackets for reference.

In general the gene expression of all PTPs appeared to be very dynamic with decreasing, increasing or stable expression levels across development. Each PTP subfamily contained members that showed expression levels above the set threshold of 5% gene expression relative to the HKGs.

Overall seven PTPs showed "extremely high" gene expression above 60%, which represents only 7% of all analysed PTPs. These highly expressed PTPs comprised the two RPTP genes *Ptprf* (355% mean relative gene expression) and *Ptprs* (156%), which were the most prevalent genes identified in DRGs across all analyzed developmental stages, the two PRL phosphatases *Ptp4a2* (122%) and *Ptp4a1* (75%), a further RPTP *Ptprr* (94%), and *Pten* (75%) and *Dusp11* (65%).

Approximately 9% of all PTPs were expressed at "very high" levels (30 and 60%), 26% at "high" levels (15 to 30%), 29% of PTPs at "moderate" levels (for 5 to 15%) and the highest proportion of 30% were expressed below the set threshold of 5%. However, since the relative comparative ΔC_T method was used for analysis, low percentage does not necessarily represent low gene expression *per se* but a large difference between the C_T value of the PTP gene and the C_T value of the set of HKGs. This means, if a strongly expressed HKG is chosen, the percentage of expression will be consequently smaller. Additionally, all these data were retrieved from whole DRGs and as described above it is possible that some of the PTPs are expressed for instance at high levels in a small proportion of cells, but show overall low or moderate expression in the whole DRGs. This latter issue was addressed using ISH (section 3.3.3 below).

3.3.1.3.1. DSP gene expression

In the present analysis most members of the PRL, MTM, PTEN subfamilies and *Acp1* showed the highest expression levels among all analyzed DSPs, followed by several members of the MKPs and atypical DSPs and at last the SSHs, CDC14s and CDC25s with the lowest, but still moderate expression levels. Members of specific DSP subfamilies show similar substrate specificities and functions, but differ in their expression patterns (for more details on PTP categorization see section 1.3). They will be described as whole subfamilies, whereas RPTP gene expression, the focus of this thesis, will be described in more detail.

Two of the three members of the PRL subfamily were among the highest expressed PTP genes in DRGs. *Ptp4a1* (122%) and *Ptp4a2* (78%) were both expressed at extremely high levels with a significant decrease in expression at the analysed stages. In contrast to this the third member *Ptp4a3* was expressed at moderate levels (13%) with no significant changes in gene expression. These phosphatases are expressed in a variety of tissues and exhibit diverse functions and therefore a role in normal tissue homeostasis has been suggested (Dumaual et al., 2006).

MTMs, PTENs and Acp1 are all involved in many homeostatic and metabolic signalling pathways, such as cell growth and survival, development and differentiation, cell migration and motility and metabolism. Thus their presence in DRGs was not unexpected.

Most members of the MTM subfamily were expressed at high levels in murine embryonic DRGs. Of the thirteen analysed MTMs four showed very high expression levels (*Mtmr2, Mtmr4, Mtmr9* and *Sbf2*) and three high expression levels (*Mtmr6, Mtmr7* and *Sbf1*). Three MTMs (*Mtmr1, Mtmr3* and *Mtmr12*) were expressed at moderately high levels and the remaining three MTMs (*Mtm1, Mtmr10* and *Mtmr11*) were expressed below the threshold at all embryonic stages. All MTMs showed a significant decrease or no changes in gene expression. MTMs comprise both catalytically inactive and active phosphatases, which are known to dephosphorylate phosphoinositides that are implicated in proliferation, differentiation and transport (Laporte et al., 2003).

Acp1 was expressed at very high levels (56%) and was among the highest expressed PTPs in DRGs at the analyzed stages. It also showed a significant decrease in

gene expression (Figure 3.3C). The low molecular weight phosphatase Acp1 is ubiquitously expressed in a variety of tissues and is known to regulate many TKRs such as PDGFR and EphR and is involved among other processes in growth inhibition (Kikawa et al., 2002, Raugei et al., 2002).

Among the four members of the PTEN subfamily the two phosphatases *Pten* (75%) and *Tns1* (23%) were expressed at extremely high and high levels respectively. *Pten* expression did not change significantly during development. Whereas uniquely among all analysed PTPs (RPTPs not included) *Tns1* expression doubled at each developmental stage, which might indicate an expression in non-neural cells and will be discussed later. The remaining two phosphatases from this subfamily *Tenc1* and *Tns3* (both 6%) were expressed at moderate levels and showed a decrease in expression during development. The PTEN family members are all tumour suppressors that modulate signalling pathways such as the PI3 kinase pathway and inhibit cell proliferation, growth, migration and survival (Leslie and Downes, 2004).

The MKPs and the atypical DSPs apart from *Dusp11* displayed slightly lower gene expression levels than the previously mentioned subfamilies, with the majority of the members showing a decrease or no change in gene expression. Both subfamilies are involved in a wide range of important cellular processes such as gene expression, differentiation, proliferation and cell survival, which are among others controlled by Trk signalling. Thus their expression in DRGs was also not surprising.

Among the ten analysed members of the MKP subfamily *Dusp1* showed highest expression (35%), four MKPs showed high expression levels (*Dusp4, Dusp6, Dusp7* and *Dusp8*), two MKPs (*Dusp10* and *Dusp16*) were expressed at moderate levels and only three MKPs were expressed below the threshold (*Dusp2, Dusp5* and *Styxl1*). Most MKPs showed a significant decrease or no changes in gene expression except *Dusp10*, which showed a significant peak in expression at E13.5. MKPs regulate MAP kinases.

Among the 15 atypical DSPs, four phosphatases were expressed below the threshold and the remaining PTPs were expressed at moderate to high levels with the exception of *Dusp11*, which showed very high expression levels (65%). Most members of this subfamily showed a decrease in gene expression or no significant changes, except *Dusp26* and *Styx* with a significant peak at E13.5 and *Dusp15* and *Dusp23* with a

significant increase in gene expression. The atypical DSPs have a broad substrate specificity ranging from proteins to mRNA; the latter is a substrate of *Dusp11*.

The SSHs, CDC14s and CDC25s, showed the lowest gene expression profile compared to other DSP subfamilies. The three SSHs were expressed at moderately high levels. *Ssh1* and *Ssh2* showed a significant decrease in expression whereas *Ssh3* expression increased. The four members of the CDC14 subfamily were all expressed at low levels with half of them even below the threshold. And all four showed significant decrease in gene expression. Two of the three PTPs from the class III Cys-based CDC25 subfamily (*Cdc25a, Cdc25b* and *Cdc25c*) showed a mean expression level above the threshold (Figure 3.3C) and a very significant decrease in gene expression across the analysed stages. These phosphatases are involved among other processes in actin dynamics and cell cycle regulation, and their expression profile possibly indicates that the proportion of proliferating cells in the DRGs decreases across development.

To sum up, several of the DSP genes show high expression levels with an interesting pattern in murine embryonic DRGs. Most DSPs are implicated in crucial signalling pathways and thus not surprisingly in human diseases, especially in cancerogenesis and neurological disorders (Pulido and Hooft van Huijsduijnen, 2008, Patterson et al., 2009). It would be interesting in future to analyse, whether their expression is specific to this tissue or rather ubiquitous and what roles they might play and whether some of them are also implicated directly and specifically in Trk signalling.

3.3.1.3.2. NPTP and RPTP gene expression

The classical Tyr-specific PTPs NPTPs and RPTPs play important roles in many different signalling pathways and their expression and function has been extensively studies in a variety of tissues among others in DRGs. In this study the gene expression levels of the 17 known murine NPTPs were relatively high for the majority of phosphatases and at similar levels as of the MKPs (Figure 3.4A). Among all NPTP genes *Ptpn12* was the most abundant (34%). The seven NPTPs *Ptpn1, Ptpn2, Ptpn3, Ptpn9, Ptpn11, Ptpn13* and *Ptpn23* were expressed at high levels and *Ptpn4* and *Ptpn5* at moderate levels. The seven remaining NPTPs were expressed below the threshold of 5% with *Ptpn6, Ptpn7, Ptpn18, Ptpn20* and *Ptpn22* even below 1%. Overall the majority of NPTPs showed a decrease in gene expression during development with the

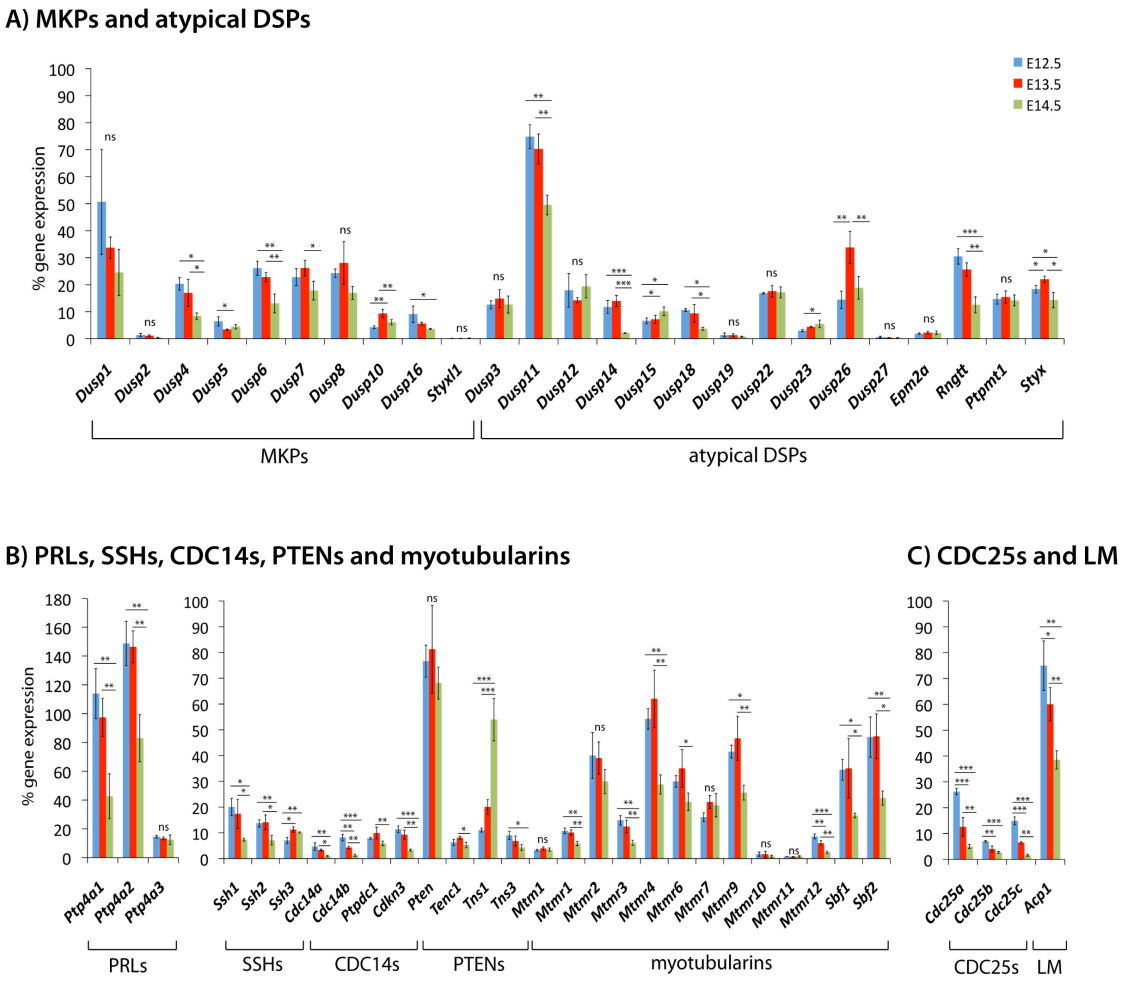

Figure 3.3. QPCR analysis of PTP gene expression during DRG development I.

PTP gene expression was measured in murine embryonic DRGs at the developmental stages E12.5 (blue), 13.5 (red) and 14.5 (green). Displayed are relative gene expression levels of **A)** MKPs and atypical DSPs, **B)** PRLs, SSHs, CDC14s, PTENs and MTMs and C) CDC25s and the LM PTP. Gene expression levels were calculated as $2^{-\Delta CT}$ % relative to the HKG set. SD and statistical analysis (ANOVA) were included in the graphs and categorized as following: $p > 0.05$ non-significant (ns), $0.01 < p < 0.05$ significant (∗), $0.001 < p < 0.01$ very significant (∗∗) and $p < 0.001$ extremely significant (∗∗∗).

exception of *Ptpn5, Ptpn20* and *Ptpn22*, which revealed a significant increase. NPTPs are involved in many important signalling mechanisms, for instance they modulate growth factor signalling pathways in the immune system, metabolism and the nervous system. They control cell adhesion and motility, and are implicated in the onset of many diseases such as cancer, diabetes and neurodegenerative disorders. NPTPs, which were at least moderately expressed in DRGs in the present study, were all implicated in signalling pathways in the nervous system. The highest expressed NPTP in DRGs PTP-PEST (*Ptpn12*) is a ubiquitously expressed regulator of integrin signalling, which is especially highly expressed during development and is implicated in vascularisation and neurogenesis (Sirois et al., 2006). Another highly expressed PTP SHP-2 (*Ptpn11*) is a known oncogene, which is implicated in several types of leukaemia and in neuroblastoma and developmental disorders (Ostman et al., 2006). Most importantly for my analysis SHP-2 has also been identified as a mediator of TrkA and TrkB signalling *in vitro* (Yamada et al., 1999, Chen et al., 2002). NPTPs, which were expressed at the lowest or almost undetectable levels, were implicated in many signalling pathways other than the nervous system, such as in haematopoiesis and the immune system, apart from SHP-1 (*Ptpn6*), which was identified in the CNS especially in glia cells but not in the PNS (Horvat et al., 2001). Altogether, some of the NPTPs are likely to be specifically involved in Trk signalling and could be analysed in future.

The analysis of the expression of all 21 known RPTP genes, the focus of this thesis, revealed that *Ptprf, Ptprs* and *Ptprr* were the most abundant PTPs in DRGs as mentioned above (Figure 3.4B). *Ptpra* was expressed at very high levels (40%) followed by *Ptpro* (28%), *Ptprz1* (22%), *Ptprn* (20%), *Ptprd* (18%) and *Ptprg* (16%) with high expression levels. *Ptprn2, Ptprj, Ptprk* and *Ptprm* showed moderate to low expression levels. The remaining eight RPTPs *Ptprb, Ptprc, Ptpre, Ptprh, Ptprq, Ptprt, Ptpru* and *Ptprv* showed expression levels at all developmental stages below the cut-off of 5%. Overall the thirteen RPTPs *Ptprf, Ptprs, Ptprr, Ptpra, Ptpro, Ptprz1, Ptprn, Ptprd, Ptprg, Ptprn2, Ptprk, Ptprj* and *Ptprm* were detected above the threshold in DRGs during development. Then again it is important as previously stated to keep in mind that we have analysed the expression in whole DRGs and that the expression of some RPTPs in specific cell populations within the DRGs might be different. For instance an RPTP gene with low expression levels in our screen might be in fact strongly expressed in a small specific subpopulation of cells within the DRGs, but its

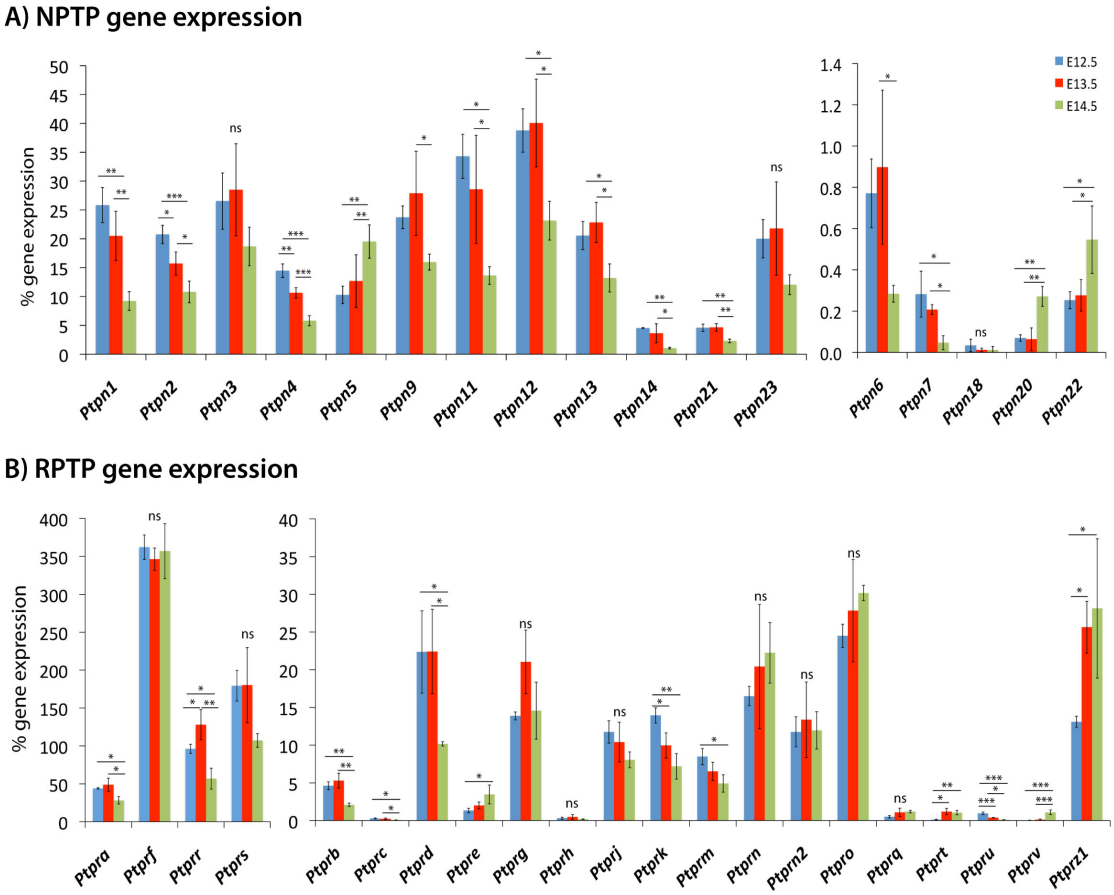

Figure 3.4. QPCR analysis of gene expression during DRG development II.

A) NPTP and **B)** RPTP gene expression in murine embryonic DRGs was measured at the developmental stages E12.5 (blue), 13.5 (red) and 14.5 (green). Results of the relative quantification analysis are displayed as mean $2^{-\Delta CT}$ % gene expression relative to the HKG set. SD and statistical analysis (ANOVA) were included in the graphs and categorized as following: $p > 0.05$ non significant (ns), $0.01 < p < 0.05$ significant (∗), $0.001 < p < 0.01$ very significant (∗∗) and $p < 0.001$ extremely significant (∗∗∗).

expression was diluted out in the analysis of whole DRGs. The analysis of the expression profiles of the RPTPs across the analyzed developmental stages revealed three different patterns. *Ptpra, Ptprb, Ptprc, Ptprd, Ptprk, Ptprm* and *Ptpru* demonstrated a significant decrease, whereas *Ptpre, Ptprt, Ptprv* and especially *Ptprz1* showed a significant increase in expression during development similar to the previously mentioned DSP gene *Tns1*. The remaining nine RPTP genes *Ptprf, Ptprs, Ptprg, Ptprh, Ptprj, Ptprn, Ptprn2, Ptpro* and *Ptprq* did not reveal any significant changes in expression across analysed developmental stages (Figure 3.4B). These patterns will be compared to Trk gene expression patterns in the following chapter (Chapter 4).

The eleven candidate RPTP genes, the strongly expressed genes *Ptprf, Ptprs, Ptprr, Ptpra, Ptpro, Ptprz1, Ptprd, Ptprg* and the marginal candidate genes *Ptprk, Ptprj* and *Ptprm*, were further analysed using ISH (section 3.3.3). *Ptprn* and *Ptprn2,* despite being positive in the qPCR analysis, were omitted from the final candidate gene set. This will be discussed later in this chapter together with the function and reported expression of the candidate RPTP genes.

3.3.2. RPTP and Trk gene expression analysis – a pilot exon microarray study

Another very popular high-throughput technique to study gene expression is microarray analysis. It allows the analysis of thousands or even millions of genes in parallel in one sample. However, it is widely known that microarray chips also suffer from high batch-to-batch variability and poor sensitivity and specificity depending on the hybridization efficiency of the probes. Thus such experiments always require further validation of the results for instance using qPCR. Several different chip types have been developed such as the commonly used 3' microarrays and the recently developed exon microarrays. The latter was tested in the present study. An exon microarray provides in addition to a global gene expression analysis, also information about differently spliced isoforms, and due to its design it compensates for some of the mentioned drawbacks. Each probe set consists on average of four different probes, which cover a specific region of an exon, and around four different probe sets cover different parts of the exon. Additionally probes are selected across the entire length of the transcript (for more

details see section 3.2). For these reasons the exon array represents a robust gene-level analysis and is not biased towards the 3' end unlike traditional 3' microarrays.

In a pilot microarray experiment to analyse PTP gene expression in DRGs I have tested the GeneChip® Mouse Exon 1.0 ST array (Affymetrix). However, due to several limitations of this experiment such as that several genes of interest were only covered by probes with low confidence ("extended probes"), as well as time intensive and challenging data analysis and high costs, this experiment was not extended to a multi-chip study. Instead, the semi-automated qPCR arrays, specifically set up for PTP gene expression analysis, became available and were then used (section 3.3.1). Nevertheless, the pilot microarray analysis was performed on an E12.5 murine DRG sample before the qPCR arrays could be used. Thus I have analysed the data obtained from this single exon microarray for several RPTP and the three Trk genes and have finally compared them to the data obtained from the qPCR screen for a partial validation of the results.

To select data I have used a stringent cut-off value of signal intensity $\log_2 7$ for an overall detected expression according to the experience of the Bloomsbury Centre for Bioinformatics, UCL (personal communication). In our analysis this was further justified by the expression of the two HKGs *Psmb2* and *Ubc*, which were both expressed above this threshold, and additionally the expression of *Ptprc* below the threshold (Figure 3.5). *Ptprc* (CD45) is expressed in haematopoietic cell types (Alexander, 2000) and no expression was reported in DRG cells to date.

Two approaches were used for data analysis. In addition to a manual analysis of selected probe sets (Figure 3.5A), I have also used the "global analysis option" of the Expression Console® software (Affymetrix) to retrieve information about global gene expression (Figure 3.5B). In general both methods agreed in their outcome, but differed in the levels of signal intensity for some of the genes. This was due to the rather stringent selection of the probe sets in the manual analysis and the removal of considered outliers. The analysis of the different probe sets additionally provided an overview of the different intensities of specific probe sets, which cover specific exons. However, since only one chip was used, an analysis of the different splice forms was not possible.

Overall, all three Trk genes were expressed at very high levels in murine E12.5 DRGs (Figure 3.5). The majority of all probe sets was expressed not only above the set

threshold but also mostly above the signal intensity of $\log_2 8$. *Ntrk1* was detected only by low confidence "extended probes" on this chip and therefore its expression was evaluated with more caution. The analysis of RPTP gene expression revealed 13 RPTPs with values above the set threshold based on the median of the signal intensity of their probe sets (Figure 3.5) and among these *Ptprf* and *Ptprs* were expressed at the highest levels. All of their probe sets were expressed highly above the threshold with signal intensities of $\log_2 9$ - $\log_2 10$ for *Ptprs* and $\log_2 10$ - $\log_2 11$ for *Ptprf*. *Ptprg* and *Ptprr* showed very high expression levels with the majority of probe sets with signal intensities of $\log_2 8$ - $\log_2 9.5$. *Ptpra, Ptprd, Ptprn* and *Ptpro* were expressed at relatively high levels with the majority of signal intensities between approximately $\log_2 7.5$ and $\log_2 9$.

The RPTP genes *Ptprj, Ptprk, Ptprm, Ptprn2* and *Ptprz1* were expressed only moderately with most signal intensities between $\log_2 7$ and $\log_2 8$. The remaining eight RPTP genes *Ptprb, Ptprc, Ptpre, Ptprh, Ptprq, Ptprt, Ptpru* and *Ptprv* were expressed below the set threshold, with *Ptprc, Ptprh and Ptprq* with lowest values. *Ptprh, Ptprq* and *Ptprz1* were detected only by low confidence "extended probes".

In summary the results from the microarray analysis agree remarkably well with the results obtained from the qPCR analysis at E12.5 (Table 3.2) and thus validate each other. Both analyses revealed expression of the same RPTP genes *Ptpra, Ptprd, Ptprf, Ptprg, Ptprj, Ptprk, Ptprm, Ptprn, Ptprn2, Ptpro, Ptprr, Ptprs* and *Ptprz1* in murine embryonic DRGs during organogenesis. Differences in expression levels between qPCR and the microarray studies are likely to be caused by alterations in primer efficiencies in the qPCR analysis and the hybridisation strengths to the probes on the chip. Another likely factor could be the detection of different transcripts on the chip and by the primers used for qPCR. However, this point cannot be further addressed, as no information on the detection of different transcripts was available from a single exon microarray. Finally, the agreement between the data sets suggests that indeed the inter-gene comparison in the qPCR is to some extent justified.

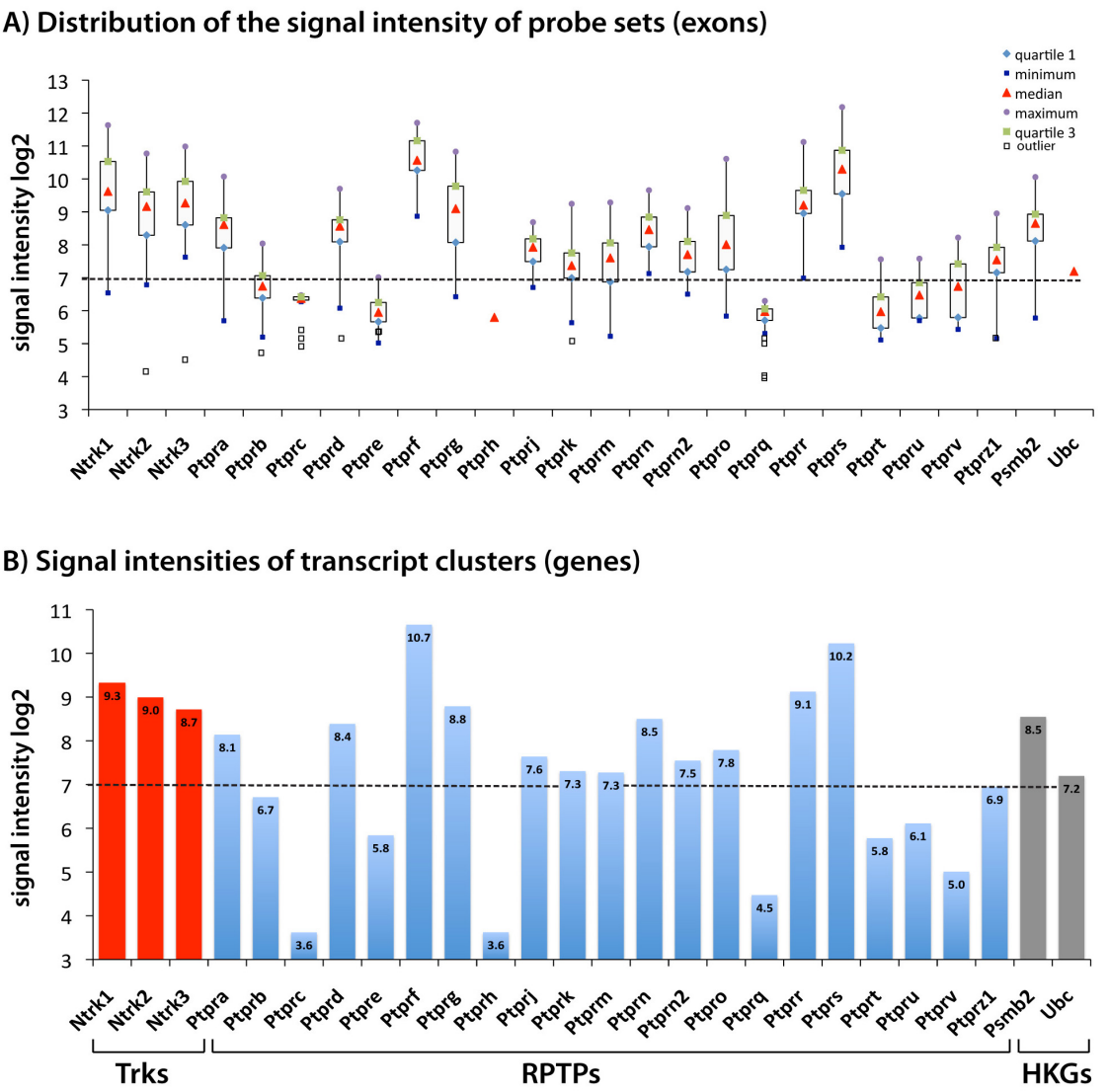

Figure 3.5. Microarray analysis of RPTP, Trk and housekeeping gene expression in E12.5 DRGs.

The expression of RPTP, Trk and housekeeping genes (HKGs) was analysed in E12.5 DRGs from CD-1 mouse embryos using a GeneChip® Mouse Exon 1.0 ST array (Affymetrix). **A**) The box plot represents the distribution of signal intensities (log_2) of detected and stringently selected probe sets (exons) for each transcript cluster (gene) as calculated manually. **B**) Medians of signal intensities (log_2) of transcript clusters as calculated by the Expression Console® software (Affymetrix) are displayed. The differences in several signal intensity values are due to the more stringent selection of probe sets in the manual analysis and the removal of considered outliers. A value of log_2 7 signal intensity was used as a cut-off point to discriminate, whether genes were present or absent in the sample (see text for more explanations).

GENE SYMBOL	PROTEIN NAME	SIGNAL INTENSITY (GENES)	SIGNAL INTENSITY (EXONS)	MICROARRAY RESULTS	QPCR RESULTS	COMPARISON
Ntrk1	**TrkA**	[9.3]	[9.6]	[+++]	++++	++++
Ntrk2	**TrkB**	9.0	9.2	+++	++	++(+)
Ntrk3	**TrkC**	8.7	9.3	+++	++++	+++(+)
Ptpra	**RPTPα**	8.1	8.6	++	+++	++(+)
Ptprb	**VE-PTP**	6.7	6.7	–	–	–
Ptprc	**CD45**	3.6	6.4	–	–	–
Ptprd	**RPTPδ**	8.4	8.6	++	++	+ +
Ptpre	**RPTPε**	5.8	6.0	–	–	–
Ptprf	**LAR**	10.7	10.6	++++	++++	++++
Ptprg	**RPTPγ**	8.8	9.1	+++	+	++
Ptprh	**SAP1**	[3.6]	[5.8]	[–]	–	–
Ptprj	**DEP-1**	7.6	7.9	+	+	+
Ptprk	**RPTPκ**	7.3	7.4	+	+	+
Ptprm	**RPTPμ**	7.3	7.6	+	+	+
Ptprn	**IA-2**	8.5	8.5	++	++	++
Ptprn2	**IA2β**	7.5	7.7	+	+	+
Ptpro	**PTP-BK**	7.8	8.0	++	++	++
Ptprq	**PTPS31**	[4.5]	[6.0]	[–]	–	–
Ptprr	**PTPRR**	9.1	9.2	+++	++++	+++(+)
Ptprs	**RPTPσ**	10.2	10.3	++++	++++	++++
Ptprt	**RPTPρ**	5.8	6.0	–	–	–
Ptpru	**RPTPλ**	6.1	6.5	–	–	–
Ptprv	**OST-PTP**	5.0	6.7	–	–	–
Ptprz1	**RPTPζ**	[6.9]	[7.5]	[+]	+	+

Table 3.2. Comparison of microarray and qPCR results in E12.5 murine DRGs.

Displayed are $\log_2$ signal intensity (si) values of probe sets (exons) as calculated manually and of transcript clusters (genes) as calculated by Expression Console® software (Affymetrix). These results were compared to the qPCR analysis of RPTP and Trk gene expression in murine E12.5 DRGs. The genes *Ntrk1*, *Ptprh*, *Ptprq*, *Ptprz1* were covered only by low confidence "extended probes" on the microarray chip and were therefore considered with caution (in square brackets "[ ]"). Keys for evaluation of qPCR expression levels (x) and $\log_2$ signal intensity (si) in microarrays:

++++ (extremely high)	$x > 50\%$	$si > \log_2 10$
+++ (very high)	$0\% > x > 30\%$	$\log_2 10 > si > \log_2 9$
++ (high)	$30\% > x > 15\%$	$\log_2 9 > si > \log_2 8$
+ (moderate)	$15\% > x > 5\%$	$\log_2 8 > si > \log_2 7$
– (low)	$5\% > x$	$\log_2 7 > si$

3.3.3. ISH analysis of Trk and RPTP gene expression

ISH is a powerful technique to visualize mRNA expression on the cellular level and so provides information about the location of mRNA transcripts. In this study I have used chromogenic ISH to confirm the results obtained from the quantitative analysis in addition to the analysis of the location of gene expression in the DRGs. Negative sense ISH controls were performed for all analysed Trk and RPTP genes with the exception of *Ptprg* and *Ptprz1* due to unknown transcription plasmids. Pictures are provided in the appendix (Appendix, Figure 3). The results from this analysis were also compared and complemented with entries from the recently developed database GenePaint (http://www.genepaint.org) (Visel et al., 2004), which contains a public collection of pictures of ISH sagittal sections from E14.5 C57BL/6 mouse embryos of almost all PTPs (Appendix, Figure 4).

3.3.3.1. RPTP genes, which were expressed in DRGs

The ISH analysis showed extremely high to very high expression of the three Trk genes in the DRGs at all analysed developmental stages in agreement with the quantitative analysis (Figure 3.6C). *Ntrk1* was expressed in the majority but not all cells in the DRGs at all analyzed stages. *Ntrk2* and *Ntrk3* expression was restricted to a specific subpopulation of DRG cells scattered within the DRGs with more $Ntrk3^+$ than $Ntrk2^+$ cells present. The proportion of both $Ntrk3^+$ and $Ntrk2^+$ cells appears to decrease during development. However, no cell counts were performed at this point. These results are in strong agreement with previously reported findings (see section 3.3.1).

High expression in DRGs, as estimated by quantitative analysis, of the candidate RPTP genes *Ptpra, Ptprd, Ptprf, Ptprg, Ptpro, Ptprr* and *Ptprs* was also confirmed by ISH (Figure 3.6A). The sense riboprobes did not provide any specific staining (Appendix, Figure 3).

Ptprf was expressed in most cells in the DRGs without apparent changes in their amount between E12.5 and E14.5. Previously *Ptprf* expression was documented in embryonic and adult murine DRGs (Schaapveld et al., 1998) specifically in neurons but not in any non-neural cells (Longo et al., 1993, Zhang et al., 1998).

Ptprs was expressed rather ubiquitously in almost all tissues but with most hybridised riboprobes in specific cells within DRGs. *Ptprs* expression was previously

found in proliferating and differentiated neurons in DRGs in embryonic and adult rodents (Yan et al., 1993, Wang et al., 1995, Haworth et al., 1998, Schaapveld et al., 1998, Van Vactor, 1998).

Ptprd expression was also detected in DRGs at all three embryonic stages. The results retrieved from the GenePaint database also demonstrate that *Ptprd* is expressed in E14.5 DRGs in the mouse (Appendix, Figure 4). Surprisingly, in contrast to these findings Shaapveld *et al*. reported no expression of *Ptprd* in murine E14.5 DRGs using the same riboprobe (Schaapveld et al., 1998). In our analysis *Ptprd* staining was also very weak to almost undetectable on some sections. To analyse whether this might be due to the location within the DRG or whether there is a difference between different DRGs depending on their position in the embryo (cervical or thoracic) ISH was performed on sagittal sections (see chapter 4 Figure 4.4). However, no differences were detected between DRGs. Potentially this might be due to a more rapid degradation of *Ptprd* mRNA in comparison to other RPTPs for unknown reasons. Therefore particular care is needed when using the *Ptprd* probe in these studies.

Ptpro was strongly expressed in the quantitative analysis, and ISH analysis showed very high expression of *Ptpro* in large and medium sized cells in the DRGs (Figure 3.6A). The neuronal *Ptpro* isoform has been previously detected in a specific subset of neurons in dorsal root, cranial and sympathetic ganglia and in specific brain areas (Haworth et al., 1998, Beltran et al., 2003).

Ptpra was ubiquitously expressed in the mouse embryos with stronger expression in DRGs. The quantitative analysis showed a decrease in the expression levels at E14.5 compared to E13.5, but no obvious changes were seen on the *in situ* hybridized sections (Figure 3.6A). *Ptpra* expression was found in DRG neurons at all three developmental stages and in adult rodents with a peak in expression at E13.5 (den Hertog et al., 1996, Haworth et al., 1998, Van Vactor, 1998).

Ptprg was moderately expressed in the quantitative analysis with no significant changes during development. Its expression in DRGs was also detected with ISH, but the staining was not very strong, and possibly restricted to specific cells within the DRGs (Figure 3.6A). Previously this phosphatase was detected in neurons in the murine embryonic CNS such as pyramidal neurons and in DRGs at E14.5 and E17.5 (Lamprianou et al., 2006).

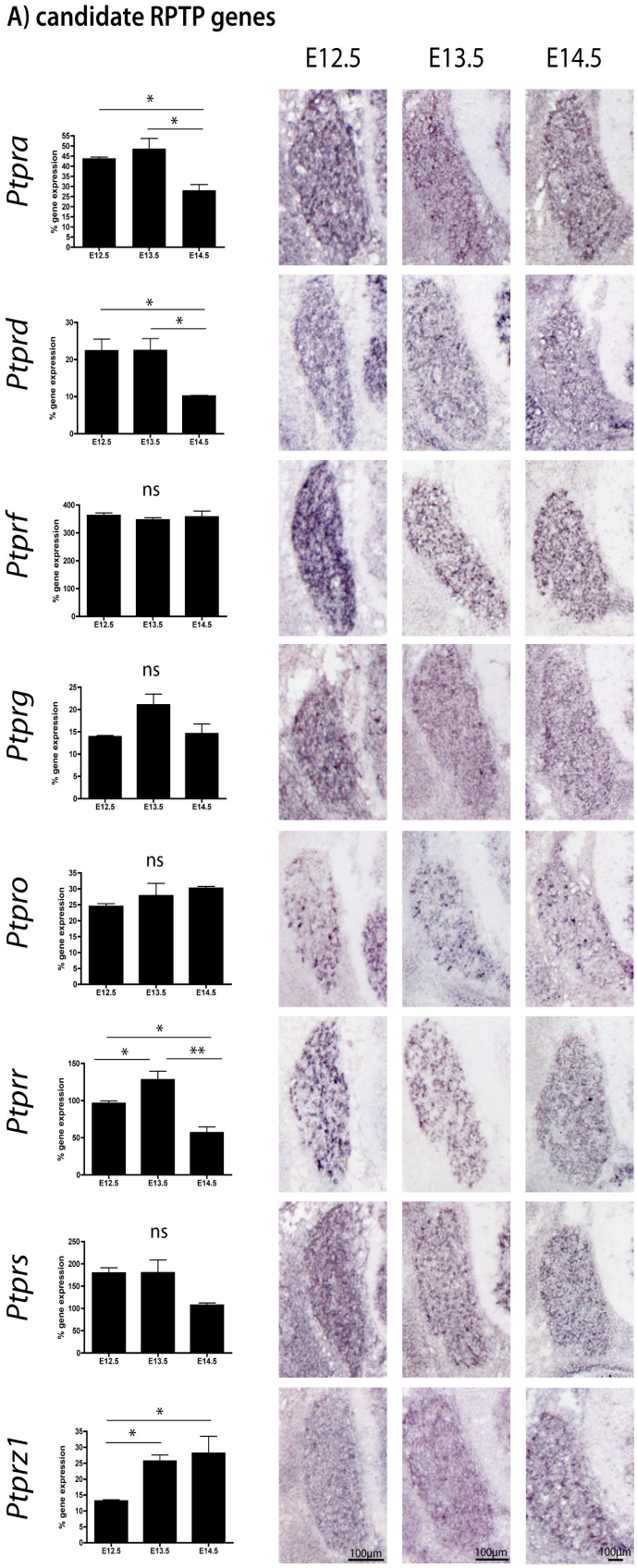
A) candidate RPTP genes
E12.5
E13.5
E14.5
Ptpra
Ptprd
Ptprf
Ptprg
Ptpro
Ptprr
Ptprs
Ptprz1
% gene expression
ns
100µm

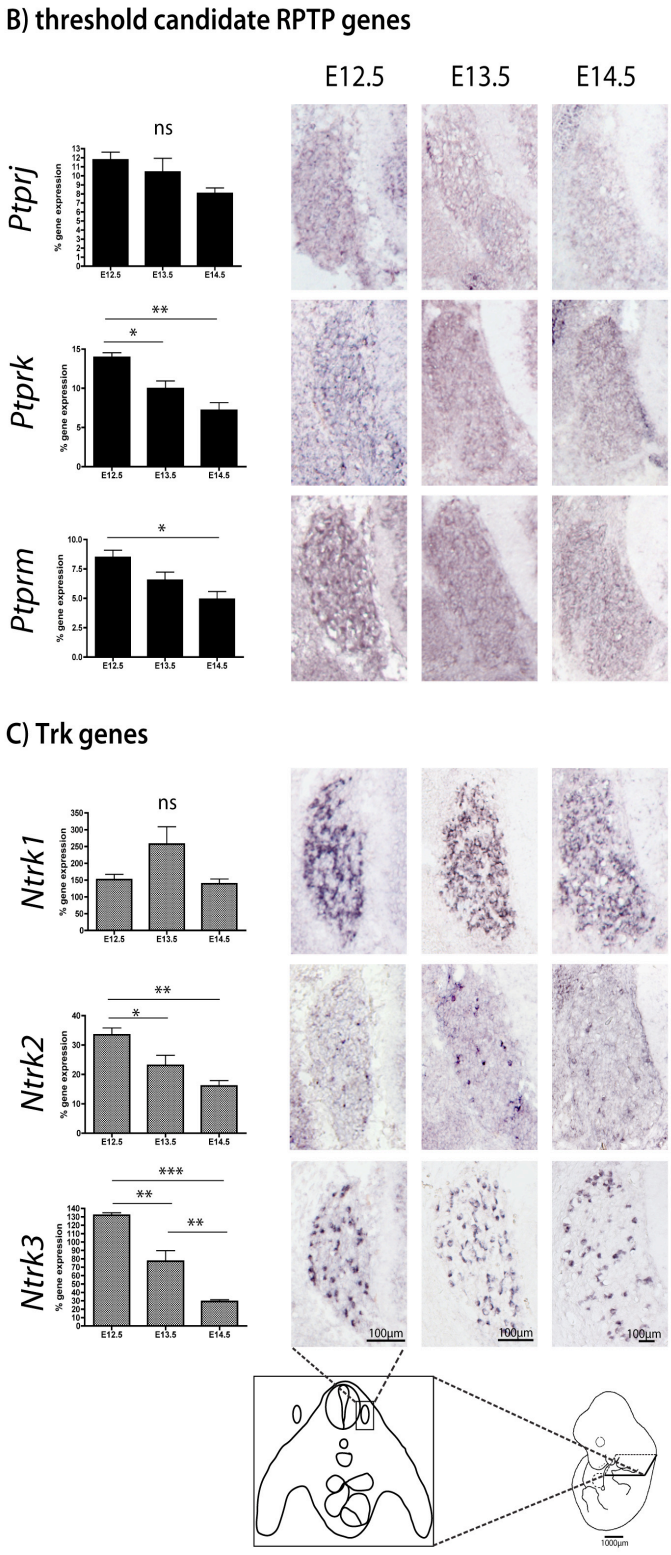

Figure 3.6. qPCR and ISH analyses on murine embryonic DRGs.

To confirm the qPCR analysis ISH was performed on transverse cryosections through limb regions of mouse embryos at the developmental stages E12.5, E13.5 and E14.5. Displayed are the results from the qPCR (graphs) and ISH analyses (DRGs) of **A**) eight candidate RPTP genes (*Ptpra, Ptprd, Ptprf, Ptprg, Ptpro, Ptprr, Ptprs* and *Ptprz1*), **B**) threshold candidate RPTP genes (*Ptprj, Ptprk* and *Ptprm*) and **C**) Trk genes (*Ntrk1, Ntrk2* and *Ntrk3*). The sense probes did not provide any specific staining (Appendix, Figure 3).

Ptprz1 was expressed at moderate levels in the qPCR screen and its expression patterns showed an interesting increase during development (Figure 3.6A). ISH staining of *Ptprz1* was not particularly strong and was developed for several days in comparison to few hours for most other riboprobes. However, *Ptprz1* expression in DRGs could be confirmed. The used riboprobe detected the long transmembrane isoform specifically, but similar results were obtained with a riboprobe that hybridized to all three known isoforms (data not shown). In agreement with the presented results, some staining could also be detected in DRGs on the E14.5 sagittal embryo section retrieved from GenePaint (Appendix, Figure 4), but the staining was very faint especially in comparison to the staining in the VZs in the brain. The expression of this phosphatase in DRGs was previously mostly attributed to SGCs (Haworth et al., 1998).

The candidate gene ***Ptprr*** was strongly and specifically expressed in DRGs in the quantitative analysis and also with ISH. Its expression is significantly downregulated at E14.5 in the qPCR analysis. ISH staining however, does not show an obvious decrease in expression. Only PTPBR7, the longest transmembrane isoform of RPTPR, was previously detected in DRGs during development at the analyzed stages and in adult mice (Van Den Maagdenberg et al., 1999).

The expression of the marginal candidate genes ***Ptprj, Ptprk*** and ***Ptprm*** was very low to almost undetectable in DRGs, in agreement with the qPCR analysis (Figure 3.6B). However, ISH is not a very sensitive technique and therefore undetected genes might still be expressed in DRGs at very low levels. To increase the signal levels the probes were left to develop for several days, but this increased the background rather than the actual signal. The riboprobes were additionally tested on brain sections and appeared to hybridize correctly and at significant levels (data not shown). These results also agree with data retrieved from GenePaint (Appendix, Figure 4). In more detail, *Ptprj* was expressed at levels above *Ptprm*, the lowest expressed gene among all candidate RPTPs in the quantitative analysis. However, in the ISH analysis almost no signal could be located within the DRGs for both *Ptprj* and *Ptprm*. *Ptprk* was expressed at slightly stronger levels than *Ptprj* and showed a significant decrease in expression in the quantitative analysis. However, ISH with a riboprobe detecting all isoforms was very weak at E12.5 with slightly increasing levels during development (Figure 3.6B). Whereas RPTPκ was previously detected in small to medium sized neurons in murine

DRGs at E14 (Jiang et al., 1993, Hantman and Perl, 2005), *Ptprm* and *Ptprj* expression in DRGs was not reported to our knowledge.

3.3.3.2. RPTP genes, which were not expressed in DRGs

The genes *Ptprb, Ptprc, Ptpre, Ptprh, Ptprq, Ptprt, Ptpru* and *Ptprv* were expressed below the set threshold in the qPCR screen and were therefore excluded from further ISH analysis in this study. Nevertheless, in order to confirm their low or absent expression in DRGs, which will support our results, I have used ISH data retrieved from the GenePaint database (Appendix, Figure 4) and previous publications.

On *in situ* hybridized sections form the GenePaint database *Ptprb* staining was absent from cells in the DRGs, but it was very strong in specific blood vessels. Indeed previous findings have associated the encoded vascular endothelial tyrosine phosphatase (VE-PTP) as its name suggests with the remodelling of blood vessels and angiogenesis (Baumer et al., 2006). *Ptprc* expression was absent in DRGs and only detectable in the thymus. As mentioned earlier the expression of the encoded CD45 protein was previously detected on all nucleated haematopoietic cells and was shown to play an important role for instance in the activation of T-cells (Alexander, 2000, Hermiston et al., 2003). *Ptpre* expression was detected in the murine NS but not in DRGs. It is expressed in the neural tube of mouse embryos at E12 and later stages and in specific brain areas such as the granular cells of the cerebellum at E14.5. It was suggested to play a role in the differentiation and maturation of these cells (Mukouyama et al., 1997). RPTPε is also involved in osteoclast formation and function (Granot-Attas et al., 2007), negative regulation of insulin receptors (Nakagawa et al., 2005) and in the myelination by Schwann cells through regulation of potassium channels (Peretz et al., 2000). *Ptpru* was not expressed in murine DRGs at E14.5 but it was previously found in various regions of the brain and within the motor columns of the spinal cord in E15.5 rat embryos (Van Vactor, 1998). *Ptprv* was not detected in DRGs of E14.5 mouse embryos (Appendix, Figure 4). The encoded OST-PTP phosphatase was not associated with the nervous system but instead is involved in bone remodelling and is a tumour suppressor and a direct target of p53 (Doumont et al., 2005). *Ptprt* was strongly expressed in the CNS apart from some stained cells in the DRGs (Appendix, Figure 4). Previous studies have shown however, that RPTPρ is exclusively expressed in the CNS, where it is involved in the regulation of synapse function (Lim et al., 2009). *Ptprq* encodes

PTPS31, which is specific for inositol phospholipids. It is expressed and exerts its function in the kidney glomeruli and the inner ear (Goodyear et al., 2003). It was among the lowest expressed genes in the developing DRGs in the qPCR screen. However, no data were available on any public ISH database to validate these results. Nevertheless, no expression has ever been reported in DRGs.

In summary, the results obtained in the quantitative gene expression analysis could be confirmed using ISH, and these data were also largely in agreement with previous reports. The strong candidate genes *Ptpra, Ptprd, Ptprf, Ptprg, Ptpro, Ptprr* and *Ptprs* were highly expressed in DRGs either in almost the entire DRG or in a subset of cells. Surprisingly, weak expression of *Ptprz1* transcripts was detected in DRGs using ISH, whereas moderately high expression was seen in the quantitative analysis. The marginal genes *Ptprj, Ptprk* and *Ptprm* were also almost undetectable in the ISH study in agreement with their low expression in the quantitative analysis.

3.4. Discussion

The aim of this chapter was to identify candidate RPTPs based on their gene expression levels in developing DRGs, which are likely to interact with Trk receptors and might so play a role in neuronal functions such as differentiation, survival and neurite outgrowth.

It is always preferable to analyse the expression of proteins instead of genes as a gene expression analysis merely reports the amount of mRNA present in the tissue. But it does not provide any information of whether the mRNA is in fact translated into active proteins, with correct folding, localization and post-translational modification or proteolytic cleavage. However, an analysis on the protein levels is limited by the availability of specific antibodies. At the moment when this study was conducted no suitable antibodies against RPTP epitopes were available to us and the lack of such antibodies still hinders the field as a whole. Under such circumstances the alternative analysis of gene expression was a valuable starting point to select candidate RPTP genes. A gene expression approach has also the great advantage that a plethora of high-tech and high-throughput techniques exists, which allows the analysis of many genes in parallel.

In the present study three different types of gene expression techniques were used. The high-throughput techniques qPCR arrays and microarrays are very valuable

tools for rapidly analysing a large group of genes, from small amounts of samples. But they also come with caveats and these limitations have to be taken into consideration for the interpretation of the results. As with all such general screening methods, not all of the parameters can be exactly determined, but instead plausible assumptions are made. For instance in the qPCR array the PCR amplification efficiency and the efficiencies of the primers, which have to be similar for target and control genes (HKGs), were not all previously experimentally examined. However, all used primers were commercially obtained as validated assays from Qiagen and Dr. Vasu Akepati (Weismann Institute, Israel) has validated a selection of primers and confirmed their approximately 100% efficiency (personal communication). Additionally the amplification curves of all primers were monitored and appeared to be approximately parallel implying similar qPCR amplification efficiencies. Similar limitations apply to classic microarrays since each individual probe has a different hybridisation affinity. In exon arrays this problem is partly compensated for by the design of the array as described earlier and thus provides a robust gene-level analysis. Since only one single microarray was run, no conclusions about technical and biological repeatability and their statistical robustness could be made. Both the qPCR and the microarrays were used in this study to create a gene expression profile and not for a comparison of individual gene expression under different conditions as is normally done. Although this is a rather unconventional way of data analysis, our data sets from the qPCR and the microarray analyses agreed with each other on the evaluation of RPTP and Trk gene expression and thus support and validate each other. Additionally the expression of all relevant candidate genes was confirmed using ISH. The advantage of this unconventional analysis method is that it allows an estimation of the gene expression levels in the samples, whereas the conventional analysis only provides information about the changes of gene expression under experimental conditions. Thus our analysis was more suitable to us for the selection of highly expressed genes for further study.

Another important point, which needs to be considered for the interpretation of the results, is that gene expression analysis on a mixed population of cells such as in the DRGs used in this analysis lacks information about the location of the mRNA in specific cell types. Although several different techniques are available to separate cells such as fluorescence-activated cell sorting (FACS) or magnetic-activated cell sorting (MACS), most of these techniques require dissociation of DRG cells, which is known to

have a fundamental impact on gene expression and represents rather a regeneration than an *in vivo* system (see chapter 6 for more details). Performing gene expression analysis directly on fresh frozen DRG tissue provides information closer to the *in vivo* state and thus was preferred to the aforementioned selection of specific cell subtypes. Moreover, the main interest of this expression analysis was to select candidate genes for further in-depth coexpression analysis with Trks (chapter 4), which also provided greater spatial information. Therefore the techniques used were well suited for this purpose.

The present study represents the only comprehensive such gene expression analysis of the PTP family and especially of RPTPs in developing sensory ganglia in the mouse at the developmental stages E12.5 to E14.5. Based on the qPCR array and exon microarray analyses I have selected eleven RPTP genes encoding RPTPα, RPTPδ, LAR, RPTPγ, RPTP-BK, RPTPR, RPTPσ, RPTPζ and the marginal candidates DEP-1, RPTPκ and RPTPμ as possible candidate genes and confirmed their expression in DRGs via ISH. The genes of the first eight RPTPs apart from RPTPζ were strongly expressed in both analyses, whereas the expression of DEP-1, RPTPκ and RPTPμ genes was detected in our quantitative analyses, but was almost undetectable in DRGs with the less sensitive ISH method. Expression of all these RPTPs was previously described in different parts of the nervous system of several species during development and in adult organisms. Their function was also implicated in neuronal events such as axon guidance, neurite outgrowth, or neuronal tissue histogenesis during development (section 1.3.3). Therefore their presence in our candidate list was not surprising. All of the candidate RPTPs apart from DEP-1, RPTPμ and also RPTPδ were also previously detected in DRGs (section 1.3.3). A reason for the presence of the latter three RPTPs in our candidate gene panel might be due to the more sensitive qPCR technique we have used compared to previous studies, which were mostly performed with ISH. However, whereas the expression of DEP-1 and RPTPμ was indeed very low in the ISH study, RPTPδ expression was clearly detectable in DRGs and its expression was also documented in the GenePaint databank. RPTPδ plays in fact a role in the nervous system as knockout mice show neuronal abnormalities such as memory deficits, hypomyelination and hyperpotentiation of hippocampal synapses, posture and motor defects (Uetani et al., 1997, Uetani et al., 2000). However, until now RPTPδ was implicated in neuronal adhesion and neurite outgrowth only in CNS neurons (Tuttle et

al., 1999, Wang and Bixby, 1999, Chilton and Stoker, 2000, Sun et al., 2000b). An expression of DEP-1 and RPTPμ in DRGs can be attributed to both non-neural cells and to neurons. DEP-1 belongs to the same PTPR3 subgroup as RPTP-BK, but in contrast to the latter it is usually expressed in hematopoietic lineages, endothelial cells, fibroblasts, and different epithelial and smooth muscle cells. It regulates cell-contact mediated growth, as it is directly related to cell-density (Ostman et al., 1994). It plays additionally an important role in vascularisation (Borges et al., 1996, Autschbach et al., 1999, Schraven, 2000, Jandt et al., 2003) and was shown to dephosphorylate VEGFRs, PDGFRs and EGFRs (Kovalenko et al., 2000, Grazia Lampugnani et al., 2003, Tarcic et al., 2009). Therefore its expression in DRGs might be attributed for instance to the presence of developing blood vessels, which express these kinases. On the other hand recently DEP-1 was also detected in retinal progenitor cells and postmitotic neurons in the mouse retina and a possible role in the regulation of proliferation and differentiation of these cells was suggested (Horvat-Brocker et al., 2008). A similar role of DEP-1 in progenitor cells within the DRGs is hence also possible. Like RPTPκ, RPTPμ is a member of the CAM-like PTPR2B subgroup, which is known to mediate neurite outgrowth and growth cone repulsion. Gene expression of RPTPμ was previously detected in different neurons in the murine CNS, but it was also found to be localized to non-neural cells for instance in blood vessels (Fuchs et al., 1998, Van Vactor, 1998, Chilton and Stoker, 2000). In this respect RPTPμ and RPTPκ were both identified in RGCs (Ledig et al., 1999b, Burden-Gulley et al., 2002, Horvat-Brocker et al., 2008), but only RPTPκ gene expression was also found in specific neurons in murine E14 DRGs (Hantman and Perl, 2005). Further RPTPμ was shown to regulate N-cadherin-dependent neurite outgrowth in chick (Burden-Gulley and Brady-Kalnay, 1999, Ensslen et al., 2003, Major and Brady-Kalnay, 2007). Therefore RPTPμ might possibly play a similar role either in non-neuronal or neuronal cells in developing murine DRGs. The expression analysis of RPTPζ provided us with some interesting results. In our qPCR analysis we observed an increase in RPTPζ gene expression throughout development possibly indicating expression in proliferative cells such as SGCs (Lawson and Biscoe, 1979). Indeed its expression was previously identified in SGCs surrounding large neurons in rat E14 DRGs and other glia cells in the CNS and PNS (Canoll et al., 1993, Shintani et al., 1998, Van Vactor, 1998, Harroch et al., 2000). Nevertheless, RPTPζ expression was previously also documented in a subset of neurons (Harroch et al.,

2000). I have detected only weak staining in DRGs using an ISH probe against all three isoforms in the current study, in contrast to its high expression in the qPCR analysis. Strangely, whereas in one ISH study strong expression of RPTPζ in murine E14 DRGs was reported (Canoll et al., 1996b), another group reported negligible levels of RPTPζ expression in rat E14 (corresponding to E12.5 in mouse) DRGs (Haworth et al., 1998). In the latter study small, scattered RPTPζ-labelled cells were also detected at E18 in rat DRGs and throughout the spinal cord, which is consistent with labelling in non-neural cells.

We have excluded the two catalytically inactive RPTPs IA2 and IA2β, encoded by *Ptprn* and *Ptprn2* respectively (Jiang et al., 1998), from further analysis although both RPTPs were strongly and specifically expressed in DRGs (Appendix, Figure 24). However, these phosphatases were previously only linked to insulin receptors and knockout mice of both phosphatases show no obvious phenotype apart from a glucose intolerance and impaired insulin secretion (Saeki et al., 2002, Kubosaki et al., 2004). The expression of these phosphatases in sensory neurons might be therefore linked to insulin receptors, since insulin-receptor-like receptors (IRR) are expressed in Trk^+ neurons (Reinhardt et al., 1994).

Together, our gene expression analysis has confirmed and expanded the knowledge of the expression patterns of Trk genes in murine embryonic DRGs at the developmental stages E12.5 – E14.5. This comprehensive analysis has further shown that specific RPTP genes are among the highest expressed PTPs in developing murine DRGs, which strengthens the case of their possible implication with Trks in neurons as previously suggested. Based on the gene expression levels in DRGs and on previous reports we have finally selected eleven candidate RPTP genes encoding RPTPα, RPTPδ, LAR, RPTPγ, RPTP-BK, RPTPR, RPTPσ, RPTPζ and the marginal candidates DEP-1, RPTPκ and RPTPμ for further in-depth analysis of their spatial expression (chapter 4). All of these RPTPs were previously implicated in functions of the nervous system and some of them were also suggested and shown to play a role in Trk signalling. In our further analysis we concentrated in particular on the coexpression of these RPTPs with Trk receptors in the same neurons in DRG (chapter 4) as their coexpression would further support a possible role of RPTPs in Trk signalling in neurons and so a function in crucial neuronal processes.

Chapter 4

Coexpression analysis of candidate RPTPs and Trks in murine embryonic DRGs

4.1. Introduction

The quantitative analysis described in the previous chapter provided first insights into the expression levels of RPTP genes in comparison to almost the entire PTP family and the Trk receptors in murine embryonic DRGs during organogenesis (E12.5-14.5). The chromogenic ISH study confirmed these results and provided further valuable information about the location of gene expression in the tissue. Altogether eleven candidate RPTP genes, the strongly expressed genes *Ptprf* (encoding LAR), *Ptprs* (RPTPσ), *Ptprr* (RPTPR), *Ptpra* (RPTPα), *Ptpro* (RPTP-BK), *Ptprz1* (RPTPζ), *Ptprd* (RPTPδ), *Ptprg* (RPTPγ) and the marginal candidates *Ptprk* (RPTPκ), *Ptprj* (DEP-1) and *Ptprm* (RPTPμ) were selected mainly based on their expression levels to further investigate their possible implication in Trk signalling.

A role for the RPTPs LAR, RPTPσ, RPTPR, RPTPα, RPTP-BK, RPTPζ and RPTPγ (see section 1.4) has been previously suggested in molecular studies mainly using over-expression approaches. Only for LAR these experiments were carried out in primary embryonic hippocampal neurons. Also, a coexpression analysis of RPTPs with Trk receptors, which would support a physiological interaction, was previously only performed for RPTP-BK in murine E16 DRGs and TG (Beltran et al., 2003). Together these studies have shown that several RPTPs seem to interact at least with one of the Trk receptors. Therefore the questions arise, whether these Trks are substrates of all of these RPTPs under physiological conditions, suggesting a possible redundancy among RPTPs, and whether RPTPs have a preference towards a specific Trk receptor under physiological conditions (see section 1.4).

The first aim of the experiments in this chapter was hence to compare the temporal and spatial expression patterns of these candidate RPTP genes with the expression of Trk genes in murine embryonic DRGs at E12.5, E13.5 and E14.5. For this purpose I have extended the previously described qPCR analysis (chapter 3) to a comparative analysis of the expression profiles of candidate RPTP genes with Trk genes during development. Further ISH analysis was used to compare the specific spatial expression patterns of Trk and selected RPTP genes not only in DRGs but also in the surrounding tissues.

The second goal was to perform a detailed coexpression analysis of the strongest expressed candidate RPTP genes and Trk genes in the dorsal root sensory neurons of E13.5 mouse embryos using a combination of fluorescent ISH and immuno-fluorescence. As described above a close coexpression of particular RPTPs and Trk members would potentially implicate the encoded enzymes in each other's signalling pathways in sensory neurons during development. In contrast, a lack of close coexpression would suggest that specific RPTPs and Trks are not in tight co-regulatory partnerships or developmentally co-regulated.

4.2. Experimental procedures

4.2.1. qPCR analysis

The qPCR protocols were described in detail in the previous chapter. For data analysis in this chapter the $\Delta\Delta C_T$-method was used. For the relative comparative gene expression analysis between different embryonic stages, $2^{-\Delta\Delta CT}$ values were calculated with $\Delta\Delta C_T$ representing the difference between normalized ΔC_T values to HKGs of two embryonic stages. Hereby each sample from a certain developmental stage was compared to all three samples from the other developmental stage and a SD was calculated. Data were displayed as fold changes ($2^{-\Delta\Delta CT}$). Statistical analysis was performed with Prism 4 (GraphPad Software) as described in section 2.7.

4.2.2. Chromogenic and double fluorescent ISH and immunofluorescence

ISH and immunofluorescence (IF) were performed on transverse cryosections of E13.5 wild type (CD-1) mouse embryos as described in 2.4. The used antibodies were described in tables 2.3. and 2.4. The details of the used riboprobes were summarized in section 3.2.1.

Following ISH and IF cells were counterstained with DAPI to visualize the nuclei and allow counting of total cell numbers. It has to be noted that some of the big neurons (TrkB and TrkC), although positive for Trk staining, did not show nuclei staining, as the section was not going through the nucleus. Additionally, staining detected in red blood cells was an artefact caused by endogenous peroxidase activity.

Pictures were taken and processed as described in section 2.6. Manual cell counting was performed on pictures, whereby only neurons, identified by their big round nuclei, were counted (Figures 1.4 and 4.1). A range of around 200-1400 neurons on 5 to 15 different pictures of randomly selected DRG regions from several embryos were counted per RPTP and Trk combination. The percentage of cells unambiguously positive for RPTP and/or Trk receptors was determined and SDs were calculated.

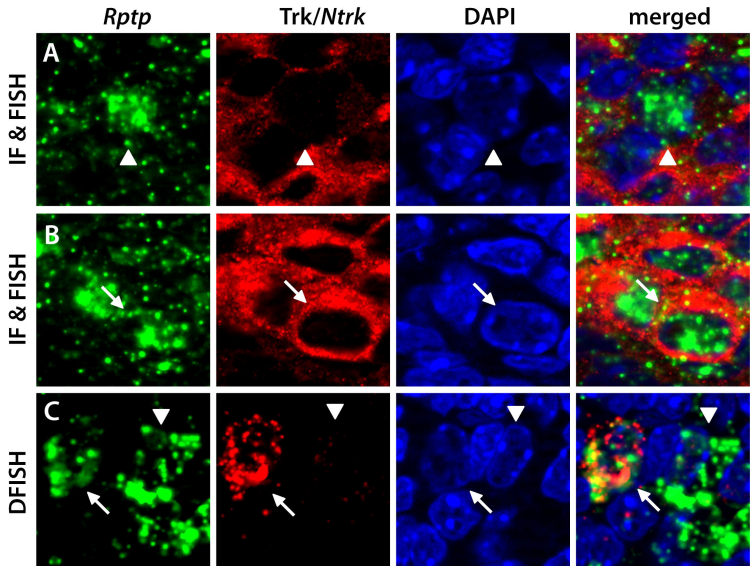

Figure 4.1. Cell counting.
Examples of coexpressing neurons (indicated by arrows) and non-coexpressing neurons (indicated by arrowheads) in the DFISH and IF and FISH expression study.

4.3. Results

4.3.1. Comparison of RPTP and Trk gene expression patterns using qPCR arrays

qPCR arrays were used to compare the expression patterns of RPTP and Trk genes. The analysis revealed that, whereas the expression patterns of some RPTP genes were similar to Trk gene expression, others showed a completely different temporal pattern (Figure 4.2). In this respect the expression pattern of *Ptprr* resembled mostly the expression of *Ntrk1,* while *Ptpra* and *Ptprd* expression and to some extent *Ptprg* expression were mostly similar to the expression of *Ntrk1* and *Ntrk2* together. *Ptprf* and *Ptpro* expression did not change significantly at any embryonic stage unlike any of the

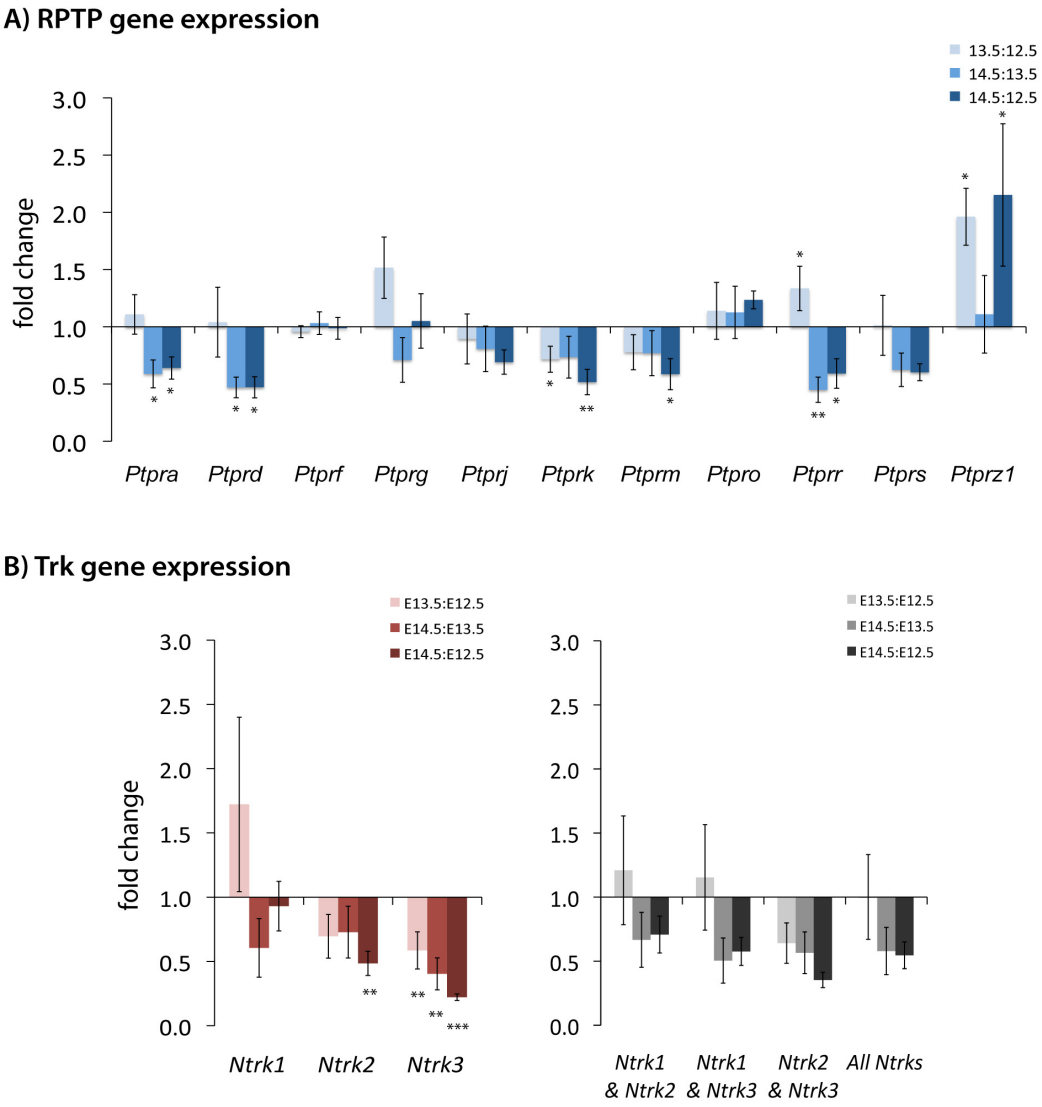

Figure 4.2. Comparison of the gene expression patterns of candidate RPTPs with Trks.

Displayed are fold changes between expression levels at different embryonic stages of **A)** candidate RPTP genes, **B)** individual Trk genes (red) and their combinations (grey), (comparative expression at two chosen stages: E13.5:E12.5; E14.5:E13.5; E14.5:E12.5). Results are displayed as bars representing mean $2^{-\Delta\Delta CT}$ values with SD. Statistical analysis (ANOVA) was included with $p > 0.05$ non-significant (ns), $0.01 < p < 0.05$ significant (∗), $0.001 < p < 0.01$ very significant (∗∗) and $p < 0.001$ extremely significant (∗∗∗). Values below the x-axis stand for a decrease and values above the x-axis for an increase in gene expression across development.

individual Trk genes or a combination of these and might indicate an expression in a subpopulation of cells. *Ptprs* expression patterns could be similar to the expression pattern of *Ntrk1,* a combination of *Ntrk1* and *Ntrk3* or all three Trk genes combined. *Ptprj*, *Ptprk* and *Ptprm* expression patterns were similar to each other and appeared to have similarity to *Ntrk2* expression alone or in combination with *Ntrk3*. *Ptprz1* expression pattern was unique among the candidate RPTP genes, as it revealed an increase during development unlike any Trk gene. A similar pattern was already observed for *Tns1*, a dual-specificity phosphatase from the PTEN subfamily, although its increase in expression during development was much higher than the increase of *Ptprz1* (chapter 3). These observations might indicate an expression in highly proliferative non-neural cells of both phosphatases as suggested in the previous chapter.

The data in Figure 4.2 collectively suggest that most RPTP genes are not straightforwardly co-regulated with specific Trk genes, either in level or temporal pattern.

4.3.2. Comparison of RPTP and Trk spatial gene expression patterns using ISH

A comparison of the spatial expression patterns of RPTPs in DRGs and surrounding embryonic tissues with those of Trks was carried out. All three Trk genes and the analysed RPTPs showed unique expression patterns especially in DRGs and the spinal cord. Among the Trk genes *Ntrk1* as well as *Ntrk3* were expressed exclusively in DRGs, whereas *Ntrk2* was also found in the ependymal layer of the VZ around the central canal in the spinal cord (Figure 4.3). The expression around this region decreased throughout development. It is the area where solely the truncated isoform of TrkB was previously detected (Armanini et al., 1995, Kumanogoh et al., 2008). Additionally, in the present study *Ntrk1*$^+$, *Ntrk2*$^+$ or *Ntrk3*$^+$ neurons were found in the DRGs without any restriction to specific areas at the analysed developmental stages. This is in agreement with previous studies in rodent DRGs. In contrast, avian DRGs display a specific segregation pattern of neuronal subtypes. For instance Rifkin *et al*. have shown that specific trk$^+$ neurons are spatially segregated in DRGs of chick embryos after E6 (corresponding to approximately E13.75 in mouse embryos). They found that trkA$^+$ neurons were located

in the dorsal medial 2/3 of the DRG, whereas trkB and trkC were mostly expressed in neurons in the ventral lateral regions (Rifkin et al., 2000).

All analysed candidate RPTP genes showed unique expression patterns in DRGs and surrounding tissues (Figure 4.4). Several of these genes were exclusively expressed in DRGs either in a scattered fashion similar to Trk gene expression or in almost the entire DRG. Some of the RPTPs showed high apparent similarity to Trk gene expression, whereas the results for other RPTPs were more ambiguous.

Ptprf was highly expressed in the majority of the cells within the DRGs and thus appears to be similar to the expression of all three Trk genes. It was also detected in the VZ around the spinal canal at E12.5 similar to *Ntrk2* expression. However, *Ptprf* staining differed from the latter in intensity and shape, as unlike *Ntrk2* it did not appear in the ependymal layer. The expression in the spinal cord almost disappeared entirely at later stages.

Ptprs expression was rather ubiquitous but stronger staining could be detected in DRGs and the VZ at E12.5. The staining in this area decreased at E13.5 and disappeared at E14.5. At E13.5 and E14.5 some expression in the ventral lateral part of the grey matter, where motor neurons reside, was also observed. *Ptprs* expression in the spinal cord resembled *Ptprf* and thus *Ntrk2* expression. But it appeared to spare the region adjacent to the spinal canal unlike *Ntrk2*. *Ptprs* expression in the DRGs therefore resembled the expression of all three Trk genes.

Ptprd was expressed in DRGs. In addition stronger expression was detected in the motor neuron pool in the spinal cord similar to *Ptprs* expression. Especially at E12.5 and partly at E13.5 staining could also be seen in the intermediodorsal and ventricular population of cells. These findings are in agreement with previous studies in mice and rats (Sommer et al., 1997, Van Vactor, 1998). *Ptprd* expression is thus different from any *Ntrk* expression in the spinal cord, but in the DRGs its expression might resemble the expression of all three Trks genes.

Ptpro expression was detected in specific cells within the DRGs at all analysed stages. It was also detected in the ventral lateral part of the grey matter in the motor neuron region similar to *Ptprs* expression. From E13.5 onwards intense staining of *Ptpro* was also detected in the roof plate, which extends from the central canal to the dorsal margin of the spinal cord, where radial glia fibres are situated. Its expression

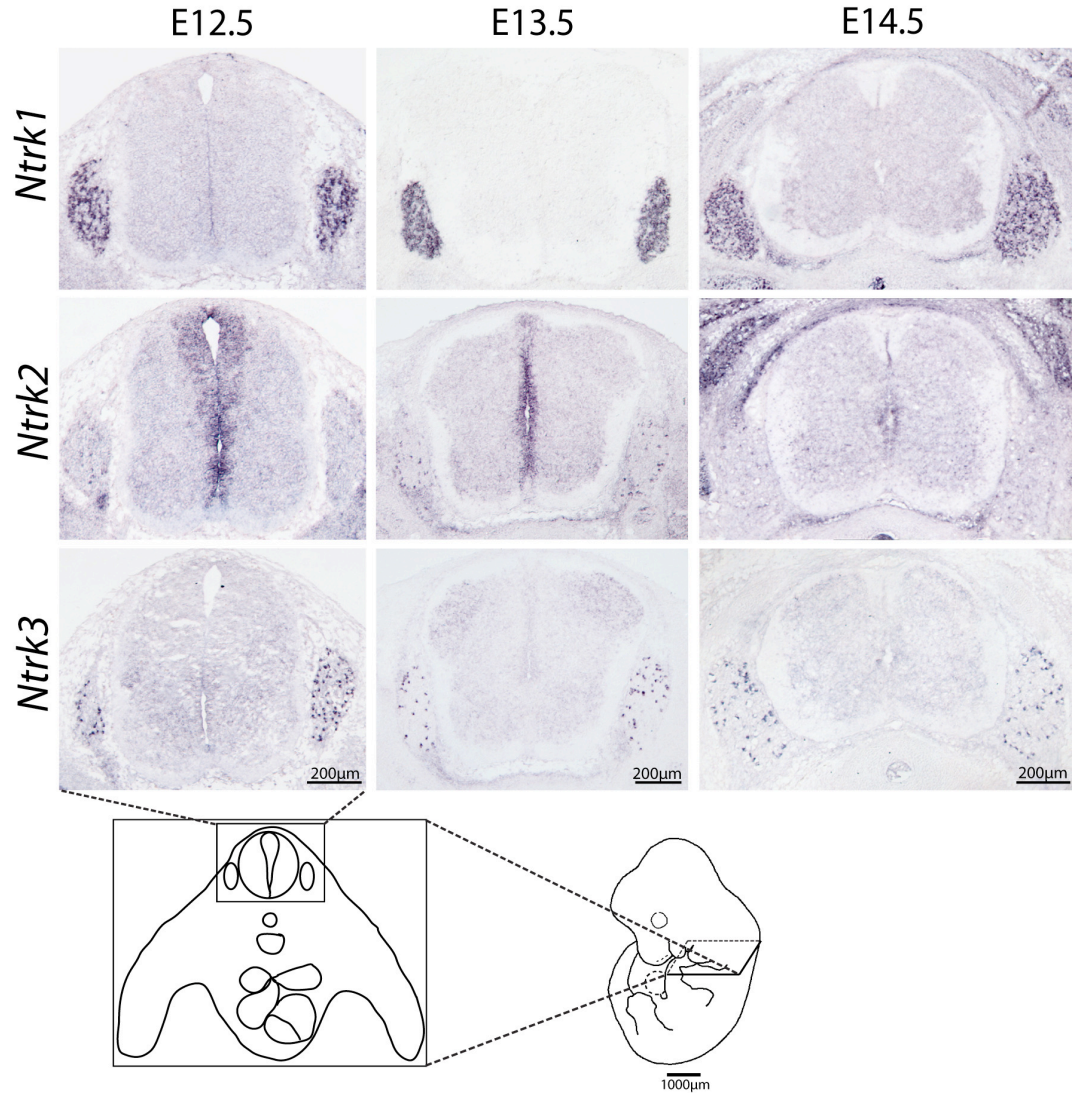

Figure 4.3. ISH analysis of Trk gene expression on transverse mouse embryo sections.

Riboprobes targeting all identified transcripts of *Ntrk1*, *Ntrk2* and *Ntrk3*, encoding TrkA, TrkB and TrkC respectively, were hybridised to transverse sections through the limb regions of mouse embryos at the developmental stages E12.5, 13.5 and 14.5. *Ntrk1*$^{+}$ cells were found most DRG cells. *Ntrk2* and *Ntrk3* were expressed in a subset of DRG cells. *Ntrk2* was additionally expressed in the VZ around the central canal in the spinal cord but this expression decreased during development. The sense probes did not provide any specific staining (Appendix, Figure 3).

pattern resembled mostly *Ntrk2* and *Ntrk3* expression, as it was detected in an obviously higher proportion of cells than either *Ntrk2* or *Ntrk3* alone. However, no cell counts were performed at this stage. Similar to previous reports the staining intensity with the *Ptpro* riboprobe ranged from faint to very strong in cells within the DRGs (Haworth et al., 1998).

Ptpra expression was rather ubiquitous but slightly stronger in DRGs, especially at later stages. Staining was also found in the motor neuron region. The corresponding sense probe showed no signal (Appendix, Figure 3). This expression pattern is in agreement with previous reports (den Hertog et al., 1996, Haworth et al., 1998). *Ptpra* expression in DRGs was similar to the expression of all Trk genes.

Ptprr was specifically expressed in the majority of cells within the DRGs and no staining could be seen either in the spinal cord or in surrounding tissues. This expression pattern was most similar to the expression of *Ntrk1*.

Ptprg expression was detected in DRGs, but the staining was not very strong. However, *Ptprg* appears to be expressed in specific cells within the DRGs. Additionally, some ubiquitous but very faint staining was detected in the surrounding nervous tissues. Its expression pattern was similar to the pattern of *Ptpra* and *Ptprs* expression and hence resembled the expression of all three Trks. Some expression was also visible in the motor neuron domain at E13.5 and E14.5.

Ptprz1 was expressed at very low levels in DRGs unlike any Trk receptor. Expression of this phosphatase was previously reported in SGCs in embryonic and adult rat DRGs (Haworth et al., 1998). Similar to the expression of the truncated TrkB isoform, *Ptprz1* expression was visible in the ventral ependymal layer at E12.5 but this expression decreased at later developmental stages. In fact, a coexpression of the truncated TrkB isoform and *Ptprz1,* mostly in non-neural cells, was reported (Snyder et al., 1996).

The expression of the threshold candidates ***Ptprj, Ptprk*** and ***Ptprm*** was lower than the expression of any other candidate RPTP gene, despite the NBT/BCIP developing time of several days. However, the staining with each probe was stronger than staining with the sense riboprobe (Appendix, Figure 3). The lowest gene expression was seen for *Ptprj* at all three developmental stages in DRGs and the surrounding tissues. Only some specific staining was detected in the ventral ependymal

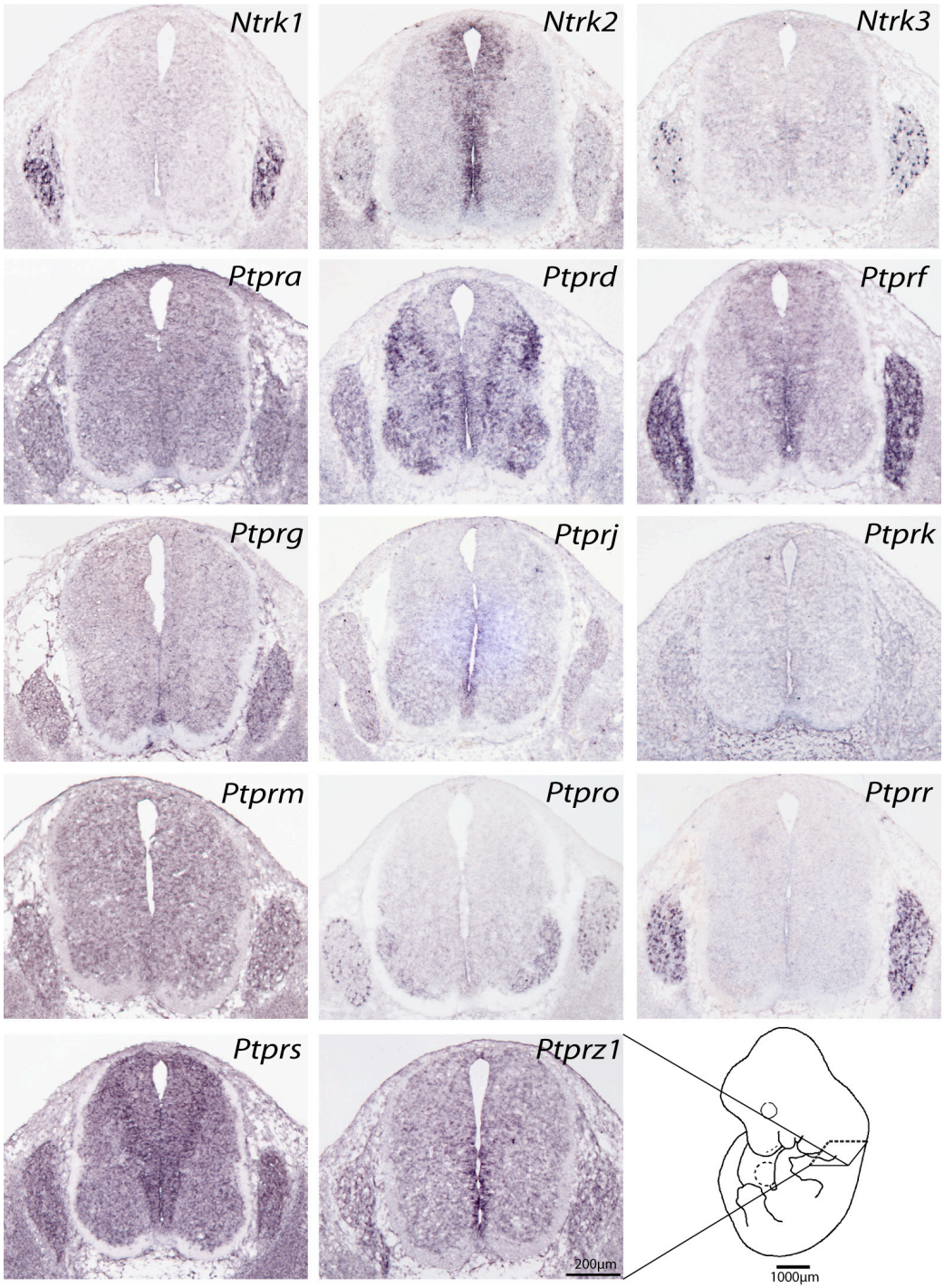

Figure 4.4A. ISH analysis of Trk and RPTP gene expression on transverse E12.5 mouse embryo sections (continued).

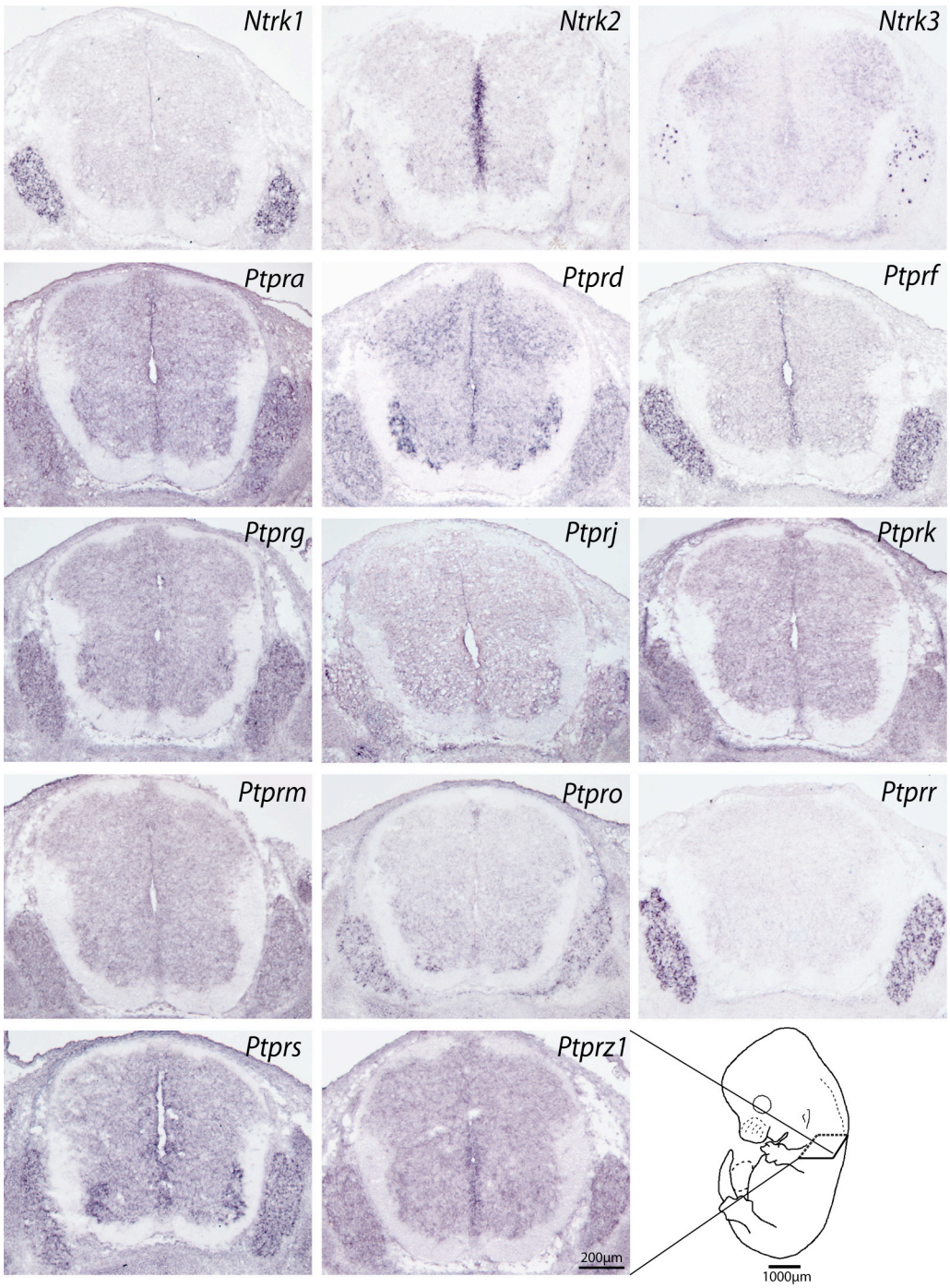

Figure 4.4B. ISH analysis of Trk and RPTP gene expression on transverse E13.5 mouse embryo sections (continued).

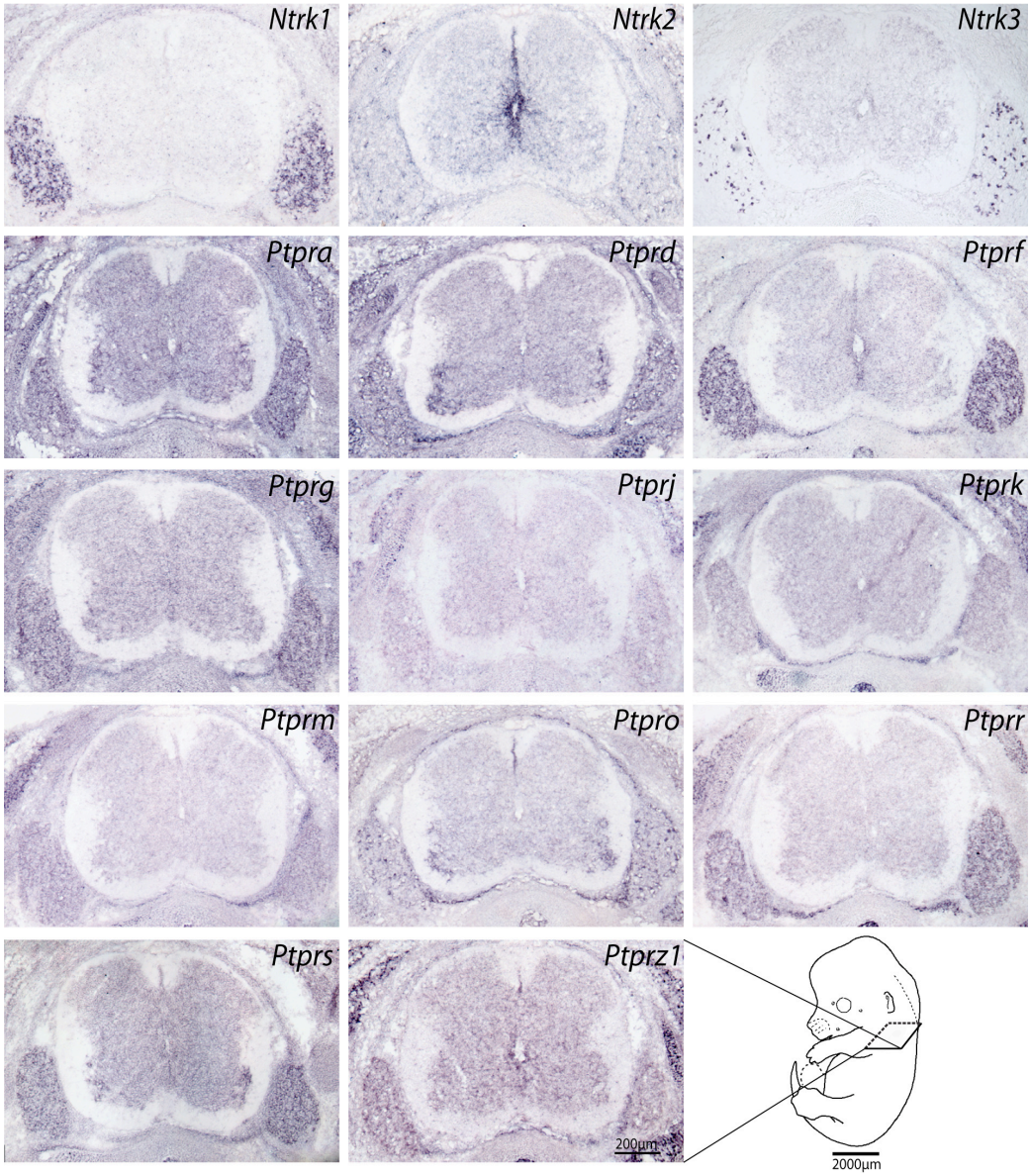

Figure 4.4. ISH analysis of Trk and RPTP gene expression on transverse E12.5, E13.5 and E14.5 mouse embryo sections.

ISH was performed on transverse cryosections through the limb region of **A)** E12.5, **B)** E13.5 and **C**) E14.5 mouse embryos with riboprobes detecting all isoforms of Trk genes and the major isoforms of candidate RPTP genes as stated in the experimental procedures section 3.2.3. The sense probes provided no specific staining (Appendix, Figure 3).

layer of the spinal cord at E12.5, similar to *Ptprz1*. *Ptprk* and *Ptprm* expression was also rather weak but slightly stronger in the DRGs than in the spinal cord at all three analysed stages. No obvious similarities to Trk expression could be detected for these three genes.

The comparison of the gene expression patterns of RPTPs with those of Trks using qPCR arrays and ISH shows that both techniques produced datasets, which broadly agree with each other. The differences stem probably from the complementary nature of the techniques, with the low sensitivity of ISH and the lack of spatial information of the qPCR analysis. All in all, most of the RPTP genes appear to have similar expression patterns to more than one Trk receptor gene (*Ptpra, Ptprd, Ptprf, Ptprg, Ptprr, Ptprs*) and some have even more similarity to a specific subpopulation of neurons (*Ptprf* and *Ptpro*) or even non-neural cells such as SGCs (*Ptprz1*). The expression pattern obtained with the qPCR arrays for the marginal candidate RPTP genes (*Ptprj, Ptprk* and *Ptprm*) appears to be similar to *Ntrk2* and/or *Ntrk3*, but the ISH analysis did not reveal any strong staining in the DRGs and thus no similarities to Trk expression.

4.3.2.1. No rostrocaudal gradient of Trk and RPTP gene expression was detected in E13.5 DRGs

The generation of mouse lumbar DRG cells begins at around E9, shows a peak at E12.5 and is complete by E14-14.5. In agreement with a known rostrocaudal gradient in development of sensory ganglia and spinal cord it was described that the generation of cervical DRG neurons is 12-24 h ahead of the lumbar DRGs (Lawson and Biscoe, 1979). Since the expression of specific Trk receptors is timed as well (reviewed in 1.1.3), an expected rostrocaudal gradient should be observed. In previous ISH studies, however, no apparent rostrocaudal gradient was reported (Klein et al., 1990b, Tessarollo et al., 1993). In contrast to this in studies using specific Trk antibodies a rostrocaudal gradient was shown in E10 mouse embryos (Farinas et al., 1998). The authors concluded that this discrepancy might suggest a translational control mechanism.

In order to analyse whether any significant differences and possible similarities are visible in the expression patterns of Trk and candidate RPTP genes in murine E13.5 DRGs across the spinal cord, I performed ISH on sagittal embryo sections. This is of particular importance for the comparison of gene expression patterns and also the

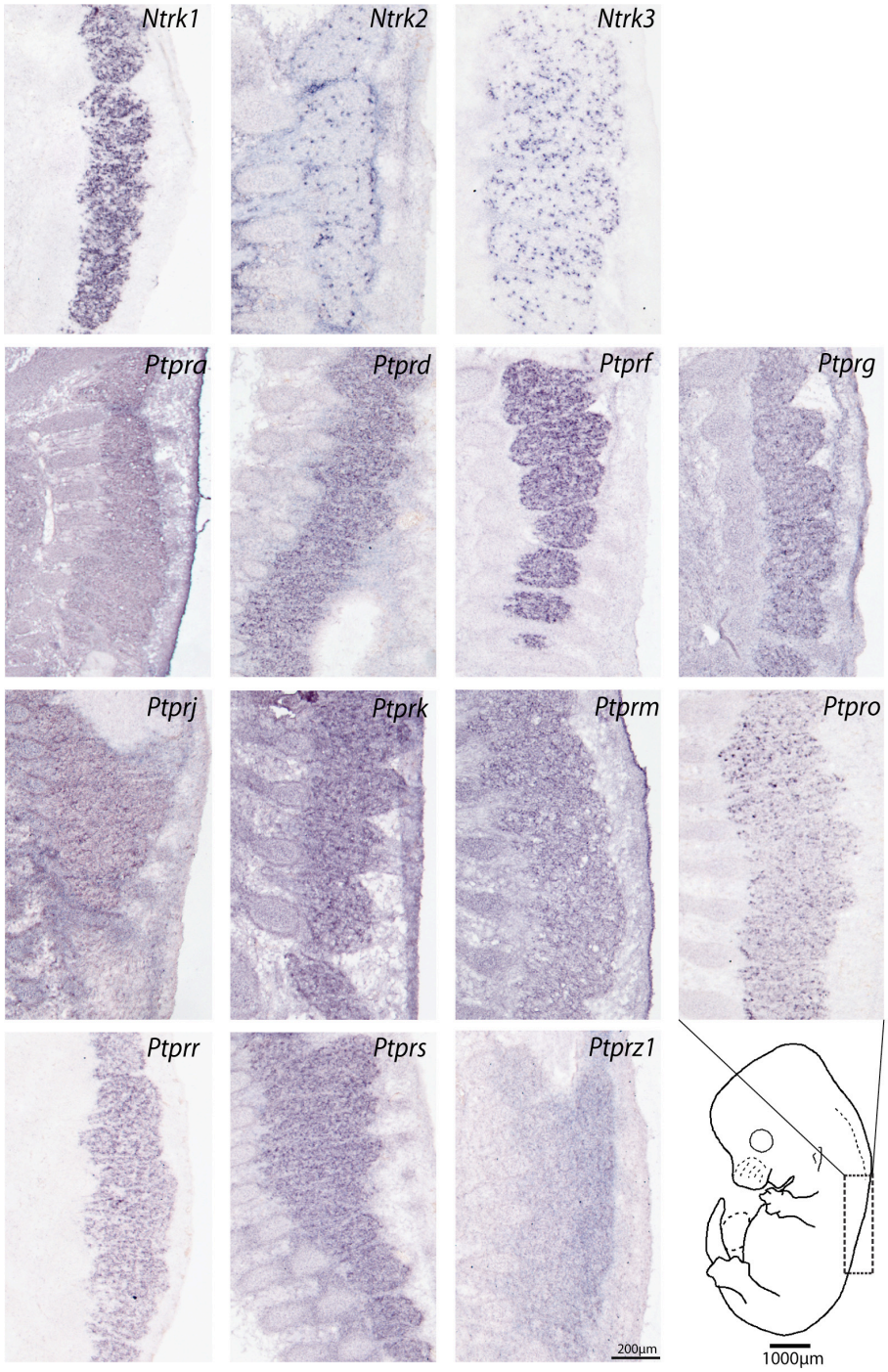

Figure 4.5. ISH of Trk and RPTP candidate genes on sagittal E13.5 mouse embryo sections.

Sagittal murine embryo sections of the cervico-thoracic and thoracic regions were *in situ* hybridised with probes against Trk genes (upper row) and eleven RPTP genes. The expression of some RPTP genes was restricted only to specific cells within the DRGs, whereas the expression of other genes was rather ubiquitous. No obvious changes in gene expression were detectable between the most caudal and rostral DRGs. No specific staining was detected with the sense probes (Appendix, Figure 3).

coexpression analysis since sections from slightly different spinal regions were used and this might alter the results. In contrast to aforementioned findings, this expression analysis (Figure 4.5) and additionally the ISH analysis of almost all RPTPs on E14.5 C57BL/6 mouse embryo sections retrieved from the GenePaint database (Appendix, Figure 4) did not reveal any obvious rostrocaudal gradient in expression of either Trk or RPTP genes at the analysed stages.

4.3.3. Coexpression analysis of Trks and RPTPs in murine E13.5 DRGs

For an accurate coexpression study of RPTPs and Trks it was important first to establish how many cells express Trk receptors in E13.5 mouse DRGs and whether a significant number of these neurons coexpresses at least two of these enzymes. Both questions were previously addressed in several IHC and ISH studies on different species of wild type and transgenic animals and most of these reports agree on the relative proportion of Trk expressing cells. They have also confirmed coexpression of at least two Trk receptors in DRGs, TG and other tissues in rodents and other species and have shown a decrease in coexpression during development. Nevertheless, these studies are conflicting on the degree of coexpression mostly due to technical differences. Therefore it was important to analyse Trk coexpression in our system before their coexpression with RPTP genes could be assessed.

In the present study I have used different combinations of FISH and IF (Figure 4.6 and Appendix, Table 2) for an expression and coexpression analysis of Trks and RPTPs in murine E13.5 DRG neurons. All Trk antibodies recognized an epitope in the ECD and thus detected all known isoforms of the specific Trk receptors (specificity test see Appendix, Figure 1). The riboprobes against Trk genes detected all known transcript variants (previously described in chapter 3).

4.3.3.1. Expression of Trk receptors

In this study $TrkA^+$ neurons represented the majority of cells in E13.5 murine DRGs with 75 +/- 12% (IF) or 60 +/- 10% (FISH). $TrkB^+$ neurons accounted for 6.5 +/-1.5% (IF) or 4.5 +/- 1.9% (FISH) and the proportion of $TrkC^+$ neurons was around 8.4 +/- 3.3% (IF) or 9.6 +/- 4% (FISH). The amounts of neurons detected with either IF or FISH in the present study differed slightly from each other. This might be

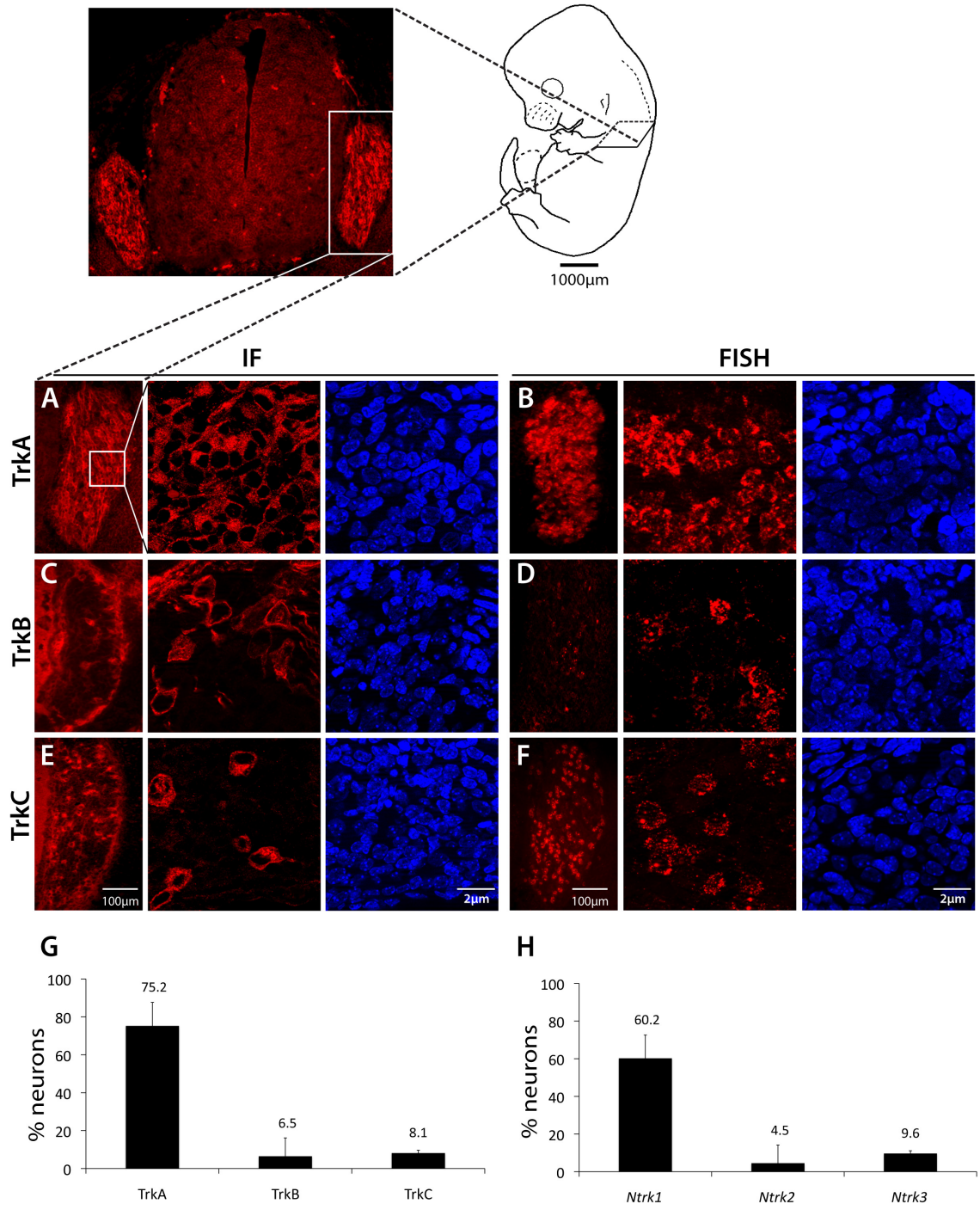

Figure 4.6. Expression of Trk receptors in murine E13.5 DRG neurons.

Immunofluorescence (IF) (**A, C, E**) and fluorescent ISH (FISH) (**B, D, F**) were performed on transverse cryosections through E13.5 mouse embryos. TrkA, TrkB and TrkC antibodies detected the ECD of the corresponding Trk receptor and the riboprobes detected all known Trk transcripts. Cell nuclei were counterstained with DAPI (blue). **G** and **H**) Percentage of Trk or *Ntrk* positive neurons. Trk^+ and $DAPI^+$ neurons were counted on pictures and the mean percentage and SD of unambiguously stained neurons was determined (Appendix, Table 2). Pictures were taken on the Zeiss Axiophot with a 20x objective and the Zeiss Imager.Z1 ApoTome with a 63x objective.

caused by technical difficulties since cell counting especially using FISH, was sometimes challenging when no cell borders were detectable. Thus due to some ambiguous cases the cell numbers could have been slightly under- or overestimated. Nevertheless, the proportions of the different Trk expressing subtypes of neurons in the DRGs were approximately the same using both techniques and agree well with prior findings where IHC demonstrated in E13 murine DRGs that almost 80% of neurons were $TrkA^+$, 8% were $TrkB^+$ and around 10% were $TrkC^+$ (Phillips and Armanini, 1996, White et al., 1996, Farinas et al., 1998, Ernsberger, 2009).

4.3.3.2. Coexpression of Trk receptors

In the present study the coexpression analysis revealed that at least two Trk receptors were coexpressed in E13.5 DRG neurons but that this proportion was small (less than 5%) in reference to the total population of Trk^+ DRG neurons (Figure 4.7F and Appendix, Table 3). Cell counts showed that around 0.9 +/- 0.7% (DFISH) and 1.3 +/- 0.9% (IF and FISH) of all DRG neurons were $TrkA^+$ and $TrkB^+$, 2.0 +/- 1% (DFISH) and 2 +/- 1.5% (IF and FISH) were $TrkA^+$ and $TrkC^+$ and 1.4 +/- 0.1% (DFISH) were $TrkB^+$ and $TrkC^+$. Since labelling with all three Trk receptors was technically not possible, it cannot be excluded that some neurons also coexpress all three Trk receptors. In reference to the individual Trk^+ subpopulations (Figure 4.7G and Appendix, Table 3) no more than approximately 3% of the total $TrkA^+$ neurons coexpressed another Trk receptor. In contrast to this, a much higher proportion of both $TrkC^+$ and $TrkB^+$ neurons coexpressed another Trk receptor. Interestingly, among $TrkB^+$ or $TrkC^+$ neurons more cells coexpressed TrkA than TrkC or TrkB respectively and both $TrkA^+/TrkB^+$ and $TrkA^+/TrkC^+$ proportions were similar (almost 1/3). I have also observed that almost twice as many $TrkB^+$ neurons coexpressed TrkC than *vice versa*.

Coexpression of Trk receptors in DRGs and other tissues was previously reported in several IHC and ISH studies and observed in transgenic mice (summarized in 1.3.). These results are mostly in agreement with the present findings. For instance Kramer *et al*. have shown that at E11.5 75% of murine lumbar DRG cells coexpressed TrkB and TrkC receptors. This amount dropped to 40% at E12 and 10% at E12.5 and at E14.5 no coexpression was detected in lumbar DRGs (Kramer et al., 2006). This is well in agreement with the current study as only around 1.4% of all neurons coexpressed TrkB and TrkC. Similar findings were made in TG (Funfschilling et al., 2004). TrkA

and TrkC coexpression was prior reported in E11.5 mouse DRGs, but was almost absent from E12.5 onwards in murine DRGs (Kramer et al., 2006, Sun et al., 2008) and TG (Huang et al., 1999). In the present study the prevalence of $TrkA^+$ and $TrkC^+$ neurons at E13.5 was around 2-3% and is thus well in agreement with these reports. TrkA and TrkB coexpression was previously detected in E10.5 until E12 mouse TG (Dykes et al., 2010), but was not analysed in murine DRGs yet to our knowledge. It is possible, however, that this is also the case in DRGs. Considering the delay in development of DRGs in comparison to TG this agrees with our findings of 1% total $TrkA^+$ and $TrkB^+$ neurons.

In summary, coexpression of Trk receptors in E13.5 murine DRG neurons is low (< 5%), but cannot be neglected as it accounts for a high percentage of the specific $TrkB^+$ and $TrkC^+$ subpopulations. We found that whereas coexpression among $TrkA^+$ neurons is rare, one third of $TrkB^+$ neurons coexpressed either TrkA or TrkC at E13.5. Among $TrkC^+$ neurons less than one third coexpressed TrkA and the $TrkB^+/TrkC^+$ population was almost half as big as the $TrkC^+/TrkB^+$ population, but still 14% and thus not negligible. Together, among all Trk^+ subpopulations, more $TrkB^+$ neurons coexpressed another Trk receptor than either $TrkA^+$ or $TrkC^+$ neurons. However, it is not known whether among these neurons some also coexpress the third Trk receptor and thus the amount of coexpressing neurons might be lower. In fact Moshnyakov *et al*. have performed RT-PCR on individual E12 and E16 rat TG neurons and have shown that several of these cells express all three Trk receptors (Moshnyakov et al., 1996). However, this study was not quantitative and no prevalence of these triple-expressing neurons was determined.

The total amount of all detected Trk^+ neurons accounts for around 87 +/- 6%, if coexpression is taken into account. Thus these results demonstrate that most of the cells in E13.5 DRGs are Trk^+. The remaining Trk^- neurons could for instance represent non-neuronal cells or possibly Ret^+ neurons or other neural subtypes. Finally, this detailed Trk expression study validates the technical approach of using DFISH and IF especially for a coexpression analysis as the results mostly agree with previous findings. In addition these data also expand previous knowledge on Trk coexpression in murine embryonic DRG neurons.

Figure 4.7. Coexpression of Trk receptors in murine E13.5 DRG neurons.

Double fluorescent ISH (DFISH) and immunofluorescence (IF) were performed sequentially on transverse cryosections through the limb region of E13.5 mouse embryos for coexpression analysis. The TrkA antibody detected the ECD and the riboprobes detected all known transcripts. Nuclei were counterstained with DAPI (blue). **A** and **C**) IF (TrkA, red) and fluorescent ISH (TrkB or TrkC, green), **B, D, E**) DFISH. Pictures were taken on the Zeiss Imager.Z1 ApoTome with a 63x objective. Scale bar = 20 μm. Arrowheads indicate non-coexpressing neurons, whereas coexpressing neurons are shown in the insets. Percentages of **F**) Trk coexpressing neurons in reference to all detected DRG neurons and **G**) of Trk coexpressing neurons among $TrkA^+$, $TrkB^+$ or $TrkC^+$ neurons. SDs were included in the graph. The lighter columns represent DFISH staining and the darker columns IF and FISH. Scale bar = 2 μm.

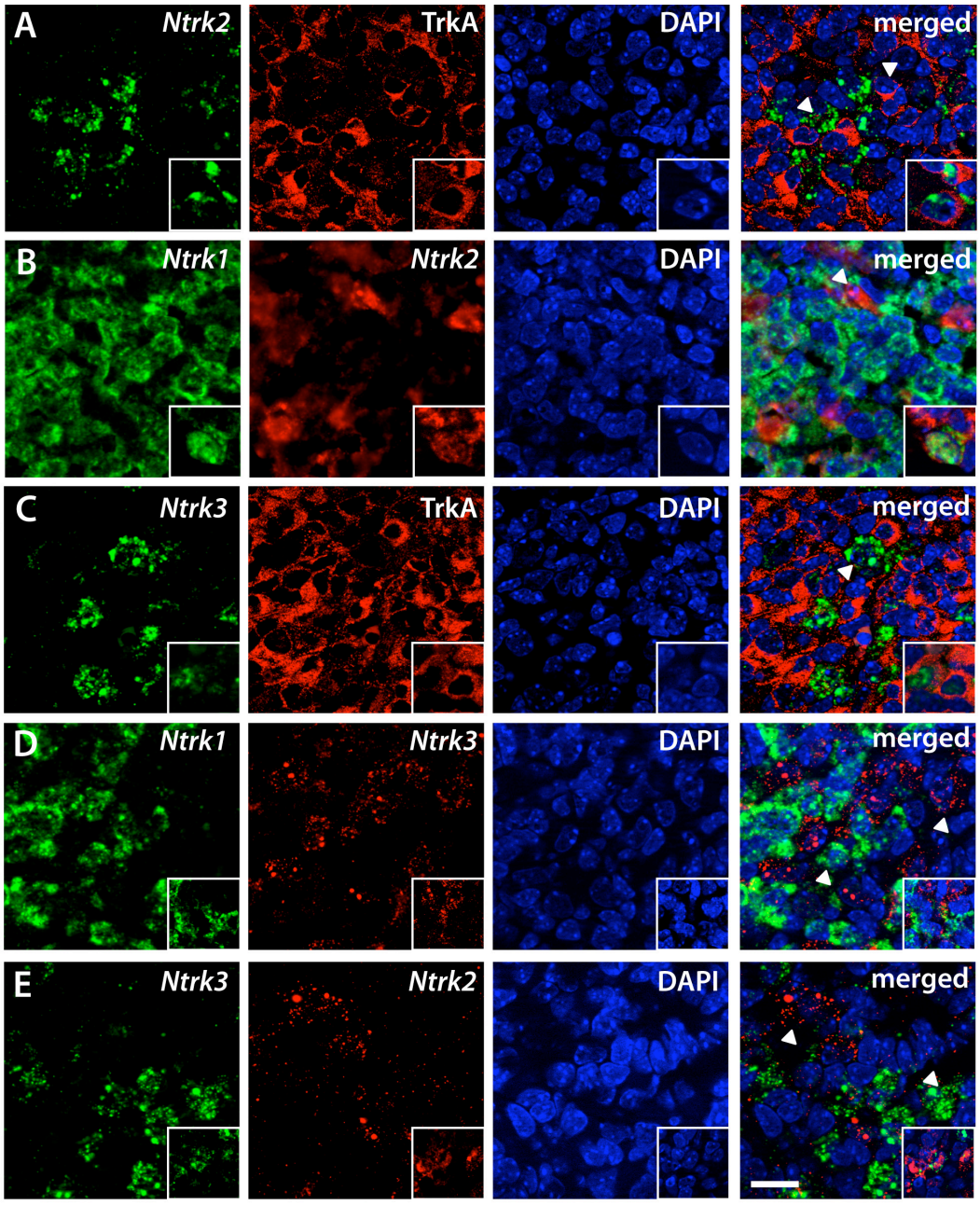
A
Ntrk2
TrkA
DAPI
merged
B
Ntrk1
Ntrk2
DAPI
merged
C
Ntrk3
TrkA
DAPI
merged
D
Ntrk1
Ntrk3
DAPI
merged
E
Ntrk3
Ntrk2
DAPI
merged

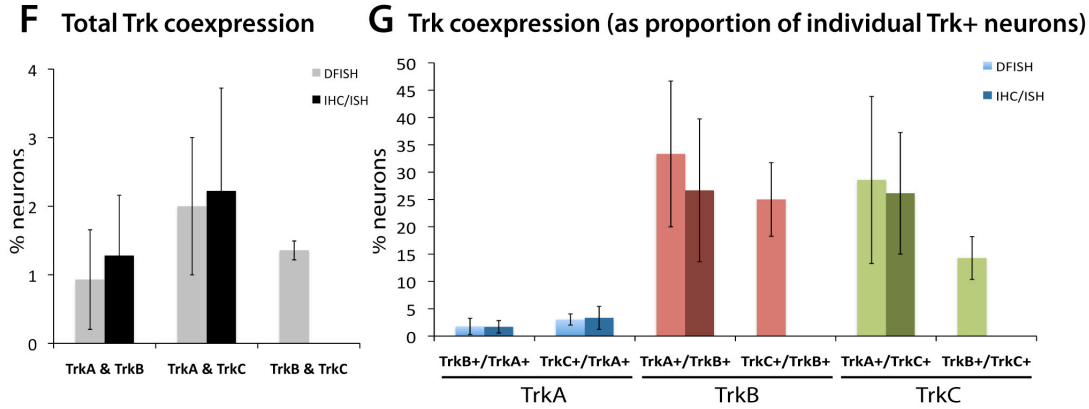
F Total Trk coexpression
G Trk coexpression (as proportion of individual Trk+ neurons)
% neurons
DFISH
IHC/ISH
TrkA & TrkB
TrkA & TrkC
TrkB & TrkC
TrkB+/TrkA+
TrkC+/TrkA+
TrkA+/TrkB+
TrkC+/TrkB+
TrkA+/TrkC+
TrkB+/TrkC+
TrkA
TrkB
TrkC

4.3.3.3. Coexpression of RPTPs and Trks

Having characterised Trk expression, I then analysed the detailed coexpression of all three Trk receptors with the seven strongest expressed candidate RPTP genes: *Ptpra, Ptprd, Ptprf, Ptprg, Ptpro, Ptprr* and *Ptprs*. The marginal candidates *Ptprj, Ptprk* and *Ptprm* and also *Ptprz1* were not included in this study due to their low expression levels in DRGs and the detection limits of ISH. FISH and IF are both powerful techniques to obtain spatial information of the expression of Trks and RPTPs simultaneously in the same cell. RPTPs were detected by FISH, and TrkA was detected with an antibody against the ECD thus recognizing all known TrkA isoforms. IF with the TrkA antibody had the advantage of visualizing the cell membrane and thereby facilitating the localization of cells. The antibodies against TrkB and TrkC epitopes could not be used because they were unfortunately destroyed during ISH, and thus DFISH was performed instead.

Among the analysed phosphatases *Ptpra, Ptprd, Ptprg* and *Ptprs* were found in over 90%, whereas *Ptprf, Ptprr* and *Ptpro* were expressed in around 82%, 70% and 12% of sensory neurons respectively (Figure 4.11A and Appendix, Table 4). All seven phosphatases were coexpressed with all three Trk receptors, but in different characteristic patterns (Figure 4.8 - 4.11 and Appendix, Table 5).

The phosphatases ***Ptpra, Ptprd, Ptprg*** and ***Ptprs*** were found in around 90% or more of $TrkA^+$ neurons and ***Ptprf*** in around 82%. These phosphatase genes were also expressed in 100% of $TrkB^+$ or $TrkC^+$ neurons (Figure 4.11C). The total proportion of Trk^+ neurons coexpressing these phosphatases (Figure 4.11B) broadly agreed with the distribution of these neuronal subtypes in the DRGs (section 4.3.4.1). As previously described TrkA was expressed in around 75% (IF), TrkB in 5% (FISH) and TrkC in 10% (FISH) of cells in E13.5 DRGs. A high SD indicated that not all $TrkB^+$ neurons appeared to coexpress *Ptprd* on all sections, which might however be due to the previously mentioned issues with the *Ptprd* riboprobe (Figure 4.11C). Additionally, although all *Ntrk3*$^+$ neurons coexpressed *Ptprg*, the proportion of these cells in comparison to the total amount of DRG cells was less than half as big compared to the total amount of $TrkC^+$ neurons in DRGs (Figure 4.11B). However, this was simply caused by the fact that sections with less $TrkC^+$ neurons than usual were picked for cell counting.

Ptprr expression was also observed in all TrkB$^+$ and almost all TrkC$^+$ neurons, but only around 80% of TrkA$^+$ neurons coexpressed this phosphatase (Figure 4.11C). The other way round 90% of all *Ptprr*$^+$ neurons were also TrkA$^+$ and around 6% and 15% coexpressed TrkB or TrkC respectively (Figure 4.11C). The number of *Ptprr*$^+$ cells coexpressing TrkA was higher than the actual proportion of these cells in DRGs, because not all cells in DRGs express *Ptprr* and these calculations refer to the total amount of cells expressing this phosphatase (Figure 4.11D, Appendix, Table 5).

The coexpression of ***Ptpro*** with Trks differed significantly from any of the other analysed phosphatases. It was expressed in only around 5% of TrkA$^+$ neurons, but 78% of TrkC$^+$ and almost all TrkB$^+$ neurons. TrkB$^+$/*Ptpro*$^+$ neurons were the most prevalent with 56% occurrence; followed closely by TrkC$^+$/*Ptpro*$^+$ neurons with 49% and only 28% of *Ptpro*$^+$ neurons coexpressed TrkA. Since these numbers do not add up to 100% this indicates that *Ptpro*$^+$ is expressed in neurons that coexpress at least two Trk receptors. So do all of these neurons coexpress TrkB? This assumption suggests itself, as all TrkB neurons coexpress *Ptpro (Ptpro*$^+$/TrkB$^+$). However comparing these numbers with the results from the Trk coexpression analysis (section 4.3.4) it appears that this is not the case. Only 14% of all TrkC$^+$ neurons were TrkB$^+$ (TrkB$^+$/TrkC$^+$) in comparison to 78% of *Ptpro*$^+$/TrkC$^+$ neurons. And in the case of TrkA 5% of the neurons were *Ptpro*$^+$/TrkA$^+$, but less than 2% of TrkA$^+$ neurons coexpressed TrkB (TrkB$^+$/TrkA$^+$). Additionally, all TrkB$^+$ neurons were *Ptpro*$^+$ but only around 50% of TrkB$^+$ neurons coexpress another Trk receptor. And the Trk coexpression study showed less than 5% total Trk coexpression, whereas 11% of all DRG cells expressed *Ptpro*. Together these findings indicate that *Ptpro* expression is not directly linked to TrkB coexpression patterns in E13.5 DRGs. Surprisingly, one correlation seems to add up however, which is that around 5 (+/- 3.2)% of TrkA$^+$ neurons coexpress either TrkB or TrkC 5 (+/- 3.2)%, almost the total amount of *Ptpro*$^+$/TrkA$^+$ neurons (5.3 +/- 2.4%). It has to be noted that my analysis was restricted to high expression intensities, but *Ptpro* expression was also found in a subset of neurons with very low staining intensity similar to previous reports in rat E14 and E18 DRGs (Haworth et al., 1998).

To sum up, first none of the analysed RPTPs was coexpressed with only one particular Trk receptor. Second, only few Trk$^+$ DRG neurons did not coexpress one of the six RPTP genes (excluding *Ptpro*). This was the case for a minority of TrkA$^+$ neurons, which did not coexpress *Ptprf, Ptprs, Ptprg* or *Ptprr*. And third, neurons

Figure 4.8. Expression of RPTP genes and TrkA in murine E13.5 DRG neurons.

Fluorescent ISH and IF were performed sequentially with riboprobes detecting RPTP genes (green) and TrkA antibody (red) on transverse cryosections of E13.5 mouse embryos. Nuclei were counterstained with DAPI (blue). Arrowheads indicate non-coexpressing neurons, whereas coexpressing neurons are indicated with full arrows. Neurons were identified by the presence of big round nuclei. Pictures were taken on the Zeiss Imager.Z1 ApoTome with a 63x objective. Scale bar = 2 μm.

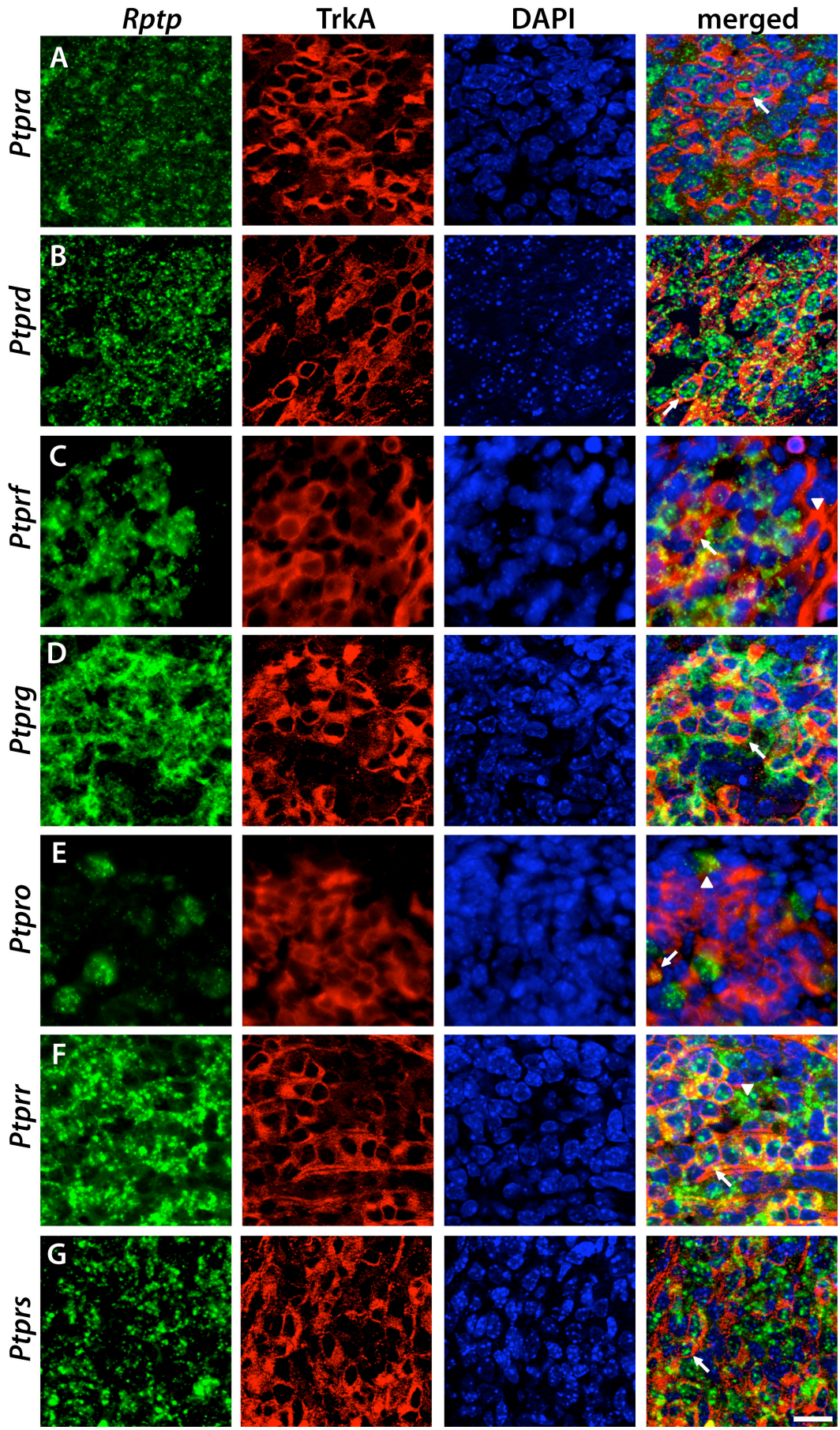
Rptp
TrkA
DAPI
merged
A
Ptpra
B
Ptprd
C
Ptprf
D
Ptprg
E
Ptpro
F
Ptprr
G
Ptprs

Figure 4.9. Expression of RPTP genes and *Ntrk2* in murine E13.5 DRG neurons.

Double fluorescent ISH was performed with riboprobes detecting RPTP genes (green) and *Ntrk2* (red) on transverse cryosections of E13.5 mouse embryos. Nuclei were counterstained with DAPI (blue). Arrows indicate coexpressing neurons (with big round nuclei). Pictures were taken on the Zeiss Imager.Z1 ApoTome with a 63x objective. Scale bar = 2 μm.

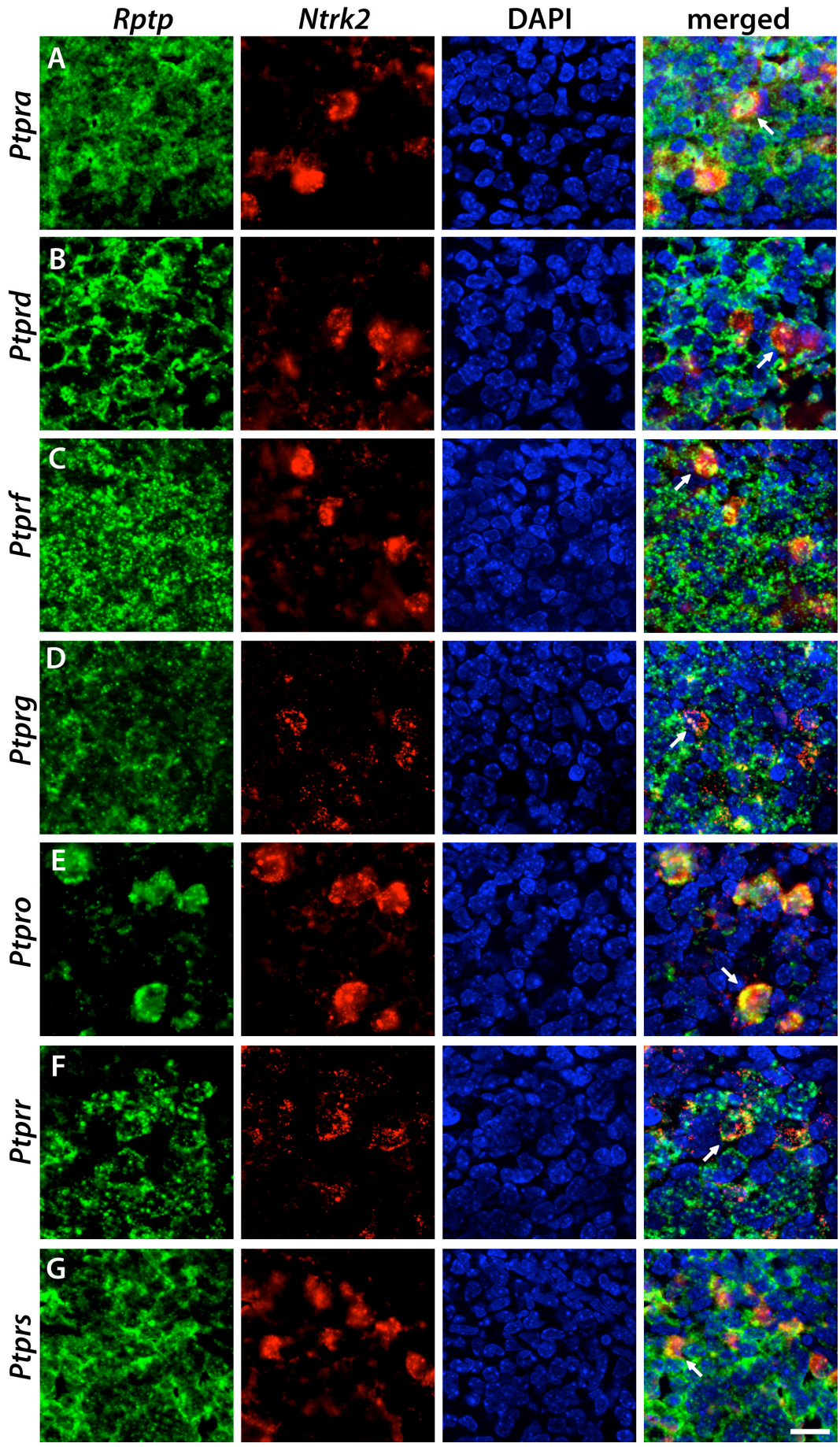
Rptp
Ntrk2
DAPI
merged
A
Ptpra
B
Ptprd
C
Ptprf
D
Ptprg
E
Ptpro
F
Ptprr
G
Ptprs

Figure 4.10. Expression of RPTP genes and *Ntrk3* in murine E13.5 DRG neurons.

Double fluorescent ISH was performed with riboprobes detecting RPTP genes (green) and *Ntrk3* (red) on transverse cryosections of E13.5 mouse embryos. Nuclei were counterstained with DAPI (blue). Arrows indicate coexpressing neurons (with big round nuclei). Pictures were taken on the Zeiss Imager.Z1 ApoTome with a 63x objective. Scale bar = 2 μm.

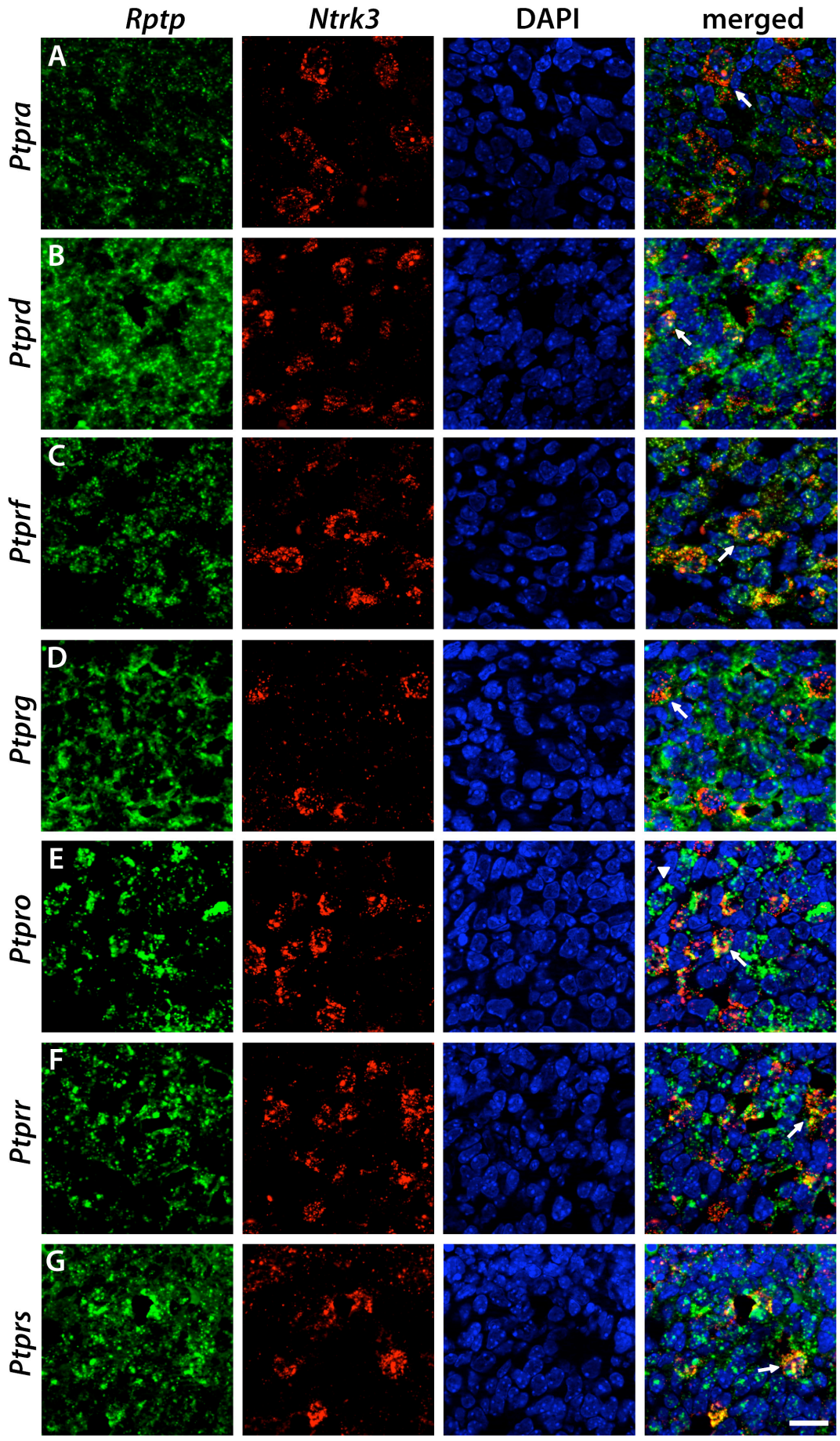
Rptp
Ntrk3
DAPI
merged
A
Ptpra
B
Ptprd
C
Ptprf
D
Ptprg
E
Ptpro
F
Ptprr
G
Ptprs

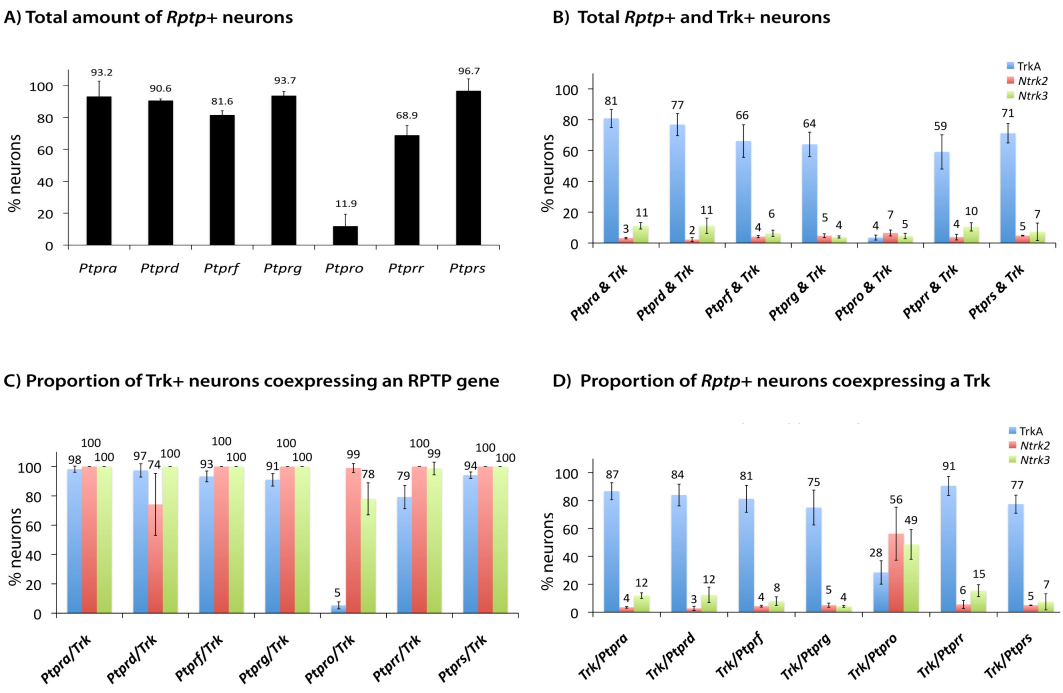

Figure 4.11. RPTP and Trk coexpressing cells in murine E13.5 DRG neurons.

Double fluorescent IHC and IF were performed on transverse cryosections of murine E13.5 embryos. TrkA was detected with an antibody against the ECD. *Ntrk2*, *Ntrk3* and *Rptps* were visualized with riboprobes. The cells were counterstained with DAPI. Trk$^+$ and/or *Rptp*$^+$ and DAPI$^+$ neurons were counted on pictures. Neurons were identified by the presence of big round nuclei. **A**) Total proportion of *Rptp*$^+$ neurons. **B)** Total proportion of Trk$^+$ & *Rptp*$^+$ neurons. **C**) Proportion of Trk$^+$ neurons, which coexpress an RPTP gene (*Rptp*$^+$/Trk$^+$). **D**) Proportion of *Rptp*$^+$ neurons, which coexpress a Trk receptor (Trk$^+$/*Rptp*$^+$). Data are additionally presented in the Appendix, Table 5.

expressing a specific Trk receptor coexpressed numerous RPTP genes. *Ptpro* was the only RPTP, which stood out in this analysis concerning its expression and coexpression patterns.

4.4. Discussion

Previous studies have shown a molecular interaction of particular RPTPs with Trk receptors mostly in over-expression systems (section 1.4). In order to assess the physiological relevance of these proposed interactions I have analysed and compared the expression profiles of selected highly expressed RPTPs with Trk receptors in murine embryonic DRGs followed by an extensive coexpression analysis of Trks with seven of the strongest expressed RPTPs in the same sensory neurons, which is a prerequisite for their possible interaction. Here I will briefly discuss the findings of particular RPTPs and compare these to previous reports.

Among the analysed phosphatase genes *Ptprf, Ptprs* and *Ptprr* were strongly and specifically but also rather ubiquitously expressed in DRG neurons. An interaction with specific Trk receptors was previously attributed to all three RPTPs (section 1.4).

Ptprf is a very good candidate gene to be implicated in Trk signalling due to its specific and very strong expression in DRG neurons at the analysed embryonic stages, similar to Trk expression. *Ptprf* was expressed in almost all Trk^+ neurons apart from a minor proportion of small $TrkA^+$ neurons. It was reported that LAR could indeed possibly regulate TrkA and TrkB receptors for instance in PC12 cells and in embryonic hippocampal neurons, respectively, either directly or through the activation of Src (Tisi et al., 2000, Tsujikawa et al., 2002, Yang et al., 2003, Yang et al., 2005a). A clear coexpression of the LAR gene with all Trk receptors indicates the additional possibility of TrkC regulation.

Ptprs expression was rather ubiquitous in all tissues but stronger expression was detected in DRGs. It has been described before that many tissues express the long isoform of RPTPσ whereas the shorter isoform is highly enriched in neurons (Stoker, 1994). We detected both isoforms in this study. *Ptprs* was expressed in all Trk^+ neurons, with the exception of a small population of $TrkA^+$ neurons. In previous over-expression studies in HEK293T cells in our lab RPTPσ could be co-immunoprecipitated with TrkA

and TrkC, but not TrkB, though it was able to dephosphorylate all three Trk receptors. Additionally, over-expression of RPTPσ in embryonic chick sensory neurons resulted in the suppression of NGF-dependent neurite outgrowth but without affecting cell survival (Faux et al., 2007). The absent binding to TrkB but its dephosphorylation by RPTPσ might indicate an indirect regulation of TrkB. Thus, *Ptprs* expression in all Trk^+ cells supports the realistic hypothesis of its possible interaction with all three Trk receptors.

Ptprr expression is almost exclusive to sensory neurons during murine development and was detected in the majority of DRG neurons in our study. The qPCR analysis revealed a similar expression profile specifically to TrkA, but in the ISH analysis a likely expression in almost all Trk^+ neurons was more apparent. Indeed, in my coexpression analysis *Ptprr* was expressed in all $TrkB^+$ or $TrkC^+$ neurons, but only around 80 (+/- 8)% of $TrkA^+$ neurons also hybridized *Ptprr*. On the one hand our findings suggest a potential interaction between RPTPR with all Trk receptor types. A current unpublished study showed that RPTPR indeed binds and dephosphorylates TrkA and even possibly controls its maturation. However, it has apparently no effect on TrkB (Noordman, Y. *et al*., unpublished data). But like in many of these interaction studies the experiments were performed in an over-expression system (COS cells) and have to be confirmed *in vivo*. On the other hand the absence of *Ptprr* in a small, yet uncharacterised population of $TrkA^+$ neurons questions the previous assumptions of an interaction of this phosphatase particularly with TrkA receptors. Therefore one might speculate that its expression in TrkA, B and C neurons might be there for other reasons than Trk signalling.

The phosphatase genes *Ptpra, Ptprd* and *Ptprg* were also rather ubiquitously expressed in DRGs, similar to the previously described RPTPs, but at much lower levels. All three were also coexpressed with Trks. And although none of these RPTPs was previously directly linked to Trk signalling, they are all implicated in neuronal functions and might play Trk-dependent or -independent roles in DRGs.

Ptpra was ubiquitously expressed in many tissues of the mouse embryos but with stronger staining in DRGs similar to *Ptprs* expression. RPTPα is implicated in the differentiation and migration of NCCs and neurons (den Hertog et al., 1993, den Hertog et al., 1996, Fang et al., 1996) and it was previously detected within neurons in DRGs (Haworth et al., 1998). The qPCR analysis revealed a similarity in the expression of *Ptpra* and all three Trk genes, in agreement with their coexpression, thus suggesting a

possible interaction with all Trk receptors. However, previous experiments in HEK293T cells in our lab have shown that RPTPα neither binds nor dephosphorylates TrkA directly (Faux et al., 2007). But RPTPα may still play an indirect role in TrkA regulation, for instance through Src, which is indeed known to be activated by RPTPα and to transactivate Trks (Zheng et al., 1992, den Hertog et al., 1993, Fang et al., 1994, Zheng et al., 2000, Johnson and Van Vactor, 2003). An effect on TrkA might have not been detected in previous experiments for instance due to low expression of Src in the used cell line. However, RPTPα might also be expressed in Trk^+ neurons for reasons unrelated to Trk regulation.

Ptprd expression showed similarity to the expression of *Ntrk1* and *Ntrk2* in the qPCR screen, but it was coexpressed with all Trk receptors by *in situ*. No interaction between RPTPδ and any Trk protein was previously reported nor was its expression actually detected in DRGs in contrast to our study. However, RPTPδ plays a role in the nervous system as knockout mice show neuronal abnormalities (Uetani et al., 1997, Uetani et al., 2000). In chick embryos RPTPδ was predominantly found in differentiated neurons in the CNS, where it promotes neuronal adhesion and regulates neurite outgrowth as an attractive and repulsive guidance cue and might be involved in synapse formation (Sommer et al., 1997, Schaapveld et al., 1998, Van Vactor, 1998, Wang and Bixby, 1999, Johnson and Holt, 2000). RPTPδ could also full-fill Trk-dependent or independent functions in DRGs.

Ptprg was also ubiquitously expressed in DRGs and surrounding tissues, and the qPCR array analysis revealed a possible similarity to TrkA and TrkB expression. The coexpression analysis additionally confirmed its expression in all Trk^+ neurons. But in similarity to *Ptprf, Ptprs* and *Ptprr,* not all $TrkA^+$ neurons expressed this phosphatase. Interestingly, RPTPγ-deficient mice did not show any abnormalities in NGF-induced neurite outgrowth (Lamprianou et al., 2006). In addition, contradictory findings have previously shown that RPTPγ and not RPTPζ inhibits TrkA-mediated neurite outgrowth in PC12 cells, but more recently the opposite has been reported. The authors of both papers postulated, that whereas RPTPγ interacts with Trk downstream pathways, RPTPζ directly dephosphorylates Y674 and/or Y675 in the catalytic domain of TrkA and thus controls its kinase activity (Shintani et al., 2001, Shintani and Noda, 2008). Therefore, RPTPγ might also play Trk-dependent or -independent functions in DRGs.

The increasing expression of ***Ptprz1*** in the qPCR analysis indicated a possible expression in glia cells. Further, strong expression was detected in the ependymal layer lining the spinal canal at earlier developmental stages and this tissue contains indeed mostly glia cells. The staining in DRGs was very faint but might be located around neurons. RPTPζ expression was previously identified predominantly in glia cells such as Schwann cells and SGCs in embryonic and adult rat DRGs but also in a subset of neurons (Canoll et al., 1993, Haworth et al., 1998, Shintani et al., 1998, Van Vactor, 1998, Harroch et al., 2000). Its expression also partly correlated with the truncated TrkB isoform in non-neuronal cells (Snyder et al., 1996). In previous coexpression studies in HEK293T cells RPTPζ dephosphorylated TrkA and an over-expression of RPTPζ in PC12 cells inhibited NGF-induced neurite outgrowth (Shintani and Noda, 2008). These findings are consistent with the elevated TrkA-phosphorylation state in RPTPζ-deficient mice, which also display aberrant motor coordination, and reduced responses to moderate nociceptive stimuli (Lafont et al., 2009). In addition these mice have also an impaired ability in the recovery from demyelination (Harroch et al., 2000, Harroch et al., 2002). The expression of *Ptprz1* in DRGs was unfortunately too low for a coexpression analysis with Trk receptors. Together with previous studies our findings support a role of RPTPζ possibly in glia cells, which might be Trk-dependent or -independent.

Ptpro expression was the most unique and interesting among all analysed RPTP genes. The qPCR analysis indicated no similarity to any specific Trk gene expression, but suggested a possible expression in a subtype of neurons. The ISH analysis showed that *Ptpro* was expressed in particular cells within the DRG, but this amount of cells appeared to be bigger than $TrkB^+$ or $TrkC^+$ neurons alone, thus suggesting an expression in these two cell types together. The coexpression analysis revealed that approximately 56% of $Ptpro^+$ neurons coexpressed TrkB (100% of $TrkB^+$ neurons), 49% coexpressed TrkC (78% of $TrkC^+$ neurons) and 28% coexpressed TrkA (5% of $TrkA^+$ neurons). These results confirm the previous assumption that a specific subpopulation of Trk^+ neurons expresses this phosphatase. Our findings partly agree with a previous expression study by Beltran *et al*. on murine cervical and cranial ganglia at E16. In their analysis, twice as many $Ptpro^+$ neurons were detected in E16 DRGs, in agreement with the increase of RPTP-BK expression during development. Of these, 50% coexpressed TrkC (80% of all $TrkC^+$ neurons) and only 15% coexpressed TrkB

(19% of all TrkB$^+$ neurons). TrkA and *Ptpro* coexpression was also abundant especially in TG but was not quantified (Beltran et al., 2003). Interestingly, a comparison between these two studies showed a possible dynamic change in the coexpression of *Ptpro* with TrkA and TrkB receptors but no changes in the proportion of TrkC and *Ptpro* expressing neurons across development between E13.5 and E16.

So, which neurons express *Ptpro*? First, *Ptpro* could be expressed in neurons that coexpress more than one Trk receptor. If this were true, its expression would be very high at earlier stages and disappear completely at later stages like TrkA/TrkB/TrkC coexpression. However, instead an increase in *Ptpro* expression throughout development from E12 onwards and a peak between E16 until P3 was detected (Van Vactor, 1998). In addition, as described above, the cell amounts of Trk-coexpressing cells do not add up to confirm an expression of *Ptpro* in Trk-coexpressing neurons only, as the amount of *Ptpro*$^+$ neurons is considerably higher than the amount of Trk-coexpressing neurons. Though interestingly the amount of TrkB/TrkA and TrkC/TrkA-coexpressing neurons together was similar to the total amount of *Ptpro*/TrkA-coexpressing neurons (both around 5%) (Figure 1.12). Additionally, my analysis was restricted to neurons with the highest expression intensities to avoid ambiguous results, but *Ptpro* expression was in fact also found in a subset of neurons with very low staining intensity similar to reported findings (Haworth et al., 1998). This might complicate matter, but also possibly explains the lack of an obvious correlation with Trk-expression.

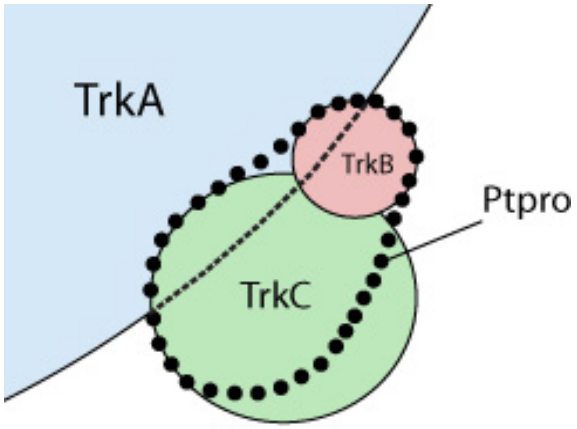

Figure 4.12. Schematic representation of *Ptpro*/Trk coexpression in murine E13.5 DRGs.
Displayed are a fraction of TrkA$^+$ neurons (blue) and the entire TrkB$^+$ (red) and TrkC$^+$ (green) neuronal populations. The dotted line represents the population of *Ptpro*$^+$ neurons. The coexpression analysis revealed that all TrkB$^+$ neurons, around 80% of TrkC$^+$ neurons and around 5% of TrkA$^+$ neurons coexpress *Ptpro*.

A coexpression and possible interaction of RPTP-BK with Trk receptors is also supported by the fact that RPTP-BK$^{-/-}$ mice show nociceptive (TrkA) and proprioceptive (TrkC) defects (Gonzalez-Brito and Bixby, 2009). Interestingly, the phenotype of RPTP-BK$^{-/-}$ mice appears to be similar to the phenotype of mice deficient in the TFs Runx1 and Runx3, which control the differentiation of TrkA and TrkC sensory neurons by initiating TrkA and TrkC expression and partly suppressing TrkB expression (Gonzalez-Brito and Bixby, 2009). So, *Ptpro* expression might be in fact linked to Trk expression on the level of transcriptional control.

Additionally, RPTP-BK homologs in *Drosophila* and chick are able to control axon guidance in CNS neurons (Desai et al., 1996, Krueger et al., 1996, Ledig et al., 1999b, Sun et al., 2000b, Stepanek et al., 2001). And RPTP-BK$^{-/-}$ mice also showed neurite guidance defects of proprioceptive and nociceptive neurons (Gonzalez-Brito and Bixby, 2009), similar to the phenotype observed in Runx3$^{-/-}$ mice (Arber et al., 2000, Inoue et al., 2002). These findings together with our coexpression data point to a yet unknown connection between RPTP-BK and Trk expression and function. In this context, RPTP-BK might control the differentiation of Trk^{+} neurons possibly on the transcriptional level. It will be of particular interest to analyse the function of this RPTP in context with Trk expression and function in more detail.

The marginal candidate genes *Ptprj, Ptprk* and *Ptprm* were expressed at the lowest levels in the qPCR analysis and almost no expression was detected using ISH. The comparative qPCR analysis revealed that these genes might be expressed in the smallest subpopulation of DRG neurons like TrkB and/or TrkC, but this similarity might also be brought about merely by their low expression. However, due to the sensitivity threshold of ISH no coexpression analysis was performed. We conclude that these phosphatases might be indeed expressed in DRG cells, either in neurons or more likely in non-neuronal cells (see also discussion chapter 3). Based on their low expression and lack of similarity to Trk-expression an implication in Trk signalling is unlikely.

Taken together the qPCR and ISH expression analyses performed on embryonic DRGs at three developmental stages (E12.5 - E14.5) displayed how dynamic the expression of Trks and RPTPs is during development. These expression profiles were used to identify similarities between Trk and RPTP expression and revealed a unique expression pattern

for all eleven analysed phosphatases. Most of the strongly expressed genes demonstrated a certain degree of similarity to the expression of Trk receptors. However, none of these phosphatases showed similarity in gene expression to one particular Trk receptor but instead to at least two but mostly all three Trks. The coexpression analysis of selected RPTP genes with Trk receptors in E13.5 DRG neurons supported these results as the majority of Trk^+ neurons expressed more than one RPTP gene and *vice versa*. The fact that with all of the RPTPs detailed here, there is a small percentage of TrkA-expressing neurons that do not express them, indicates that there can be no hard link between the regulation of TrkA signalling and any specific RPTP. Presumably if RPTPs are to be seen as key regulators of TrkA as previously suggested, then in any particular neuron TrkA has many RPTPs to choose from. This in turn should imply a high potential for functional redundancy in RPTP action and in turn confirm, indirectly, the likely promiscuity in RPTP target specificity. This also agrees with the molecular studies of some RPTPs and Trks to date.

Among the RPTPs studied here, RPTP-BK showed the most interesting coexpression patterns with Trks. Along with the highly expressed RPTPs LAR and RPTPσ, RPTP-BK function and their possible implication in Trk signalling, which governs crucial neuronal processes such as neurite outgrowth and cell survival, as was previously suggested mostly in over-expression systems, was further studied in knockdown experiments in dissociated primary murine embryonic DRG cells (chapter 6).

Chapter 5

Development of a method to knockdown RPTP gene expression in embryonic sensory neurons

5.1. Introduction

The function of some RPTPs in Trk signalling was previously analysed but mostly in over-expression assays (section 1.4). The aim of these experiments was therefore to establish an assay for the analysis of the physiological function of specific RPTPs in Trk signalling in primary murine embryonic sensory neurons.

In general the physiological function of proteins can be analysed by reducing or even eliminating them from a particular system such as a cell or a whole organism and examining the effects thereafter. For this purpose either knockout animals are generated or knockdown techniques such as RNA interference (RNAi) tools are used. A transgenic animal allows analysis of the protein function in its endogenous environment and even behavioural studies can be carried out. However, it is not always the best solution as it is expensive and time-consuming to generate a transgenic animal and in many cases these animals have either no particular phenotype or die prenatally, which complicates the analysis. RNAi represents a very powerful tool to analyse the function of a protein in a rather simple and straightforward manner and was therefore used in this study.

RNA interference (RNAi) is a naturally occurring highly conserved mechanism in certain organisms and cell types, which is thought to be part of a natural defence system against exogenous viral agents, or is involved in transposon-silencing or gene regulation. During this posttranscriptional gene silencing mechanism, double-stranded RNA (dsRNA) causes degradation of the homologous mRNA and thus prevents its translation into a protein. Gene silencing was long known to exist only in plants, until Fire and Mello identified dsRNA as the initiators of the RNAi pathway also in *Caenorhabditis elegans* (Fire et al., 1998). Later on its existence in eukaryotic cells such as in mammals was also proven. The RNAi pathway is known to consist of five steps. First the dsRNA is cleaved into short 21-25 nucleotide small interfering RNAs (siRNAs) by the ribonuclease Dicer. In the second step the siRNAs assemble with several proteins into the RNA-inducing silencing complex (RISC). In the next step the ATP-generated unwinding of the siRNA activates RISC, which then binds to the homologous mRNA transcript by base pairing interactions and cleaves it. The mRNA pieces are no longer protected by the poly-A-tail and the cap-structure and are thus degraded by exonucleases (Dykxhoorn et al., 2003).

Scientists have exploited this gene silencing mechanism to study gene function. In simple organisms such as *C. elegans* and *Drosophila,* RNAi can be induced by long dsRNA. In complex mammalian organisms however, dsRNA longer than 30 bp activates a non-specific, interferon-mediated response, which shuts down any translation and initiates apoptosis. To overcome this problem, siRNA, which mimic the first step of the endogenous RNAi pathway, are used in mammalian cells. These siRNA molecules can be chemically synthesised, transcribed *in vitro* or generated by digestion of long dsRNA by RNAse III or Dicer, and are then introduced into the cells. However, this achieves only transient effects and once the siRNA pool is depleted the mRNA is no longer destroyed. To overcome this problem, plasmids were developed that intracellularly express siRNA in the form of small hairpin RNA (shRNA). The shRNA is encoded by sense and antisense RNA strands which are separated by a short loop. After transcription it folds into an shRNA and is cleaved by Dicer into siRNA, which initiates the RNAi response (Mittal, 2004, Sandy et al., 2005).

However, the introduction of the si/shRNA molecules into the cells of choice remains one of the main hurdles for a successful knockdown experiment. This has proven to be especially challenging for postmitotic primary cells such as primary sensory neurons, which were used in this study. Therefore in this chapter I have explored possibilities to introduce shRNA molecules targeting candidate RPTP genes into primary sensory neurons with highest efficiency, which is essential to achieve a proper knockdown of these genes.

Many different gene delivery techniques are being developed to introduce foreign nucleic acids into the cells of choice. These are on the one hand non-viral chemical or mechanical transfection techniques such as liposome-based methods or electroporation and on the other hand transduction with viral particles. Both techniques have advantages and disadvantages. Non-viral techniques are less costly and easy to use, but are not efficient in all cell types and can also be cytotoxic. Viral techniques are very efficient in postmitotic cells, but depending on the virus type could also cause advert effects such as an immunological response, or disruption of genes in the case of integrating viruses. They are also more time-consuming and costly.

In this chapter I have analysed both non-viral and viral gene delivery methods for their efficiency to introduce DNA plasmids into murine embryonic sensory neurons. Whereas different non-viral methods proved to be inefficient, the lentiviral approach

was very successful. Subsequently, I have set-up a lentivirus-mediated gene knockdown assay and have analysed the effects of lentiviral transduction on gene expression and morphology of the sensory neurons. The final RPTP knockdown experiments and the analysis of the effects on NT signalling pathways will be described in Chapter 6.

5.2. Experimental procedures

Protocols for cell culture techniques, DNA preparation and the preparation and maintenance of murine DRG cultures were described in the General Materials and Methods section (chapter 2).

5.2.1. Transient transfection techniques

5.2.1.1. Calcium phosphate transfection

Dissociated murine embryonic DRG cells were seeded at a confluence of 50-60% in a precoated (PLL and FN) 6-well-plate. Before transfection the medium was replaced with fresh growth medium. The transfection mixture was prepared as following: per transfection 2 μg of sterile high quality DNA in 90 μl ddH_2O were mixed with 10 μl of 2.5 M $CaCl_2$. One hundred μl of 2x HeBS (280 mM NaCl, 50 mM HEPES, 1.5 mM Na_2HPO_4, pH 7.05 adjusted with 5 M NaOH) were preloaded in a sterile Eppendorf tube and the DNA/$CaCl_2$ mixture was added drop-wise to the 2x HeBS whilst bubbling air up through the mixture. The DNA/$CaCl_2$/2x HeBS solution was incubated for 20 min at room temperature in order to allow crystal formation and then added drop-wise to the cells. After an incubation time of 6 to 16 h the cells were washed with PBS and fresh complete medium was added. 48 h after transfection the cells were examined for transgene expression and pictures were taken and processed as described in section 2.7.

5.2.1.2. Transfection with Lipofectamine™ and PLUS™ reagent

Dissociated murine embryonic DRG cells were seeded at a confluence of 70-80% in a precoated 12-well-plate. Before transfection the medium was replaced with fresh growth medium. For transfection of one well, 1 μg of sterile high quality plasmid DNA

was mixed with 200 µl Opti-MEM® I Reduced medium without serum (GIBCO). One µl of PLUS™ reagent (Invitrogen) was added to the diluted DNA and gently mixed. The mixture was incubated for 5-15 min at room temperature and 2.5 µl of Lipofectamine™ LTX reagent (Invitrogen) were gently added to the DNA/Plus reagent mixture and incubated for 30 min at room temperature to allow formation of complexes. One hundred µl of DNA/PLUS™-reagent/ Lipofectamine™ LTX complexes were added to each well. For optimisation of the transfection efficiency varying ratios of DNA to PLUS reagent (DNA (µg): PLUS reagent (µl): 1:0.5, 1:1, 1:2) and amounts of these complexes (1x, 2x and 3x) were tested. After incubation of the cells with the complexes for 6 h fresh medium was added. 48 h after transfection the cells were examined for transgene expression as described above.

5.2.1.3. Transfection with Lipofectamine™ and ME27 peptide

Dissociated murine embryonic DRG cells were seeded at a confluence of 70-80% in a precoated 6-well-plate. Per transfection reaction 1 µl lipofectamine was diluted in 60 µl OptiMEM and 40 µl (4 µg) of peptide ME27 and 1 µg of plasmid DNA diluted in 100 µl ddH_2O were added. After the growth medium was replaced with 1 ml fresh medium per well the lipid/protein/DNA solution was added. After incubation for 4-6 h the medium was replaced. 24-48 h after transfection, the cells were examined for transgene expression as described above.

5.2.2. Test of lentiviral pseudotypes

All viral preparations for this experiment were kindly provided by Dr. Natalie Ward. The eGFP-lentiviruses (pLNT/SFFV-eGFP-WPRE) were pseudotyped with envelop proteins from Vesicular Stomatitis Virus (VSVg), Baculovirus gp64 (gp64), Ebola Zaire (EboZ), Ross River Virus (RRV), Murine Leukaemia Virus – Amphotropic (MLV-A), Murine Leukaemia Virus – Ecotropic (MLV-E) and Hanta virus.

Dissociated DRGs from E13.5 CD-1 mouse embryos were seeded at a density of 30% (40.000 cells per well) in two 12-well-plates coated with PLL and FN and transduced as above at three different MOIs (25, 50 and 100) with the seven differently pseudotyped eGFP-expressing lentiviruses. The MOIs were determined by measurement of the mass of HIV-1 p24 antigen in the lentiviral vector preparation using

the Beckman Coulter HIV-1 p24 antigen assay according to the manufacturer's instructions (physical titration). Three wells were left untransduced. The cells were cultured in NGF-containing (50 ng/ml) complete medium for 96 h before fixation with 4% PFA (section 2.4.3). The cells were daily examined for eGFP-expression with the Zeiss Axiovert-135 and approximately ten pictures were taken per virus type as above. Exposure BF: 100 msec, GFP: 1 sec, Gain: 0, Digital gain: 1x.

To calculate transduction efficiency, fluorescent and total amount of neurons (120 to 290 neurons were counted per lentiviral type) was determined by manual cell counting on pictures using Openlab software and the percentage of transduced cells was calculated.

5.2.3. Production of HIV-1-derived replication deficient lentiviruses

5.2.3.1. Plasmids for virus production (2nd generation)

The packaging GAG-POL plasmid pCMVΔR8.74 was a gift of Dr. Natalie Ward in Prof. Adrian Thrasher's laboratory (Molecular Immunology Unit, ICH; originally obtained from Prof. Luigi Naldini, Istituto Scientifico H, San Raffaele, Italy).

The envelope plasmid pCEE encoding the envelope glycoproteins for murine leukaemia virus ecotropic (MLV-E) was a gift of Dr. Natalie Ward (originally obtained from Prof. Michael Green, University of Massachusetts).

For the virus production and titration studies the previously described vector plasmid pLNT/SFFV-eGFP-WPRE was used (Demaison et al., 2002). It is a variant of the pHR second-generation HIV-1-based vector containing a self-inactivating 3' LTR, a central polypurine tract (cppt), the spleen focus-forming virus U3 promoter (SFFV), an enhanced green fluorescent protein reporter gene (eGFP), and the woodchuck hepatitis virus posttranscriptional regulatory element (WPRE).

For knockdown experiments, I used the MISSION™ TRC lentiviral expression vector pLKO.1 containing shRNA directed against murine RPTP genes (Sigma, described in Figure 5.4 (Moffat et al., 2006)), which was kindly provided by Dr. Jörg Mueller and Prof. Frank Böhmer (PTPNET member, University of Jena, Germany).

5.2.3.2. Preparation of MLV-E pseudotyped lentiviruses

For virus production, 12 x 10^6 HEK293T cells were seeded in T175 cm^2 flasks the day before transfection (~ 80% confluence) as described in section 2.5.1. Per flask a DNA solution consisting of 19.2 µg vector construct, 28.8 µg envelope plasmid pCEE and 28.8 µg packaging plasmid pCMVΔR8.74 was prepared in a total volume of 1080 µl sterile ddH_2O. 120 µl $CaCl_2$ were mixed with the DNA solution and immediately added drop by drop to 1200 µl 2x HBS solution whilst bubbling it with an automated pipette. The mixture was allowed to form crystals for 20 min at room temperature. Meanwhile the medium was changed on the cells to 8 ml medium containing DMEM, 1% P/S antibiotics, 10% FBS, 20 mM HEPES buffer and 25 µM chloroquine to enhance virus production. Cells were overlaid with the transfection mix and incubated at 37ºC, 5% CO_2 for 6 h. After the incubation time the medium was changed to 15 ml normal growth medium. The cell supernatant was harvested after 48 and 72 h and concentrated as described below.

5.2.3.3. Concentration of MLV-E pseudotyped lentiviruses

5.2.3.3.1. Centrifugation method

Virus containing supernatants from three transfected T175 cm^2 flasks collected at 48 h and 72 h were pooled and cell debris was removed by filtering through a 0.22 µm filter (Millipore) (supernatant was stored at 4ºC for 24 h). 45 ml of this supernatant were spun in a 50 ml Falcon tube at 4000 rpm for 20 h at 4ºC in a centrifuge with a swing-rotor. Virus pellets were carefully resuspended in 120 µl OptiMEM (GIBCO) and incubated on ice for 20 min. The virus pellets were pooled and aliquots stored at -80ºC.

5.2.3.3.2. Filter Devices

Virus-containing supernatant from two transfected T175 cm^2 flasks collected at 48 h were passed through 0.22 µm filters (Millipore). 15 ml filtered supernatant were loaded into each Amicon Ultra-15 Centrifugal Filter Device (Millipore) and spun at 2500 rpm for 45 min at 4ºC. This step was repeated with an additional 15 ml supernatant using the same filter. The flow-through was discarded and the virus containing filtrate was stored at -80ºC.

5.2.3.4. Transduction of target cells with MLV-E pseudotyped lentiviruses

Target cells of interest (3T3 cells or murine dissociated DRGs) were seeded at a desired density one day before transduction. The culture medium was renewed shortly before infecting the cells with the lentiviruses. 24 h after transduction the culture medium was renewed and the cells were cultured for 48-72 h. The cells were daily examined for GFP-expression and morphological changes and pictures were taken and processed as described in section 2.7.

5.2.3.5. Titration of MLV-E pseudotyped lentiviruses – expression titre

Multiplicity of infection (MOI) is used as a parameter for the prediction of gene transfer events or viral infectivity in a population of target cells. MOI represents the ratio of input infectious units (titred on the target cell line) to the number of cells available for transduction (MOI = TU/amount of target cells). Hereby "infectious units" (IU), also referred to as transduction units (TU), represent the smallest amount of virus capable of infecting a cell. The "titre" of the original virus stock is defined as the number of infectious units per unit volume of the virus preparation. In theory the relationship between virus titre, its dilution, volume of viral stock used, and the proportion of infected cells, should be linear. However, in reality the transduction of cells to estimate viable virus titres is non-linear and depends on many different factors such as number of target cells, inoculum volume, time of transduction etc. Thus all calculations are rather estimates than exact values (Zhang et al., 2004).

To estimate the titre (TU/ml) of eGFP-lentiviral vectors, target cells of interest (NIH 3T3 cells or DRG cells) were seeded into a multi-well-plate at a confluence of 50-60% one day before transduction. A one-fold dilution series of lentiviruses from 60, 30, 10 µl down to 10^{-6} µl in 100 µl aliquots of OptiMEM (GIBCO) was prepared and the target cells were immediately transduced with each dilution per well (100 µl) in a constant final volume. 72 h after transduction the cells were examined under a fluorescent microscope and five pictures were taken per well as described above. The amount of fluorescent neurons and total number of neurons were determined by manual cell counts on pictures with 5-50% positive cells as values below 5% are close to background and above 50% have an increased chance for multiple infections per cell. The area of the plate and the proliferation rate of NIH 3T3 cells (doublings time of

approximately 24 h) were taken into consideration. The average of the titres from all dilutions represented the final estimated titre of the virus preparation.

5.2.4. Initial test of the effects of MLV-E lentivirus infection on gene expression in primary sensory neurons

To assess the effect of MLV-E pseudotyped lentivirus transduction, non-targeting shRNA (Sigma or Qiagen) and two different concentration techniques (ultracentrifugation (centri) or filtration with Amicon Ultra-15 Centrifugal Filter Devices (filtered)) on the gene expression of dissociated DRG cultures from E13.5 CD-1 mouse embryos, the cells were infected with different MLV-E control lentiviruses and gene expression of Trks and several RPTPs was assessed with qPCR.

DRG cells were seeded at a density of 50% (250.000 cells per well) in 12-well-plates coated with PLL and FN and transduced with the following MLV-E pseudotyped control viruses: centri or filtered eGFP lentiviruses (pLNT/SFFV-eGFP-WPRE) and centri or filtered control lentiviruses containing non-targeting shRNA from Sigma or Qiagen in pLKO.1 puro. The cells were infected in duplicates with half of the whole virus production in a total volume of 450 µl per well. The cells were cultured in NGF- and BDNF-containing (50 ng/ml) complete medium for 72 h, daily examined and pictures were taken as described above.

QPCR analysis was performed to assess the effect of viral infection on gene expression in DRGs. RNA was extracted from the transduced cells after 72 h, reverse transcribed and qPCR was performed on 15ng cDNA of each sample on 96-well plates with primers against all three Trk genes and the RPTP genes *Ptpra, Ptprf, Ptpro, Ptprr* and *Ptprs. Psmb2* was used as a HKG for comparative data analysis. The experiments were performed in duplicates. Detailed protocols can be found in Chapter 2.2.

NOTE: To eliminate any viral residues all disposable equipment and cells, which came in contact with the virus particles, were treated with Virkon disinfectant (Anachem) for at least 24 h before appropriate disposal.

5.3. Results

5.3.1. Non-viral DNA delivery techniques

Different non-viral transfection techniques have been developed to introduce DNA into eukaryotic cells by either chemical reagents such as calcium phosphate ($CaPO_4$) and liposomes or physical methods such as microinjection and electroporation. They are mostly technically easy to use, not expensive, cause little or no cytotoxicity and unrestricted amounts of DNA can be used. Transfection is a transient event and the integration of foreign DNA into the chromosome of the target cell or stable episomal maintenance occurs at very low frequency. Therefore reporter gene systems such as drug resistance or fluorescent reporters for instance the green fluorescent protein (GFP) and its derivatives are used, which allow us not only to monitor the transfection efficiency but also to select for successfully (stably) transfected cells. Non-viral techniques are the method of choice to introduce nucleic acids quickly and efficiently into many different cell types. However, the transfection efficiency is the main limiting factor and it is known that some cell types such as primary neurons are difficult to transfect.

5.3.1.1. Non-viral DNA delivery techniques were unsuccessful in introducing plasmids into murine embryonic DRGs

Three different non-viral gene delivery methods available in our laboratory were tested for their efficiency to introduce an eGFP-expressing plasmid into primary sensory neurons from dissociated murine embryonic DRGs (Figure 5.1). The routinely used $CaPO_4$ transfection is based on the formation of a precipitate containing $CaPO_4$ and DNA. The precipitate adheres to the cell surface and is internalized via endocytosis or phagocytosis by the cell. This method was very efficient for plasmid delivery into cell lines such as HEK293Ts (see chapter 7), but no transfection of neurons was observed using this technique (Figure 5.1A).

Further, liposome-mediated transfection techniques were tested, which are very sensitive and non-toxic to primary cells. In principle lipids are mixed with DNA and build complexes, which are taken into the cells via endocytosis or membrane fusion. The lipids disrupt the endosome and the DNA is released into the cytoplasm and thus

escapes endosomal degradation. In this study I have used Lipofectamine™ Reagent (Invitrogen), which is a 3:1 liposome formulation of the polycationic lipid DOSPA and the neutral lipid DOPE. Lipofectamine alone did not transfect primary sensory neurons (data not shown). Current research investigates possibilities to enhance lipid-mediated transfection into cell types, which are non-permissive to many non-viral transfection methods such as primary neurons, for instance by addition of reagents or proteins. In this study I have tested two such methods.

First, a lipofection-based formulation containing the integrin-targeting peptide ME27 kindly provided by Dr. S. Hart (Molecular Immunology Unit, ICH) was tested. The peptide ME27 consists of an integrin targeting cyclic RGD domain and a sixteen lysine domain for DNA binding, separated by a four-amino-acid-linker sequence, which is cleavable by endosomal enzymes (Hart et al., 1998). Endosomal cleavage promotes disengagement from the integrin receptor and its release into the cytoplasm. A similar lipid-peptide formulation was previously used for transfection of neuroblastoma cells very efficiently (Grosse et al., 2010). The transfection rate for sensory neurons in this study however, was very low. Only non-neural cells were fluorescent green with the exception of one or two neurons (Figure 5.1B).

I have then assessed the transfection efficiency of lipofectamine™ LTX with PLUS™ reagent (Invitrogen). Different DNA:PLUS reagent ratios and varies amounts of the mixture to transfect dissociated murine DRG cultures were tested. The efficiency of transfection of the whole DRG cell population was highest at a ratio of 1:1 and increased with the amount of the liposome-DNA-PLUS reagent mixture added onto the cells. But almost exclusively non-neural cells were transfected using this method (Figure 5.1C).

The mechanical non-viral delivery method nucleofection, a type of electroporation, was previously tested by Dr. Claire Faux (Stoker's group). However, this had also a low transfection rate and caused a high amount of cell death (Faux et al., 2007). Thus it was not appropriate for our study especially since the cells would be very stressed, causing an alteration of their signalling pathways.

In summary, none of the non-viral techniques tested in this study have proven to be efficient enough to transfect primary sensory neurons. Therefore the viral gene delivery system was assessed.

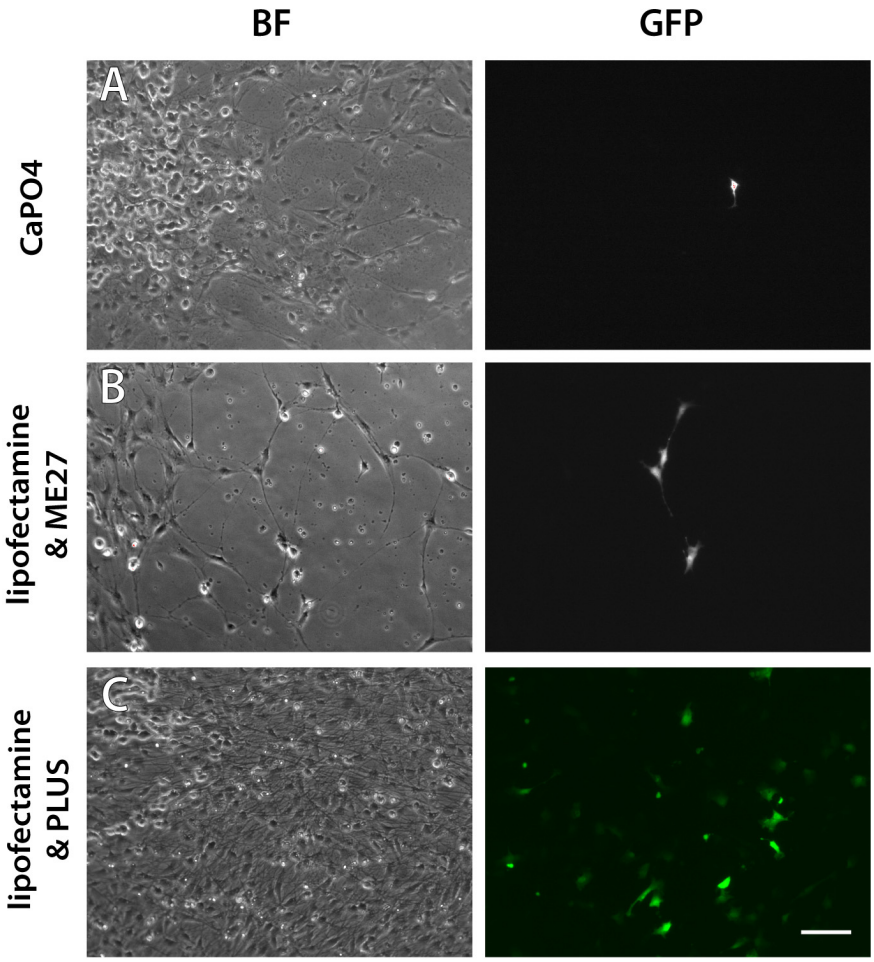

Figure 5.1. Non-viral gene delivery techniques.

Three different non-viral gene delivery techniques were tested for their transfection efficiency of murine embryonic sensory neurons. **A**) $CaPO_4$ transfection, **B**) transfection with lipofectamine (Invitrogen) and peptide ME27 **C**) transfection with lipofectamine LTX with PLUS reagent (Invitrogen). All three techniques were inefficient to introduce an eGFP-plasmid into murine embryonic DRG cells. Pictures were taken with the Zeiss Axiovert-135 fluorescent microscope in bright field (BF) or FITC channel for GFP detection. Scale bar = 10 μm.

5.3.2. Viral gene delivery techniques – Transduction with HIV-1-derived replication-deficient lentiviruses

Viral techniques have proven to be very efficient in transducing cells, which are hardly or not at all permissive or too sensitive for transfection, such as primary neurons. Many different well-characterized viruses i.e. adenoviruses, adeno-associated-viruses (AAV) and retroviruses have been genetically modified, and are commonly used as gene delivery vehicles for instance in gene therapy. They are either non-integrating or integrating and can infect non-dividing cells or are dependent on the mitotic cycle of the host cell. Whereas integration is desirable as it provides stable gene delivery, it is also rather random and can lead to insertional mutagenesis and subsequent cell damage. The immune response is another major problem especially for gene therapy.

One of the most popular viruses used as a gene delivery vehicle is the retrovirus and it was also the virus of choice for the first successful experiments to introduce dsRNA into primary almost non-transfectable cells and to induce RNAi (Barton and Medzhitov, 2002). Retroviruses are naturally occurring pathogens, which infect host cells in order to use their cellular machinery for the production of new progeny. For their life cycle they require proteins, which are encoded by the viral RNA. This RNA is replicated into DNA and integrated into the host chromosomes after infection. Thus proteins for the viral infection and production such as the reverse transcriptase/integrase POL, GAG for viral structural proteins and ENV for the viral envelope glycoproteins are produced and new viral particles assembled. The latter determines the tropism or host specificity of the virus by interaction with receptors on the surface of the host cells. Scientists have exploited these very efficient mechanisms of cell entry for stable gene delivery but developed replication-deficient virus particles for safety reasons (see below). Moreover as the encoded sequence such as a transgene or an shRNA construct integrates into the genome of the target cells, it allows a long-term transgene expression or knockdown and they are not silenced during development. Nevertheless, one major caveat of retroviruses is that they can only integrate their viral genome during the mitotic phase and thus differentiated or non-cycling cells such as neurons are resistant to these viruses.

Lentiviruses such as the human immunodeficiency virus type 1 (HIV-1) are a type of retrovirus and thus encompass all the beneficial characteristics of retroviruses,

but can additionally integrate into the genome at both mitotic and post-mitotic stages. Therefore lentiviruses have been the tool of choice for the generation of replication-deficient viral transfer tools (Somia and Verma, 2000, Quinonez and Sutton, 2002, Sinn et al., 2005).

5.3.2.1. Efficiency screening of pseudotyped HIV-1-based replication deficient lentiviruses on murine embryonic DRG cultures

Pseudotyping is a naturally occurring event. It has been observed long ago that when a retrovirus and a Vesicular Stomatitis Virus (VSV) infect the same host cell, progeny virions contain the genome of one virus encapsidated by the envelope of the other virus and are called pseudotypes (Zavada, 1972). In the lab lentiviral vectors can be produced with virtually any kind of tropism and this has been exploited to generate species- and tissue-specific viral vehicles (Cronin et al., 2005).

In order to find the most efficient lentivirus with the right tropism for murine embryonic sensory neurons, we have tested seven differently pseudotyped eGFP-expressing lentiviruses. We used glycoproteins from VSV (VSVg), Baculovirus gp64 (gp64), Ebola Zaire (EboZ), Ross River Virus (RRV), Murine Leukaemia Virus – Amphotropic (MLV-A), Murine Leukaemia Virus – Ecotropic (MLV-E) and Hanta virus. All viruses used in this experiment were produced and kindly provided by Dr. Natalie Ward. We infected dissociated murine embryonic DRG cells with the listed viruses at three different multiplicities of infection (MOI) 25, 50 and 100 and examined the transduced cells daily (Figure 5.2).

The first fluorescent cells were detected after 48 h in wells infected with MLV-E and VSVg pseudotyped lentiviruses at all MOIs. Both viruses infected different cell types in the culture including neurons. The intensity of the transduced cells however, was higher for MLV-E pseudotyped than VSVg pseudotyped lentiviruses. Very faint green non-neural cells were also detected in wells pseudotyped with glycoproteins from RRV and Hanta virus. After 72 h transduced cells were seen in all wells with the exception of cells transduced with MLV-A pseudotyped viruses. At lowest MOIs some glia cells but no neurons were transduced by RRV, Hanta, EboZ and gp64 pseudotyped viruses. Many green cells, mostly neurons, were detected in wells transduced with VSVg and MLV-E pseudotyped viruses at all MOIs, but the latter virus generated stronger fluorescent signals. 96 h post transduction no changes were detected in

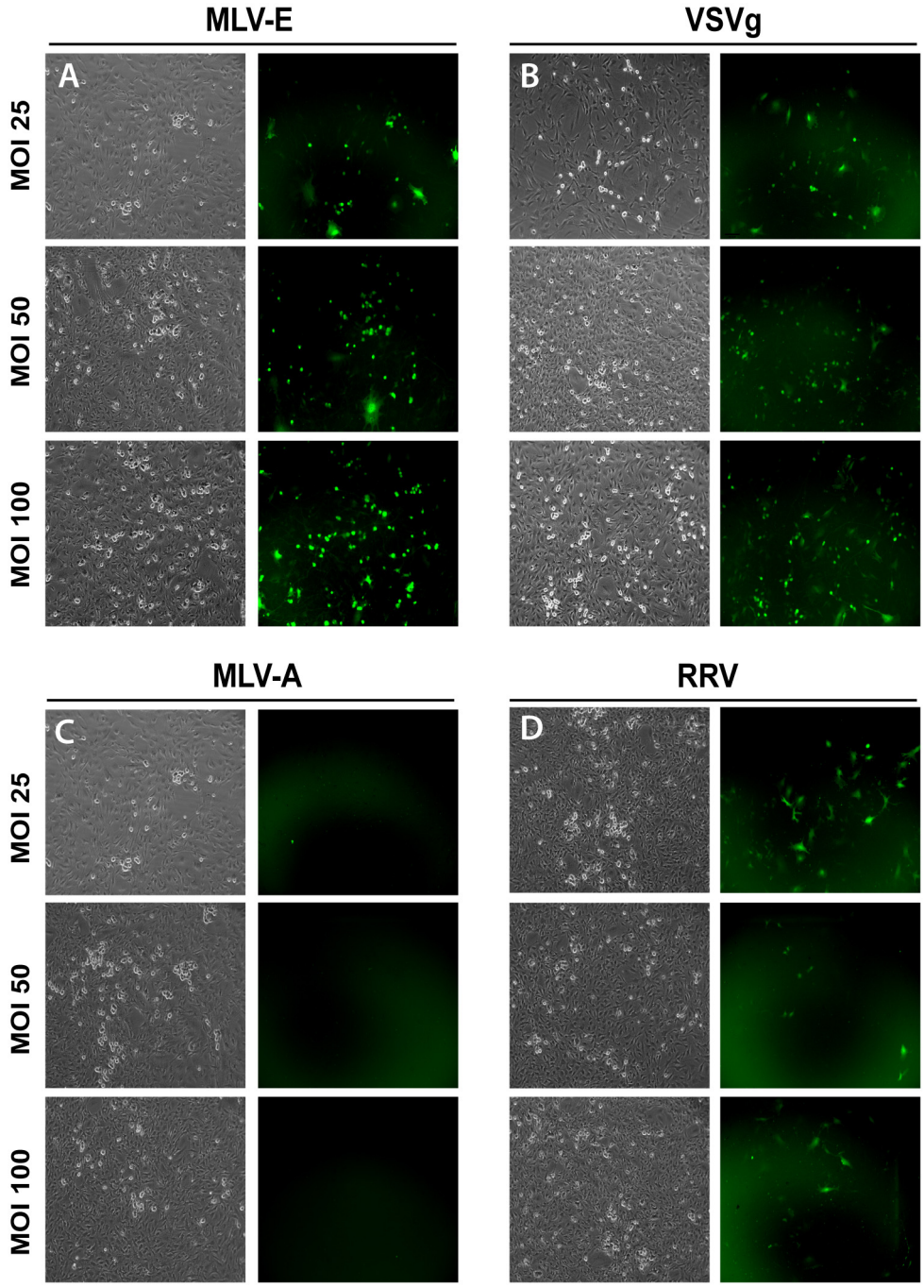
MLV-E
VSVg
MLV-A
RRV
A
B
C
D
MOI 25
MOI 50
MOI 100
MOI 25
MOI 50
MOI 100

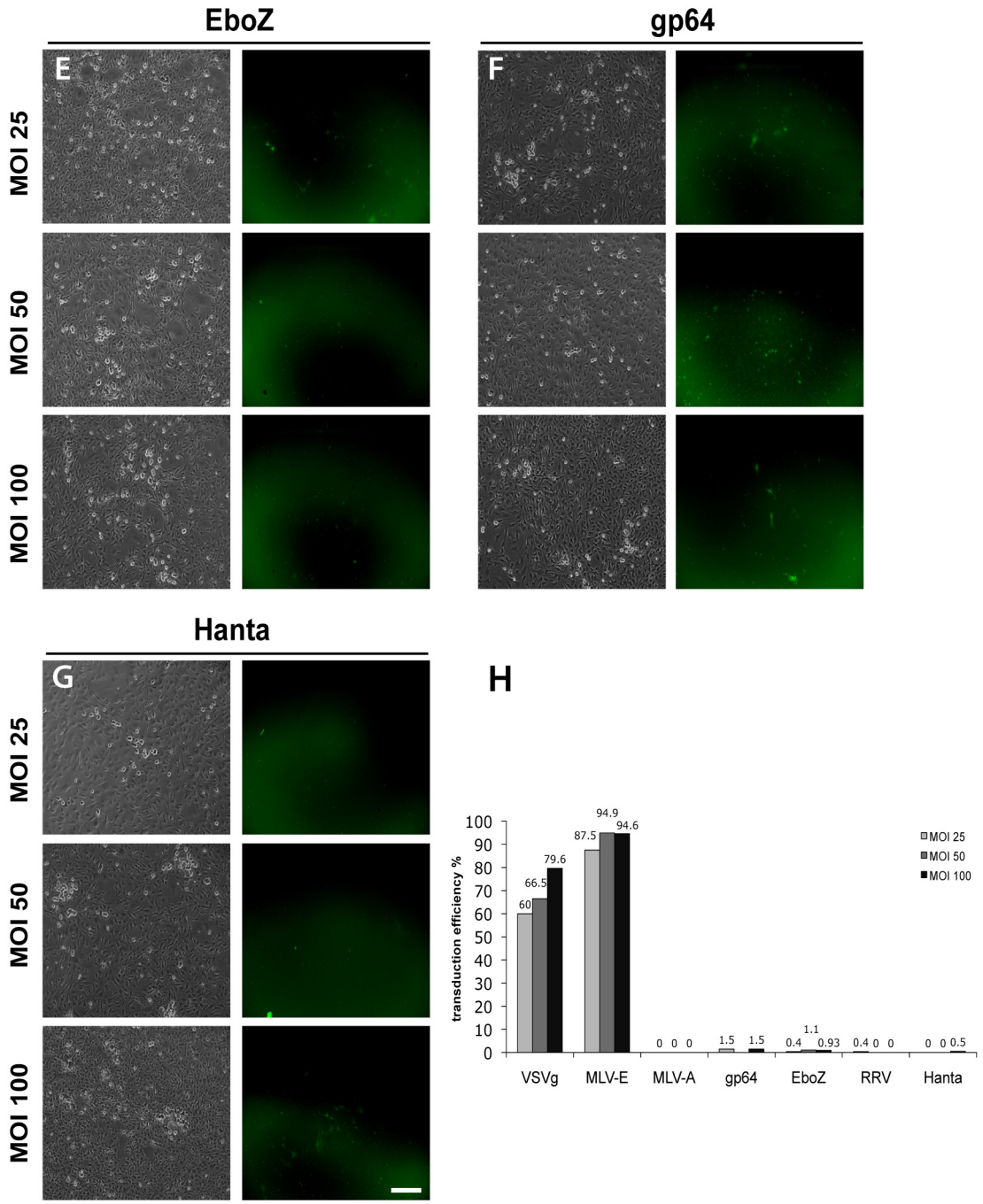

Figure 5.2. Screen of seven different pseudotypes of HIV-1 derived lentiviruses on murine E13.5 DRG neurons.

Primary dissociated murine embryonic DRG cultures were infected with HIV1-derived replication deficient eGFP-lentiviruses (pLNT/SFFV-eGFP-WPRE) pseudotyped with seven different envelope proteins from **A**) Murine Leukaemia Virus – Ecotropic (MLV-E), **B**) Vesicular Stomatitis Virus (VSVg), **C**) Murine Leukaemia Virus – Amphotropic (MLV-A), **D**) Ross River Virus (RRV), **E)** Ebola Zaire Virus (EboZ), **F**) Baculovirus gp64 (gp64) and **G)** Hanta virus (kindly provided by Dr. Natalie Ward, IMU). Three different MOIs (25, 50 and 100) per virus were tested. Scale bar = 10 μm. **H**) Transduction efficiency. 165-330 neurons were counted on pictures using Openlab software and efficiencies were calculated (Appendix, Table 5).

comparison to 72 h apart from the cells infected with the Hanta pseudotyped virus, which showed brighter intensity.

Among all seven differently pseudotyped lentiviruses tested in the present experiment the virus pseudotyped with MLV-E proved to be the most efficient at transducing sensory neurons with 95% transduction efficiency at an MOI of 50. No improvement could be seen at an MOI of 100. This was closely followed by the lentivirus pseudotyped with VSVg, which infected the primary neurons with an efficiency of 80% at an MOI of 100. All other viruses transduced preferably non-neural cells. Unexpectedly the MLV-A pseudotyped lentivirus did not transfect any cells at all. Since this experiment was performed just once, it cannot be excluded that something might have been wrong with this batch of MLV-A virus solution. Other batches of this virus, however, were tested on other cell types and successfully infected different cell types (personal communication with Dr. Natalie Ward). Cell death was not experimentally evaluated, but observations did not show any remarkable increase in cell death compared to untransduced controls.

Lentiviruses pseudotyped with glycoproteins from the ecotropic gammaretrovirus MLV (MLV-E) belonging to the Moloney strain have proven to be the most efficient to transduce almost all of the murine embryonic DRG neurons at an MOI of 50. MLV-E encodes $Pr80^{env}$, a glycosylated envelope precursor, which is proteolytically cleaved into the extraviral surface subunit (SU) gp70, which mediates viral binding, and the transmembrane (TM) subunit p15E, which mediates viral fusion. The final envelope complex is a trimer of heterodimers of both subunits (Pinter and Fleissner, 1979). The murine receptor on the host cells is the cationic amino acid transporter (CAT1), which can only be found on murine and rat cells (Kim et al., 1991). As expected MLV-E pseudotyped lentiviruses did not infect human HEK293T cells but did infect murine NIH 3T3 cells (data not shown).

Glycoproteins from the rhabdovirus VSV are today used the most to pseudotype lentiviral vectors due to their broad tropism. VSVg interacts with a ubiquitous cellular "receptor" of most eukaryotic cells. Additionally VSVg pseudotyped virus particles are very stable and can be therefore concentrated to a high titre by ultracentrifugation. However, VSVg is highly cytotoxic on the packaging cell line and may stimulate the host antiviral immune response. Since it can also infect human cells, it harbours a great risk for the scientist and many precautions have to be taken when work with this virus

type is carried out. In this respect MLV-E pseudotypes are more convenient for daily work (Schambach et al., 2006) on top of being more efficient for the transduction of primary sensory neurons. Therefore they were the pseudotype of choice in this study.

5.3.2.2. Production of MLV-E pseudotyped lentiviruses

For the production of HIV-1 derived replication-deficient lentiviruses usually a "third-generation" split plasmid system is used. Producer cells such as HEK293Ts are transfected simultaneously with three recombinant plasmids, which separately encode only essential genes for virus assembly and infection. One plasmid encodes the proteins GAG and POL for packaging and production of new viral particles and the second encodes envelope glycoproteins of the virus such as MLV-E. The third plasmid is the modified HIV-1 backbone vector, which harbours the gene or sequence of interest such as an shRNA construct to be transferred into the target cell. The producer cells then generate new replication-deficient viral particles, which are harvested, concentrated, titred and finally used to infect the target cells (Kutner et al., 2009). Each of these steps has to be optimized for the target cells of choice and thoroughly tested.

A sufficiently high titre for an efficient infection of the target cells is crucial for any experiment and for this purpose the produced viruses are further concentrated. Two different techniques for the concentration of MLV-E pseudotyped lentiviral particles were tested, the concentration via ultracentrifugation (centri) and concentration using Amicon Ultra-15 Centrifugal Filter Devices (Millipore) (filtered). The functional virus titres of the differently concentrated eGFP-HIV1-derived lentivirus preparations were determined by infection of NIH 3T3 cells and dissociated DRG cells. Although usually Fluorescent-activated cell sorting (FACS) methods are used for this purpose, due to the heterogeneity of the DRG cultures we have instead performed cell counts on pictures to determine the transduction efficiency specifically for neurons. Transduction of NIH 3T3 cells was performed as an estimation of the actual virus titre, whereas transduction of DRG cultures with the same virus preparation was used to assess specifically the transduction of neurons.

All in all the filtered viruses appeared to be twice as infectious as lentiviruses concentrated via ultracentrifugation on both NIH 3T3 and DRG cells (Table 5.2). One of the reasons for this result might be the damage of sensitive MLV-E glycoproteins by long ultracentrifugation. The differences in the titre values obtained on the different

cells are not unusual and in our study additionally explained by the fact that only transduced neurons were counted in the DRG cultures neglecting transduced non-neural cells (Zhang et al., 2004). Nevertheless, these numbers were only used as crude estimates and sufficient for the knockdown experiments (chapter 6).

CONCENTRATION TECHNIQUE	TITRE (TU/ml)
NIH 3T3 cells	
ultracentrifugation	$3.3*10^6$
Amicon Ultra-15 Centrifugal Filters	$7.7*10^6$
Murine embryonic DRG cells*	
ultracentrifugation	$2.1*10^6$
Amicon Ultra-15 Centrifugal Filters	$5.9*10^6$

Table 5.1. Test of two different concentration techniques for MLV-E pseudotyped eGFP-HIV1-derived lentiviral particles.
Murine embryonic DRG cultures and NIH 3T3 cells were infected with MLV-E pseudotyped HIV1-derived replication deficient eGFP-lentiviruses (pLNT/SFFV-eGFP-WPRE) from two virus preparations, which differed in the concentration technique used, either ultracentrifugation or filtration using Amicon Ultra-15 Centrifugal Filter Devices, to prepare them. * In the case of the DRGs these values refer only to transduced neurons.

5.3.3. Lentivirus-mediated knockdown of RPTPs using shRNA constructs

5.3.3.1. The MISSION™ TRC shRNA lentiviral vector pLKO.1 puro (Sigma)

For the knockdown of specific RPTPs the commercially available MISSION™ TRC (The RNAi Consortium) lentiviral expression vector pLKO.1 puro from Sigma containing shRNA sequences directed against murine RPTP genes were used. This HIV-1 derived lentiviral vector contains several important features for the assembly of replication incompetent viral particles, integration into the genome of the target cell, transcription of the shRNA transcript, and resistance genes for selection in bacterial and in transduced cells. Specifics are described in Figure 5.3. The shRNA sequence contains 21 “sense” bases, which are identical to the GOI, a loop containing an *Xho*I restriction site and 21 “antisense” bases, which are complementary to the “sense” bases, followed by a poly T-termination sequence for the RNA Polymerase III. These shRNA constructs

are designed using a proprietary algorithm (Ref.1, Ref.2) and most of them were also validated experimentally. Here I will briefly describe this system and several test experiments, which are crucial for a successful knockdown study.

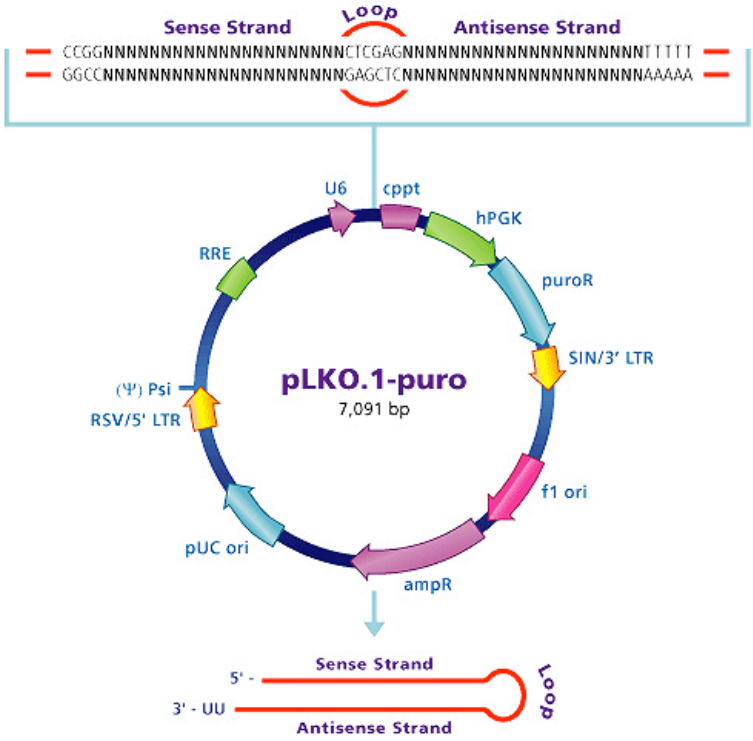

Figure 5.3. MISSION™ TRC lentiviral expression vector pLKO.1.
The HIV-1 derived replication incompetent lentiviral vector (Sigma) comprises a 5' long terminal repeat (RSV/5'LTR), an RNA packaging sequence Ψ, a Rev response element (RRE), the shRNA sequence under the transcriptional control of the U6 promoter (U6), a central polypurine tract (cppt), a puromycin resistance gene (puroR) under the control of the human phosphoglycerate kinase promoter (hPGK), a 3' self-inactivating long terminal repeat (SIN/3'LTR) and f1 origin of replication (f1 ori), the ampicillin resistance gene (ampR) and pUC origin of replication (pUC ori) (Moffat et al., 2006).

5.3.3.2. MISSION™ TRC shRNA-containing lentiviral vectors are stable and not immunogenic

For virus preparation, large amounts of vector DNA are needed. To test the stability of the pLKO.1 puro plasmids and assess whether any recombination occurred during plasmid preparation diagnostic restriction enzyme digests with *Hind*III were performed. No evidence of recombination was observed (data not shown).

One major concern when using RNAi constructs in mammalian cells is the induction of a non-specific defence mechanism (as mentioned above), which results in

an interferon response of the host cell leading to the complete shutdown of protein synthesis. However, TRC researchers at the Broad Institute, who have developed the shRNA containing vectors used in this study, have shown that these shRNA constructs did not induced any interferon response in the tested adenocarcinoma human alveolar basal epithelial cells (Moffat et al., 2006, Ref.3).

5.3.3.3. Effects of the transduction with MLV-E pseudotyped lentiviral particles on gene expression in primary sensory neurons

To assess whether the infection of dissociated murine E13.5 DRG cells with lentiviruses has any effects on their morphology and gene expression, which could potentially affect the interpretation of the results after the knockdown of RPTPs, I have performed an initial test experiment.

The sensory neurons were infected with different types of MLV-E pseudotyped lentiviruses that either contained eGFP in pLNT/SFFV-eGFP-WPRE or a non-targeting shRNA from Sigma or Qiagen in the pLKO.1 puro backbone vector or the cells were treated only with media, either Opti-MEM® or filtered HEK 293T supernatant consisting of highly concentrated DMEM medium supplemented with FBS and antibiotics, which were used as a carriers for the differently concentrated viruses. The cells were infected with half of the whole virus production per well in the same volume at an approximate MOI of 3 - 8 for the eGFP-encoding viruses (section 5.3.2.2). The MOI of the lentiviruses containing shRNA sequences could not be determined due to the lack of appropriate reporter genes in the constructs and titration tools. However, to some extent it can be assumed to be in the range of the MOI of the eGFP-lentiviruses, although differences in the backbone vectors might affect virus production and expression of the GOI slightly. The shRNAi-containing lentiviruses were successfully produced and were functional as gene knockdown was observed and the integration PCR assay was positive (chapter 6). In the initial test experiment the effects of the transduction with these lentiviruses on gene expression, specifically of all three Trk genes and the RPTP genes *Ptpra, Ptprf, Ptpro, Ptprr* and *Ptprs,* were assessed using qPCR analysis. Additionally cell morphologies were also examined.

First, the effect of the virus-containing media (filtered HEK 293T supernatant and Opti-MEM®) on the sensory neurons was assessed and compared to untreated cells (Figure 5.3A). Overall, gene expression was not much affected by these media. Further,

the effects of the differently concentrated viruses normalized to the medium of the virus preparation were compared with each other and all showed an effect on gene expression but with a varying degree (Figure 5.4B). In the case of the filtered lentiviruses, mostly eGFP-expressing viruses (eGFP filtered) and non-targeting Sigma control lentiviruses (ctrl S filtered) affected gene expression. The filtered eGFP-lentivirus boosted gene expression only of the three RPTPs *Ptpra*, *Ptpro* and *Ptprr* but did not alter Trk gene expression. Cells treated with the filtered non-targeting Sigma control lentiviruses showed increased expression of *Ntrk1, Ptpra* and to a higher degree of *Ptpro* and *Ptprs*, but slightly suppressed expression of *Ntrk2*. The control lentivirus containing a non-targeting shRNA from Qiagen also boosted the expression of *Ptpro* but to a lesser degree than the non-targeting Sigma control lentivirus. All centrifuged lentiviruses had a stronger effect on gene expression in sensory neurons than the described filtered lentiviruses and suppressed gene expression in some cases even to less than half of their expression in the Opti-MEM® control. The strongest effects were observed in cells transduced with eGFP-lentiviruses and non-targeting Sigma control viruses, which strongly suppressed gene expression of all Trks and RPTPs apart from *Ptprf*. The lentiviruses containing non-targeting shRNA from Qiagen also suppressed gene expression of all Trks and *Ptprf, Ptprr* and *Ptpra* but to a slightly smaller degree than the described non-targeting Sigma control virus; or boosted it instead of suppressing it for *Ptprs* and *Ptpro.*

Overall the lentiviruses concentrated via ultracentrifugation had a strong suppressing effect on gene expression, whereas the filtered viruses showed a smaller suppressing and sometimes even boosting effect on gene expression. However, no obvious morphological changes were observed in the cell cultures infected with either virus type (Figure 5.5). Additionally the non-targeting Sigma shRNA appears to have a stronger effect on gene expression than the non-targeting Qiagen shRNA. These results agree with observations made by Prof. F. Böhmer and Dr. J. Mueller (personal communication). It has to be noted that also the non-targeting Qiagen shRNA caused up to 20-30% changes in gene expression. However, this experiment was performed only once and at least two more repeats would be necessary for a reliable estimation. Finally, it was decided that the filtered MLV-E-pseudotyped lentiviruses and the non-targeting Qiagen shRNA were to be used in the knockdown study (chapter 6).

Figure 5.4. Effects of lentiviral infection of dissociated E13.5 DRGs on gene expression.

Primary dissociated murine DRG cultures were infected with MLV-E pseudotyped HIV1-derived replication deficient eGFP-lentiviruses (pLNT/SFFV-eGFP-WPRE) and control (ctrl) lentiviruses containing non-targeting shRNA from Sigma (S) or Qiagen (Q). Two different concentration techniques, ultracentrifugation (centri) and filtration (filtered), were tested and lentiviral infection was compared to cells incubated with Opti-MEM® (OPTI) or HEK293T supernatant (sup) depending on the concentration technique. **A)** Average gene expression in infected and control cells (ΔC_T) normalised to *Psmb2*. **B**) Changes in gene expression ($\Delta\Delta C_T$) upon infection with different viruses. Corresponding pictures of the cell cultures are displayed in Figure 5.5.

A) Average gene expression (dCT)

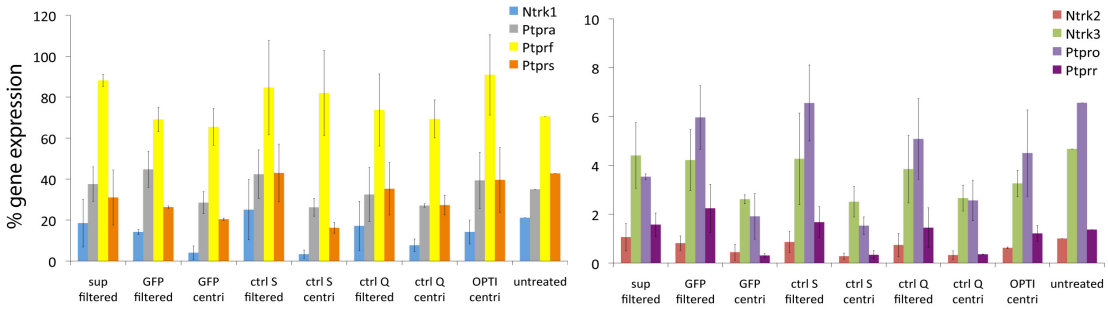

B) Changes in gene expression (ddCT)

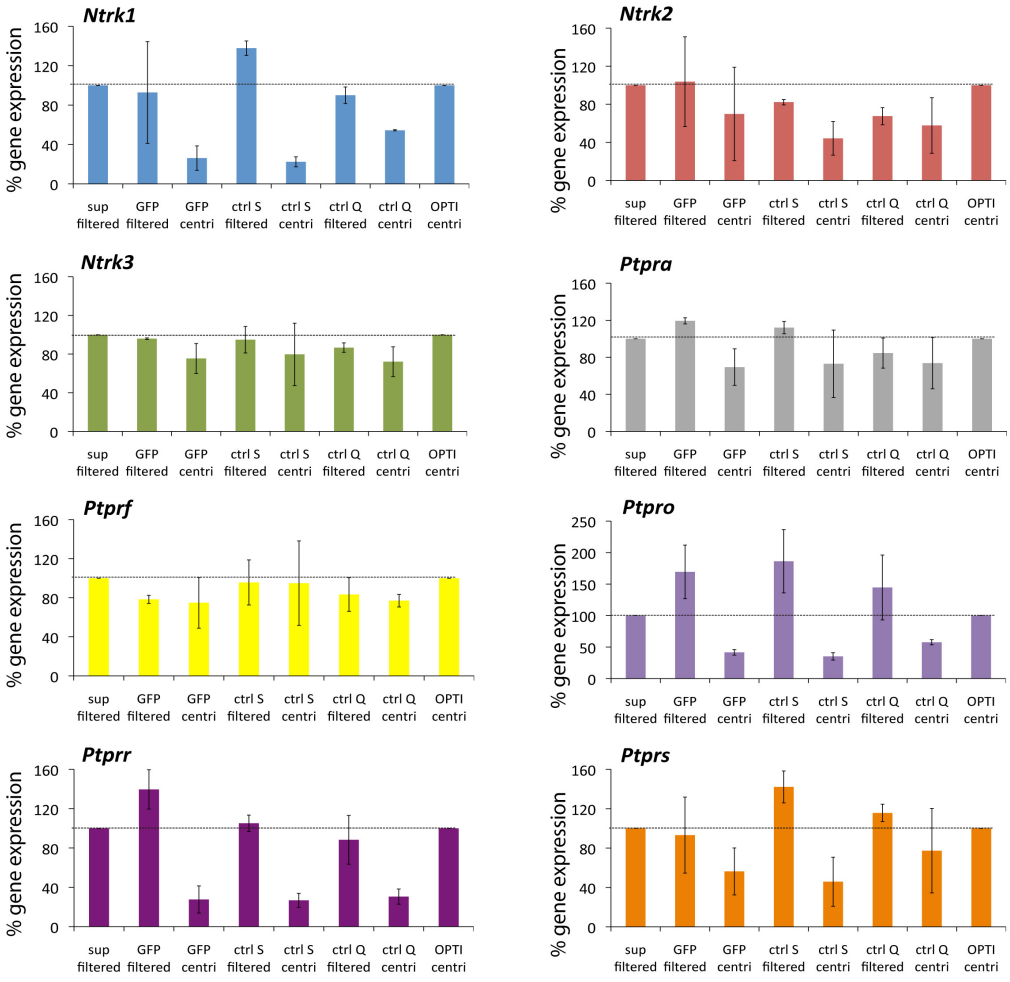

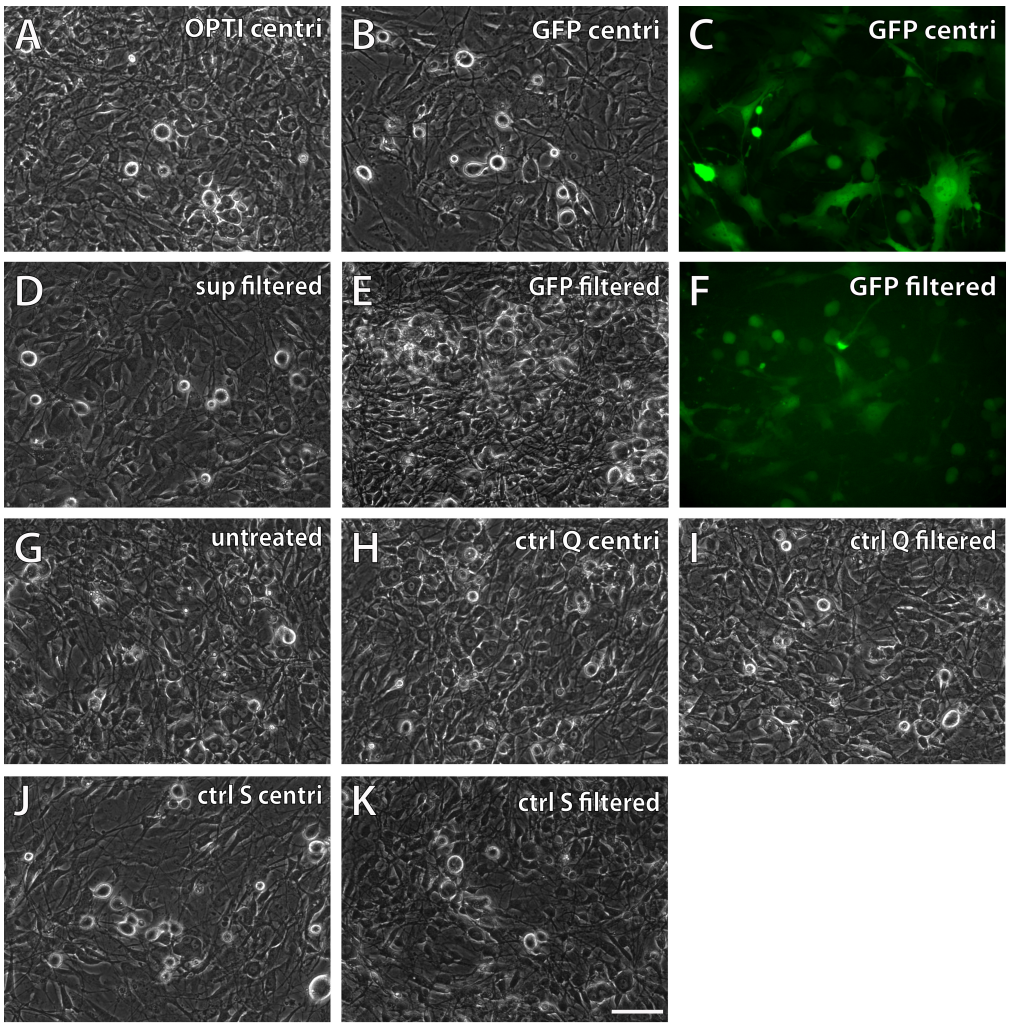

Figure 5.6. Effects of lentiviral infection of dissociated E13.5 DRGs on cell morphology.
Displayed are pictures of primary dissociated murine DRG cultures with different treatments corresponding to the qPCR results displayed in Figure 5.4. Cells were infected with MLV-E pseudotyped HIV1-derived replication deficient eGFP-lentiviruses (GFP) and control (ctrl) lentiviruses containing non-targeting shRNA from Sigma (ctrl S) or Qiagen (ctrl Q) that were concentrated either by ultracentrifugation (centri) or filtration (filtered) or cells were treated with Opti-MEM® (OPTI centri) or HEK293T supernatant (sup filtered). Scale bar = 10 μm.

5.4. Discussion

The results in these experiments have demonstrated that a lentivirus-mediated shRNA knockdown assay can be used in order to study the physiological function of RPTPs in Trk signalling in dissociated primary murine embryonic sensory neurons.

Primary sensory neuron cultures are a very suitable cell model system to analyse Trk signalling. However, these cells are difficult to manipulate in terms of the introduction of foreign DNA. As efficient introduction of shRNA constructs into the cells is the main requirement for a successful RNAi effect, different techniques were tested here to introduce DNA such as eGFP and shRNA constructs into primary sensory neurons. Whereas different transfection methods resulted in very low efficiency, the lentiviral approach was more promising. In a pseudotype screen we could show that MLV-E pseudotyped lentiviral particles transduced DRG cells with more than 90% efficiency. They are additionally safe to use as they only infect murine cells. Many different commercial lentivirus-based RNAi systems are nowadays available and we have tested the MISSION™ TRC lentiviral expression vector pLKO.1 from Sigma containing shRNA sequences targeting GOIs such as RPTPs.

In an initial test experiment the infection of DRG cells with non-targeting shRNA-containing lentiviral particles revealed no major changes in the morphology or gene expression of these cells after transduction with lentiviral particles concentrated via filtration at an MOI between 3 and 8. This number is noticeably much lower than the MOI used in the pseudotype screen, but cells infected with eGFP-lentiviruses were still sufficiently fluorescent. Also MOIs do not represent an exact value and depend on the methods used for their determination. In this study the MOI of viruses used in the pseudotype screen is based on a physical titre, which only calculates the amount of viral particles but not their infectivity. In contrast the MOI calculated for the test experiments is based on a functional titre and thus reflects the actual infectious nature of the virus. In the end it is solely important for our experiments that the viruses are successfully produced and infect neurons, which was shown to be the case. In fact a low MOI is preferable for our knockdown study as an overexpression of shRNA could overwhelm the RNAi machinery and produce aberrant results (Huppi et al., 2005).

Together, the lentiviral approach to introduce DNA into sensory neurons was successful and very efficient. Additionally, since lentiviruses are integrating, the shRNA

constructs will be constantly produced and thus provide a stable and long-term knockdown. Therefore the lentiviral approach was finally used to knockdown RPTP genes in sensory neurons in order to assess their function in Trk signalling (chapter 6).

Chapter 6

Effects of RPTPσ, LAR and RPTP-BK knockdown on Trk signalling in embryonic sensory neurons

6.1. Introduction

NT signalling controls vital functions of neurons such as survival or death, and proliferation and differentiation and thus it has been extensively studied since the discovery of NTs and Trk receptors (section 1.2). However, the regulation of the signalling cascades is still poorly understood and many questions remain unanswered. In recent years work has been carried out to analyse the implication of phosphatases including RPTPs in Trk signalling, but the vast majority of these studies was performed in artificial over-expression systems and their physiological relevance needs to be demonstrated (section 1.4).

In this study I have aimed for the challenging analysis of the physiological effects of specific RPTPs on Trk signalling in their endogenous environment, the sensory neurons from embryonic DRGs. In particular I was interested in the functional analysis of the three RPTPs, which were previously implicated in Trk signalling; the two strongest expressed RPTPs in DRGs, LAR and RPTPσ, and also RPTP-BK, which has a unique and very interesting coexpression pattern with Trks in DRGs (chapter 4). For this purpose I have employed the lentiviral-mediated RNAi approach (described in chapter 5) to knockdown these RPTPs and analyse the effects on Trk signalling on the protein and mRNA level.

One of the major advantages of the analysis of endogenous proteins in primary cells is the natural environment of these proteins. Unlike in artificial over-expression systems, all cell signalling components are present and thus results will not be altered for instance by missing adaptor proteins or the presence of different protein isoforms. Additionally, over-expression of proteins might cause adverse effects on cell signalling, and so this might be avoided by studying endogenous proteins in primary cell cultures. Thus the latter represents a valid approach to analyse the actual physiological function of the proteins of interest. It is important to take into account that sensory neurons from dissociated DRG cultures as used in the current study show many characteristics of regenerating sensory neurons *in vivo,* due to axotomy of their processes during culture preparation. But as many developmental processes are in fact recapitulated during regeneration, deciphering the active signalling pathways during this event can also lead to the understanding of neural development.

Trk signalling pathways and the involvement of RPTPs in those were thoroughly described in sections 1.2.3. and 1.4. Here, I will briefly recapitulate the major aspects relevant for the current study.

Trk signalling is initiated upon NT-binding, which leads to receptor dimerization, autophosphorylation of ten tyrosine residues and activation of the kinase activity. The Tyr autophosphorylation has two main purposes. On the one hand the phosphorylation of the three Tyr residues Y670, Y674 and Y765 (human TrkA) in the kinase domain potentiates kinase activity and the phosphorylation of the other residues. On the other hand phosphorylated Tyr residues represent docking or recognition sites for other signalling proteins (Schlessinger and Ullrich, 1992, Kaplan and Stephens, 1994). The best-analysed Tyr residues outside the catalytic domain are Y490, Y751 and Y785 mostly due to the availability of antibodies against these epitopes. Phosphorylated Y490 is required for Shc or Frs2 association and activation of the Ras-MAPK pathways leading to proliferation, differentiation, cell growth and neurite outgrowth. Phospho-Y785 binds directly to PLCγ-1, which leads for instance either to PKCδ-mediated MAPK pathway activation or Ca^{2+}-mediated regulation of synaptic plasticity through enhanced neurotransmitter release. The phosphorylation at Y751 is required for PI3K association and activation of the Akt signalling cascade, which inhibits apoptosis and activates prosurvival factors. All these pathways are interlinked and can activate each other under certain circumstances. As it has become apparent in recent years, an important component of the regulation of Trk signalling seems to occur through the tyrosine phosphatases.

In this study I have primarily analysed the phosphorylation of Trk Y785, due to the availability of good antibodies. This is a docking site for PLCγ-1, and upon binding PLCγ-1 is phosphorylated and can initiate neurite outgrowth via the PLCγ-1/PKCδ/MAPK pathway (Corbit et al., 1999). It can also enhance neurotransmitter release via the PLCγ-1/Ca^{2+}/CaMPK and PLCγ-1/Ca^{2+}/PKA pathways and is thus implicated in synaptic plasticity (Lessmann, 1998). The pTrk Y785/PLCγ-1 signalling additionally controls expression and activity of many proteins such as ion channels (Toledo-Aral et al., 1995, Klein et al., 2005). Mice with a specific mutation in the TrkB Y816 show impaired hippocampal LTP in the CNS (Minichiello et al., 2002) and also structural abnormality of synapses and impaired fibre guidance in vestibular neurons in the PNS (Sciarretta et al., 2010). I have additionally looked at the MAPK

Erk1/2 pathway and the Akt pathway, which both control neurite outgrowth and cell survival. These three pathways are mainly initiated through pY490 and pY751 in Trk signalling. However, Trk signalling pathways are cross-linked with many other pathways and remain poorly understood.

One of the best-analysed RPTPs implicated in this signalling pathway is LAR. Both augmenting and inhibitory roles for LAR on Trk-mediated and Trk–independent neurite outgrowth, cell survival and synapse morphogenesis depending on the context were discovered. For instance a knockdown study in hippocampal neurons presented an augmenting role of LAR on TrkB Y515 initiated signalling and a positive effect of LAR on the MAPK and Akt pathways. LAR knockdown resulted in a decrease in protein expression after 3 days, leading to a decrease in TrkB Y515 phosphorylation upon BDNF-treatment and a decrease in phosphorylation of the analysed downstream pathway components Shc, Erk and Akt and of the TF CREB. Additionally a deactivation of Src and a decrease in the BDNF-induced neurotrophic activity were observed. These data suggested an activation of Src by LAR, which then phosphorylates TrkB Y515 (Yang et al., 2006). In DRG explant cultures LAR activation showed also an augmenting effect on neurite outgrowth (Yang et al., 2005a). In PC12 cells LAR plays an inhibitory role on TrkA, as LAR downregulation resulted in an increase in NGF-mediated neurite outgrowth and decreased apoptosis (Moshnyakov et al., 1996, Tisi et al., 2000). In support of these findings inhibition of LAR in PC12 cells through a specific wedge peptide also resulted in an augmented NGF-induced phosphorylation of Tyr 490 of TrkA and its downstream pathway components Erk and Akt and enhanced neurite outgrowth (Xie et al., 2006). The effect of LAR on the phosphorylation state of Trk-Y785 was previously not directly assessed in any study. But in one report augmented LAR function in hippocampal $TrkB^{+}$ neurons lead to an increase in PLCγ phosphorylation. In the same study Erk phosphorylation was only slightly elevated (Yang et al., 2005a). Nevertheless, in this study these effects could also possibly be attributed to an effect of LAR on other growth factor receptors, which signal through the PLCγ-pathway. LAR could also have either a positive or a negative effect on Trk phosphorylation in sensory neurons. Therefore I have aimed to analyse the direct effect of LAR on Trk Y785 phosphorylation in DRG cells in my knockdown experiments.

RPTPσ is another RPTP, which was implicated in Trk signalling. RPTPσ is strongly expressed in the entire nervous system and $RPTP\sigma^{-/-}$ mice display the most

obvious neurological defects among all RPTP knockout mice (Elchebly et al., 1999, Wallace et al., 1999, Batt et al., 2002, Meathrel et al., 2002). Therefore the implication of this phosphatase especially in neurite outgrowth was previously analysed in several studies also in context with Trk signalling. Faux *et al.* have shown that RPTPσ can dephosphorylate all three Trks in an over-expression system in HEK293T cells and that an over-expression of RPTPσ in embryonic chick sensory neurons from dissociated DRGs resulted in the suppression of NGF-dependent neurite outgrowth without affecting their survival (Faux et al., 2007). These results support previous findings in adult retinal cells in RPTPσ$^{-/-}$ mice, in which increased neurite outgrowth was observed after a lesion. These mice displayed a constitutive elevation of the MAPKs Erk1/2 and Akt kinases, but PLCγ activation was not observed. An implication of RPTPσ in these downstream signalling pathways was suggested and possibly linked to Trk and EGFR signalling (Sapieha et al., 2005). However, in contrast to LAR the affected Trk Tyr residues were not identified yet and the physiological relevance of its interaction with Trk receptors also remains to be shown. Therefore its function in Trk signalling was also assessed in my knockdown study.

RPTP-BK appears to have a specific function in DRGs possibly mediated through Trk receptors. The importance of RPTP-BK in sensory neurons is most apparent in RPTP-BK$^{-/-}$ mice, which clearly display nociceptive and proprioceptive abnormalities such as the loss of the response to thermal pain (Gonzalez-Brito and Bixby, 2009). An interaction of RPTP-BK with TrkC was also previously studied and it was shown that both enzymes could interact with each other, whereby RPTP-BK also dephosphorylates TrkC (Hower et al., 2009). However, these experiments were performed in an over-expression system and the physiological relevance of this interaction remains to be assessed and the dephosphorylated TrkC tyrosines identified. Especially in regard to our findings in chapter 4, which have shown that RPTP-BK is expressed not only in TrkC^{+}, but also TrkA^{+} and TrkB^{+} RPTP-BK could play a role in the signalling pathways of all three Trk receptors.

The main focus in this study was to assess whether Trk receptors could be direct substrates of the RPTPs LAR, RPTPσ and RPTP-BK by analysing the phosphorylation state of Trk receptors, in particular of Tyr 785, following RPTP knockdown. To complement this analysis the function of two downstream signalling pathways, the Erk1/2-MAPK and to some extent the PI3K/Akt pathway, was studied.

6.2. Experimental procedures

6.2.1. Generation of lentiviruses and transduction of sensory neurons

The generation of MLV-E pseudotyped lentiviruses and transduction of sensory neurons was thoroughly described in chapter 5.

6.2.2. ShRNA and control plasmids

In this study MISSION™ TRC shRNA lentiviral vectors pLKO.1-puro (Sigma) targeting the murine RPTP genes *Ptprf, Ptpro* and *Ptprs* encoding LAR, RPTP-BK and PTPRσ respectively were used (Figure 6.1). A set of 4-5 sequence-verified shRNA constructs was provided per gene with a guaranteed knockdown efficiency of at least 70% (Sigma). As a non-targeting control (ctrl) I have used the pLKO.1-puro vector containing a non-targeting shRNA sequence from Qiagen kindly provided to us by Dr. Jörg Mueller (University of Jena, Germany).

	CONSTRUCT	TRC No.	TARGETED SEQUENCE (5'→3')
LAR	**SH 1**	TRCN0000029944	GCCTCGAATTACGTGGATGAA
	SH 2	TRCN0000029945	GCCGTATGTGAAATGGATGAT
	SH 3	TRCN0000029946	CCACCAGTGTTACTCTGACAT
	SH 4	TRCN0000029947	GCCCTTCAAGATCCTGTACAA
	SH 5	TRCN0000029948	CGCTTTGAGGTAATTGAGTTT
RPTP-BK	**SH 1**	TRCN0000029984	CCAGAGTTGATTCAACAGTTT
	SH 2	TRCN0000029985	CGATTCTTACATCAAGGATAT
	SH 3	TRCN0000029986	GCGCTCATACCGAATGTCAAT
	SH 4	TRCN0000029987	CCATTCACAGAAGAACCCATT
	SH 5	TRCN0000029988	CCTACAACAGAAGTCCCACAT
PTPRσ	**SH 1**	TRCN0000029994	CCTTCCTCATTCCCTTCTGAT
	SH 2	TRCN0000029995	CCAGCTTTATCGACGGCTATA
	SH 3	TRCN0000029996	CGAAATCACAATTCATGCAAA
	SH 4	TRCN0000029997	GCAGAACTACTTCATTGTGAT
	SH 5	TRCN0000029998	CCACGGCCATATTGGTAAGTT
	Ctrl Q	non-targeting shRNA from Qiagen in pLKO.1 puro	

Table 6.1. MISSION™ pLKO.1-puro lentiviral expression vectors.

The pLKO.1-puro constructs (Sigma) contain shRNA sequences directed against the murine RPTP genes *Ptprf, Ptprs, Ptpro* and a non-targeting control shRNA from Qiagen. SH = small hairpin, ctrl = control.

6.2.3. Lentivirus-mediated knockdown of RPTP genes

The day before transduction, DRGs were dissected from E13.5 CD-1 mouse embryos and dissociated and cultured as described in section 2.5.3. Approximately 250,000 cells were seeded per well of a PLL and FN pre-coated 12-well-plate. One day after plating the cells were infected with shRNA-containing lentiviruses, whereby one entire production of filtered lentivirus was equally distributed onto three wells in a final volume of 1 ml complete DRG medium. After 24 h the cells were washed gently with PBS and cultured for 72 or 96 h. The cells were examined for morphological changes each day starting 24 h after plating and pictures were taken as described in section 2.6. Finally the cells were harvested for mRNA and protein extraction (section 2.2.11) and gDNA isolation (section 2.1.18). Experiments were performed first without and then with mitotic inhibitors.

6.2.4. Integration PCR

To test whether the lentiviruses integrated into the genome of the target cells as a proof of presence of lentiviruses, PCR was performed on extracted gDNA from infected cells.

Each PCR reaction contained 5 µl 25 mM $MgCl_2$, 5 µl 5x GoTaq® Flexi Buffer, 200 µM dNTPs (Bioline), 10 µM integration primers, 1 unit GoTaq® Hot Start Polymerase (Promega) and 200 ng gDNA or 50 ng plasmid DNA template in a final volume of 25 µl ddH_2O. The reaction was run in a PCR thermo cycler under following conditions with a heated lid at 104ºC: polymerase activation: 94ºC for 5 min, 3-step-cycling: 40x (30 sec at 94ºC (denaturation), 30 sec at 50ºC (annealing), 45 sec at 72ºC (extension)), final extension: 5 min at 72ºC. The forward primer anneals to U6 and the reverse primer to cppt in the pLKO.1-puro vector (Table 6.2) producing a PCR product of 309 bp.

INTEGRATION PRIMER	SEQUENCE (5' → 3')	TM (ºC)
Forward (iF) – cppt	TAC AAA ATA CGT GAC GTA GAA A	52.8
Reverse (iR) – U6	TTT GTT TTT GTA ATT CTT TA	43

Table 6.2. Integration primers.

6.2.5. Assessment of the knockdown effects

6.2.5.1. QPCR

RNA was extracted from transduced cells, reverse transcribed and qPCR was performed on 15 ng cDNA of each sample in duplicates on 96-well plates as described in section 2.2.

6.2.5.2. WB analysis

Protein samples were obtained from infected DRG cultures during mRNA-extraction by acetone precipitation (section 2.2.1.1). Samples were removed from the freezer and warmed to 65ºC. For estimation of protein amounts different Bradford assays were tested. However, this approach was technically not feasible for the DRG samples due to unknown reasons. Therefore, instead, aliquots of the samples were electrophoresed on PAGE gels and commassie stained (section 2.3.4) followed by densitometry analysis to broadly estimate protein concentration. Western blotting and quantitative densitometry analysis were performed as described in section 2.3. Antibody details are described in Tables 2.3 and 2.4. The Trk antibodies specifically detect only the corresponding TrkA, TrkB or TrkC receptor (Appendix, Figure 1). The two antibodies pTrkA Y794 (rat) and pTrkB Y816, referred to as pTrk* and pTrk** respectively, detected endogenous levels of Trk receptors phosphorylated at the Y785 (human TrkA). The pTrk** antibody cross-reacted with the corresponding phosphorylated Tyr residues of all Trk receptors in contrast to previous reports. The pTrk* antibody also recognized phosphorylated TrkC and possibly also phosphorylated TrkB (see also explanations in the text in section 6.3.1)(Appendix, Figure 2). For data analysis the protein expression was normalized to the HKG β-tubulin or to the expression of the total unphosphorylated protein. In the case of phospho-Trk expression, data for each of the two pTrk antibodies (pTrk* = pTrkA Y785 and pTrk** = pTrkB Y816) were normalized to the expression of panTrk, which detects the ICD of all Trk receptors and thus the full-length isoforms. Results were expressed as ratios of normalized volume with respect to the mock treated or wild type control (= 1) with standard errors (see Materials and Methods section 2.3.3.7 for more details).

6.3. Results

6.3.1. Design of knockdown experiments

All knockdown experiments were performed with independent lentiviral preparations on freshly prepared dissociated DRG cultures. Four to five different shRNA lentiviral constructs were used per gene to knockdown *Ptprf* (LAR), *Ptprs* (RPTPσ) or *Ptpro* (RPTP-BK) mRNA. The non-targeting shRNA from Qiagen in the pLKO.1 vector was used as a control (and reference) in all experiments (Table 6.1). All shRNA sequences have different knockdown efficiencies depending on the cell type and additionally some shRNA constructs might cause "off-target" effects. In recent studies some researchers have used a pool of different shRNA constructs. However, a possible off-target effect might be mixed with target-specific effects in such experiments thus altering the results of the RNAi phenotype (Moffat et al., 2006). For these reasons different shRNA constructs to knockdown RPTP gene expression in our study were used in independent experiments.

Lentiviruses carrying shRNA were prepared, and dissociated murine E13.5 DRG cells were infected at an MOI of around 3-8 as described in chapter 5. As these viruses do not contain any suitable marker to assess or track infection, in order to confirm successful transduction, I have performed PCR with primers annealing to the integrating part of the shRNA pLKO.1 construct (cppt and U6, Table 6.2) on gDNA extracted from selected infected cells. PCR on all of these samples from infected cells and the positive controls (lentiviral backbone vectors) yielded a characteristic band of 309 bp, and as expected untreated DRGs and cells infected with eGFP viruses remained negative (data not shown).

In general the cells were cultured for 3 days after transduction in medium containing NGF, BDNF and NT-3, apart from one *Ptpro* knockdown experiment, which was extended to 4 days. The two first *Ptprf* and *Ptprs* experiments were also performed without NT-3 due to its unavailability. As my amendments and improvements of the DRG culturing system and the knockdown experiments caught up at this point, one of each of the knockdown experiments was performed with the mitotic inhibitors FdUrd and Uridine. These inhibitors reduced the amount of proliferating cells such as glia cells and fibroblasts in the culture from 80% to 60% after 3 days and even to 40% after

4 days and improved the read-out of the RNAi phenotype in neurons (Appendix, Figure 5).

The knockdown efficiency of the small hairpins (from now on referred to as SH) was assessed on the mRNA level with qPCR using primers from the qPCR screen (chapter 3). Data were normalized to *Psmb2* only, instead of three HKGs like in the qPCR arrays, due to a restricted amount of mRNA from the samples available. Nevertheless, since analysis on only one embryonic stage was performed, a relatively stable gene like *Psmb2* was fully sufficient for this purpose. As some proteins might have a long half-life, it is best to confirm the knockdown also on the protein level. However, this was not possible due to the lack of specific antibodies against RPTPs.

The effects of the RPTP knockdowns were analysed via WB with antibodies against specific phosphorylation sites of Trk receptors and components of several downstream signalling pathways such as Erk1/2, Akt1/2 and Stat3. Although I believe this was broadly successful, it was a very challenging task given that little material from primary cells was available, the protein levels were difficult to quantify (see material and methods section 6.2) and only low endogenous levels of Trk receptors were present.

As a control for Trk expression I have used TrkA, TrkB and TrkC specific antibodies, which recognized the ECD of the corresponding Trk receptors thus detecting all Trk protein isoforms, and a panTrk antibody, which recognizes the ICD of all Trk receptors thus detecting only the full-length isoforms (Appendix, Figure 1). In the case of TrkA, several protein sizes exist: the 80 kDa core protein, which is immediately glycosylated to an immature 110 kDa protein (gp 110) and a fully mature 140 kDa glycoprotein (gp140), as well as a shed membrane-bound ICD of 41 kDa and a soluble ECD (Martin-Zanca et al., 1989). In the case of TrkB and TrkC the full-length mature 145 kDa glycoproteins (gp145) and different non-catalytic glycosylated 95 kDa (gp95) isoforms are the most predominant (Klein et al., 1989, Lamballe et al., 1991, Middlemas et al., 1991). I have concentrated my analysis on the full-length 140 and 145 kDa proteins.

Further, I have tested several phospho-Trk antibodies. However, despite enormous efforts to find appropriate conditions for these antibodies, in order to improve the background to signal ratios, only two antibodies provided reasonable results. The commercially available antibodies recognizing phosphorylated Y490 or Y674/Y675

(from different companies) worked only on over-expressed Trk receptors, but not well on phosphorylated endogenous Trk receptors in lysates from primary sensory neurons. In contrast to this the two antibodies pTrkA Y794 (rat) and pTrkB Y816, referred to as pTrk* and pTrk** respectively, both detected endogenous levels of Trk receptors phosphorylated at the Y785 (human TrkA). These antibodies were kindly provided by Dr. Sheilla Harroch (PTPNET member, Institute Pasteur Paris, France) and were originally generated by Dr. M. Chao's lab (Rajagopal et al., 2004, Arevalo et al., 2006). The pTrk** antibody cross-reacted with the corresponding phosphorylated Tyr residues of all Trk receptors in contrast to previous reports (Appendix, Figure 2). The pTrk* antibody also recognized phosphorylated TrkC but not phosphorylated TrkB in agreement with published results (Rajagopal et al., 2004). However, the TrkB control sample in my test did not produce a strong band with the pTrkB (pTrk**) antibody as well, thus possibly indicating poor TrkB phosphorylation levels in this sample. Therefore it cannot be completely excluded that the pTrk* antibody in fact also cross-reacts with TrkB. Both antibodies were used to assess directly the phosphorylation state of the Trk receptors following RPTP knockdown.

The effects on the Trk downstream signalling pathways were examined with antibodies against phospho-Akt, -Erk1/2 and -Stat3. The kinase Akt is a major executer of the PI3K pathway, mainly initiated by phosphorylated Y751 and also Y490 in the Trk receptors. It controls cell survival by inhibiting apoptosis through phosphorylation and inactivation of Bad, forkhead TFs, c-Raf and caspase-9 etc. Akt is activated by phospholipid binding and phosphorylation of T308 within the activation loop and S473 in the C-terminus. Our antibody detected the latter. Erk1 (p44) and Erk2 (p42) are mediators of the classical MAPK pathway, which is initiated in Trk signalling mainly through phosphorylated Y490 residues. Additionally the MAPK pathway is also initiated through phosphorylated Y785, which activates the PLCγ-1 pathway. Erk1/2 activation leads to cell proliferation, differentiation and survival. Furthermore the available phospho-Stat3 Y705 antibody was used. The signal transducer and transcription activator 3 (Stat3) is a TF and is activated by phosphorylation of its Y705 and its S727 depending on the cell type, which induces dimerization, nuclear translocation and DNA binding. Stat3 is involved in cell proliferation and regulates the expression of anti-apoptotic genes (Darnell, 1997). In addition to its nuclear function as a TF Stat3 also regulates cell migration (Gao and Bromberg, 2006). Initially discovered

as a cytokine signal transducer, Stat3 was recently also identified as a signal transducer of TrkA signalling (Ng et al., 2006). In PC12 cells TrkA leads to Stat3 phosphorylation at S727 but not Y705, and the activation of several TrkA downstream pathways such as cell proliferation and neural differentiation. More recently, it was also shown that Trk oncogenes mediate phosphorylation of Stat3 additionally at T705, which is targeted by our antibody. This phosphorylation is partially mediated through the MAPK pathway and is possibly due to the high expression levels of Trk (Miranda et al., 2010). In our experiments we should not detect the T705 phosphorylation under normal conditions. All WB experiments were performed with several technical replicates and the expression levels were densitometrically estimated.

Together the different knockdown experiments were carried out with several SHs per gene and at least twice, but under different culturing conditions, and the effects of the knockdowns were assessed on the mRNA and protein levels. Repeats of the experiments were attempted, but unfortunately due to a unit-wide contamination of the tissue culture facility for several months, all these experiments were lost. Nevertheless, since several different SHs for each gene were used in each experiment, a comparison between these provided us with several effective replicates and thus valuable results.

6.3.2. *Ptprf* knockdown in murine embryonic sensory neurons

Two independent knockdown experiments targeting *Ptprf* were performed. In both experiments the cells were cultured for 3 days after transduction, but in the first experiment no mitotic inhibitors and no NT-3 were used. The first experiment was also conducted with three shRNA-containing lentiviruses (SH1, SH3 and SH5), whereas the second one was carried out with all five available different shRNA-containing lentiviruses. Overall, all SH constructs caused a knockdown of *Ptprf* mRNA in both experiments. SH1 caused a knockdown of 63 and 46%, SH2 of 55%, SH3 of 28 and 63%, SH4 of 53% and SH5 of 63 and 69% (Figures 6.1D and 6.2D).

In the first experiment the analysis of the expression of all *Ntrk* genes and the corresponding proteins revealed a decrease in *Ntrk2* and *Ntrk3* gene expression and TrkA, B and C protein expression in the knockdown samples SH1 and SH3. The expression in the SH5 sample remained mostly unchanged (Figure 6.1A-C). The expression of *Ptprs*, another member of the PTPR2A group like *Ptprf,* did not change

significantly upon knockdown in any sample. This indicates that no compensation for a deficiency in LAR took place by this phosphatase at this time point. The phosphorylation of Trk Y785 (pTrk** antibody) appeared to be elevated in all knockdown samples compared to the mock-treated control. This was accompanied by a slightly increasing trend in Erk1/2 phosphorylation. The phosphorylation of Stat3 was decreased in the samples SH1 and SH3 and of Akt in sample SH1. The cell morphologies in all samples were comparable to each other (Figure 6.1E). The unstable Trk gene and protein expression mostly complicated the interpretation of the results in samples SH1 and SH3 but not of SH5, which showed rather stable Trk expression. In this sample the 63% *Ptprf* knockdown resulted in a twofold increase in Trk pY785 phosphorylation but with no major changes in Erk1/2 or Akt phosphorylation.

In the second experiment the expression of the *Ntrk* genes fluctuated again across the samples (Figure 6.2A). However, for most of the samples these changes were within the previously observed range of up to 30% (chapter 5). The elevated amount of Trk proteins mostly correlated with their gene expression. Once again in sample SH5 Trk protein expression was least varying and although the gene expression levels were decreased, they were still within the usual fluctuation range. *Ptprs* expression was especially increased in samples SH2 and SH3, but rather stable in the remaining samples. Both pTrk Y785 antibodies (pTrkA Y794 = pTrk* and pTrkB Y816 = pTrk**) worked on these samples and the results agreed on an overall increase in Trk Y785 phosphorylation in samples SH4 and SH5. Whereas SH1 showed an elevation and SH3 a decrease in phosphorylation with the pTrk* antibody, no changes were visible with the pTrk** antibody (Figure 6.2B-C). The phosphorylation of Erk1/2 was either decreased or mostly unchanged, especially in sample SH5. Akt phosphorylation was possibly decreased in samples SH1 and SH4, but unchanged in all other samples with a similarity in this pattern to Erk1 phosphorylation. Stat3 phosphorylation was decreased in all knockdown samples, with highest values for SH5. Too little protein was present in sample SH2 for accurate densitometry analysis of Trk expression and phosphorylation. The morphology of the cells in all samples was similar (Figure 6.2E), but in comparison to the first experiment more neurons and less glia cells were present. Together, in this experiment the knockdown of *Ptprf* caused an overall increase in the phosphorylation state of Trk Y785 and possibly no effect or a downregulation of Erk1/2 phosphorylation

Figure 6.1. Effects of *Ptprf* knockdown in murine E13.5 sensory neurons. Experiment 1.

This experiment was carried out with three shRNA (SH1, 3 and 5) lentiviruses targeting *Ptprf* and a non-targeting control (ctrl) lentivirus, but without mitotic inhibitors and NT-3 for 3 days. The effects on gene expression and protein phosphorylation were analysed. **A**) qPCR analysis of gene expression of *Ntrk1-3, Ptprf* and *Ptprs*. Results were normalized to *Psmb2* as a HKG and the difference in ΔC_T values between cells infected with shRNA targeting *Ptprs* and the non-targeting control (ctrl) virus, were used to generate percentage expression levels ($2^{-\Delta\Delta C_T}$ %). The error bars represent SDs between samples from separate wells, which were infected with the same virus. **B**) Representative WB and **C**) densitometry analysis. Results were compared to protein expression in cells infected with the ctrl virus. In the case of phospho-antibodies, expression was normalized to the protein amount (with the exception of pAkt, as the Akt antibody was not available). Several technical repeats were performed. And when data were available for the antibody from more than one western blot, standard errors were calculated and included in the graphs. pTrk** = pTrkB Y816 antibody detecting phosphorylated TrkA, TrkB and TrkC Y785 sites. **D**) Knockdown (kd) efficiencies. **E**) Cell morphologies. Scale bar = 10 μm.

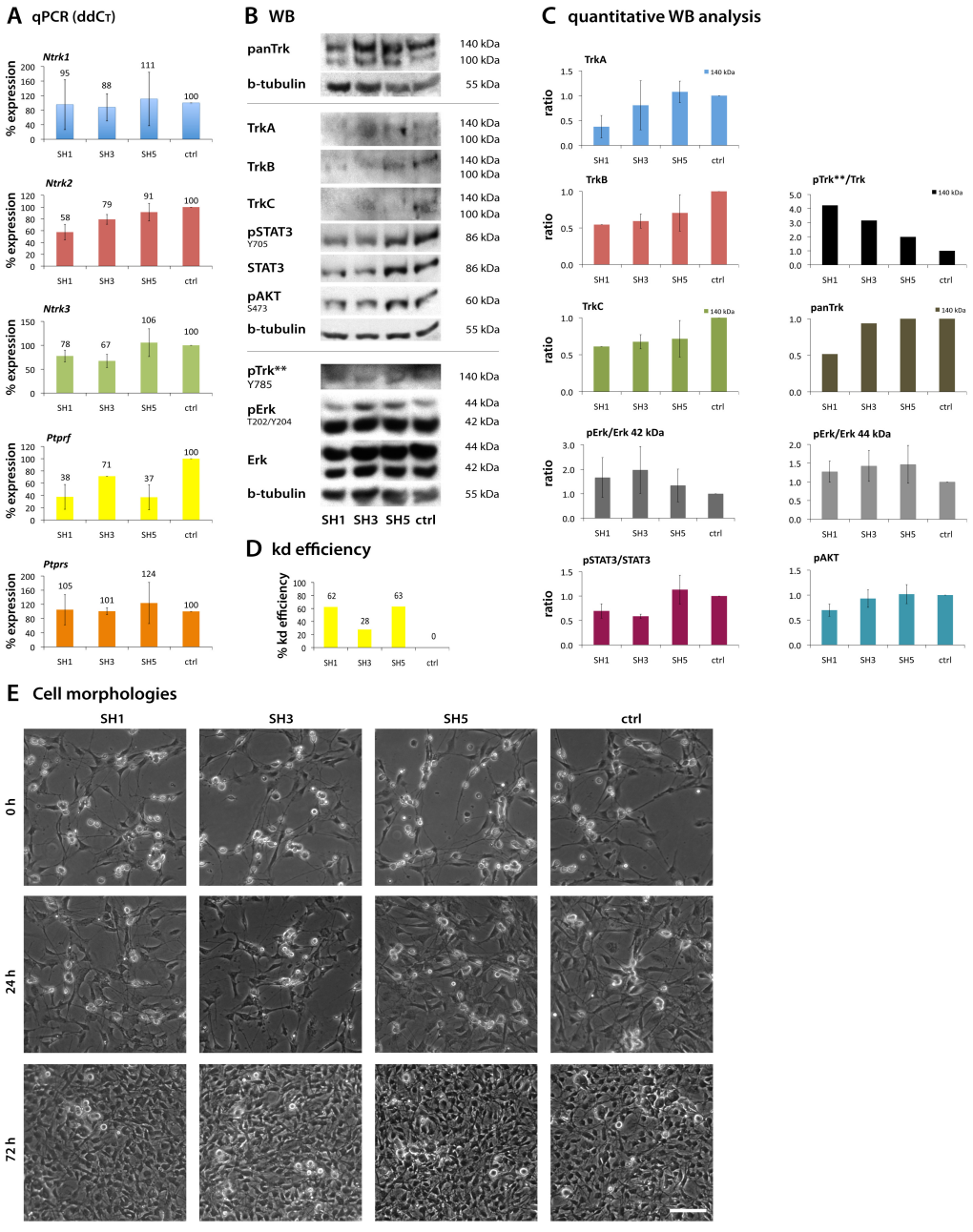

***Ptprf* knockdown. Experiment 1.**

Figure 6.2. Effects of *Ptprf* knockdown in murine E13.5 sensory neurons. Experiment 2.

This experiment was carried out with five shRNA (SH1-5) lentiviruses targeting *Ptprf* and a non-targeting control (ctrl) lentivirus and with mitotic inhibitors for 3 days. The effects on gene expression and protein phosphorylation were analysed. **A**) qPCR analysis of gene expression of *Ntrk1-3, Ptprf* and *Ptprs*. Results were normalized to *Psmb2* as a HKG and the difference in ΔC_T values between cells infected with shRNA targeting *Ptprs* and the non-targeting control (ctrl) virus, were used to generate percentage expression levels ($2^{-\Delta\Delta C_T}$ %). The error bars represent SDs between samples from separate wells, which were infected with the same virus. **B**) Representative WB and **C**) Results were compared to protein expression in cells infected with the ctrl virus. In the case of phospho-antibodies, expression was normalized to the protein amount (with the exception of pAkt, as the Akt antibody was not available). Several technical repeats were performed. And when data were available for the antibody from more than one western blot, standard errors were calculated and included in the graphs. pTrk* = pTrkA Y794 antibody detecting phosphorylated TrkA and TrkC Y785 sites, pTrk** = pTrkB Y816 antibody detecting phosphorylated TrkA, TrkB and TrkC Y785 sites. **D**) Knockdown (kd) efficiencies. **E**) Cell morphologies. Scale bar = 10 μm.

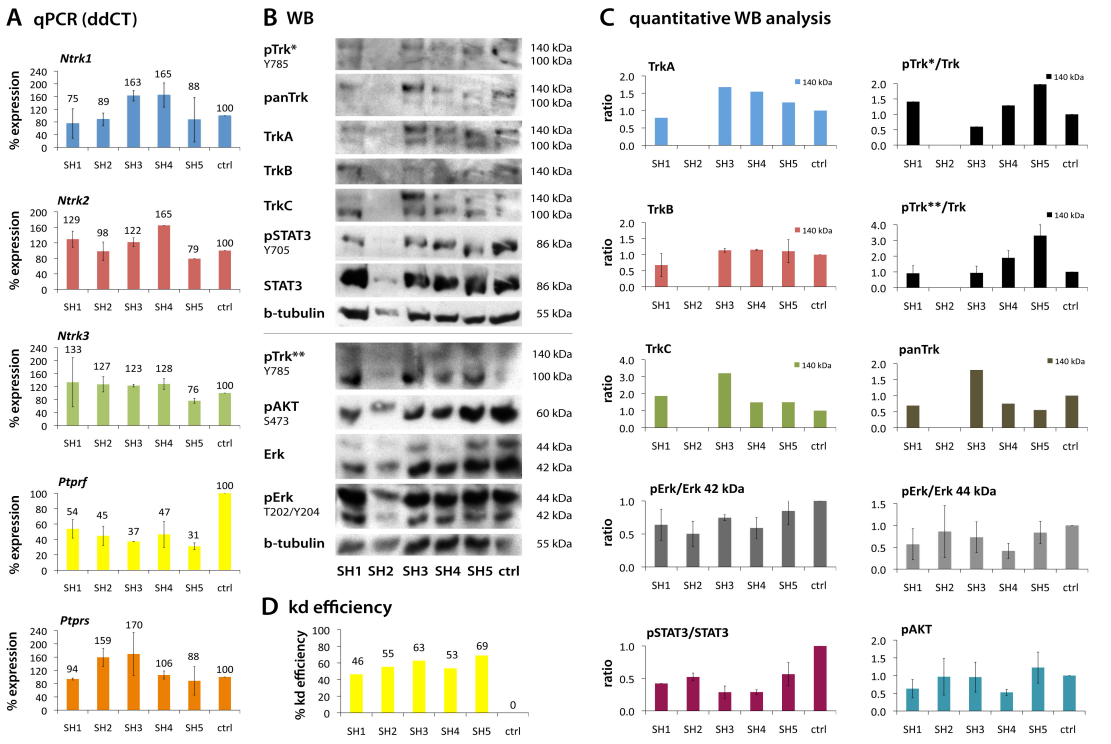

Ptprf knockdown. Experiment 2.

in most knockdown samples. Akt phosphorylation was slightly affected. *Ntrk* expression was unstable and Stat3 phosphorylation was decreased. Once again in sample SH5 Trk expression was the most stable among the analyzed samples and the phosphorylation state of Trk Y785 in this sample was upregulated, but Erk1/2 and Akt phosphorylation remained not significantly changed, and Stat3 was the least decreased.

The results from these two *Ptprf* knockdown experiments were difficult to interpret due to unstable Trk expression. But overall the downregulation of LAR possibly resulted in an upregulation of Trk Y785 phosphorylation. The MAPK and Akt signalling pathways were possibly unaffected in the first experiment but slightly downregulated in the second.

6.3.3. *Ptprs* knockdown in murine embryonic sensory neurons

Two knockdown experiments, each with four different shRNA lentiviruses targeting *Ptprs* mRNA and a non-targeting control virus, were performed. Similar to the *Ptprf* knockdown experiments the cells were cultured for 3 days after transduction either with or without mitotic inhibitors. The first experiment also lacked NT-3 in the culture medium.

The knockdown efficiencies of the four shRNA were comparable in both experiments apart from SH3 (Figures 6.3.D and 6.4D). Two of the shRNA constructs (SH1 and SH2) knocked down *Ptprs* mRNA expression in both experiments, but with higher knockdown efficiency in the second experiment (> 78%) compared to the first one (> 43%). The SH4 did not result in any knockdown in both experiments, whereas SH3 reduced mRNA expression by > 60% in the second experiment, but had an effect only in one out of two samples (same virus, two different wells) in the first experiment. Integration PCR was performed on gDNA from cells of the first experiment and showed that viruses were integrated in the cell chromosomes. Thus the complete lack of knockdown by SH4 was not caused by an absence of the virus. Also, the constructs appeared not to have recombined during large-scale propagation when analysed by RE digests (data not shown), which could lead otherwise to their inactivation. Interestingly, when tested in HEPA cells by researchers from the Broad Institute (Sigma), only SH4 caused a 65% decrease in mRNA expression of *Ptprs* (Sigma) and no knockdown was reported for any of the other hairpin sequences. This might be explained by the fact that

different hairpins can target different transcript variants or transcript regions containing single nucleotide polymorphisms (SNPs) and thus cause a particular shRNA to work in one cell type but not as effectively or at all in another, if this protein isoform is missing.

In the first experiment the analysis of gene expression of all *Ntrk* genes demonstrated that in both samples with a successful *Ptprs* knockdown (SH1 and SH2) the expression of these genes was downregulated. Especially in sample SH2 these changes were higher than the frequently observed fluctuation ratio of up to 30% (Figure 6.3A) and correlated with decreased protein levels (Figures 6.3B and C). The strongest decrease in expression in this sample was observed for TrkB. The gene expression levels in sample SH1 were also decreased (Figure 6.3A), but the expression on the protein level was upregulated (Figures 6.3B and C). Interestingly, *Ptprf* expression was also downregulated in the samples with a successful knockdown. The phosphorylation of Trk Y785 in samples SH1 and SH2 was upregulated in comparison to the control sample. Increased phosphorylation of Trk Y785 was also detected for SH3, but not SH4, which showed no knockdown of *Ptprs* at all. The phosphorylation state of the downstream pathway components Erk1/2, Stat3 and Akt appeared to be mostly unaltered in the successful knockdown samples. No obvious differences in cell morphologies were detected upon knockdown of *Ptprs* (Figure 6.3E). These results show a possible up regulation of Trk Y785 phosphorylation upon *Ptprs* knockdown, which was however not accompanied by any changes in the analysed downstream pathway components.

In the second experiment *Ntrk1-3* and *Ptprf* expression fluctuated again (Figure 6.4A). Among the samples with a *Ptprs* knockdown these changes were, however, within the ratio of 30% for the samples SH1 and SH2. But in the sample SH3 *Ntrk2* expression was highly upregulated, whereas *Ptprf* expression was downregulated by over 30%. In sample SH4, which showed a high upregulation of *Ptprs* expression instead of a knockdown, *Ntrk1* expression was also highly upregulated. Interestingly no such increase in gene expression was detected for the other *Ntrk* genes or *Ptprf* in this sample, thus showing no obvious possible systematic error during data collection. On the protein level the expression of all Trks was upregulated in all knockdown samples, but panTrk expression, which detects the full-length isoforms, was rather downregulated or unchanged (Figure 6.4B and C). The phosphorylation state of Trk Y785 was upregulated in all knockdown samples, except for sample SH4, which did not

Figure 6.3. Effects of Ptprs knockdown in murine E13.5 sensory neurons. Experiment 1.

The experiment was carried out with four shRNA (SH1-4) lentiviruses targeting *Ptprs* and a non-targeting control (ctrl) lentivirus without mitotic inhibitors and NT-3 for 3 days. The effects on gene expression and protein phosphorylation were analysed. **A**) qPCR analysis of gene expression of *Ntrk1-3, Ptprf* and *Ptprs*. Results were normalized to *Psmb2* as a HKG and the difference in ΔC_T values between cells infected with shRNA targeting *Ptprs* and the non-targeting control (ctrl) virus, were used to generate percentage expression levels ($2^{-\Delta\Delta C_T}$ %). The error bars represent SDs between samples from separate wells, which were infected with the same virus. **B**) Representative WB and **C**) densitometry analysis. Results were compared to protein expression in cells infected with the ctrl virus. In the case of phospho-antibodies, expression was normalized to the protein amount (with the exception of pAkt, as the Akt antibody was not available). Several technical repeats were performed. And when data were available for the antibody from more than one western blot, standard errors were calculated and included in the graphs. pTrk** = pTrkB Y816 antibody detecting phosphorylated TrkA, TrkB and TrkC Y785 sites. **D**) Knockdown (kd) efficiencies. **E**) Cell morphologies. Scale bar = 10 μm.

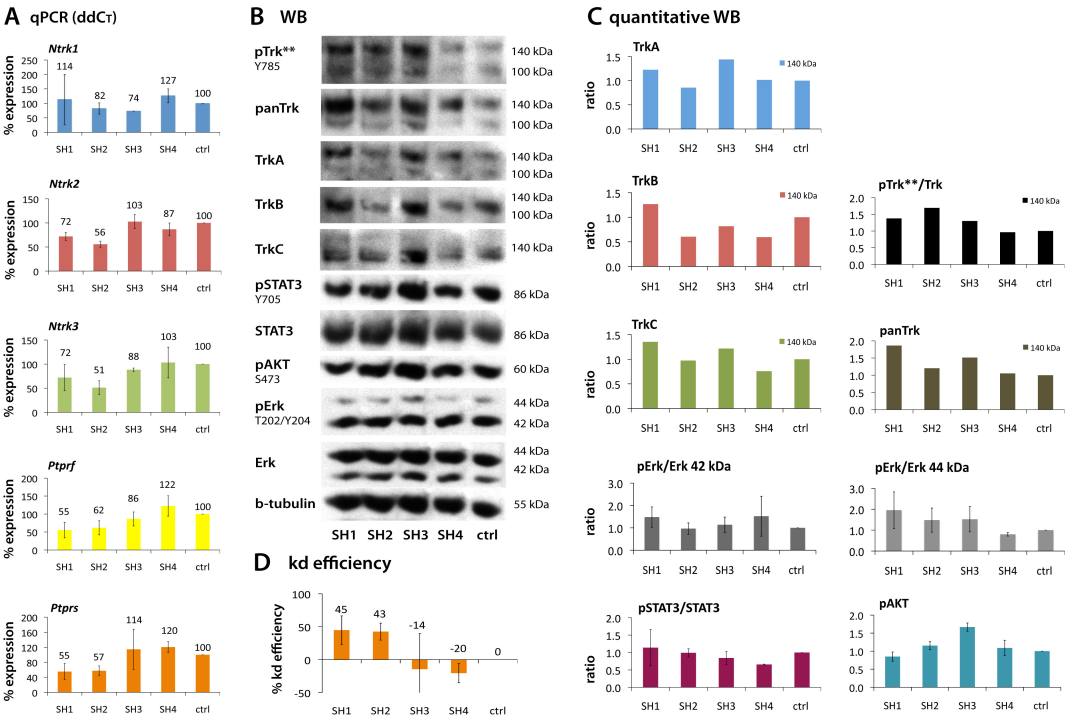

Ptprs knockdown. Experiment 1.

Figure 6.4. Effects of *Ptprs* knockdown in murine E13.5 sensory neurons. Experiment 2.

The experiment was carried out with four shRNA (SH1-4) lentiviruses targeting *Ptprs* and a non-targeting control (ctrl) lentiviruses and with mitotic inhibitors for 3 days. The effects on gene expression and protein phosphorylation were analysed. **A**) qPCR analysis of gene expression of *Ntrk1-3, Ptprf* and *Ptprs*. Results were normalized to *Psmb2* as a HKG and the difference in ΔC_T values between cells infected with shRNA targeting *Ptprs* and the non-targeting control (ctrl) virus, were used to generate percentage expression levels ($2^{-\Delta\Delta C_T}$ %). The error bars represent SDs between samples from separate wells, which were infected with the same virus. **B**) Representative WB and **C**) densitometry analysis. Results were compared to protein expression in cells infected with the ctrl virus. In the case of phospho-antibodies, expression was normalized to the protein amount (with the exception of pAkt, as the Akt antibody was not available). Several technical repeats were performed. And when data were available for the antibody from more than one western blot, standard errors were calculated and included in the graphs. pTrk** = pTrkB Y816 antibody detecting phosphorylated TrkA, TrkB and TrkC Y785 sites. **D**) Knockdown (kd) efficiencies. **E**) Cell morphologies. Scale bar =10 μm.

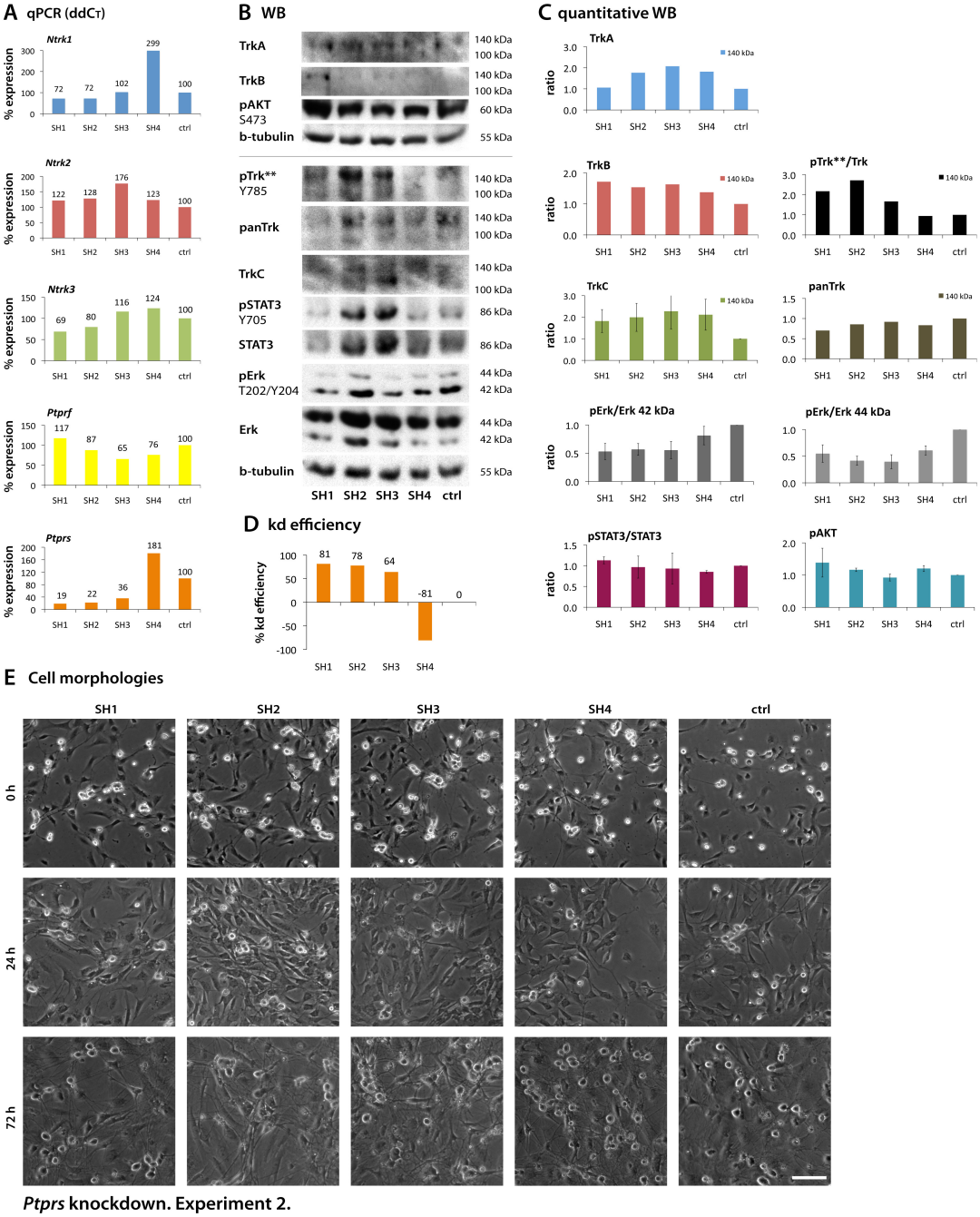

Ptprs knockdown. Experiment 2.

knock down. In contrast to the previous experiment Erk1/2 phosphorylation was slightly reduced in all SH-treated samples with a smaller effect in the sample SH4. The phosphorylation of Stat3 and possibly Akt was not significantly affected. The morphology of the cells appeared also unaltered in all samples with more neurons and less glia cells present in this experiment compared to the previous one (Figure 6.4E).

Together the results from both *Ptprs* knockdown studies showed an increase in the phosphorylation of Trk Y785 and no changes in Stat3 or Akt phosphorylation upon *Ptprs* knockdown. Whereas this increase in Trk phosphorylation was not accompanied by any changes in pErk1/2 in the first experiment, we observed a significant decrease of these MAPK downstream pathway components in the second experiment. This downregulation is however marginal when compared to sample SH4 with no knockdown. These differences might be explainable by different culturing conditions and thus the composition of the cell cultures. The majority of cells in the first experiment were glia cells and due to mitotic inhibitors less glia cells and more neurons were present in the second experiment.

6.3.4. *Ptpro* knockdown in murine embryonic sensory neurons

Two independent knockdown experiments, each with five different shRNA lentiviruses targeting *Ptpro* mRNA and a mock virus, were performed. The first experiment was carried out for 3 days without mitotic inhibitors, whereas in the second experiment the cells were cultured for 4 days with mitotic inhibitors. Independent of the differences in the composition of the cell cultures, knockdown efficiency of *Ptpro* in both experiments ranged between 82 and 96%, with SH5 and SH1 being most successful in both experiments (Figures 6.5 and 6.6).

In the first experiment a striking downregulation of *Ntrk1* expression by over 80% in all samples apart from SH1, in which it was downregulated by approximately 20%, was observed. The corresponding TrkA protein expression was in contrast to this elevated in all samples, especially in sample SH5. *Ntrk2* expression was upregulated in the samples SH1 and SH2 but downregulated in samples SH4 and SH5. *Ntrk3* expression was upregulated in samples SH1 and SH3 and downregulated in samples SH4 and SH5. Both TrkB and TrkC expression levels were upregulated especially in samples SH1 and SH2. *Ptprr* expression was also assessed as it was suggested to

interact with TrkA, whose expression might be influenced by *Ptpro* downregulation. And in fact *Ptprr* expression was decreased in all knockdown samples similar to TrkA expression. Trk Y785 phosphorylation was slightly upregulated in sample SH2 but downregulated in the remaining samples. Erk1/2 phosphorylation was only marginally affected. Stat3 phosphorylation was downregulated in samples SH1 and slightly in SH3 but unchanged in the remaining samples. Akt phosphorylation was highly upregulated in sample SH1, and also to some extent in samples SH4 and SH5, whereas it remained unchanged in samples SH2 and SH3. Together, the samples SH1 and SH5 revealed in comparison to the other three samples a strange pattern in gene and/or protein expression. No apparent changes in cell morphologies were visible (Figure 6.5E).

In the second experiment (Figure 6.6) *Ntrk1* expression was repeatedly strongly decreased, whereas TrkA expression remained unchanged. *Ntrk2* and *Ntrk3* expression was also strongly downregulated in the samples SH1, SH3 and SH5 but to a lesser extent in samples SH2 and SH4. TrkB was mostly unchanged, whereas TrkC levels were decreased apart from sample SH5. *Ptprr* expression was downregulated in most samples apart from sample SH5. Overall a decrease in the expression of all genes was observed in sample SH1 with no corresponding changes in protein expression. This might be caused by a systematic error such as an inhibitory effect on the qPCR. This particular hairpin already altered gene and protein expression in comparison to other samples in the first experiment, thus suggesting an additional problem with its sequence. The analysis of the phosphorylation of the downstream signalling pathway components has shown that Erk1/2 phosphorylation was mostly unchanged apart from an upregulation of pErk1 in sample SH2 and of pErk2 in samples SH1 and SH4. Stat3 phosphorylation was not meaningfully affected. Akt phosphorylation was possibly not affected as well. The phosphorylation of Trk Y785 was upregulated in all samples, when detected with the pTrk** antibody, and upregulated in samples SH1-3 but decreased in samples SH4-5, when detected with the pTrk* antibody. The cells looked very healthy and their morphology remained unchanged in all samples in comparison to the mock control sample (Figure 6.6E).

Together these findings show a possible downregulation of pTrk Y785 in all samples apart from SH2 in the first experiment, but an upregulation in the second experiment, when using the same pTrk** antibody. An explanation for the contradicting outcomes might be the difference in the culturing systems (+/- growth inhibitors).

Figure 6.5. Effects of *Ptpro* knockdown in murine E13.5 sensory neurons. Experiment 1.

The experiment was carried out with five shRNA (SH1-5) targeting *Ptpro* and a non-targeting control (ctrl) lentiviruses and without mitotic inhibitors for 3 days. The effects on gene expression and protein phosphorylation were analysed. **A**) qPCR analysis of gene expression of *Ntrk1-3, Ptpro* and *Ptprr*. Results were normalized to *Psmb2* as a HKG and the difference in ΔC_T values between cells infected with shRNA targeting *Ptprs* and the non-targeting control (ctrl) virus, were used to generate percentage expression levels ($2^{-\Delta\Delta C_T}$ %). In contrast to the *Ptprf* and *Ptprs* knockdown experiments no error bars (SD) were available as samples from all wells were pooled and analysed together. **B**) Representative WB and **C**) densitometry analysis. Results were compared to protein expression in cells infected with the ctrl virus. In the case of phospho-antibodies, expression was normalized to the protein amount (with the exception of pAkt, as the Akt antibody was not available). Several technical repeats were performed. And when data were available for the antibody from more than one western blot, standard errors were calculated and included in the graphs. pTrk** = pTrkB Y816 antibody detecting phosphorylated TrkA, TrkB and TrkC Y785 sites. **D**) Knockdown (kd) efficiencies. **E**) Cell morphologies. Scale bar = 10 μm.

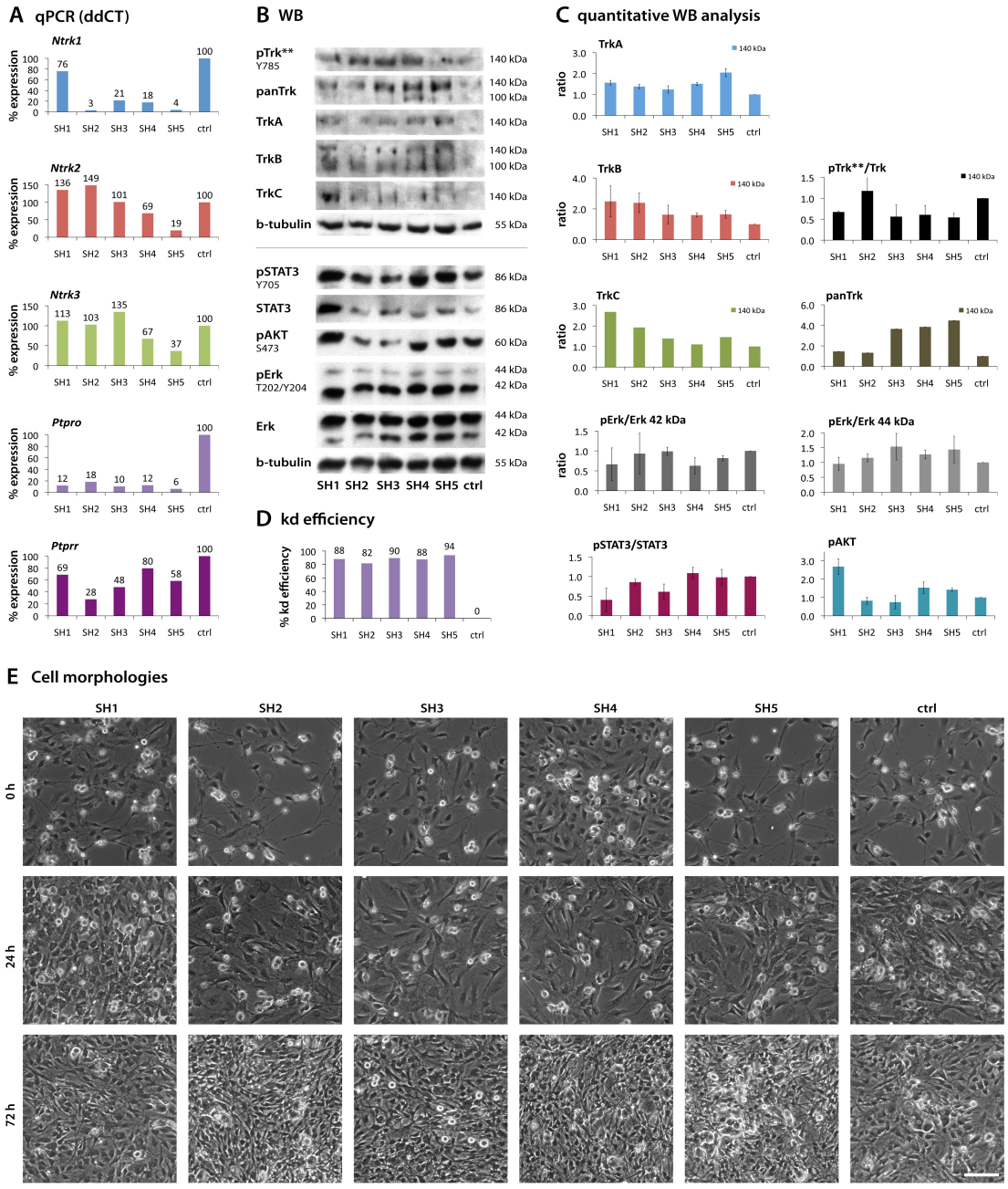

Ptpro knockdown. Experiment 1.

Figure 6.6. Effects of *Ptpro* knockdown in murine E13.5 sensory neurons. Experiment 2.

The experiment was carried out with five shRNA (SH1-5) targeting *Ptpro* and a non-targeting control (ctrl) lentiviruses and without mitotic inhibitors for 4 days. The effects on gene expression and protein phosphorylation were analysed. **A**) qPCR analysis of gene expression of *Ntrk1-3, Ptpro* and *Ptprr*. Results were normalized to *Psmb2* as a HKG and the difference in ΔC_T values between cells infected with shRNA targeting *Ptprs* and the non-targeting control (ctrl) virus, were used to generate percentage expression levels ($2^{-\Delta\Delta C_T}$ %). In contrast to the *Ptprf* and *Ptprs* knockdown experiments no error bars (SD) were available as samples from all wells were pooled and analysed together. **B**) Representative WB and **C**) densitometry analysis. Results were compared to protein expression in cells infected with the ctrl virus. In the case of phospho-antibodies, expression was normalized to the protein amount (with the exception of pAkt, as the Akt antibody was not available). Several technical repeats were performed. And when data were available for the antibody from more than one western blot, standard errors were calculated and included in the graphs. pTrk* = pTrkA Y794 antibody detecting phosphorylated TrkA and TrkC Y785 sites, pTrk** = pTrkB Y816 antibody detecting phosphorylated TrkA, TrkB and TrkC Y785 sites. **D**) Knockdown (kd) efficiencies. **E**) Cell morphologies. Scale bar = 10 μm.

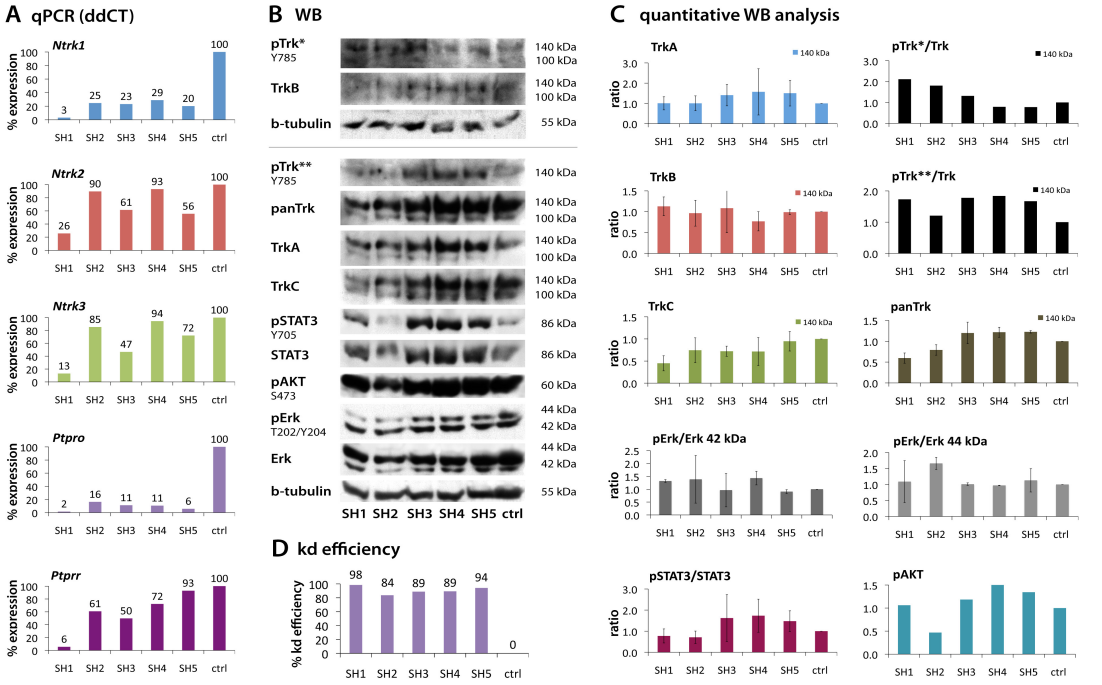

Ptpro knockdown. Experiment 2.

No particular changes in Erk1/2, Akt or Stat3 phosphorylation correlated with any other observation. The most striking result in both *Ptpro* knockdown experiments was the strong downregulation of *Ntrk1* gene expression in all five knockdown samples and to some extent also *Ntrk2* and *Ntrk3*. However, these changes were mostly not reflected on the protein levels.

6.4. Discussion

The knockdown experiments in this study provided interesting insights into the possible function of the three analysed RPTPs LAR, RPTPσ and RPTP-BK in Trk signalling pathways and their potential role in DRG regeneration and development. But before I will discuss the findings in this chapter, it is important to address several important issues concerning the experimental set-up and the cells used in this study.

In general knockdown experiments are a powerful tool to analyse the physiological function of proteins. But they can harbour several pitfalls and thus have to be interpreted carefully. As the mRNA level might not reflect actual protein levels, the knockdown efficiency should be assessed on the protein level. But this requires specific antibodies, which were unfortunately not available to us for the RPTPs, as mentioned earlier. Thus we can only speculate at this point, whether the phenotypes we observe can be really attributed to a deficiency of the RPTP of interest. However, the knockdown efficiency on the mRNA level was repeatedly higher than 45% and mostly above 50% for several small hairpin constructs in each experiment. Further, the experiments in this study have been conducted for 3-4 days, which was an appropriate amount of time to induce a successful knockdown on the protein level in previous studies. For instance in the case of LAR, an siRNA-induced knockdown resulted in a 45% decrease in protein expression after 3 days and lead to molecular changes (Yang et al., 2006). One might argue that the experiments should be carried out for a longer period of time especially since the half-life time of the proteins is unknown. But long-term studies might suffer from compensatory effects caused for instance by functional redundancy of other RPTPs or an upregulation of compensatory proteins or even pathways and feedback mechanisms and thus will not reveal an RNAi phenotype of the particular RPTP.

Additionally, before any conclusions can be drawn from the current knockdown study some thoughts should be assigned to the cell system used in this study. DRGs are commonly used in neuroscience research as a primary cell system due to many advantages (see introduction section 1.5). Nevertheless, it is in fact a complicated system due to its diverse cell composition of glia cells and at least 20 different subtypes of sensory neurons. In general, it is believed that embryonic DRG cultures display characteristics of a regeneration assay due to the axotomy of the axons. For instance in TG, which contain like DRGs sensory neurons, several changes in gene expression of Trk receptors were observed in dissociated cultures compared to ganglia *in vivo* and explant cultures (Friedel et al., 1997). Further, in culture experiments of dissociated rat E15 TG (corresponding to E13.5 in mouse) the cells showed altered Trk expression and responsiveness to NTs, whereas explant cultures rather resembled an *in vivo* model. Interestingly, all TG neurons coexpressed all three Trk receptors and survival rates were independent of whether cells were cultured with one or several NTs (Genc et al., 2005).

In regard to the documented responsiveness of sensory neurons to all NTs, I have also not observed any changes on the gene or protein level in the current experiment, which could have been attributed to the lack of NT-3 in one of the LAR and RPTPσ experiments. In this thesis I have performed gene expression analysis on DRGs *in vivo* (chapter 3) and on dissociated DRG cultures (chapter 5), which allowed us a broad comparison of both systems. Trk gene expression showed a consistent proportion of the TrkA, TrkB and TrkC receptors both in dissociated DRGs and *in vivo* (Figures 3.2 and 5.4). It is possible though that neurons express in addition to their specific dominant Trk receptor, smaller amounts of the other two receptors, which would not skew the expression profile in general, but allow a survival response mediated by all NTs. Moreover, I have compared the expression of RPTP genes between DRGs *in vivo* and in dissociated cultures and detected substantial differences (Figures 3.4 and 5.4). The gene expression of four of the five analysed RPTPs LAR, RPTPσ, RPTP-BK and especially RPTPα was greatly elevated in dissociated cultures when compared to Trk expression. The expression levels of LAR and RPTPσ were broadly threefold and in the case of RPTPα tenfold higher than *in vivo.* Expression levels of all three RPTPs were above TrkA levels in dissociated cultures, but only LAR was expressed at higher levels than TrkA *in vivo*. RPTP-BK expression was fivefold increased and higher than the expression of TrkB and TrkC, although its expression *in vivo* was at a similar level as

TrkB expression. RPTPR expression was by tenfold decreased and below the expression level of TrkC in dissociated cultures unlike *in vivo*.

In previous studies on adult rat DRGs and sciatic nerves after injury RPTPσ mRNA was increased by 50% during regeneration *in vivo*, whereas both LAR and RPTPα were decreased by 50 and 20% respectively after 3 days. The gene expression of RPTP-BK remained unchanged (Haworth et al., 1998, McLean et al., 2002). However, in another study, LAR protein expression was increased in DRGs upon sciatic nerve crush *in vivo* (Xie et al., 2001). In contrast to these studies, our experiments were performed on embryonic DRG cultures, which might explain the differences in gene upregulation.

Together, these findings demonstrate that dissociated DRG cultures show a different gene expression profile especially of RPTPs compared to DRGs *in vivo*. The observed changes in gene expression might be caused for instance by axotomy followed by regeneration of the neurons in culture or it may be a specific effect of the disaggregation of the neurons in culture. Nevertheless, keeping this in mind this model system is still a good starting point to decipher the implication of RPTPs in Trk signalling in an endogenous environment and in fact represents an interesting study of regeneration.

The knockdown experiments in this study showed that a likely downregulation of LAR upon *Ptprf* knockdown resulted in a possible upregulation of Trk Y785 phosphorylation. These findings therefore support our hypothesis of a likely regulation of the Trk-mediated PLCγ pathway by LAR and hint towards a possible inhibitory effect of LAR on the Trk-Y785-PLCγ-pathway. However, this is in contrast to a previous report, in which augmented LAR function lead to an increase in PLCγ phosphorylation in hippocampal neurons (Yang et al., 2005a). The differences between published data and our results might be attributed to the action of LAR on different Trk subtypes, as our cultures contained predominantly TrkA neurons, whereas hippocampal neurons express almost exclusively TrkB. This is similar to the previously shown opposite effects of LAR on Trk Y490 phosphorylation in $TrkB^+$ hippocampal neurons and $TrkA^+$ PC12 cells (Yang et al., 2005a, Yang et al., 2006, Xie et al., 2006).

The analysed downstream signalling pathways were mostly not affected in these knockdown experiments but the MAPK pathway was possibly slightly downregulated in the second experiment. No changes in Akt phosphorylation were detected. Taking into account that more glia cells (around 80%) were present in the first experiment (around 60% in the second experiment), which also signal through the MAPK and Akt pathways, the effects in the neurons might have been masked in the first experiment and LAR deficiency might in fact lead to a downregulation in the MAPK pathway in neurons as observed in the second experiment. This supports therefore an augmenting role of LAR on the MAPK pathway in these cells possibly through Src as previously suggested in similar studies (Yang et al., 2006). However, this finding is somewhat unexpected, if compared to the results on the Trk-Y785 phosphorylation described above, since it agrees with the effect of LAR in $TrkB^+$ hippocampal cells and not in $TrkA^+$ PC12 cells (Yang et al., 2005a, Xie et al., 2006). Then again different mechanisms exist in different cell types, which might explain the observed differences. In addition the signalling mechanisms controlling neurite outgrowth are largely unknown and also MAPK-independent pathways exist. Moreover, Trks are not the only LAR substrate, and so the effects on the MAPK pathway might be attributed to other growth factor receptors in these cells. And this might explain the controversy.

Together, a possible implication of LAR in the PLCγ pathway mediated through direct dephosphorylation of Trk Y785 (Figure 6.7) is therefore likely and represents an interesting new aspect and a good starting point for further investigations.

The *Ptprs* knockdown experiments showed also an increase in the phosphorylation state of Trk Y785, which could lead to the activation of the PLCγ-1/PKCδ-pathway and subsequently to MAPK-independent neurite outgrowth or could activate the PLCγ-1/Ca^{2+} pathway and lead to synaptogenesis. This was previously not reported and agrees with our hypothesis.

Similar to the LAR experiments, the Akt pathway was not affected, whereas the MAPK pathway was downregulated in the second experiment, but remained unaltered in the first experiment. As mentioned above, signalling in glia cells and through other growth factor receptors might have masked the changes in neurons induced by Trk phosphorylation in the first experiment. The potential downregulation of the MAPK pathway might be attributed to an augmenting role of RPTPσ, and similar to LAR might

be mediated via Src. However, Src was not yet identified as a substrate of RPTPσ. Instead, many other kinases and growth factor receptors are dephosphorylated by RPTPσ such as EGFR *in vitro* (Suarez Pestana et al., 1999), which might be responsible for the effects in the downstream signalling pathways in DRGs upon *Ptprs* knockdown.

Together these findings might display a possible new role of RPTPσ in synaptogenesis and/or neurite outgrowth mediated through the Trk Y785-PLCγ-pathway (Figure 6.7), which is an interesting question for future research.

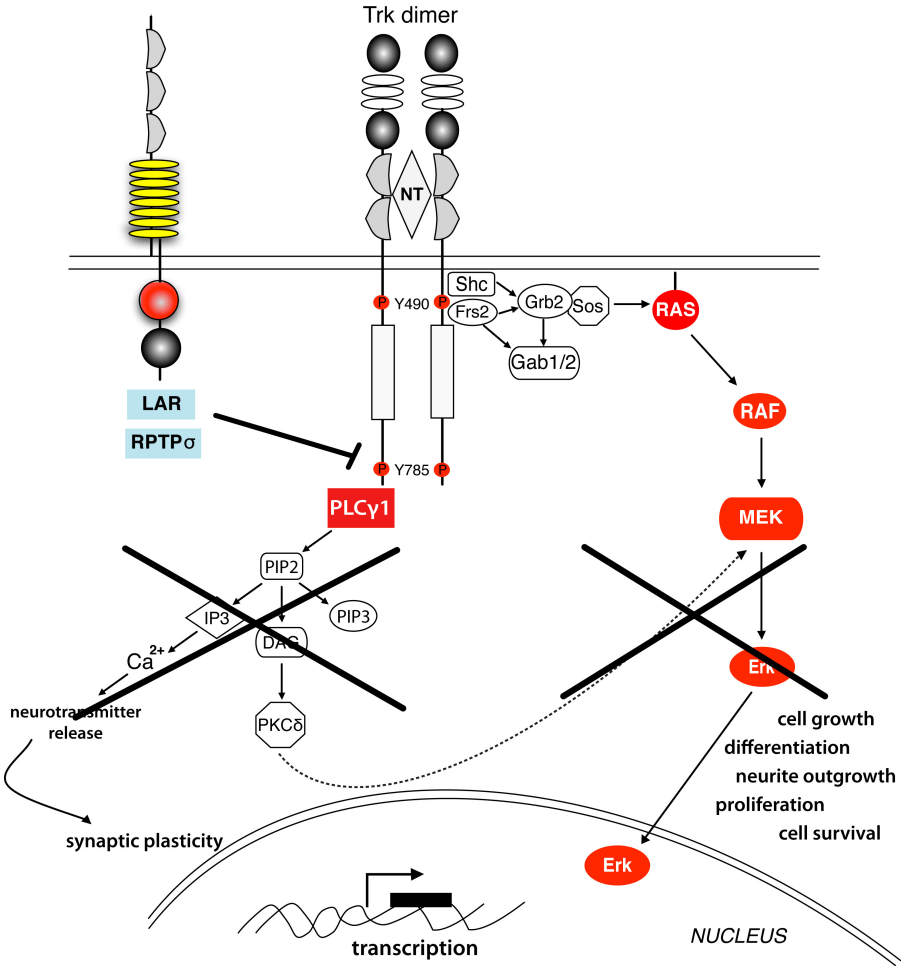

Figure 6.7. Possible function of LAR and RPTPσ in Trk signalling in sensory neurons.
LAR and RPTPσ might both dephosphorylate the Y785 residue and thus negatively affect the PLCγ-pathway and subsequently synaptic plasticity and MAPK-pathway mediated functions such as differentiation including neurite outgrowth, proliferation and cell survival. These effects might be most probably attributed to TrkA receptors, which are predominantly expressed in neurons in dissociated DRG cultures.

The results from the *Ptpro* knockdown experiments were very surprising. A dephosphorylation of TrkC by RPTP-BK was previously shown in overexpression systems (Hower et al., 2009). This might also be the case under physiological conditions and in fact also true for TrkA and TrkB. Our findings in the analysis of the effects of a decrease in RPTP-BK on Trk phosphorylation however were most contradictory between the two experiments and do not allow a conclusion. Whereas in the first experiment a possible downregulation of pTrk Y785 was observed in the majority of samples, in the second experiment Trk Y785 phosphorylation was upregulated. No particular changes were observed in Erk1/2 or Akt phosphorylation in both experiments. A possible explanation for this controversy might be the different culturing techniques between experiments. Subsequent studies are required to draw conclusions from this analysis.

One striking and unexpected finding in this study was the significant downregulation of *Ntrk1* gene expression and to some extent also of *Ntrk2* and *Ntrk3* upon *Ptpro* knockdown. This was reproducible in both experiments and was caused by all shRNAs, suggesting a specific, not off-target effect. These changes were not reflected on the protein level, but this might be due to compensation on the translational level or a decrease in Trk degradation. Thus, the question arises, how can RPTP-BK influence the gene expression especially of TrkA?

Our data are of particular interest in regard to the phenotype of RPTP-BK$^{-/-}$ mice, which display nociceptive abnormalities such as the loss of the response to thermal pain (Gonzalez-Brito and Bixby, 2009). These mice in fact showed a downregulation of GCRP on TrkA^{+} neurons by 50%, but with no significant changes in the total amount of neurons in DRGs. In our experiments we also did not observe an obvious increase in cell death or a change in Akt signalling. But this requires further experimental assessment. Based on the observations that overexpression of Runx1, which controls the expression of TrkA in neurons during DRG development and represses the generation of TrkB^{+} neurons, resulted in a similar phenotype as observed in the RPTP-BK$^{-/-}$ mice (Chen et al., 2006b, Dykes et al., 2010) an antagonizing effect of RPTP-BK on the TF Runx1 was suggested (Gonzalez-Brito and Bixby, 2009). This is supported by the phenotype of Runx1$^{-/-}$ animals, which show an increase in the amounts of TrkA^{+}, TrkC^{+} and CGRP^{+} neurons (Yoshikawa et al., 2007) (see also chapter 4, discussion and chapter 8). However, it is important to note that Runx1

function differs at early and late developmental stages. Early on it initiates TrkA expression and suppresses TrkB expression, whereas after approximately E17 it suppresses TrkA expression in favour of Ret expression (Molliver and Snider, 1997, Molliver et al., 1997, Chen et al., 2006b). Therefore a comparison between the phenotype of knockout mice and the results in our study has to be made with caution. In our experiments RPTP-BK seems to play an agonistic role on Runx1 function, as it suppresses *Ntrk1* expression consistent with a late function of Runx1 although the cultures were obtained from E13.5 embryos.

RPTP-BK$^{-/-}$ mice also display neurite guidance defects of proprioceptive neurons, similar to the phenotype observed in Runx3$^{-/-}$ mice (Arber et al., 2000, Inoue et al., 2002). It is known that Runx3 drives the generation of TrkC^{+} neurons and represses the generation of TrkB^{+} neurons (Kramer et al., 2006, Inoue et al., 2007, Dykes et al., 2010). Thus a possible regulation of RPTP-BK expression by Runx3 or a collaboration of these two proteins in the regulation of other proteins was also suggested. In our *Ptpro* knockdown experiments a possible regulation of the TrkC and TrkB gene and protein expression were also observed. However, these changes were subtler compared to TrkA gene regulation.

Finally the question arises, how can RPTP-BK influence the expression of *Ntrk1* to such an extent, when it is expressed only in a small proportion of TrkA^{+} neurons *in vivo*? In my gene expression analysis (chapters 3 and 4) I have observed additionally to the strong expression of *Ptpro* in a small subset of neurons, lower staining in other neurons similar to reported findings in rat E14 and E18 DRGs (Haworth et al., 1998). Therefore a low level of *Ptpro* in the majority of neurons in DRGs cannot be excluded. Additionally, the gene expression in dissociated DRG cells is fivefold upregulated in comparison to the *in vivo* state (see above). But it is still much smaller compared to the expression of *Ntrk1*. One other possible explanation for the impact of RPTP-BK on *Ntrk1* gene expression might be the translational control of RPTP-BK, which might compensate for the smaller amount of RPTP-BK mRNA. However, in an immunohistochemical analysis the amount of *Ptpro* and RPTP-BK roughly agreed with each other in E16 mouse DRGs *in vivo* (Beltran et al., 2003). It will be of great importance to address this question also in dissociated DRGs in future, possibly with immunocytochemistry, if antibodies become available.

Together with findings from other groups our *Ptpro* knockdown study provides data, which might support a possible role of RPTP-BK in the transcriptional regulation of Trk expression. These findings represent interesting starting points for a possible analysis of RPTP-BK function in the specification of sensory neurons.

In conclusion, the results in this chapter suggest a potential role of LAR and RPTPσ in the inhibition of Trk Y785 phosphorylation (Figure 6.7), the major mediator of the PLCγ-1 signalling pathway. Additionally, both phosphatases might potentially have an augmenting effect on the MAPK pathway. However, especially since the changes on the MAPK pathway are rather marginal, a compensatory effect by one another, which was often suggested, is possible. It will be interesting in the future to further investigate the possible activation of the PLCγ-1/PKCδ pathway by LAR and RPTPσ for instance by analysing PLCγ phosphorylation and its effects on neurite outgrowth and possibly synapse plasticity. The effect of RPTP-BK on the phosphorylation state of Trk Y785 was most controversial and it might not be involved in these regulatory processes. RPTP-BK might be instead involved in the control of Trk gene expression, since especially *Ntrk1* expression was highly decreased in these experiments. We have also observed a possible control of Trk expression by another RPTP. In an analysis of Trk gene expression in DRGs from different knockout mice, we detected a downregulation of all Trk receptors in RPTPγ$^{-/-}$ mice and to some extent in RPTPζ$^{-/-}$/RPTPγ$^{-/-}$ double knockouts (Appendix, Figure 6). As anatomical abnormalities in DRGs were not reported in these mice, these findings further support a possible role of RPTPs in the regulation of Trk gene expression.

Together our findings provide a good platform for further experiments to decipher the role of these phosphatases in DRG development and regeneration and particularly in the control of Trk function and possibly expression. However, any future such experiments must address several issues that have complicated the interpretation of the results in our study.

First, dissociated DRG cells are a mixed population of cells including glia cells and different neuronal subtypes, which complicates the read-out of the experiments. A physical separation of different cell subtypes would be therefore desirable, but in our study such an approach was not possible, as sensory neurons consist of many different

subpopulations of cells and no marker can be used currently to select a specific subpopulation for instance by separation using FACS sorting. Not only will the selected population of neurons, which might express a common marker such as Trk receptors, still differ in the composition of other receptors etc., but it would also be very difficult to generate an appropriate amount of cells for a molecular study like the one presented in this work. Additionally this is complicated by the apparent changes in gene expression in dissociated sensory ganglia cultures (Genc et al., 2005). Further, the presence of non-neural cells in the culture also complicates the analysis. In my study, I did use mitotic inhibitors to reduce the amount of glia cells in the culture to improve the read-out of the effects on neurons, and this may have lead to more reliable data. However, glia cells play crucial roles for instance in the control of the neuronal microenvironment and clearing of apoptotic cells, and are involved in chronic pain and can thus direct neuronal function (Hanani, 2005, Wu et al., 2009, Hanani, 2010b, Hanani, 2010a). Their reduction after mitotic inhibition might have affected the signalling responses in neurons including Trk signalling. Therefore although this cell model of primary cells with endogenously expressed Trk and RPTP proteins still has more advantages than an overexpression system, it will be of added benefit if future studies could be performed on a specific, selected population of neurons. For this purpose a generation of Trk expressing cells using embryonic stem cells like in other studies on Trk receptors (Nikoletopoulou et al., 2010) would be a good alternative.

The second major obstacle in my study was the lack of RPTP-specific antibodies and good antibodies against Trk phosphorylation sites. RPTP-specific antibodies are especially important for the assessment of an actual knockdown on the protein level, and this could be alternatively assessed in over-expression studies of tagged-RPTPs for instance in HEK293T cells. The phospho-Trk antibodies were especially difficult to use on lysates from a limited amount of primary cells despite enormous efforts to improve WB conditions. Possibly an increase in cell material might improve these issues as several of the antibodies worked on over-expressed samples but not on lysates from primary cells (data not shown). These Trk-specific antibodies are especially important because many of the Trk downstream signalling pathway components such as Erk, Akt, PLCγ, and PI3K etc. are also used by other growth factors and cytokines etc. For instance FGFR stimulation leads to increased activation of the MAPK, PI3K, PLCγ and Akt pathways (Huang and Reichardt, 2003) and FGF is also involved in neurite

outgrowth in PC12 cells (Togari et al., 1985). For this reason in order to test whether the effect of RPTP knockdown is mediated through Trks and not FGFR, EGFR etc., inhibitors against FGF/EGF etc. receptors could be used in addition to Trk specific antibodies. However, the selectivity of some inhibitors is questionable and has to be tested extensively first.

Chapter 7

Analysis of the interaction of Trk receptors and RPTPs using a Bimolecular Fluorescent Complementation Assay (BiFc)

7.1. Introduction

Protein-protein interactions (PPIs) describe a physical association between different proteins, which is essential for their function (Papin et al., 2005). Thus it is important for the characterization of the function of these proteins to identify their binding partners. Therefore in order to understand a possible direct function of RPTPs on Trk receptors their interaction has to be examined. For this reason the aim of this chapter was to establish an assay to analyse the direct interaction of RPTPs and Trk receptors.

Several different assays have been developed for the analysis of PPIs, such as yeast two-hybrid (Y2H) assays and co-immunoprecipitation (co-IP), or the direct visualization of protein interactions *in vivo* using Förster resonance energy transfer (FRET) assays or protein fragment complementation assays (PCAs). The latter is a simple direct visualization technique, which is based on the split of a reporter protein into two non-functional fragments linked to two possibly interacting proteins. When the proteins associate with each other, the two reporter fragments come together and form a functional reporter molecule. Depending on the reporter molecule such as β-galactosidase, ubiquitin, luciferase or fluorescent proteins (FPs), different PCA assays have been developed (Kerppola, 2008, Morell et al., 2009).

One such PCA assay is the Bimolecular fluorescent complementation (BiFc) assay, which utilizes as a reporter molecule a split FP such as the enhanced yellow fluorescent protein (EYFP) or its less temperature-sensitive mutant Venus (Hu and Kerppola, 2003, Shyu et al., 2006). The principle behind BiFc is very simple. The two proteins of interest are both covalently linked to a complementary FP fragment that upon interaction of the proteins associate with each other and form a functional FP, which can be simply detected with an inverted fluorescent microscope in living cells (Hu et al., 2002). BiFc assays can be used in a plethora of applications to answer many different questions. It is possible to use BiFc assays to detect PPIs *in vitro* and *in vivo* in almost any cell type and in specific subcellular compartments, and it allows the detection of interactions in response to developmental, environmental etc. changes.

BiFc assays have also many advantages compared to other protein interaction assays such as the Y2H assays, Co-IPs and the other *in vivo* method FRET. For instance Y2H assays would have the disadvantage of potential false post-translational

modifications of mammalian proteins as it is carried out in *Saccharomyces cerevisiae,* which might affect their interactions with other proteins. Co-IP, another widely accepted method to analyse protein interactions, depends on high affinity of the interacting proteins with each other and on the availability of specific antibodies. This problem can be overcome by introducing covalently bound tags such as HA or myc, which however might interfere with protein folding or might become inaccessible for the antibodies. Additionally cell lysis and mixing of contents from different subcellular compartments might change protein interactions. In contrast to this, since a BiFc assay is performed in living cells, not only is the environment of the proteins accounted for but also experimental manipulations, which can alter the results, are minimized (Hu et al., 2002). Especially the endogenous environment of the proteins is of great importance since proteins have specific functions in different cell types and respond differently to a variety of extracellular signals, in different subcellular localizations, and at different developmental stages of the cell, which all determine the availability of interacting partners. However, like any other technique, the BiFc assay has its limitations. One main disadvantage is the delay between the interaction of the proteins and the time when fluorescence can be detected due to the slow folding of the protein fragments and the autocatalytic cyclization reactions required to produce a functional fluorophore (12-24 hours). Therefore detection of real-time interaction is not possible with BiFc. Additionally, this reaction is irreversible and does not allow the detection of association and dissociation of the interacting proteins. However, because of this permanent interaction, this assay is very sensitive and can detect even very weak transient interactions between proteins (Kerppola, 2008).

BiFc assays have been successfully used to demonstrate different PPIs and were also expanded to visualize multiple protein interactions to detect competition between different interaction partners based on the formation of fluorescent complexes with different spectra. The majority of these BiFc studies however analysed interaction of cytoplasmic proteins or receptor-type proteins in combination with cytoplasmic proteins. Very few studies have been documented with receptor-type proteins only like RPTPs and Trks. For instance one study has used BiFc to monitor homodimerization of the α_{1b}-adrenoceptor and its mislocalisation due to introduced mutations (Lopez-Gimenez et al., 2007). Another study analysed the formation of the adenosine A_{2A} and the dopamine D_2 receptors in neuronal cells using multicolour BiFc (Vidi et al., 2008).

And an earlier study has also shown the interaction of the amyloid precursor protein (APP) with Notch receptors. It was reported that these heterodimers produced the strongest fluorescence signals in comparison to weaker signals of the APP homodimers and almost no signals of the Notch homodimers. This is in agreement with findings that APP but not Notch receptors form homodimers and these were therefore used as positive and negative controls (Chen et al., 2006a). Additionally, another PCA method was used to successfully detect and analyse dimerization and activation of erythropoietin receptors (EpoRs) upon ligand-binding using the dehydrofolate reductase (DHFR) as a reporter (Remy et al., 1999). These studies demonstrate that it is indeed possible to perform successful BiFc or other PCA assays also on receptor-type proteins such as RPTPs and Trks under topological constrains.

A direct and selective interaction of RPTPs with Trk receptors has been previously shown using co-IPs. For instance RPTPσ but not RPTPα was demonstrated to selectively and strongly bind to TrkA and C, but only weakly to TrkB (Faux et al., 2007). Further, also LAR co-immunoprecipitates with TrkA and TrkB either via direct interaction or in a complex for instance with Src, as Src knockdown prevented TrkB-LAR co-immunoprecipitation (Xie et al., 2006, Yang et al., 2006). Apart from the fact that co-IPs have several disadvantages as pointed out above, more than one assay has to be used in order to prove a genuine PPI. Therefore in these experiments we have assessed the functionality and specificity of a BiFc assay to analyse the potential interactions of RPTPs with Trk receptors.

7.2. Experimental procedures

7.2.1. Cloning of BiFc constructs

7.2.1.1. Cloning strategy

The host plasmids pEYFP1 or pEYFP2 containing an N-terminal YFP 1 or a C-terminal YFP2 fragment in pcDNA3.1 were used for cloning of the negative controls (RPTPα and CD34) and the TrkA constructs. These plasmids were modified versions of the zipper-EYFP plasmid kindly provided by JF Paradis in SW Michnick's lab. The zipper between the *Not*I and *Cla*I RE sites in front of the linker was deleted and an *Xba*I RE site was introduced for non-directional cloning. The *Xba*I site following the YFP fragment was deleted. The flexible linker consists of 12 glycines and serines (GGGGSGGGGSSG). The RPTP or TrkA sequences were PCR amplified with primers containing an *Xba*I site and ligated into the host plasmids in reading frame with the linker and the YFP fragment. Their expression was driven by the cytomegalovirus (CMV) promoter. I will refer in this thesis to YFP1 as VNT and YFP2 as VCT in respect to plasmids provided by Dr. Radu Aricescu (see below). YFP1/VNT and YFP2/VCT interact with each other and form a functional fluorophore.

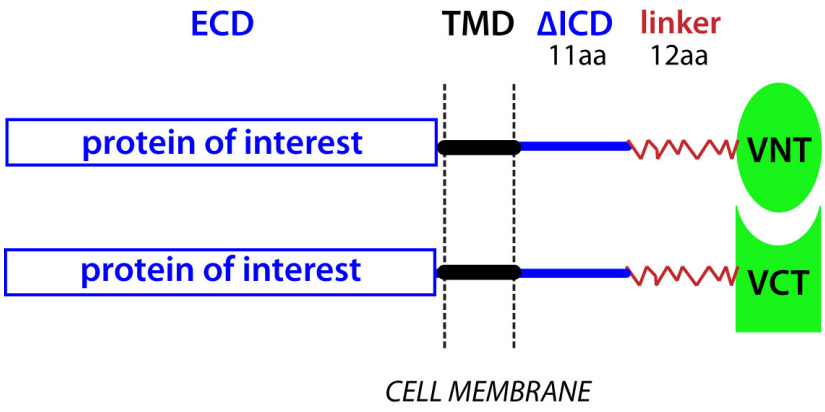

Figure 7.1. Schematic representation of truncated BiFc constructs.
TM = transmembrane domain (~ 24 aa), ECD = extracellular domain, linker consisting of 12 aa, VNT/YFP1 and VCT/YFP2 are N- and C-terminal Venus or eYFP fragments respectively.

7.2.1.2. BiFc constructs

Two types of constructs were generated. They contained either a cDNA sequence encoding the full-length TrkA or RPTP protein, or a truncated version, which mostly contained the ECD and the TMD. To design the truncated BiFc constructs the RPTP or TrkA annotated sequences were retrieved from the NCBI database (http://www.ncbi.nlm.nih.gov/nucleotide/) and examined thoroughly to identify the Kozak consensus sequence and the TMD using primarily the program Protean Lasergene® (DNASTAR) and entries from a variety of databases such as UniProtKB/Pfam (http://pfam.sanger.ac.uk/) as references. The Kozak consensus sequence is a short recognition sequence that greatly facilitates the initial binding of eukaryotic mRNAs to the small subunit of the ribosome. The consensus sequence for initiation of translation in vertebrates is known to be (GCC)RCCAUGG with R representing a purine (A or G) and contains the start codon AUG (Kozak, 1987). The TMD consists mostly of hydrophobic amino acids (aa) and was identified using the Kyte-Doolittle-hydrophobicity plot. Once these sequence regions were located PCR primers were designed upstream the Kozak sequence and 11 aa downstream of the TMD. The 11 aa bridging the TMD and the linker were included in the sequence design to match further constructs kindly provided by Dr. Radu Aricescu (see below).

pEYFP-TrkA-TM-VNT/VCT and -FL-VNT/VCT constructs

For the generation of the target constructs TrkA-FL- and TrkA-TM-VNT or -VCT a template plasmid containing a chimera of a mouse and rat TrkA sequence was used for PCR amplification (pSP72-TrkA, originally provided by Dr. Elspeth in Dr. S. Meakin's lab, Roberts Research Institute, Ontario, Canada). The first 220 bp of the TrkA sequence corresponded to mouse TrkA (NM001033124), whereas the rest was a rat TrkA sequence (NM021589). The mouse sequence encoded the signalling peptide (bp 62-164), which is usually cleaved off after the transport of the mRNA to its target location, and the first amino acid of the TrkA protein, which was a valine instead of a threonine. The TrkA-TM-construct covers bp 56-1429 and the TrkA-FL construct covers bp 56-2455 of rat TrkA cDNA (NM021589).

pEYFP-RPTPα-TM-VNT/VCT constructs

pSG-HA-RPTPα-P135-C and pSG-HA-RPTPα wild type plasmids containing the murine *Ptpra* cDNA sequence (NM_008980) in-frame with an N-terminal Haemagglutinin (HA)-tag at bp 25-79 were used as templates for the PCR reaction (kindly provided by Prof. J. den Hertog). pSG-HA-RPTPα-P135-C plasmid contains a functional mutant of RPTPα, which was generated by site-directed mutagenesis of the Phe residue at position 135 in the ECD to a Cys residue, resulting in a disulfide bridge between monomers and thus constitutive dimerization of the molecule and consequently its inactivation (Jiang et al., 1999). The TMD was located at bp 711-785. The final constructs contained bp 272-818 of the RPTPα cDNA (NM_008980).

pEYFP-CD34-TM-VNT/VCT constructs

The plasmid MPSVleader71tCD34scTKhz containing the human CD34 cDNA kindly provided by Dr. Hong in Dr. Kenth Gustafson's lab (MIU, ICH) was used as a template. The human CD34 gene encodes two protein isoforms due to alternative splicing: isoform CD34-F, the "canonical" sequence, and CD34-T, which lacks the aa 329-385 and encodes GEDP instead of ELEP at aa 321-328. The provided CD34 encodes CD-F but the first 12 aa are missing in the signalling peptide. The TMD corresponds to bp 1129-1191. The PCR product covered bp 295-1230 of the hCD34 cDNA (NM_001025109).

pHLsec-CD45/RPTPσ/LAR-TM/FL-VNT/VCT constructs

Several constructs (Table 7.1) contained human or chick truncated or full-length CD45, RPTPσ or LAR sequences in the pHLsec plasmid and were kindly provided by Dr. Radu Aricescu (University of Oxford, UK). The pHLsec vector is based on the pLEXm backbone and contains additionally a Kozak sequence, a secretion signal sequence and a Venus fragment either VNT154 or VCT155 followed by a Lys-His_6-tag. The RPTP sequences were introduced between the *Age*I and *Kpn*I sites and were under the transcriptional control of the chick β-actin promoter with an additional CMV enhancer (Aricescu et al., 2006).

BIFC CONSTRUCT	PROTEIN	SPECIES	REGION	PLASMID	
rTrkA-TM-VNT	TrkA	rat	ECD+TM	pEYFP1	A.S.
rTrkA-TM-VCT	TrkA	rat	ECD+TM	pEYFP2	V.T.
rTrkA-FL-VCT	TrkA	rat	full length	pEYFP2	A.S.
hRPTPσ-FL-VCT/VNT	RPTPσ	human	full length	pHLsec	R.A.
hRPTPσ-TM-VCT/VNT	RPTPσ	human	ECD+TM	pHLsec	R.A.
Cryp-TM-VCT/VNT	RPTPσ	chick	ECD+TM	pHLsec	R.A.
Cryp-TM-mV	RPTPσ	chick	ECD+TM	pHLsec	R.A.
Cryp-FL-mV	RPTPσ	chick	full length	pHLsec	R.A.
hLAR-TM-VCT/VNT	LAR	human	ECD+TM	pHLsec	R.A.
mRPTPα-HA-TM-VNT/VCT (Cys-mut)	RPTPα	mouse	ECD+TM	pEYFP1/2	V.T.
mRPTPα-HA-TM-VNT/VCT (wt)	RPTPα	mouse	ECD+TM	pEYFP1/2	V.T.
CD45 (RO)-TM-VNT/VCT	CD45	human	ECD+TM	pHLsec	R.A.
hCD34-TM-VNT/VCT	CD34	human	ECD+TM	pEYFP1/2	V.T.
EYFP1 (YFP1/VNT)				pEYFP1	A.S.
EYFP2 (YFP2/VCT)				pEYFP2	A.S.

Table 7.1. BiFc constructs.
The constructs were cloned by Dr. Andrew Stoker (A.S.), Dr. Radu Arcescu (R.A.) and Viktoria Tchetchelnitski (V.T.). EYFP1=VNT154, EYFP2=VCT155.

7.2.1.3. Cloning techniques

All general cloning techniques were described in section 1.1.

Briefly, 5 μg of the host plasmid were digested with *Xba*I and purified using the QIAquick PCR purification Kit, then treated with AP to prevent self-ligation and purified again. The RPTP or Trk sequence was PCR amplified with specifically designed primers containing an *Xba*I restriction site (Table 7.2) using plasmids described above as templates. The PCR product was gel purified, digested with *Xba*I and then purified using QIAquick PCR purification Kit and finally ligated into the digested host plasmid. Recombinant plasmids were subjected to analytical RE digest to confirm the predicted maps. Finally the plasmids were sequenced with custom primers, which annealed to the *Xba*I site (F, forward primer) and the VNT or VCT (R, reverse primer) for all products, apart from TrkA-FL, which needed additional sequencing primers in the middle of the sequence (Table 7.3).

PRIMER	SEQUENCE (5' → 3')	TM (°C)
mRPTPα–TM F	GG-TCTAGA-TCTTGTCCTGTTTGGCAGTG	60.5
mRPTPα-TM R	GG-TCTAGA-ATGACTCCCAGCTTGCTTGT	61.9
rTrkA-FL	GG-TCTAGA-GATCCCAAATTTGCTCCTCTGTCCACA	61.9
hCD34-TM F	GG-TCTAGA-ATGCCGCGGGGCTGGACC	68.5
hCD34-TM R	GG-TCTAGA-CAGCCTTTCTCCTGTGGG	62.1

Table 7.2. Cloning primers.

PRIMER	SEQUENCE (5' → 3')	TM (°C)
F EYFP1/2	CCAAGCTGGCTAGCGTTTA	52.6
R EYFP2 (VCT)	CGATGTTGTGGCGGATCT	55.6
R EYFP1 (VNT)	TCCAGCTCGACCAGGATG	61.1
TrkA FL iF	TCTCCTTCAGTGCCTTGACA	57.3
TrkA FL iR	CAAGAAGAATGTGACGTGCTG	57.3

Table 7.3. Sequencing primers.

7.2.2. Transfection of HEK293T cells with BiFc constructs

HEK293T cells were seeded at a density of 50% the day before transfection in a 12-well-plate. The cells were transfected with 1 or 0.5 µg of each BiFc plasmid per well using $CaPO_4$ as described in 2.5.1.3. Pictures were taken 48 h after transfection as described in section 2.6. The exposure times for eGFP were 2, 1, 0.5 and for BF 0.25 sec and 8 msec.

7.3. Results

7.3.1. Design of BiFc plasmids and experiments

The workflow of a BiFc assay is rather straightforward. Constructs, which contain a complementary FP fragment covalently bound to the protein of interest, are transfected into living cells such as HEK293T cells and fluorescence is detected with an inverted fluorescent microscope after a certain time.

The most challenging part for a successful BiFc experiment is the design of the constructs. Several important criteria have to be met. For instance the linkers between the protein of interest and the FP fragments are crucial, as they determine whether an interaction will occur and whether it is specific. These linkers usually consist of a flexible serine and glycine sequence of around 10-12 aa and are empirically chosen. The positioning of the FP fragments at the N- or C-terminals of the proteins of interest depends on the expected association of the binding partners. Further, it is important to express the fusion proteins close to endogenous levels, since high expression levels might result in non-native interactions, complex mislocalisation or spontaneous reassembly of the FP fragments. This can be achieved by using weak endogenous promoters or alternatively transfection with low amounts of plasmid DNA. It is especially important to control for the specificity of the assay using negative controls. Such controls could be the substitution of the protein partners with a known non-binding polypeptide or the introduction of mutations, which reduce or eliminate protein interaction. It is also important to swap the FP fragments in the constructs to ensure this does not cause any changes in the read-out. Finally, it has also to be established whether the YFP fragments interfere with the folding of the proteins by changing the position of the fragments in the fusion proteins (Kerppola, 2006, Morell et al., 2009).

7.3.2. Interaction of BiFc constructs in HEK293T cells

In this study we have assessed the interaction of rat TrkA receptors with chick, mouse or human RPTPs and other receptor proteins in HEK293T cells. We used either full-length (FL) proteins or truncated (TM) versions containing only the ECD and the TMD with a C-terminally bound YFP/Venus fragment (Figures 7.1 and 7.2). As positive

controls LAR and RPTPσ constructs were used, based on previously reported homodimerization and interaction of these RPTPs with Trk proteins (see previous chapters). This allowed us to assess the functionality of this assay. Further, to assess the specificity of the assay, we used RPTPα, CD45 and CD34 as negative controls with no previous records of an interaction with Trk receptors. In fact, RPTPα was previously even shown not to interact with TrkA directly in a co-IP study (Faux et al., 2007). In this study, we have used a constitutively dimerized mutant (Jiang et al., 1999, van der Wijk et al., 2005) as well as a wild type form of RPTPα. The leukocyte common antigen CD45 is expressed exclusively in hematopoietic cells, where it is involved for instance in the regulation of the activity of the SFKs Lck in T cells and Lyn in B cells (Trowbridge and Thomas, 1994). In this study we used the shortest isoform, CD45RO, which is specifically located on T cells (Tonks et al., 1990, Lammers et al., 1993, Way and Mooney, 1994). CD34 is a monomeric cell surface glycophosphoprotein and adhesion molecule that is expressed on early lympho-hematopoietic stem and progenitor cells, embryonic fibroblasts and small-vessel endothelial cells (Krause et al., 1996).

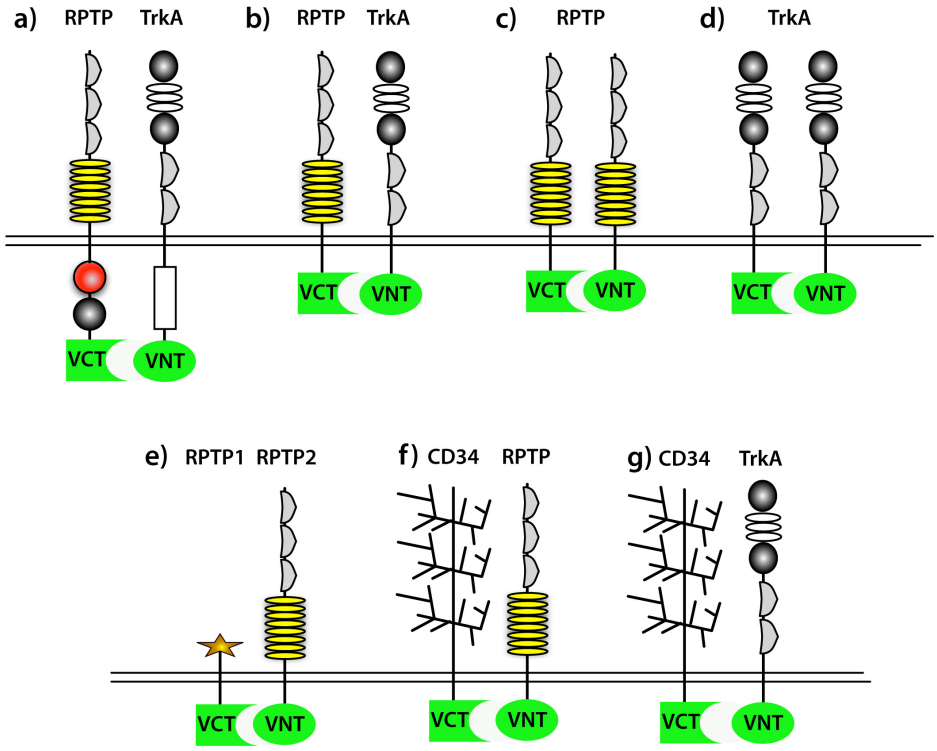

Figure 7.2. Different combinations of truncated and full-length BiFc constructs.
Displayed are representative combinations of **a**) full-length and **b-g**) truncated TrkA, different types of RPTPs (both were described in more detail in Figures 1.1 and 1.2) and the heavily glycosylated CD34 receptors, which were used in the BiFc assay. VNT/YFP1 and VCT/YFP2 are N- and C-terminal Venus or eYFP fragments respectively.

7.3.2.1. The positive controls RPTPσ and LAR do interact with TrkA

The RPTPσ-FL- or TM-VNT/VCT and LAR-TM-VNT/VCT constructs formed homodimers in our BiFc assay as expected (summarized in 1.2.1) (Figure 7.2G-L). The transfected cells looked healthy and very bright fluorescent signals localized to the plasma membrane were visible. In contrast to this, fluorescent cells transfected only with TrkA-TM constructs were mostly small in size and their frequency was very low (Figure 7.2I). Our experiments were performed without NGF and therefore although a high level of Trk expression usually leads to their ligand-independent dimerization and activation, this does not occur frequently. This could explain the low abundance of fluorescent cells (Hempstead et al., 1992). The differences in fluorescence intensities between TrkA and RPTPσ or LAR constructs could be additionally caused by the different promoters that drive their expression and thus control the amount of expressed proteins. We have used constructs with either a very strong chick β-actin promoter with an additional CMV enhancer in the case of RPTPσ and LAR, but a weaker CMV promoter for TrkA. Additionally to fluorescence localized to the plasma membrane, in some cells the fluorescent clusters were visible in intracellular compartments. This is most probably due to unspecific interaction of excess proteins in constrained spaces such as the Golgi apparatus or the endoplasmatic reticulum after translation. When we reduced the amounts of plasmid DNA used for transfection from 1 µg to 0.5 µg, this unspecific interaction was minimized. All transfections with a single plasmid were negative as expected (data not shown).

Rat TrkA-TM and human and chick RPTPσ-TM or human LAR-TM constructs interacted with each other in the plasma membrane (Figure 7.2A-C). Interestingly also the full-length TrkA interacted with truncated RPTPσ or LAR proteins (Figure 7.2E-F). The interaction of full-length TrkA with full-length RPTPσ was also observed (Figure 7.2D). However the fluorescence signal was very weak and only detectable at higher exposure times (1-2 sec longer). An interaction was also not detectable in every performed experiment. Similar to the observations made with the TrkA-TM constructs alone, the majority of cells transfected with TrkA-FL constructs in different combinations with other proteins were detected at low frequency and the cells were small in size. The reason for this poor interaction might be the stereochemistry of the proteins. Especially in the case of TrkA-FL interaction with RPTPσ-FL the D2 PTP domain and the TrkA catalytic domain may point away from each other. This issue was

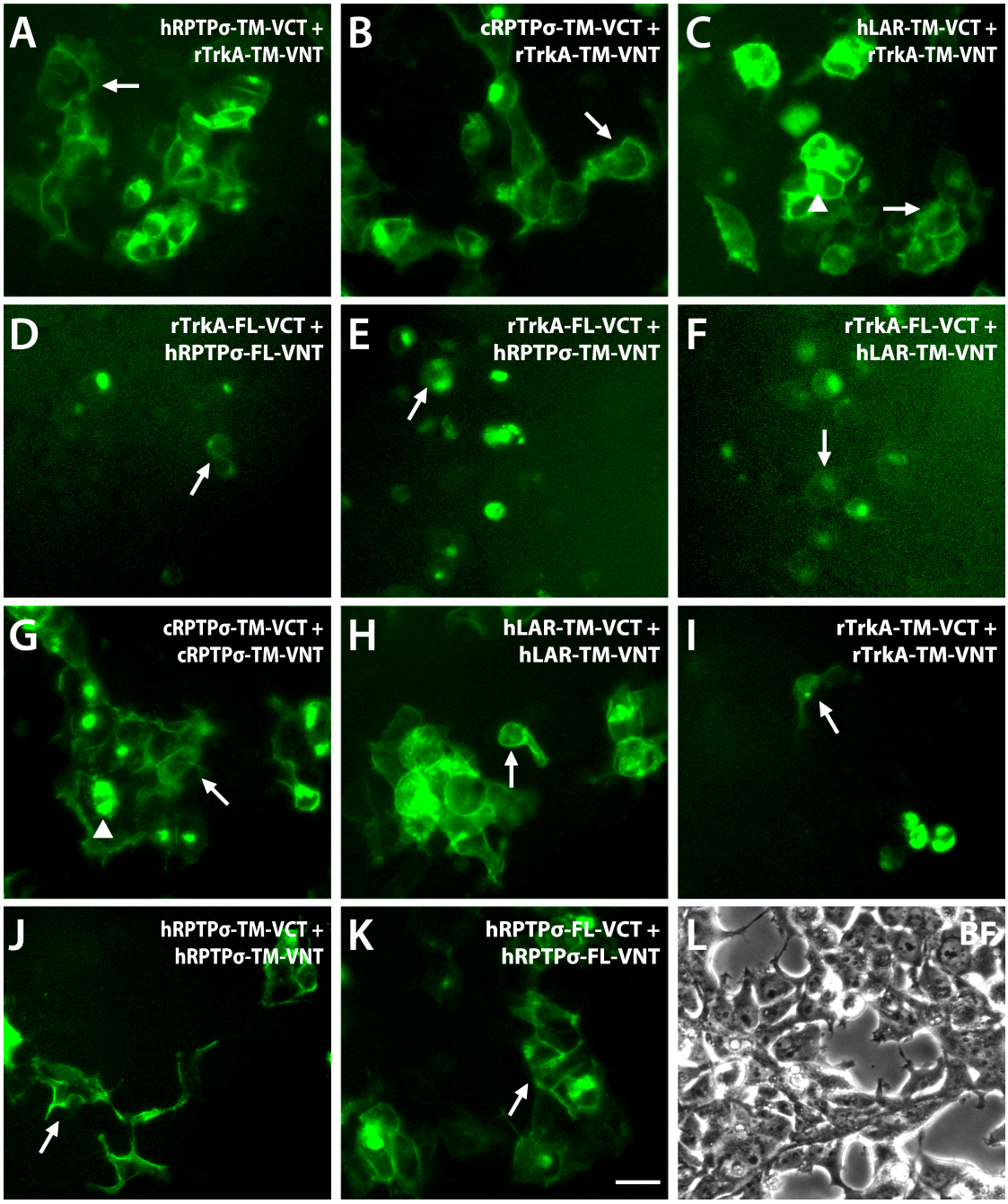

Figure 7.3. Positive BiFc controls: Interaction of RPTPs with TrkA.

Interaction of **A-C**) rTrkA-TM-VNT with chick or human RPTP-TM-VCT constructs (exposure time 0.7 sec). Interaction of rTrkA-FL-VCT with **D**) hRPTPσ-FL-VNT constructs and with **E-F**) RPTP-TM-VNT constructs (exposure times 2.5 sec). **G-K**) Homodimerization of truncated TrkA and RPTP or full-length RPTPσ constructs (exposure time 0.7 sec). **L**) Representative bright field picture. C = chick, h = human, r = rat, BF = bright field. Scale bar = 5 μm. Arrows point to staining in the plasma membrane and arrow heads to intracellular staining.

previously an apparent problem in FRET experiments (personal communication from Prof. Jeroen den Hertog and Dr. Andrew Stoker). Interestingly, similar to our analysis the interaction of APP with the truncated form of Notch was much stronger than with its full-length form. The authors suggested two reasons, the different length of the ICD of the proteins or an interference of the YFP fragments with the binding (Chen et al., 2006a).

In summary, these results show that all tested constructs formed homodimers, and that the TrkA-TM constructs interacted strongly with the RPTPσ- and LAR-TM constructs. Additionally, TrkA-FL constructs interacted with RPTPσ- and LAR-TM and RPTPσ-FL constructs, however, at lower frequency. Taken together this data demonstrate the functionality of the BiFc assay.

7.3.2.2. The negative controls RPTPα, CD45 and CD34 interact with TrkA

In order to assess whether the BiFc assay is specific, we have carefully assessed the interaction of TrkA with the putative negative control plasmids expressing RPTPα, CD45 and CD34. In our experiments the RPTPα- and CD45-TM constructs formed homodimers and were thus functional in the BiFc assay (Figure 7.3F, I and J). CD34 does not normally form homodimers and fluorescence was mostly undetectable in the transfected cells (Figure 7.3C). The detected fluorescence in very few cells might indicate an unspecific interaction of the YFP fragments on their own due to an over-expression of the CD34 constructs. A transient interaction of the YFP halves might trap them in a conformation able to form a functional fluorescent protein.

When we co-transfected these control constructs with TrkA-TM or TrkA-FL, we detected fluorescent cells in every possible combination. However, whereas the positive controls RPTPσ and LAR formed very bright fluorophores with TrkA-TM constructs, the interaction of RPTPα-TM Cys mutant or wild type form with TrkA-TM was much weaker and only detectable at a higher exposure of more than 2 sec compared to 0.5 sec for the positive controls. The differences in frequencies and fluorescent signal strengths detected might be due to higher amounts of proteins present in transfections with the positive controls and CD45 constructs, which had another backbone with a stronger promoter than the negative controls RPTPα and CD34. An additional indication for the higher protein amounts was also reflected by the presence of cytoplasmic staining

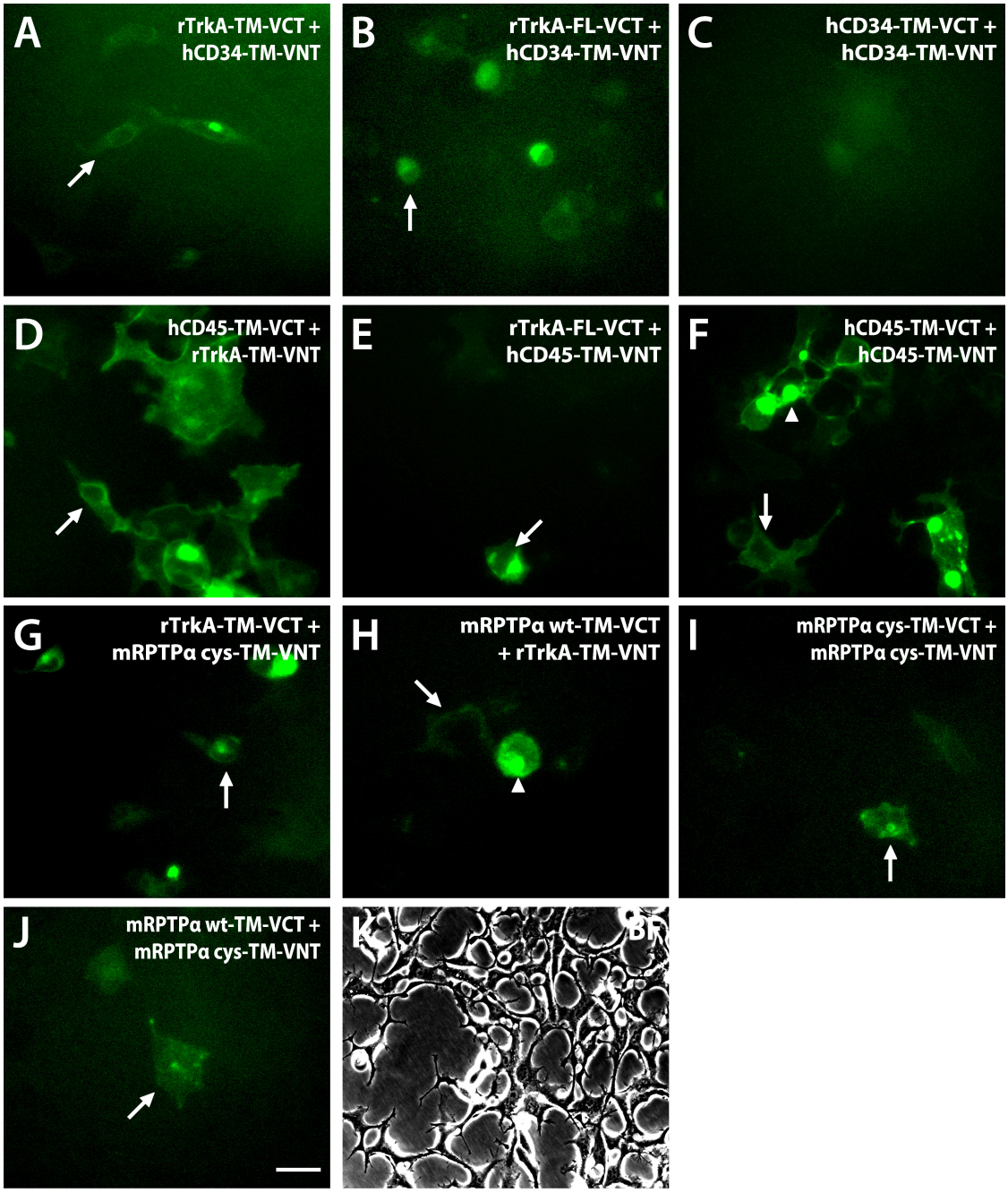

Figure 7.4. Negative controls: Interaction of CD45, RPTPα and CD34 with TrkA.

Interaction of **A-C**) hCD34-TM-VNT full-length or truncated rTrkA constructs and homodimerization (exposure time 2 - 2.5 sec), **D-F**) hCD45-TM-VNT/VCT with full-length or truncated TrkA constructs and homodimerization (exposure times 2.5, 2 and 1.4 sec respectively), **G-J**) mRPTPα wt/Cys-TM-VNT/VCT with rTrkA-TM-VCT/VNT constructs or homodimerization (exposure time 2.5 sec). **K**) Representative bright field picture. h = human, m = mouse, r = rat, BF = bright field, Cys = cysteine mutation, wt = wild type. Scale bar = 5 μm. Arrows point to staining in the plasma membrane and arrow heads to intracellular staining.

in cells transfected with the positive control constructs especially in contrast to RPTPα-TM. However, specific fluorescent signals localized to the plasma membrane could be seen in all transfections with the negative control plasmids and TrkA fusion proteins.

7.3.2.3. Interaction of RPTP receptors with each other

When we tested the interaction of all RPTPs and the CD34 receptor in different combinations with each other, we observed an interaction of all these constructs (Figure 7.4). Not only did all TM-constructs interact with each other but also RPTPσ-FL interacted with LAR- and CD45-TM (Figure 7.4D and L) and with CD34-TM (data not shown). Cells transfected with all of these constructs apart from RPTPσ-FL and CD45-TM showed a normal and healthy morphology. In comparison to the interaction of CD45-, RPTPσ- and LAR-constructs among each other, all interactions with the RPTPα and CD34-constructs were detected at 1-2 sec higher exposure times. Therefore once again the constructs driving transgene expression with the strong β-actin promoter showed brighter signals possibly due to higher amounts of proteins in the transfected cells as mentioned above.

7.4. Discussion

In this short study I have shown clearly that the BiFc assay does work well with type I transmembrane proteins that are known to dimerize such as RPTPσ and LAR and to interact with TrkA. However, all tested BiFc constructs, the full-length and truncated forms of TrkA receptors, the RPTPs LAR, RPTPα, RPTPσ and further negative controls CD45 and CD34, interact with each other in any combination, even though with differing fluorescence intensities. This was a disappointment, and at this point it is not possible to draw a final conclusion, whether these detected PPIs are specific and genuine under the experimental conditions or an artefact due to the current design of the assay, or whether these receptor-type molecules are generally unsuitable targets for BiFc assays. In order to find an answer to these questions, improvements to the design of the BiFc assay must be made.

On the one hand, the observed PPIs might be genuine and the analysed proteins including the negative controls might indeed interact with each other indirectly or

Figure 7.5. Interaction of RPTPs with each other.

Interaction of **A-F**) hCD45-TM-VNT with full-length or truncated RPTP constructs (exposure times A-E: 0.7-1 sec, F: 2.7 sec), **E-J**) mRPTPα wt/Cys -TM-VCT with RPTP-TM-VNT constructs (exposure times F-J 2.7 sec), **K, L**) hLAR-TM-VNT/VCT with full-length or truncated RPTPσ constructs (exposure times 0.7 sec), **M-O**) hCD34-TM-VNT with truncated RPTP constructs (exposure times M: 1.5 sec, N-O: 2.7 sec). C = chick, h = human, m = mouse, r = rat, BF = bright field. Scale bar = 5μm. Arrows point to staining in the plasma membrane and arrowheads to intracellular staining.

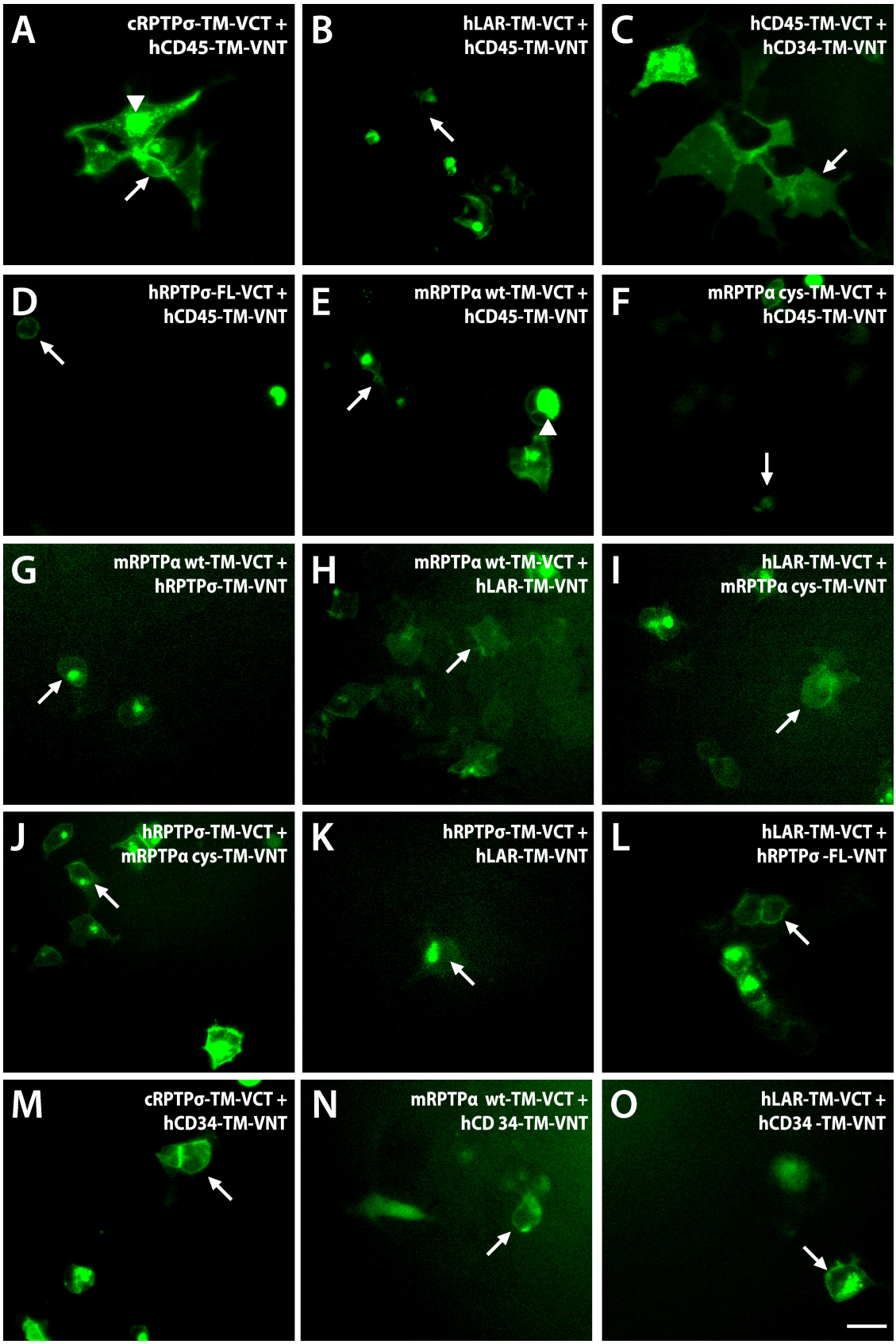
A
cRPTPσ-TM-VCT +
hCD45-TM-VNT
B
hLAR-TM-VCT +
hCD45-TM-VNT
C
hCD45-TM-VCT +
hCD34-TM-VNT
D
hRPTPσ-FL-VCT +
hCD45-TM-VNT
E
mRPTPα wt-TM-VCT +
hCD45-TM-VNT
F
mRPTPα cys-TM-VCT +
hCD45-TM-VNT
G
mRPTPα wt-TM-VCT +
hRPTPσ-TM-VNT
H
mRPTPα wt-TM-VCT +
hLAR-TM-VNT
I
hLAR-TM-VCT +
mRPTPα cys-TM-VNT
J
hRPTPσ-TM-VCT +
mRPTPα cys-TM-VNT
K
hRPTPσ-TM-VCT +
hLAR-TM-VNT
L
hLAR-TM-VCT +
hRPTPσ -FL-VNT
M
cRPTPσ-TM-VCT +
hCD34-TM-VNT
N
mRPTPα wt-TM-VCT +
hCD 34-TM-VNT
O
hLAR-TM-VCT +
hCD34 -TM-VNT

directly. Fluorescence complementation does not require direct interaction of the proteins, but only that the YFP fragments are brought close enough together to associate and form a mature fluorophore. Therefore it is possible that depending on the design of the BiFc assay, an interaction of proteins, which are for instance localized in the same complex and/or bound to the same scaffold, might be detected. The intensity of the fluorescence has been shown by others to be proportional to the strength of the interaction and thus a possible indicator for a direct or indirect interaction. Hereby stronger fluorescence levels suggest a direct or close interaction, whereas lower levels indicate an interaction within a complex (Morell et al., 2007). For instance in our assay the fluorescence intensity from an interaction of RPTPσ and TrkA was high, whereas the intensity from the interaction between RPTPα and TrkA was much weaker. In a previous study RPTPσ was shown to co-IP with TrkA possibly via a direct interaction, whereas RPTPα did not (Faux et al., 2007). The BiFc assay is more sensitive than co-IPs and so the interaction between TrkA and RPTPα might be genuine but indirect and therefore the signal intensity was much lower. However, the fluorescence intensity in our assay should be considered carefully, as we have used constructs with either a very strong chick β-actin promoter with an additional CMV enhancer or with a weaker CMV promoter. In this respect it was difficult to compare the signals from the interactions with the positive controls to the interactions with CD34 and RPTPα, as the weaker signals for the latter two might be caused by smaller protein amounts. However, the constructs of CD45 or RPTPσ were similar and their interaction with TrkA showed equally strong fluorescence levels. CD45 and in this context also CD34 are not expressed in the nervous system and a physiological interaction between TrkA and these receptors was never reported. Nevertheless, they are in fact coexpressed with TrkA in hematopoietic stem cells (Trowbridge and Thomas, 1994, Krause et al., 1996, Mulloy et al., 2005). An interaction in our BiFc assay between these receptors may therefore possibly be a physiological interaction, although it is unlikely, and might be direct.

Further, the observed interactions such as the RPTP heterodimerisation might also be direct regardless of the intensity of the signals due to the aforementioned reasons. In fact heterodimers between different vertebrate RPTPs were previously shown and several mechanisms were suggested. For instance an interaction between the D2 and D1 domains was proposed (Blanchetot and den Hertog, 2000). However, as we

have replaced the entire ICD with the YFP fragments in the majority of the BiFc constructs, a direct interaction between different RPTP molecules and other receptors might be in fact attributed to the binding of their ECDs or TMDs. In a genetic screening system in *E.coli*, which allows identification and quantitative analysis of TMD oligomerization, all 19 analysed human RPTPs formed homodimers through their TMD with different strengths (Chin et al., 2005). Similar results were also obtained prior to the mentioned study for RPTPα, RPTPσ, RPTP-BR7 and CD45 (Kitamura et al., 1995, Jiang et al., 2000, Tertoolen et al., 2001b, Chin et al., 2005, Lee et al., 2007, Noordman et al., 2008). The interaction of receptor proteins through their TMD was also suggested for homodimerization of ErbB tyrosine kinase receptors, integrins, and TrkA with one of its substrates the ankyrin-rich membrane spanning protein (ARMS) (Mendrola et al., 2002, Arevalo et al., 2004). Additionally, in a co-IP study in our lab RPTPσ and TrkA were suggested to interact with each other through their TMD and the immediate juxtamembrane regions (Faux et al., 2007). In a recent analysis an interaction of RPTPs with Trks was also assessed using a binding assay in COS cells. In this study a soluble form of the ECD of RPTPσ interacted with a soluble TrkC-ECD, but not TrkA- or TrkB-ECD. This interaction was attributed to the binding between the Ig domain in the ECD of RPTPσ and the LRR and Ig1 domains in the ECD of TrkC. Additionally, RPTPσ-ECD did not bind in a homophilic manner or to a soluble form of LAR or RPTPδ in this assay (Takahashi et al., 2011). If the TMD is in fact responsible for the binding between some of the phosphatases and Trks, as previously suggested, the lack of an interaction in these experiments might be attributed to the lack of a TMD in the constructs. This would support our hypothesis and in addition would point out differences in the interaction mechanisms between RPTPs with different Trks. First, in our assay, we show an interaction of the TMD-containing TrkA- and RPTPσ-constructs, whereas an interaction just between the ECDs of these receptors did not occur in the described study. And second, the mechanisms between RPTPσ-TrkA and RPTPσ-TrkC interactions seem to involve different domains. And in addition, the RPTPσ-TrkC interaction was shown to be trans-synaptic, whereas the RPTPσ-TrkA interaction in our BiFc assay occurs in the same cell. But as mentioned above at this point we do not know, whether all of our observed interactions are genuine.

On the other hand, the detected interactions between different RPTPs, CD34 and TrkA might be non-specific and are caused by topological constraints and/or an

overexpression of the proteins. Due to the localization of all constructs in the plasma membrane at potentially high densities, the target proteins might then come close enough together to cause the association of the YFP fragments. Additionally a self-assembly of the YFP fragments might be independent from the interaction of the target proteins causing a background signal, which is a known issue with some BiFc assays and new fluorescent proteins are currently being developed to minimize this problem (Shyu and Hu, 2008). Generally in order to minimize nonspecific interactions, weak promoters should be used to ensure that the target proteins are not over-expressed (Cabantous et al., 2005). In our study we have used a very strong and a weaker promoter and reduced the amount of plasmid DNA for transfections. However, this was still not enough to eliminate possibly unspecific intracellular interactions for some constructs. Additionally, the length of the flexible linker (currently 12 aa) could be shortened to reduce the chance of a possible self-association of the YFP fragments. This could also reduce BiFc detection of proteins, which do not interact directly but are localized within a complex (Shyu and Hu, 2008). And at last, additional negative controls should be used, such as plasmids with mutations in the potential interaction sites in order to prove specific interactions. This would also improve the measurements of fluorescent signals as indicators of the strength of the interactions, which might be skewed, if different constructs are used. Improving the current design of the BiFc assay might then solve the problem of possibly false positives due to unspecific interactions. Due to time constraints, I was not able to make these amendments.

Independent from our studies and in agreement with our results, Charlotte Coles in Dr. Radu Aricescu's group (University of Oxford, UK) was also performing a BiFc assay using some of the same constructs, but with an automated read-out using a fluorescence plate reader to measure the intensity of the signals. She has additionally performed a dilution curve of DNA amounts to analyse whether there is a specific threshold for negative and positive controls. However despite all efforts, she also came to the conclusion that it is not possible to distinguish between specific and unspecific PPIs using the BiFc assay in its current design (personal communication).

To sum up, the current design of the BiFc assay has to be improved in order to possibly use this assay for the analysis of the interaction of RPTPs with Trk receptors. Also further negative controls should be used. Once the specificity of the assay is established, it could have a great potential to be expanded to a high-throughput study, to

a competitive analysis using multicolour assays, and also to search for ligands, which cause dimerization of RPTPs and similar applications.

Alternatively, FRET another promising technique could be used, which similar to BiFc also allows direct visualization of PPIs in living cells. It is based on the energy transfer between two spectrum-overlapped fluorophores. A donor fluorophore such as CFP is linked to a bait protein and an acceptor fluorophore such as GFP is linked to the prey molecule. Once the fluorophores come into proximity, which allows FRET, the emitted light of one fluorophore activates the other fluorophore, which is visualized by the colour of the fluorophore. One of the great advantages of FRET is the possible detection of real-time complex formation and dissociation, which is not possible with BiFc assays. However, it suffers from several disadvantages such as background signals or photo bleaching. The proteins also have to be expressed at very high levels and the design of the FRET constructs might be very challenging, as the two fluorophores have to be as close together as 100Å for a successful FRET. This requires prior detailed knowledge about the structure of the proteins, which is often not available (Jares-Erijman and Jovin, 2003, Sekar and Periasamy, 2003). In a previous study in Stoker's and also in den Hertog's labs a FRET approach with RPTPσ or RPTPα constructs was not successful due to lack of knowledge about their confirmation (personal communication with Dr. Andrew Stoker). However several years later and with more information available on the protein structures it might be possible to establish a successful FRET assay to determine the interaction of RPTPs with Trk receptors.

In the end, all mentioned methods in this study such as BiFc, FRET, Y2H and co-IP not only vary in their sensitivity but might also provide different results. Therefore in order to prove a real interaction between proteins more than one assay has to be employed. Several methods can also be combined with each other such as BiFc and FRET for instance to analyse oligomerization of proteins (Vidi and Watts, 2009). Nevertheless, all of these PPI assays are based on over-expression of the proteins of interest and their actual coexpression and interaction has to be confirmed under physiological conditions such as in animal models.

Chapter 8

Concluding remarks

The story of NTs began over half a century ago, when Levi-Montalcini, Cohen and Hamburger discovered NGF. This groundbreaking finding was crowned with the Nobel Price in Physiology or Medicine in 1986 and started a long history of NT research. The role of NTs remains of most importance in the nervous system, where they control cell survival, precursor proliferation, commitment, and axon and dendrite growth and guidance of neurons as well as synapse formation, function and plasticity in the developing and adult PNS and CNS. Additionally, they also have important immunotrophic and metabotrophic functions and play a crucial role for instance in cardiac development, neovascularisation and the immune system. Their relevance is most apparent from their implication in the manifestation of several human genetic, neurodegenerative, and inflammatory, cardiovascular or metabolic diseases and carcinogenesis. The discovery of Trks several decades after the identification of their ligands, the NTs, stimulated this research area greatly. However, despite extensive studies on Trk-NT signalling, many questions remain unanswered and this reflects the complexity of this subject.

For instance one of the most important aspects is the implication of phosphatases, the counter-partners of kinases, in Trk signalling pathways. This remains poorly understood. A role of several PTPs in Trk signalling has been suggested in the literature and an interaction and direct dephosphorylation of Trks by these PTPs has been shown. However, because most of these analyses were performed in over-expression systems, their physiological relevance remains to be demonstrated. Unfortunately work with phosphatases is not a trivial task and the progress is obstructed by the nature of these PTPs. Not only do they show a promiscuity towards substrates *in vitro,* but the lack of antibodies against these enzymes and a possible compensation by other related phosphatases, as well as lack of knowledge about their physiological substrates and ligands, all complicate the research and, as a consequence, their implication in Trk signalling.

Nevertheless, the importance of some phosphatases in Trk signalling is unquestionable especially since several PTP knockout mice show mild to severe sensory abnormalities. The two main goals of this thesis were hence to identify RPTPs that could potentially interact with Trks, and to characterize their function in Trk signalling in a knockdown study using a primary cell model of sensory neurons from embryonic DRGs.

The expression of PTPs and Trks in the same tissue and possibly in the same cells is a prerequisite for their interaction. Therefore I have performed an extensive analysis of the gene expression of 94 of the 106 known PTPs using qPCR arrays on murine embryonic DRGs. I have identified several PTP members with high expression levels and noted some interesting temporal expression patterns. Although my further analysis was concentrated on RPTPs, an investigation of several other highly interesting PTPs in future will be worthwhile. The detailed analysis of the spatiotemporal expression patterns of RPTPs in comparison to Trk receptors during development, as well as the analysis of the coexpression of these receptor families, was a starting point to select candidate RPTPs for further functional analysis.

I could clearly show that 13 of the total 21 RPTPs are present in DRGs at relatively high levels during organogenesis (E12.5-14.5). Eleven of these RPTPs encoded by *Ptpra, Ptprd, Ptprf, Ptprg, Ptprj, Ptprk, Ptprm, Ptpro, Ptprr, Ptprs* and *Ptprz1* were in fact previously implicated in neuronal processes in different species in the CNS and/or PNS.

The spatiotemporal expression patterns of all candidate genes and a further in-depth coexpression analysis of the seven strongest candidate RPTPs with Trk receptors in murine E13.5 DRGs revealed unique patterns for all analysed phosphatases. Among these, the six RPTP genes *Ptpra, Ptprd, Ptprg, Ptprr, Ptprf* and *Ptprs* were strongly and ubiquitously expressed in almost all Trk^+ DRG neurons. Interestingly, in contrast to previous reports by other groups, I could also clearly show that *Ptprd* is expressed in DRGs. A small, yet uncharacterised subpopulation of $TrkA^+$ neurons did not coexpress *Ptprr, Ptprs, Ptprg* and *Ptprf*, and the proportion of $TrkA^+$/*Ptprr*$^-$ was particularly high. Over 20 different subtypes of sensory neurons exist in DRGs and it would be interesting to analyse which specific subpopulations of $TrkA^+$ neurons lack expression of these RPTPs and whether it is actually one subpopulation that does not express any of these RPTPs.

Together these findings suggest that these phosphatases could feasibly be implicated in the signalling pathways of all Trk types. The role of the phosphatases RPTPσ, LAR, RPTPR and RPTPγ in Trk signalling was in fact already looked at, but in contrast to previous assumptions an interaction with all Trk types is likely, based on their coexpression with all Trk receptors in my study. However, especially in regard to a lack of an expression in a specific subpopulation of $TrkA^+$ neurons, one might speculate

that these RPTPs are also expressed in DRGs for additional reasons not directly related to Trk signalling. The data also strongly suggest a functional redundancy in RPTP action, since arithmetically most Trk neurons must express a significant cohort of RPTP family members.

RPTP-BK revealed the most striking gene expression and coexpression patterns as it was found in a specific, small subpopulation of DRG neurons unlike any other RPTP. The coexpression analysis revealed its presence in all $TrkB^+$ neurons, the majority of $TrkC^+$ neurons and around 5% of $TrkA^+$ neurons in E13.5 DRGs. A comparison to a previous study by Beltran *et al*. in E16 DRGs has also unveiled an interesting dynamic expression pattern (Beltran et al., 2003). Whereas the $TrkC^+$/*Ptpro*$^+$ population remained constant at around 50%, the $TrkB^+$/*Ptpro*$^+$ population decreased and the $TrkA^+$/*Ptpro*$^+$ population increased during development. I have also observed a similarity in the amount of *Ptpro*$^+$/$TrkA^+$ and the amount of TrkB/TrkA and TrkC/TrkA-coexpressing cells. But the expression pattern of *Ptpro* is further complicated by differences in the amounts of mRNA molecules in different neurons (Haworth et al., 1998). It will be of great interest to further analyse the dynamics of the coexpression pattern of this RPTP with Trks over its major expression period from E12 to E16 in DRGs. Together, these findings hint towards an interesting mechanism possibly in the regulation of sensory neuron specification and Trk expression by RPTP-BK (see below).

Together, this is the first such analysis of the gene expression of almost the entire family of PTPs and in particular of eleven RPTPs in murine embryonic DRGs, and a comparison of their expression patterns to Trk receptors. The further unique coexpression analysis of seven candidate RPTPs with Trk receptors revealed rather unexpected coexpression with all three kinases. My investigation also demonstrated that many Trk^+ neurons express most of these RPTPs, hinting towards a possible functional redundancy possibly within an RPTP subgroup as suggested above. On the other hand not all RPTPs were expressed in DRGs and this also shows some degree of specificity.

In my analysis I have shown the expression of all or the most common neuronal isoforms of Trk and RPTP receptors. An even more complete picture of gene expression and coexpression would benefit from an analysis of the different isoforms of Trk receptors and RPTPs, since these isoforms are differentially expressed and have different functions (Forrest et al., 2006).

Since coexpression is a prerequisite, but not an ultimate proof for an interaction of proteins, I have further analysed the function of the RPTPs LAR, RPTPσ and RPTP-BK in Trk signalling in primary dissociated E13.5 DRG cultures. For this, I developed an efficient lentivirus-mediated shRNA-induced knockdown assay for silencing particular RPTPs in these primary neurons. LAR and RPTPσ are the highest expressed PTPs in DRGs and were previously both analysed as possible interaction partners of Trk receptors and my expression analysis showed a clear coexpression of these RPTPs with all Trk receptors. However, apart from a study of LAR and TrkB in hippocampal neurons, the majority of these experiments was performed in over-expression systems or PC12 cells, hence these data may lack some physiological relevance. In this respect my lentiviral study of endogenous proteins performed in primary DRG cultures may have one advantage.

The knockdown of LAR and RPTPσ in these cells suggested an inhibitory role of LAR and RPTPσ in Trk Y785 dephosphorylation, and in both cases possibly an augmenting effect on the MAPK pathway but no effect on the Akt pathway (Figure 6.7). This suggests an involvement of both RPTPs in the control of the Trk-mediated PLCγ signalling pathway, possibly leading to the control of synaptogenesis or MAPK- and Akt-independent neurite outgrowth. However, these signalling mechanisms remain largely unknown and my findings represent a good starting point for further investigation. Interestingly, while the similarities in the effects of the knockdown of both phosphatases suggest potential functional redundancy, they also show that removal of single RPTPs is still sufficient to moderately perturb the system. It would therefore be worthwhile to analyse a double knockdown of both RPTPs, especially since no LAR/ RPTPσ double-knockout mice are available, to address this very important issue.

The important role of RPTP-BK in Trk^{+} sensory neurons is undoubted since RPTP-$BK^{-/-}$ mice clearly display proprioceptive (TrkC) and nociceptive (TrkA) abnormalities and neurite guidance defects (Gonzalez-Brito and Bixby, 2009). RPTP-BK was also previously suggested to interact with Trks and particularly it was shown to dephosphorylate TrkC receptors (Hower et al., 2009). My coexpression study, however, clearly shows a coexpression of this phosphatase with all three Trk receptors, which makes an interaction with all Trk types possible. The results from my knockdown study showed contradicting effects on the dephosphorylation of Trk Y785 by this phosphatase and no effects on the MAPK or Akt pathways. Subsequent studies are

required to draw conclusions from this analysis concerning an implication of RPTP-BK in the Trk signalling cascade.

One striking and unexpected finding in these knockdown experiments was the very strong downregulation of *Ntrk1* gene expression and to some extent also of *Ntrk2* and *Ntrk3* upon very efficient *Ptpro* downregulation with five different small hairpins. Although these changes were not reflected on the protein level, but this might be caused by compensating translational mechanisms and requires some additional research. Together with my results from the coexpression analysis of RPTP-BK with Trk receptors, these data fit the hypothesis of a potential regulation of Trk expression and therefore sensory neuron specification by RPTP-BK. This raises a whole lot of new questions and with additional findings from many independent previously reported studies my results represent pieces of a puzzle that creates a possible picture of RPTP-BK function and strengthens its case in the specification of Trk neurons in DRGs.

The first piece of the puzzle comes from the comparison of the phenotypes of RPTP-BK $^{-/-}$ mice and other mouse models. RPTP-BK$^{-/-}$ mice display proprioceptive and nociceptive abnormalities such as neurite guidance defects and the loss of the response to thermal pain and an additional downregulation of the calcitonin gene-related peptide (CGRP) on TrkA^{+} neurons by 50%, but with no significant changes in the total amount of neurons in DRGs (Gonzalez-Brito and Bixby, 2009). In comparison, mice with abnormal expression of the TFs Runx1 and Runx3 revealed similar nociceptive and proprioceptive defects (Gonzalez-Brito and Bixby, 2009). For instance an overexpression of Runx1 resulted in a similar phenotype as observed in the RPTP-BK$^{-/-}$ mice (Chen et al., 2006b, Dykes et al., 2010) and Runx1$^{-/-}$ animals show an increase in the amounts of TrkA^{+}, TrkC^{+} and CGRP^{+} neurons displaying a negative regulation of TrkA and TrkC expression in DRGs by Runx1 (Yoshikawa et al., 2007). Therefore an antagonizing effect of RPTP-BK on Runx1 was suggested (Gonzalez-Brito and Bixby, 2009). However, Runx1 function differs at early and late stages of development. At early embryonic stages it does in fact initiate TrkA expression and suppresses TrkB expression, whereas approximately after E17 Runx1 suppresses TrkA expression in favour of Ret expression (Molliver and Snider, 1997, Molliver et al., 1997, Chen et al., 2006b). Further, RPTP-BK$^{-/-}$ mice display a similar phenotype as Runx3$^{-/-}$ mice in terms of neurite guidance defects of proprioceptive neurons (Arber et al., 2000, Inoue et al.,

2002), but RPTP-BK$^{-/-}$ mice show also defects in neurite guidance of nociceptive neurons. Runx3 drives the generation of TrkC^{+} neurons and represses the generation of TrkB^{+} neurons (Kramer et al., 2006, Inoue et al., 2007, Dykes et al., 2010) and interestingly, Runx3$^{-/-}$ mice show a decrease in the amounts of TrkA^{+}, TrkC^{+} and CGRP^{+} neurons (Nakamura et al., 2008). Therefore RPTP-BK might also play an agonistic effect on Runx3.

The second piece of the puzzle comes from the comparison of the previously reported expression patterns of Runx genes with *Ptpro* and my coexpression data of *Ptpro* with Trk receptors in E13.5 DRGs. *Ptpro* expression begins at E12 and shows a peak between E16 until P3 (Van Vactor, 1998). Runx3 expression in DRGs has an onset at E10.5 and a decline from E16 on. And in contrast to *Ptpro* no coexpression with TrkB was detected, which is not surprising as it represses TrkB expression (Levanon et al., 2002). In contrast to this, Runx1 expression begins at E12.5 and in addition to TrkA neurons it is also expressed in TrkB and TrkC neurons (Chen et al., 2006b). And so Runx1 suggests the highest similarity in gene expression to RPTP-BK. To confirm these assumptions, a coexpression analysis of RPTP-BK with Runx1 and Runx3 could be performed.

The third piece of the puzzle comes from my knockdown analysis. A possible downregulation of *Ntrk1* upon *Ptpro* knockdown but not to such an extent of *Ntrk2* and *Ntrk3* also hints mainly towards a regulation of Runx1 expression or function by RPTP-BK. However, in contrast to the comparison of the knockout animals above, in this scenario RPTP-BK would rather hint towards an agonistic role to Runx1. This might be explained by the different functions of Runx1 at early and late stages.

Several further pieces of the puzzle support a general role of RPTP-BK in sensory neuron specification. For instance *Ptpro* was identified as a target gene of Wnt signalling, with Wnt3a as a possible ligand for RPTP-BK (Kim et al., 2010). The Wnt/β-catenin pathway is known to drive NCCs towards a sensory fate (Le Douarin and Kalcheim, 1999) and might so implicate RPTP-BK in this process.

Recently another puzzle piece was found when Met, a HGFR kinase, was shown to be required for Runx1 extinction and differentiation of peptidergic CGRP^{+} nociceptors together with TrkA, whose expression is downregulated in RPTP-BK$^{-/-}$ mice. Additionally, Runx1 represses Met expression in non-peptidergic neurons

(Gascon et al., 2010). Met is a kinase and a substrate for some RPTPs such as DEP-1 (Palka et al., 2003) and LAR (Kulas et al., 1996) and could as well be a substrate of RPTP-BK. It will be intriguing to analyse Met as a potential substrate and link of RPTP-BK to Runx and thus the control of sensory neuron specification.

And at last Runx (Kaminker et al., 2002, Kramer et al., 2006) and RPTP-BK (Desai et al., 1996, Krueger et al., 1996, Sun et al., 2000b, Stepanek et al., 2001) were both implicated in axon targeting and guidance in many different studies and knockout mice of either protein also show defects in neurite guidance (Arber et al., 2000, Inoue et al., 2002). Hence these proteins were once again implicated in the same processes.

In this respect my results provide one or two valuable and testable puzzle pieces for this complex research field, which is however still controversial in some aspects.

In conclusion, this thesis has provided valuable insights into the potential role of RPTPs in Trk signalling, possibly pointing towards roles in controlling synaptogenesis, neurite outgrowth and also neuronal specification. Further studies will be able to expand this analysis and contribute to the understanding and possible control of Trk signalling. The very efficient lentiviral knockdown approach, with some important improvements as discussed in chapter 6, provides a very valuable tool in this respect. Nevertheless, research on the function of RPTPs still remains challenging. My findings further support the possibility of a degree of redundancy among some RPTPs, but also some specificity. This is especially important if RPTPs are considered as potential drug targets possibly to control Trk function, which is deregulated in many different diseases. Especially the possibility of the control of Trk gene expression by RPTP-BK opens many new doors. Understanding the transcriptional regulation of Trk receptor expression is not only of importance to decipher neuronal cell fate specification mechanisms, but could in fact also provide new strategies for therapeutic implications for the treatment of neurodegenerative diseases, chronic pain, neuropathies, cancers etc. For instance Runx3 is a tumor suppressor and TrkB is an oncogene in several tumor types including neuroblastoma. Since Runx3 represses TrkB expression in DRGs it would be interesting to find out what controls Runx3 function (Inoue et al., 2007) and in this context RPTP-BK might be a good candidate. Further, Runx1 controls the development, survival and function of the majority of nociceptive neurons by controlling for instance the expression of TrkA and many ion channels (Chen et al.,

2006b, Marmigere et al., 2006) and RPTP-BK may well be implicated in the control of Runx1 expression and/or function. It is therefore of great importance to decipher these transcriptional pathways for instance in regard to future pain therapies.

This thesis thus provides novel data about the potential functional interactions and co-expression dependencies of RPTPs and Trk enzymes in primary sensory neurons and suggests several starting points for further research that will lead to an understanding of the complex, functional interactions between Trks and RPTPs and their possible implication in disease.

Appendix

Chapter 2

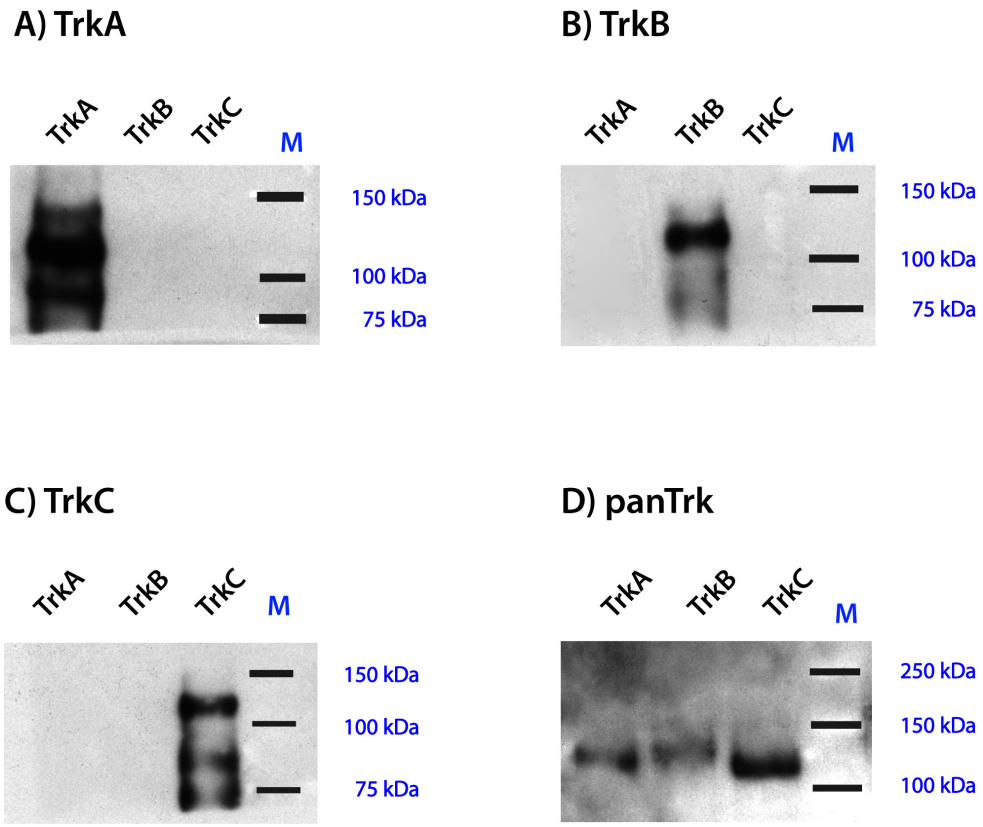

Figure 1. Specificity of Trk antibodies on WBs.

The antibodies against TrkA, TrkB and TrkC ECDs detected all isoforms of TrkA, TrkB or TrkC receptors respectively in transfected HEK293T cells on WBs. No cross-reaction with any of the other Trk receptors was detected. The panTrk antibody detected the ICD and hence only the full-length isoforms of all three Trk receptors. M = marker.

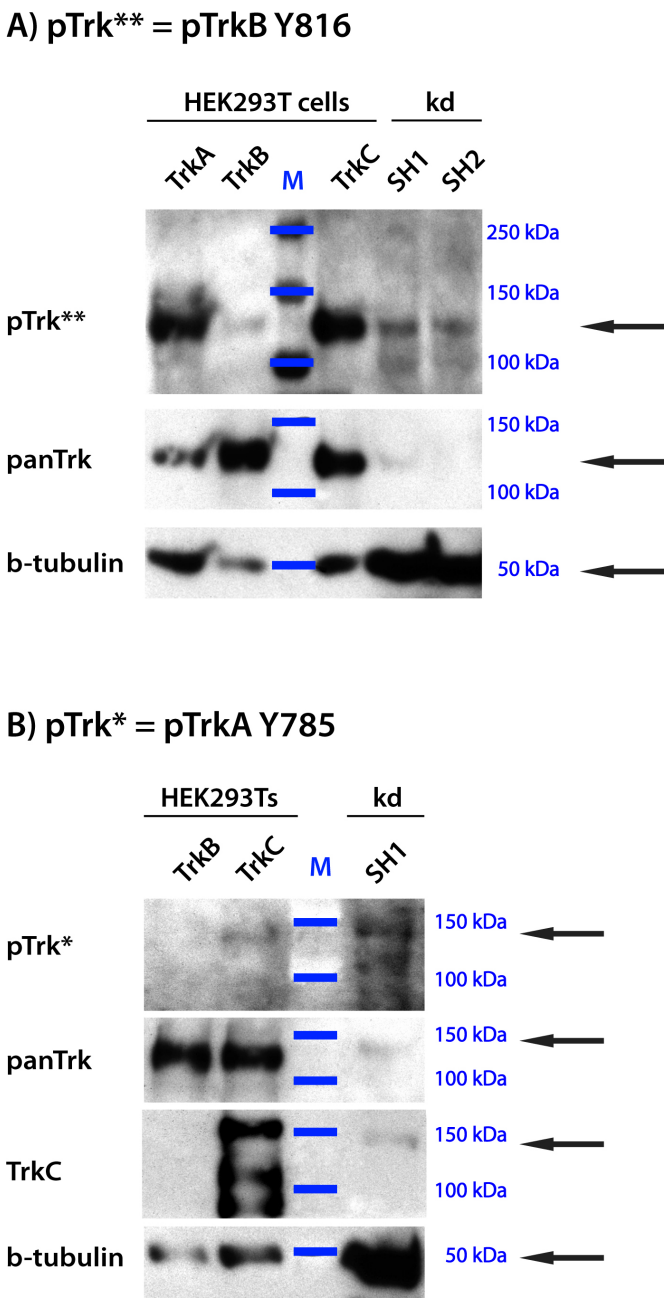

Figure 2. Cross-reaction of pTrk antibodies on WBs.

The antibody pTrk* = pTrkA recognizes phosphorylated Y785 on TrkA and TrkC and pTrk** = pTrkB recognizes phosphorylated Y785 on all three Trk receptors. M = marker, SH = small hairpin, kd = knockdown. See chapter 6 for more explanations.

Chapter 3

	PROTEIN NAME	GENE NAME	ID NUMBER
MKPs	**MKP1**	*Dusp1*	QT00288638
	PAC1	*Dusp2*	QT00248283
	MKP2	*Dusp4*	QT00140357
	hVH3	*Dusp5*	QT01065617
	MKP3	*Dusp6*	QT00101997
	PYST2	*Dusp7*	QT00155337
	hVH5	*Dusp8*	QT00118650
	MKP4	*Dusp9*	PPM25836A
	MKP5	*Dusp10*	QT00152257
	MKP7	*Dusp16*	QT00097272
	MK-Styx	*Styxl1*	PPM34884A
atypical DSPs	**FMDSP**	*Dusp1*	not existing
	VHR	*Dusp3*	QT00138467
	PIR1	*Dusp11*	QT00104867
	HYVH1	*Dusp12*	QT00124600
	TMDP	*Dusp13b*	QT00168882
	MKP6	*Dusp14*	QT00284424
	VHY	*Dusp15*	QT00171605
	LMW DSP20	*Dusp18*	QT00119322
	SKRP1	*Dusp19*	QT00169624
	LMW DSP21	*Dusp21*	QT00267064
	JSP1	*Dusp22*	QT00158431
	MOSP/VHZ	*Dusp23/25*	QT01075487
	MKP8	*Dusp26*	QT00112630
	FMDSP/DUPD1	*Dusp27*	QT01064378
	LAFORIN	*Epm2a*	QT00261842
	PTPMT1	*Ptpmt1*	QT00114772
	MCE	*Rngtt*	QT00151564
	Styx	*Styx*	QT01531992
SSHs	**SSH1**	*Ssh1*	QT00165011
	SSH2	*Ssh2*	QT00101199
	SSH3	*Ssh3*	QT00150227
PTENs	**PTEN**	*Pten*	QT00141568
	TPIP	*Tpte*	QT00161126
	TENSIN-1	*Tns1*	PPM33341A
	TENSIN-3	*Tns3*	QT01557437
	TENSIN-2, C1-TEN	*Tenc1*	QT01066800
PRLs	**PRL1**	*Ptp4a1*	QT00156464
	PRL2	*Ptp4a2*	QT00143332
	PRL3	*Ptp4a3*	QT00138243
CDC14s	**Cdc14a**	*Cdc14a*	QT01051764
	Cdc14b	*Cdc14b*	QT01079148
	KAP1	*Cdkn3*	QT01561763
	PTP 9q22	*Ptpdc1*	QT00161973

continued

	PROTEIN NAME	GENE NAME	ID NUMBER
Myotubularins	**MTM1**	*Mtm1*	QT01066079
	MTMR1	*Mtmr1*	QT00147070
	MTMR2	*Mtmr2*	QT00144795
	MTMR3	*Mtmr3*	QT01068655
	MTMR4	*Mtmr4*	QT00148757
	MTMR5	*Sbf1*	QT01549450
	MTMR6	*Mtmr6*	QT00147994
	MTMR7	*Mtmr7*	QT00175868
	MTMR9	*Mtmr9*	QT00102305
	MTMR10	*Mtmr10*	QT01067675
	MTMR11	*Mtmr11*	QT00157318
	MTMR12	*Mtmr12*	QT00132384
	MTMR13	*Sbf2*	QT00125951
CDC25s	**CDC25a**	*Cdc25a*	QT01058778
	CDC25b	*Cdc25b*	QT00127806
	CDC25c	*Cdc25c*	QT01055222
NPTPs	**PTP1B**	*Ptpn1*	QT00166418
	TCPTP	*Ptpn2*	QT01063573
	PTPH1	*Ptpn3*	QT00264649
	MEG1	*Ptpn4*	PPM35219A
	STEP	*Ptpn5*	QT01063580
	SHP1	*Ptpn6, Hcph*	QT00155967
	HePTP	*Ptpn7*	QT01073611
	LyPTP	*Ptpn22/Ptpn8*	QT00103943
	MEG2	*Ptpn9*	QT00170520
	SHP2	*Ptpn11*	QT00103362
	PEST	*Ptpn12*	QT00168126
	PTPBAS	*Ptpn13*	QT00097244
	PEZ	*Ptpn14*	QT01553097
	BDP1	*Ptpn18*	QT00097027
	PTPTyp	*Ptpn20*	PPM25464A
	PTPD1	*Ptpn21*	QT00197862
	HDPTP	*Ptpn23*	QT01560692
	LMW PTP	*Acp1*	QT00135135
HKGs	**GPS1**	*Gps1*	QT00120113
	HPRT1	*Hprt1*	QT00166768
	PSMB2	*Psmb2*	QT00113701
	UBC	*Ubc*	QT00245189
Trks	**TrkA**	*Ntrk1*	QT01046143
	TrkB	*Ntrk2*	QT00132111
	TrkC	*Ntrk3*	QT00146153

Table 1. qPCR primers used on the qPCR array.

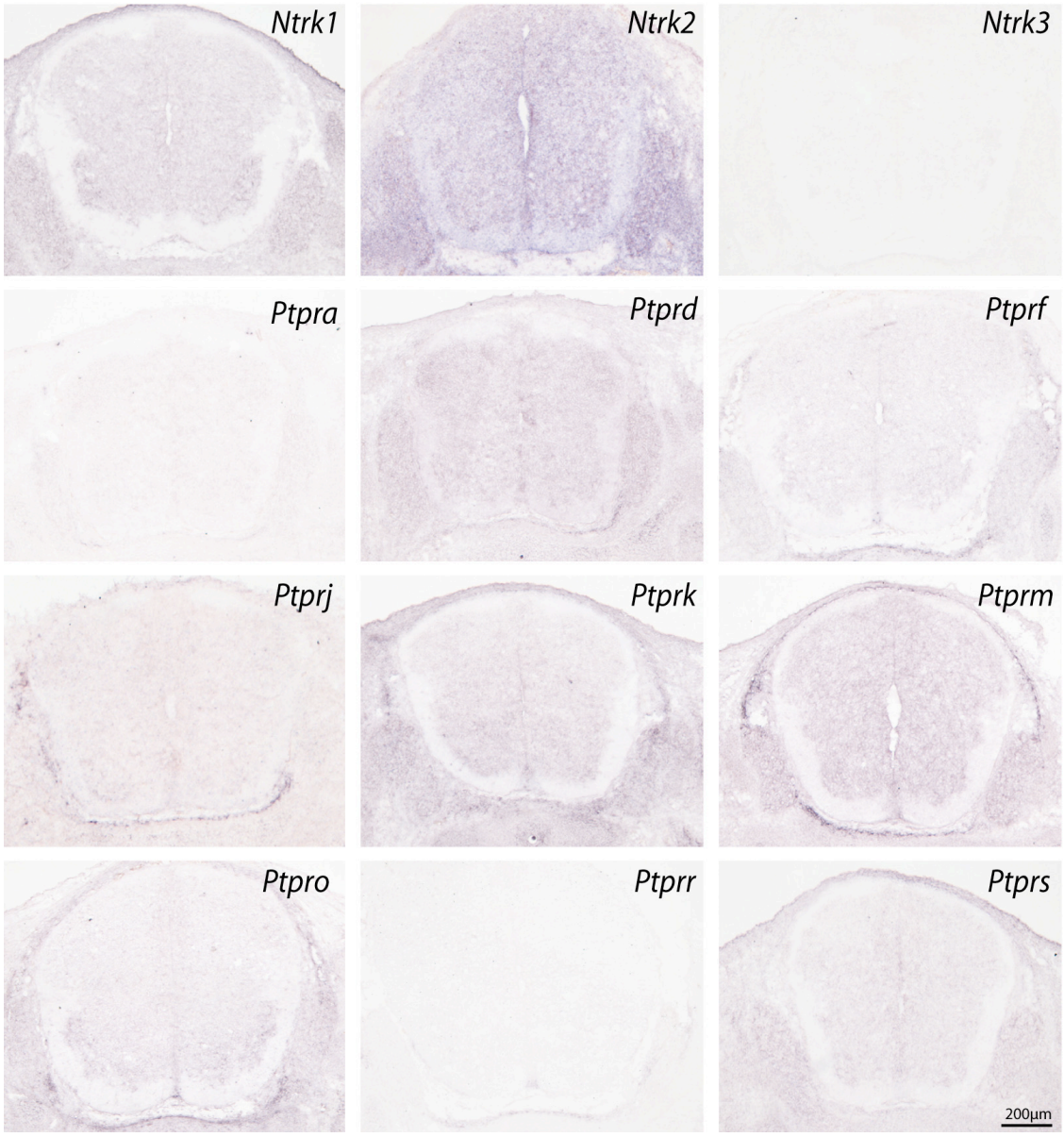

Figure 3. ISH with sense Trk and RPTP riboprobes on transverse E13.5 mouse cryosections.

Pictures with corresponding anti-sense probes are displayed in Figures in chapters 3 and 4.

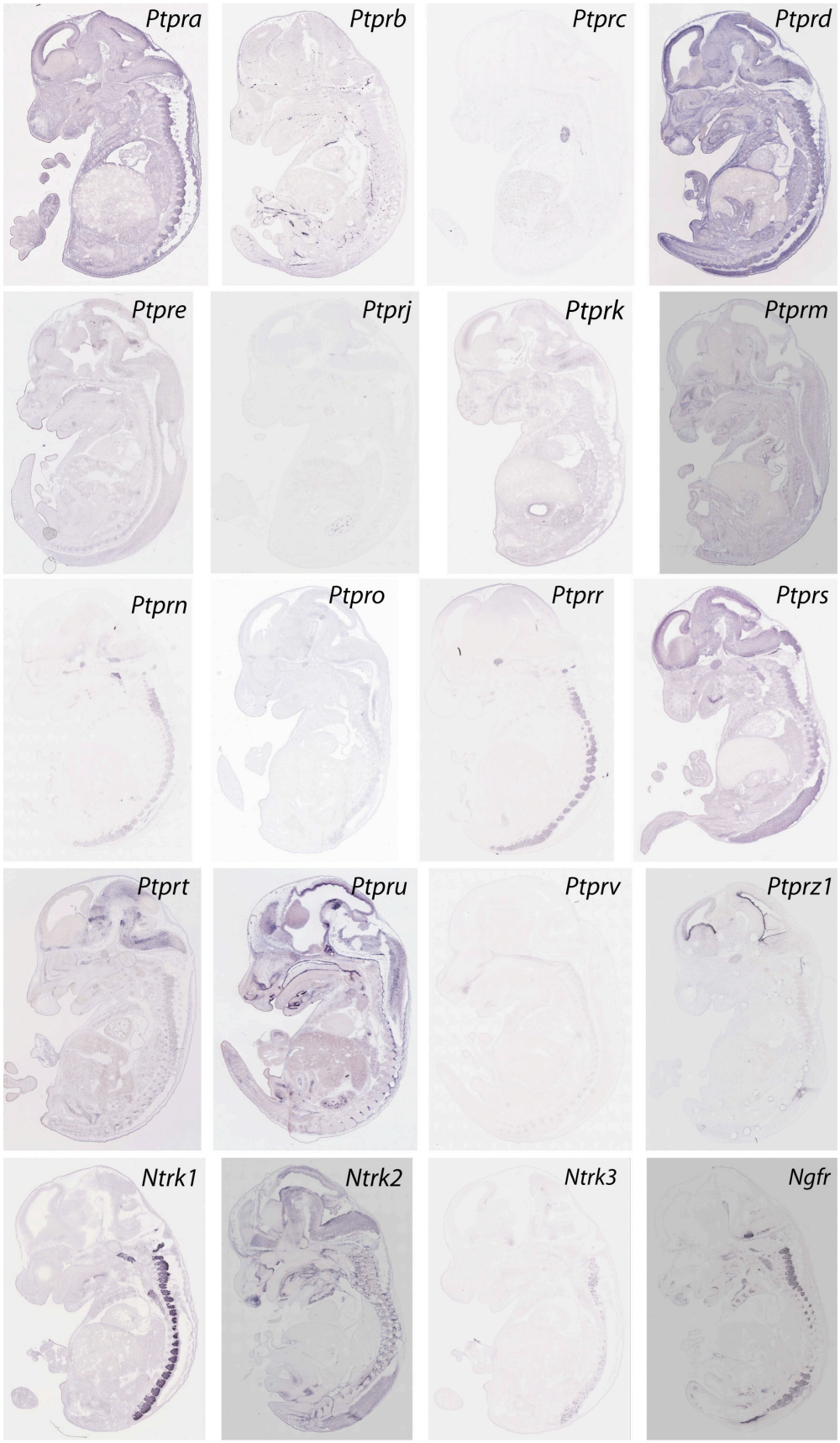

Figure 4. ISH on transverse murine E14.5 embryo sections retrieved from GenePaint databank.

Figures of ISH with RPTP and Trk anti-sense probes on sagittal murine E14.5 embryos were retrieved from the GenePaint database (www.genepaint.org). *Ngfr* = $p75^{NTR}$ gene.

Chapter 4

	TrkA$^+$ neurons	TrkB$^+$ neurons	TrkC$^+$ neurons
IHC	75.2 +/- 12.4% (7236)	6.5 +/- 1.5% (2502)	8.1 +/- 3.3% (2984)
ISH	60.2 +/- 9.7% (1164)	4.5 +/- 1.9% (4454)	9.6 +/- 4% (5297)

Table 2. Percentage of Trk$^+$ neurons in E13.5 mouse DRGs.

Trk$^+$ and DAPI$^+$ neurons were counted on pictures and the mean percentage and SD of unambiguously stained neurons was determined. Total number of neurons counted is included in brackets. Displayed in form of a graph in Figure 4.6.

	Double ISH (DISH)	IHC and ISH
TrkA$^+$ neurons		
TrkA$^+$/TrkB$^+$	1.8+/- 1.5% (805)	1.7 +/- 1.1% (1176)
TrkA$^+$/TrkC$^+$	3.0 +/- 1.0% (526)	3.3 +/- 2.1% (1510)
TrkB$^+$ neurons		
TrkB$^+$/TrkA$^+$	33.3 +/- 13.3% (805)	26.7 +/- 13.1% (1176)
TrkB$^+$/TrkC$^+$	25.0 +/- 6.7% (214)	
TrkC$^+$ neurons		
TrkC$^+$/TrkA$^+$	28.6 +/- 15.3% (526)	26.1 +/- 11.1% (1510)
TrkC$^+$/TrkB$^+$	14.3 +/- 3.9% (214)	

Table 3. Percentage of Trk coexpression in E13.5 mouse DRG neurons.

For calculations Trk$^+$ and DAPI$^+$ neurons were counted on pictures and the mean percentage of neurons unambiguously stained for the Trk receptors was determined. Mean percentage of Trk coexpressing neurons among TrkA$^+$, TrkB$^+$ or TrkC$^+$ neurons and SD were determined for each staining technique separately. Total number of neurons counted is displayed in brackets. Displayed in form of a graph in Figure 4.6.

Ptpra	***Ptprd***	***Ptprf***	***Ptprg***	***Ptpro***	***Ptprr***	***Ptprs***
93.2 +/- 2.2	91.5 +/- 2.6	79.3 +/- 14	88.4 +/- 5.5	12.1 +/- 3.4	65.9 +/- 14	92.1 +/- 5.4
92.5 +/- 1.9	82.1 +/-9.5	95.3 +/- 2.9	94.5 +/- 3	11.9 +/- 1.9	69.6 +/- 6.3	96.7 +/- 0.6
94.5 +/- 3.1	90.6 +/- 6.2	81.6 +/- 7.5	93.7 +/- 6.2	9.3 +/- 2.8	68.9 +/- 9.3	97.2 +/- 1
93.2 +/- 2.2	90.6 +/- 6.2	81.6 +/-7.5	93.7 +/- 5.5	11.9 +/- 2.8	68.9 +/- 9.3	96.7 +/- 1

Table 4. Percentage of RPTP$^+$ neurons in E13.5 mouse DRGs.

Mean percentages and SD of unambiguously stained neurons from coexpression counting and their median (lowest row). Displayed in form of a graph in Figure 4.10.

Trk$^+$/Rptp$^+$ neurons	TrkA$^+$ neurons		TrkB$^+$ neurons		TrkC$^+$ neurons	
TrkX$^+$/Ptpra$^+$	98.2 +/- 2.1%		100%		100%	
Ptpra$^+$ /TrkX$^+$	86.7 +/- 6.1%	(710)	3.5 +/- 0.6%	(502)	11.8 +/- 2%	(567)
Total neurons	80.8 +/- 5.9%		3.2 +/- 0.5%		11.2 +/- 2.1%	
TrkX$^+$/Ptprd$^+$	97.4 +/- 4.5%		74.2 +/- 21.2%		100%	
Ptprd$^+$ /TrkX$^+$	84.0 +/- 7.8%	(924)	2.7 +/- 1.6%	(520)	12.4 +/- 5.5%	(568)
Total neurons	76.8 +/- 7.8%		2.2 +/- 1.3%		11.2 +/- 5%	
TrkX$^+$/Ptprf$^+$	93.3 +/- 3.7%		100%		100%	
Ptprf$^+$ /TrkX$^+$	81.2 +/- 9.7%	(470)	4.3 +/- 0.7%	(389)	7.9 +/- 3.1%	(534)
Total neurons	66.1 +/- 10.6%		4.1 +/- 0.7%		6.3 +/- 2.1%	
TrkX$^+$/Ptprg$^+$	91.0 +/- 4.3%		100%		100%	
Ptprg$^+$ /TrkX$^+$	75.0 +/- 12.5%	(868)	5.0 +/- 1.5%	(479)	4.2 +/- 0.6%	(533)
Total neurons	64 +/- 7.9%		4.7 +/- 1.2%		3.9 +/- 0.7%	
TrkX$^+$/Ptpro$^+$	5.3 +/- 2.4%		99.0 +/- 3%		78.0 +/- 10.9%	
Ptpro$^+$ /TrkX$^+$	28.4 +/- 8.4%	(1373)	56.3 +/- 19%	(996)	48.6 +/- 10.7%	(1184)
Total neurons	3.5 +/- 1.6%		6.5 +/- 1.9%		4.6 +/- 1.7%	
TrkX$^+$/Ptprr$^+$	79.3 +/- 8%		100%		98.7 +/- 4.3%	
Ptprr$^+$ /TrkX$^+$	90.5 +/- 6.9%	(470)	5.6 +/- 2.9%	(282)	15.4 +/- 4.3%	(1244)
Total neurons	59.1 +/- 11.1%		3.8 +/- 1.8%		10.5 +/- 2.7%	
TrkX$^+$/Ptprs$^+$	94.1 +/- 2.2%		100%		100%	
Ptprs$^+$ /TrkX$^+$	77.4 +/- 6.5%	(619)	5 +/- 0.2%	(249)	7.4 +/- 5.8%	(613)
Total neurons	71.2+/- 6.3%		4.8 +/-0.2%		7.3 +/- 5.7%	

Table 5. Percentage of Trk and RPTP coexpressing neurons in E13.5 mouse DRGs.

Trk$^+$, RPTP$^+$ and DAPI$^+$ neurons were counted on pictures and the mean percentage of neurons unambiguously stained for Trk receptors and RPTP genes was determined. Mean percentage of coexpressing neurons among TrkA$^+$, TrkB$^+$ or TrkC$^+$ neurons and SD were determined. Total number of neurons counted is displayed in brackets. A graphical representation of these data can be seen in Figure 4.10.

Chapter 5

MOI		MLV-E	VSVg	MLV-A	RRV	EboZ	gp64	Hanta
25	Total neurons	249	205	189	243	275	331	165
	GFP^+ neurons	218	123	0	1	1	5	0
	Efficiency %	**87.5**	**60**	**0**	**0.4**	**0.4**	**1.5**	**0**
50	Total neurons	272	224	201	187	181		232
	GFP^+ neurons	258	149	0	0	2		0
	Efficiency %	**94.9**	**66.5**	**0**	**0**	**1.1**		**0**
100	Total neurons	224	216	177	217	215	262	187
	GFP^+ neurons	212	172	0	0	2	4	1
	Efficiency %	**94.6**	**79.6**	**0**	**0**	**0.93**	**1.5**	**0.5**

Table 6. Transduction efficiency of seven different lentiviral pseudotypes on murine E13.5 DRG neurons.

HIV1-derived replication deficient eGFP-lentiviruses (pLNT/SFFV-eGFP-WPRE) were pseudotyped with envelop glycoproteins of seven different viruses: Murine Leukaemia Virus – Ecotropic (MLV-E), Vesicular Stomatitis Virus (VSVg), Murine Leukaemia Virus – Amphotropic (MLV-A), Ross River Virus (RRV), Ebola Zaire (EboZ), Baculovirus gp64 (gp64), or Hanta virus. The primary sensory neurons were infected with these pseudotyped lentiviruses at an MOI of 25, 50 and 100. To determine the transduction efficiency 165-330 neurons were counted on pictures using Openlab software. Displayed in Figure 5.2.

Chapter 6

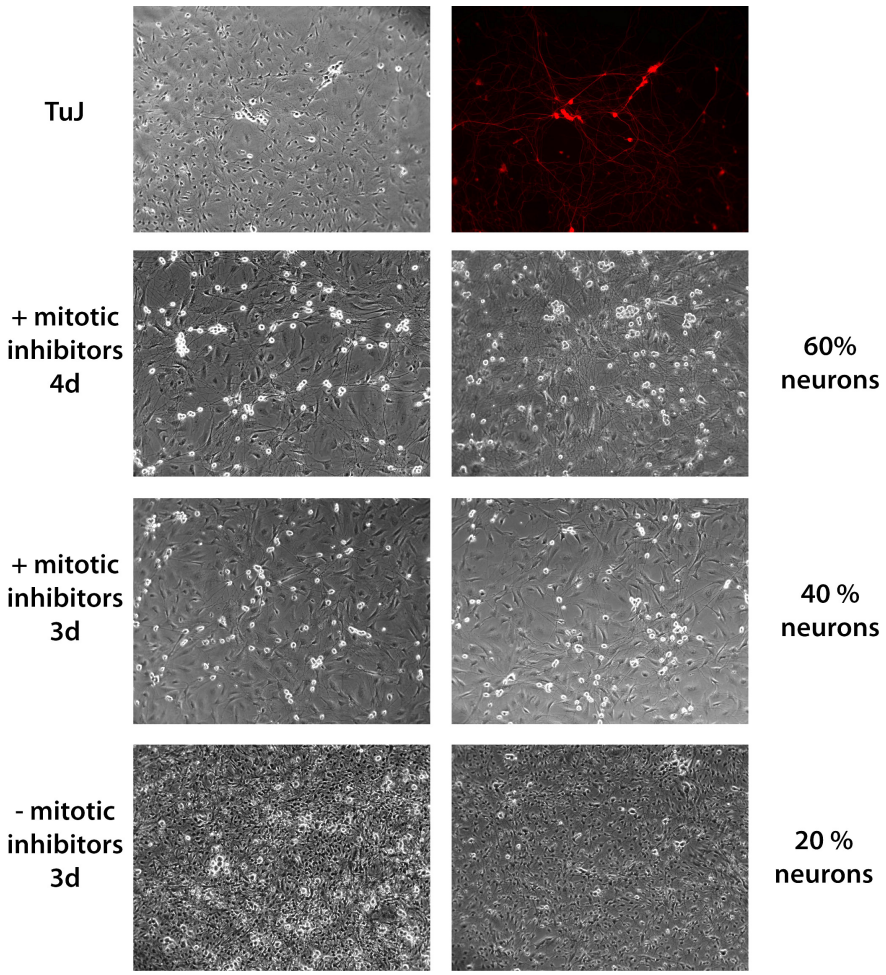

Figure 4. Dissociated murine embryonic DRG cultures with and without mitotic inhibitors.

Dissociated DRG cultures from murine E13.5 embryos were cultured either with mitotic inhibitors floxuridine (FdUrd; 50 mM) and Uridine (150 mM) or without for 3 or 4 days. The amount of neurons and non-neural cells is based on cell counts of 3 to 4 pictures for each condition. Upper panel: ICC on dissociated E13.5 DRG cells with a TuJ antibody, which recognizes β III-tubulin and thus detects all neurons in the mixed cell culture. This was used as a reference to identify the neurons in the cultures.

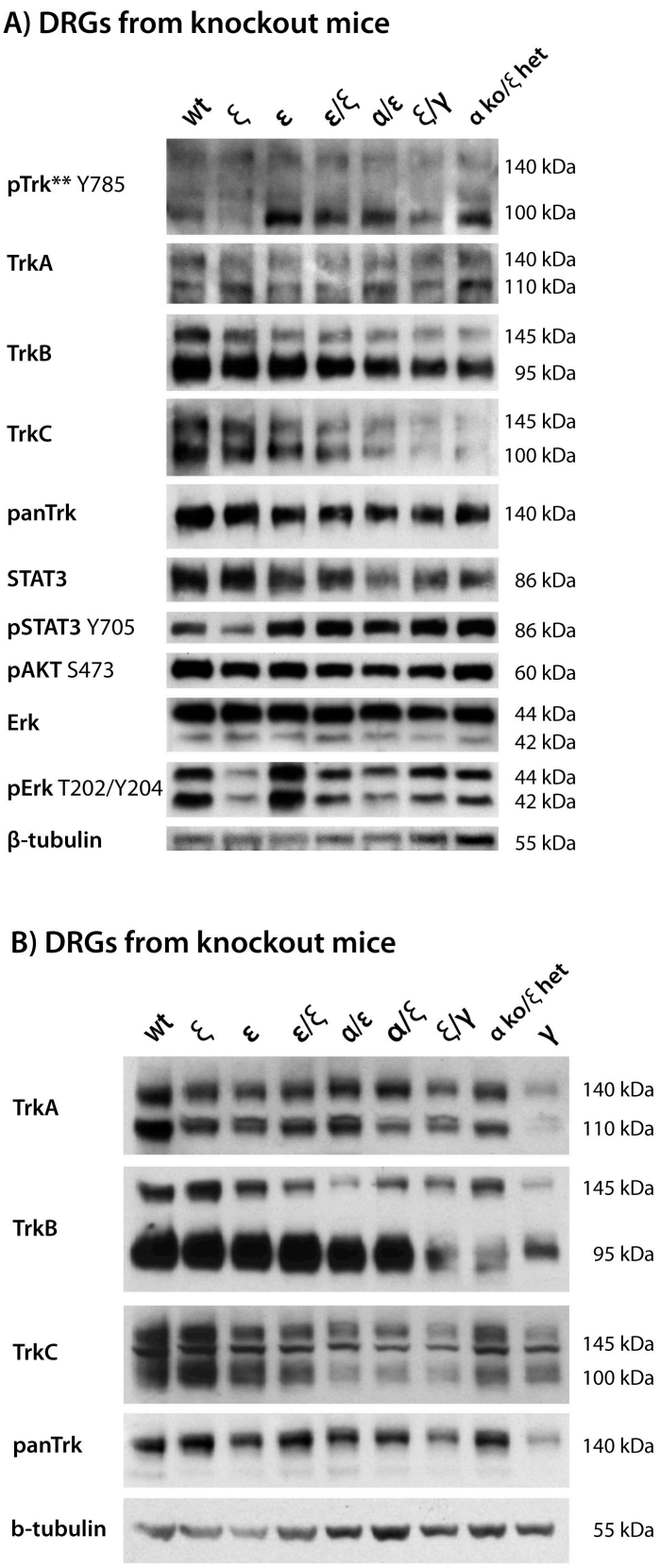

Figure 6. WB on DRG samples from knockout mice.
DRG samples from knockout mice for WB were kindly provided by Dr. Sheilla Harroch.

References

AFFYMETRIX (2005) GeneChip exon array design. Technical note. *Affymetrix, Santa Clara, CA*.

ALBERCH, J., PEREZ-NAVARRO, E. & CANALS, J. M. (2004) Neurotrophic factors in Huntington's disease. *Prog Brain Res,* 146**,** 195-229.

ALDERSON, R. F., ALTERMAN, A. L., BARDE, Y. A. & LINDSAY, R. M. (1990) Brain-derived neurotrophic factor increases survival and differentiated functions of rat septal cholinergic neurons in culture. *Neuron,* 5**,** 297-306.

ALETE, D. E., WEEKS, M. E., HOVANESSION, A. G., HAWADLE, M. & STOKER, A. W. (2006) Cell surface nucleolin on developing muscle is a potential ligand for the axonal receptor protein tyrosine phosphatase-sigma. *Febs J,* 273**,** 4668-81.

ALEXANDER, D. R. (2000) The CD45 tyrosine phosphatase: a positive and negative regulator of immune cell function. *Semin Immunol,* 12**,** 349-59.

ALONSO, A., SASIN, J., BOTTINI, N., FRIEDBERG, I., OSTERMAN, A., GODZIK, A., HUNTER, T., DIXON, J. & MUSTELIN, T. (2004) Protein tyrosine phosphatases in the human genome. *Cell,* 117**,** 699-711.

ANAND, P. (2004) Neurotrophic factors and their receptors in human sensory neuropathies. *Prog Brain Res,* 146**,** 477-92.

ANDERSEN, C. L., JENSEN, J. L. & ORNTOFT, T. F. (2004) Normalization of real-time quantitative reverse transcription-PCR data: a model-based variance estimation approach to identify genes suited for normalization, applied to bladder and colon cancer data sets. *Cancer Res,* 64**,** 5245-50.

APARICIO, L. F., OCRANT, I., BOYLAN, J. M. & GRUPPUSO, P. A. (1992) Protein tyrosine phosphatase activation during nerve growth factor-induced neuronal differentiation of PC12 cells. *Cell Growth Differ,* 3**,** 363-7.

ARBER, S., LADLE, D. R., LIN, J. H., FRANK, E. & JESSELL, T. M. (2000) ETS gene Er81 controls the formation of functional connections between group Ia sensory afferents and motor neurons. *Cell,* 101**,** 485-98.

AREVALO, J. C., WAITE, J., RAJAGOPAL, R., BEYNA, M., CHEN, Z. Y., LEE, F. S. & CHAO, M. V. (2006) Cell survival through Trk neurotrophin receptors is differentially regulated by ubiquitination. *Neuron,* 50**,** 549-59.

AREVALO, J. C., YANO, H., TENG, K. K. & CHAO, M. V. (2004) A unique pathway for sustained neurotrophin signaling through an ankyrin-rich membrane-spanning protein. *Embo J,* 23**,** 2358-68.

ARICESCU, A. R., LU, W. & JONES, E. Y. (2006) A time- and cost-efficient system for high-level protein production in mammalian cells. *Acta Crystallogr D Biol Crystallogr,* 62**,** 1243-50.

ARICESCU, A. R., MCKINNELL, I. W., HALFTER, W. & STOKER, A. W. (2002) Heparan sulfate proteoglycans are ligands for receptor protein tyrosine phosphatase sigma. *Mol Cell Biol,* 22**,** 1881-92.

ARICESCU, A. R., SIEBOLD, C., CHOUDHURI, K., CHANG, V. T., LU, W., DAVIS, S. J., VAN DER MERWE, P. A. & JONES, E. Y. (2007) Structure of a tyrosine phosphatase adhesive interaction reveals a spacer-clamp mechanism. *Science,* 317**,** 1217-20.

ARMANINI, M. P., MCMAHON, S. B., SUTHERLAND, J., SHELTON, D. L. & PHILLIPS, H. S. (1995) Truncated and catalytic isoforms of trkB are co-expressed in neurons of rat and mouse CNS. *Eur J Neurosci,* 7**,** 1403-9.

AUGUSTINE, K. A., SILBIGER, S. M., BUCAY, N., ULIAS, L., BOYNTON, A., TREBASKY, L. D. & MEDLOCK, E. S. (2000) Protein tyrosine phosphatase (PC12, Br7,S1) family: expression characterization in the adult human and mouse. *Anat Rec,* 258**,** 221-34.

AUTSCHBACH, F., PALOU, E., MECHTERSHEIMER, G., ROHR, C., PIROTTO, F., GASSLER, N., OTTO, H. F., SCHRAVEN, B. & GAYA, A. (1999) Expression of the membrane protein tyrosine phosphatase CD148 in human tissues. *Tissue Antigens,* 54**,** 485-98.

BAKER, M. W. & MACAGNO, E. R. (2000) The role of a LAR-like receptor tyrosine phosphatase in growth cone collapse and mutual-avoidance by sibling processes. *J Neurobiol,* 44**,** 194-203.

BAKER, M. W. & MACAGNO, E. R. (2010) Expression levels of a LAR-like receptor protein tyrosine phosphatase correlate with neuronal branching and arbor density in the medicinal leech. *Dev Biol,* 344**,** 346-57.

BAKER, M. W., RAUTH, S. J. & MACAGNO, E. R. (2000) Possible role of the receptor protein tyrosine phosphatase HmLAR2 in interbranch repulsion in a leech embryonic cell. *J Neurobiol,* 45**,** 47-60.

BARBACID, M. (1995a) Neurotrophic factors and their receptors. *Curr Opin Cell Biol,* 7**,** 148-55.

BARBACID, M. (1995b) Structural and functional properties of the TRK family of neurotrophin receptors. *Ann N Y Acad Sci,* 766**,** 442-58.

BARDE, Y. A., EDGAR, D. & THOENEN, H. (1982) Purification of a new neurotrophic factor from mammalian brain. *Embo J,* 1**,** 549-53.

BARKER, P. A., LOMEN-HOERTH, C., GENSCH, E. M., MEAKIN, S. O., GLASS, D. J. & SHOOTER, E. M. (1993) Tissue-specific alternative splicing generates two isoforms of the trkA receptor. *J Biol Chem,* 268**,** 15150-7.

BARR, A. J. & KNAPP, S. (2006) MAPK-specific tyrosine phosphatases: new targets for drug discovery? *Trends Pharmacol Sci,* 27**,** 525-30.

BARR, A. J., UGOCHUKWU, E., LEE, W. H., KING, O. N., FILIPPAKOPOULOS, P., ALFANO, I., SAVITSKY, P., BURGESS-BROWN, N. A., MULLER, S. & KNAPP, S. (2009) Large-scale structural analysis of the classical human protein tyrosine phosphatome. *Cell,* 136**,** 352-63.

BARTON, G. M. & MEDZHITOV, R. (2002) Retroviral delivery of small interfering RNA into primary cells. *Proc Natl Acad Sci U S A,* 99**,** 14943-5.

BATEMAN, J., SHU, H. & VAN VACTOR, D. (2000) The guanine nucleotide exchange factor trio mediates axonal development in the Drosophila embryo. *Neuron,* 26**,** 93-106.

BATT, J., ASA, S., FLADD, C. & ROTIN, D. (2002) Pituitary, pancreatic and gut neuroendocrine defects in protein tyrosine phosphatase-sigma-deficient mice. *Mol Endocrinol,* 16**,** 155-69.

BAUMER, S., KELLER, L., HOLTMANN, A., FUNKE, R., AUGUST, B., GAMP, A., WOLBURG, H., WOLBURG-BUCHHOLZ, K., DEUTSCH, U. & VESTWEBER, D. (2006) Vascular endothelial cell-specific phosphotyrosine phosphatase (VE-PTP) activity is required for blood vessel development. *Blood,* 107**,** 4754-62.

BAXTER, G. T., RADEKE, M. J., KUO, R. C., MAKRIDES, V., HINKLE, B., HOANG, R., MEDINA-SELBY, A., COIT, D., VALENZUELA, P. & FEINSTEIN, S. C. (1997) Signal transduction mediated by the truncated trkB receptor isoforms, trkB.T1 and trkB.T2. *J Neurosci,* 17**,** 2683-90.

BELTRAN, P. J. & BIXBY, J. L. (2003) Receptor protein tyrosine phosphatases as mediators of cellular adhesion. *Front Biosci,* 8**,** D87-99.

BELTRAN, P. J., BIXBY, J. L. & MASTERS, B. A. (2003) Expression of PTPRO during mouse development suggests involvement in axonogenesis and differentiation of NT-3 and NGF-dependent neurons. *J Comp Neurol,* 456**,** 384-95.

BIBEL, M. & BARDE, Y. A. (2000) Neurotrophins: key regulators of cell fate and cell shape in the vertebrate nervous system. *Genes Dev,* 14**,** 2919-37.

BILWES, A. M., DEN HERTOG, J., HUNTER, T. & NOEL, J. P. (1996) Structural basis for inhibition of receptor protein-tyrosine phosphatase-alpha by dimerization. *Nature,* 382**,** 555-9.

BIXBY, J. L. (2001) Ligands and signaling through receptor-type tyrosine phosphatases. *IUBMB Life,* 51**,** 157-63.

BLANCHETOT, C. & DEN HERTOG, J. (2000) Multiple interactions between receptor protein-tyrosine phosphatase (RPTP) alpha and membrane-distal protein-tyrosine phosphatase domains of various RPTPs. *J Biol Chem,* 275**,** 12446-52.

BLANCHETOT, C., TERTOOLEN, L. G. & DEN HERTOG, J. (2002a) Regulation of receptor protein-tyrosine phosphatase alpha by oxidative stress. *Embo J,* 21**,** 493-503.

BLANCHETOT, C., TERTOOLEN, L. G., OVERVOORDE, J. & DEN HERTOG, J. (2002b) Intra- and intermolecular interactions between intracellular domains of receptor protein-tyrosine phosphatases. *J Biol Chem,* 277**,** 47263-9.

BLUME-JENSEN, P. & HUNTER, T. (2001) Oncogenic kinase signalling. *Nature,* 411**,** 355-65.

BODRIKOV, V., LESHCHYNS'KA, I., SYTNYK, V., OVERVOORDE, J., DEN HERTOG, J. & SCHACHNER, M. (2005) RPTPalpha is essential for NCAM-mediated p59fyn activation and neurite elongation. *J Cell Biol,* 168**,** 127-39.

BORGES, L. G., SEIFERT, R. A., GRANT, F. J., HART, C. E., DISTECHE, C. M., EDELHOFF, S., SOLCA, F. F., LIEBERMAN, M. A., LINDNER, V., FISCHER, E. H., LOK, S. & BOWEN-POPE, D. F. (1996) Cloning and characterization of rat density-enhanced phosphatase-1, a protein tyrosine phosphatase expressed by vascular cells. *Circ Res,* 79**,** 570-80.

BRADFORD, M. M. (1976) A rapid and sensitive method for the quantitation of microgram quantities of protein utilizing the principle of protein-dye binding. *Anal Biochem,* 72**,** 248-54.

BRADY-KALNAY, S. M., FLINT, A. J. & TONKS, N. K. (1993) Homophilic binding of PTPμ, a receptor-type protein tyrosine phosphatase, can mediate cell-cell aggregation. *J. Cell Biol.,* 122**,** 961-972.

BRENNAN, C., RIVAS-PLATA, K. & LANDIS, S. C. (1999) The p75 neurotrophin receptor influences NT-3 responsiveness of sympathetic neurons in vivo. *Nat Neurosci,* 2**,** 699-705.

BRODEUR, G. M. (2003) Neuroblastoma: biological insights into a clinical enigma. *Nat Rev Cancer,* 3**,** 203-16.

BUCHMAN, V. L. & DAVIES, A. M. (1993) Different neurotrophins are expressed and act in a developmental sequence to promote the survival of embryonic sensory neurons. *Development,* 118**,** 989-1001.

BUCKLEY, P. F., MAHADIK, S., PILLAI, A. & TERRY, A., JR. (2007) Neurotrophins and schizophrenia. *Schizophr Res,* 94**,** 1-11.

BURDEN-GULLEY, S. M. & BRADY-KALNAY, S. M. (1999) PTPmu Regulates N-Cadherin-dependent Neurite Outgrowth. *J Cell Biol,* 144**,** 1323-1336.

BURDEN-GULLEY, S. M., ENSSLEN, S. E. & BRADY-KALNAY, S. M. (2002) Protein tyrosine phosphatase-mu differentially regulates neurite outgrowth of nasal and temporal neurons in the retina. *J Neurosci,* 22**,** 3615-27.

BURRIDGE, K., SASTRY, S. K. & SALLEE, J. L. (2006) Regulation of cell adhesion by protein tyrosine phosphatases 1. Cell-matrix adhesion. *J Biol Chem*.

CABANTOUS, S., TERWILLIGER, T. C. & WALDO, G. S. (2005) Protein tagging and detection with engineered self-assembling fragments of green fluorescent protein. *Nat Biotechnol,* 23**,** 102-7.

CANOLL, P. D., BARNEA, G., LEVY, J. B., SAP, J., EHRLICH, M., SILVENNOINEN, O., SCHLESSINGER, J. & MUSACCHIO, J. M. (1993) The expression of a novel receptor-type tyrosine phosphatase suggests a role in morphogenesis and plasticity of the nervous system. *Brain Res Dev Brain Res,* 75**,** 293-8.

CANOLL, P. D., MUSACCHIO, J. M., HARDY, R., REYNOLDS, R., MARCHIONNI, M. A. & SALZER, J. L. (1996a) GGF/neuregulin is a neuronal signal that promotes the proliferation and survival and inhibits the differentiation of oligodendrocyte progenitors. *Neuron,* 17**,** 229-43.

CANOLL, P. D., PETANCESKA, S., SCHLESSINGER, J. & MUSACCHIO, J. M. (1996b) Three forms of RPTP-beta are differentially expressed during gliogenesis in the developing rat brain and during glial cell differentiation in culture. *J Neurosci Res,* 44**,** 199-215.

CANTLEY, L. C. & NEEL, B. G. (1999) New insights into tumor suppression: PTEN suppresses tumor formation by restraining the phosphoinositide 3-kinase/AKT pathway. *Proc Natl Acad Sci U S A,* 96**,** 4240-5.

CAPORALI, A. & EMANUELI, C. (2009) Cardiovascular actions of neurotrophins. *Physiol Rev,* 89**,** 279-308.

CARR, V. M. & SIMPSON, S. B., JR. (1978) Proliferative and degenerative events in the early development of chick dorsal root ganglia. I. Normal development. *J Comp Neurol,* 182**,** 727-39.

CHAO, M. V. (2003) Neurotrophins and their receptors: a convergence point for many signalling pathways. *Nat Rev Neurosci,* 4**,** 299-309.

CHEN, B. & BIXBY, J. L. (2005) A novel substrate of receptor tyrosine phosphatase PTPRO is required for nerve growth factor-induced process outgrowth. *J Neurosci,* 25**,** 880-8.

CHEN, B., HAMMONDS-ODIE, L., PERRON, J., MASTERS, B. A. & BIXBY, J. L. (2002) SHP-2 Mediates Target-Regulated Axonal Termination and NGF-Dependent Neurite Growth in Sympathetic Neurons. *Dev Biol,* 252**,** 170-187.

CHEN, C. D., OH, S. Y., HINMAN, J. D. & ABRAHAM, C. R. (2006a) Visualization of APP dimerization and APP-Notch2 heterodimerization in living cells using bimolecular fluorescence complementation. *J Neurochem,* 97**,** 30-43.

CHEN, C. L., BROOM, D. C., LIU, Y., DE NOOIJ, J. C., LI, Z., CEN, C., SAMAD, O. A., JESSELL, T. M., WOOLF, C. J. & MA, Q. (2006b) Runx1 determines nociceptive sensory neuron phenotype and is required for thermal and neuropathic pain. *Neuron,* 49**,** 365-77.

CHEN, Z., SIMMONS, M. S., PERRY, R. T., WIENER, H. W., HARRELL, L. E. & GO, R. C. (2008) Genetic association of neurotrophic tyrosine kinase receptor type 2 (NTRK2) With Alzheimer's disease. *Am J Med Genet B Neuropsychiatr Genet,* 147**,** 363-9.

CHEUNG, A. T., WANG, J., REE, D., KOLLS, J. K. & BRYER-ASH, M. (2000) Tumor necrosis factor-alpha induces hepatic insulin resistance in obese Zucker (fa/fa) rats via interaction of leukocyte antigen-related tyrosine phosphatase with focal adhesion kinase. *Diabetes,* 49**,** 810-9.

CHILTON, J. K. & STOKER, A. W. (2000) Expression of receptor protein tyrosine phosphatases in embryonic chick spinal cord. *Mol Cell Neurosci,* 16**,** 470-80.

CHIN, C. N., SACHS, J. N. & ENGELMAN, D. M. (2005) Transmembrane homodimerization of receptor-like protein tyrosine phosphatases. *FEBS Lett,* 579**,** 3855-8.

CHIRIVI, R. G., DILAVER, G., VAN DE VORSTENBOSCH, R., WANSCHERS, B., SCHEPENS, J., CROES, H., FRANSEN, J. & HENDRIKS, W. (2004) Characterization of multiple transcripts and isoforms derived from the mouse protein tyrosine phosphatase gene Ptprr. *Genes Cells,* 9**,** 919-33.

CHIRIVI, R. G., NOORDMAN, Y. E., VAN DER ZEE, C. E. & HENDRIKS, W. J. (2007) Altered MAP kinase phosphorylation and impaired motor coordination in PTPRR deficient mice. *J Neurochem,* 101**,** 829-40.

CLANDININ, T. R., LEE, C. H., HERMAN, T., LEE, R. C., YANG, A. Y., OVASAPYAN, S. & ZIPURSKY, S. L. (2001) Drosophila LAR regulates R1-R6 and R7 target specificity in the visual system. *Neuron,* 32**,** 237-48.

CLARY, D. O. & REICHARDT, L. F. (1994) An alternatively spliced form of the nerve growth factor receptor TrkA confers an enhanced response to neurotrophin 3. *Proc Natl Acad Sci U S A,* 91**,** 11133-7.

CLARY, D. O., WESKAMP, G., AUSTIN, L. R. & REICHARDT, L. F. (1994) TrkA cross-linking mimics neuronal responses to nerve growth factor. *Mol Biol Cell,* 5**,** 549-63.

COHEN, R. I., MARMUR, R., NORTON, W. T., MEHLER, M. F. & KESSLER, J. A. (1996) Nerve growth factor and neurotrophin-3 differentially regulate the proliferation and survival of developing rat brain oligodendrocytes. *J Neurosci,* 16**,** 6433-42.

COHEN, S. & LEVI-MONTALCINI, R. (1956) A Nerve Growth-Stimulating Factor Isolated from Snake Venom. *Proc Natl Acad Sci U S A,* 42**,** 571-4.

COHEN, S. & LEVI-MONTALCINI, R. (1957) Purification and properties of a nerve growth-promoting factor isolated from mouse sarcoma 180. *Cancer Res,* 17**,** 15-20.

CONOVER, J. C., ERICKSON, J. T., KATZ, D. M., BIANCHI, L. M., POUEYMIROU, W. T., MCCLAIN, J., PAN, L., HELGREN, M., IP, N. Y., BOLAND, P. & ET AL. (1995) Neuronal deficits, not involving motor neurons, in mice lacking BDNF and/or NT4. *Nature,* 375**,** 235-8.

CORBIT, K. C., FOSTER, D. A. & ROSNER, M. R. (1999) Protein kinase Cdelta mediates neurogenic but not mitogenic activation of mitogen-activated protein kinase in neuronal cells. *Mol Cell Biol,* 19**,** 4209-18.

CORDON-CARDO, C., TAPLEY, P., JING, S., NANDURI, V., O'ROURKE, E., LAMBELLE, F., KOVARY, K., KLEIN, R., JONES, K. R., REICHARDT, L. F. & BARBACID, M. (1991) The *trk* tyrosine protein kinase mediates the mitogenic properties of nerve grwoth factor and neurotrophin-3. *Ce;;,* 66**,** 173-183.

CRONIN, J., ZHANG, X. Y. & REISER, J. (2005) Altering the tropism of lentiviral vectors through pseudotyping. *Curr Gene Ther,* 5**,** 387-98.

CULMSEE, C., GERLING, N., LEHMANN, M., NIKOLOVA-KARAKASHIAN, M., PREHN, J. H., MATTSON, M. P. & KRIEGLSTEIN, J. (2002) Nerve growth factor survival signaling in cultured

hippocampal neurons is mediated through TrkA and requires the common neurotrophin receptor P75. *Neuroscience,* 115**,** 1089-108.

CURTIS, R., ADRYAN, K. M., STARK, J. L., PARK, J. S., COMPTON, D. L., WESKAMP, G., HUBER, L. J., CHAO, M. V., JAENISCH, R., LEE, K. F. & ET AL. (1995) Differential role of the low affinity neurotrophin receptor (p75) in retrograde axonal transport of the neurotrophins. *Neuron,* 14**,** 1201-11.

DARNELL, J. E., JR. (1997) STATs and gene regulation. *Science,* 277**,** 1630-5.

DAVIES, A. M. (1987) Molecular and cellular aspects of patterning sensory neurone connections in the vertebrate nervous system. *Development,* 101**,** 185-208.

DAVIES, A. M. (1996) The neurotrophic hypothesis: where does it stand? *Philos Trans R Soc Lond B Biol Sci,* 351**,** 389-94.

DAVIES, A. M., MINICHIELLO, L. & KLEIN, R. (1995) Developmental changes in NT3 signalling via TrkA and TrkB in embryonic neurons. *Embo J,* 14**,** 4482-9.

DEBANT, A., SERRA PAGES, C., SEIPEL, K., O'BRIEN, S., TANG, M., PARK, S. H. & STREULI, M. (1996) The multidomain protein Trio binds the LAR transmembrane tyrosine phosphatase, contains a protein kinase domain, and has separate rac-specific and rho-specific guanine nucleotide exchange factor domains. *Proc Natl Acad Sci U S A,* 93**,** 5466-5471.

DEMAISON, C., PARSLEY, K., BROUNS, G., SCHERR, M., BATTMER, K., KINNON, C., GREZ, M. & THRASHER, A. J. (2002) High-level transduction and gene expression in hematopoietic repopulating cells using a human immunodeficiency [correction of imunodeficiency] virus type 1-based lentiviral vector containing an internal spleen focus forming virus promoter. *Hum Gene Ther,* 13**,** 803-13.

DEN HERTOG, J., GROEN, A. & VAN DER WIJK, T. (2005) Redox regulation of protein-tyrosine phosphatases. *Arch Biochem Biophys,* 434**,** 11-5.

DEN HERTOG, J. & HUNTER, T. (1996) Tight association of GRB2 with receptor protein-tyrosine phosphatase alpha is mediated by the SH2 and C-terminal SH3 domains. *Embo,* 15**,** 3016-3027.

DEN HERTOG, J., OSTMAN, A. & BOHMER, F. D. (2008) Protein tyrosine phosphatases: regulatory mechanisms. *Febs J,* 275**,** 831-47.

DEN HERTOG, J., OVERVOORDE, J. & DE LAAT, S. W. (1996) Expression of receptor protein-tyrosine phosphatase alpha mRNA and protein during mouse embryogenesis. *Mech Dev,* 58**,** 89-101.

DEN HERTOG, J., PALS, C. E., JONK, L. J. & KRUIJER, W. (1992) Differential expression of a novel murine non-receptor protein tyrosine phosphatase during differentiation of P19 embryonal carcinoma cells. *Biochem Biophys Res Commun,* 184**,** 1241-9.

DEN HERTOG, J., PALS, C. E., PEPPELENBOSCH, M. P., TERTOOLEN, L. G., DE LAAT, S. W. & KRUIJER, W. (1993) Receptor protein tyrosine phosphatase alpha activates pp60c-src and is involved in neuronal differentiation. *Embo J,* 12**,** 3789-98.

DEN HERTOG, J., TRACY, S. & HUNTER, T. (1994) Phosphorylation of receptor protein-tyrosine phosphatase alpha on Tyr789, a binding site for the SH3-SH2-SH3 adaptor protein GRB-2 in vivo. *Embo J,* 13**,** 3020-32.

DESAI, C. J., GINDHART, J. G., JR., GOLDSTEIN, L. S. & ZINN, K. (1996) Receptor tyrosine phosphatases are required for motor axon guidance in the Drosophila embryo. *Cell,* 84**,** 599-609.

DESAI, C. J., KRUEGER, N. X., SAITO, H. & ZINN, K. (1997) Competition and cooperation among receptor tyrosine phosphatases control motoneuron growth cone guidance in Drosophila. *Development,* 124**,** 1941-52.

DIAZ-RODRIGUEZ, E., CABRERA, N., ESPARIS-OGANDO, A., MONTERO, J. C. & PANDIELLA, A. (1999) Cleavage of the TrkA neurotrophin receptor by multiple metalloproteases generates signalling-competent truncated forms. *Eur J Neurosci,* 11**,** 1421-30.

DIERSSEN, M., GRATACOS, M., SAHUN, I., MARTIN, M., GALLEGO, X., AMADOR-ARJONA, A., MARTINEZ DE LAGRAN, M., MURTRA, P., MARTI, E., PUJANA, M. A., FERRER, I., DALFO, E., MARTINEZ-CUE, C., FLOREZ, J., TORRES-PERAZA, J. F., ALBERCH, J., MALDONADO, R., FILLAT, C. & ESTIVILL, X. (2006) Transgenic mice overexpressing the full-length neurotrophin receptor TrkC exhibit increased catecholaminergic neuron density in specific brain areas and increased anxiety-like behavior and panic reaction. *Neurobiol Dis,* 24**,** 403-18.

DOUMONT, G., MARTORIATI, A. & MARINE, J. C. (2005) PTPRV is a key mediator of p53-induced cell cycle exit. *Cell Cycle,* 4**,** 1703-5.

DROSOPOULOS, N. E., WALSH, F. S. & DOHERTY, P. (1999) A soluble version of the receptor-like protein tyrosine phosphatase kappa stimulates neurite outgrowth via a Grb2/MEK1-dependent signaling cascade. *Mol. Cell. Neurosci.,* 13**,** 441-9.

DUMAUAL, C. M., SANDUSKY, G. E., CROWELL, P. L. & RANDALL, S. K. (2006) Cellular localization of PRL-1 and PRL-2 gene expression in normal adult human tissues. *J Histochem Cytochem,* 54**,** 1401-12.

DUNAH, A. W., HUESKE, E., WYSZYNSKI, M., HOOGENRAAD, C. C., JAWORSKI, J., PAK, D. T., SIMONETTA, A., LIU, G. & SHENG, M. (2005) LAR receptor protein tyrosine phosphatases in the development and maintenance of excitatory synapses. *Nat Neurosci,* 8**,** 458-67.

DWIVEDI, Y. (2009) Brain-derived neurotrophic factor: role in depression and suicide. *Neuropsychiatr Dis Treat,* 5**,** 433-49.

DYKES, I. M., LANIER, J., ENG, S. R. & TURNER, E. E. (2010) Brn3a regulates neuronal subtype specification in the trigeminal ganglion by promoting Runx expression during sensory differentiation. *Neural Dev,* 5**,** 3.

DYKXHOORN, D. M., NOVINA, C. D. & SHARP, P. A. (2003) Killing the messenger: short RNAs that silence gene expression. *Nat Rev Mol Cell Biol,* 4**,** 457-67.

EGAN, M. F., KOJIMA, M., CALLICOTT, J. H., GOLDBERG, T. E., KOLACHANA, B. S., BERTOLINO, A., ZAITSEV, E., GOLD, B., GOLDMAN, D., DEAN, M., LU, B. & WEINBERGER, D. R. (2003) The BDNF val66met polymorphism affects activity-dependent secretion of BDNF and human memory and hippocampal function. *Cell,* 112**,** 257-69.

EIDE, F. F., VINING, E. R., EIDE, B. L., ZANG, K., WANG, X. Y. & REICHARDT, L. F. (1996) Naturally occurring truncated trkB receptors have dominant inhibitory effects on brain-derived neurotrophic factor signaling. *J Neurosci,* 16**,** 3123-9.

ELCHEBLY, M., WAGNER, J., KENNEDY, T. E., LANCTOT, C., MICHALISZYN, E., ITIE, A., DROUIN, J. & TREMBLAY, M. L. (1999) Neuroendocrine dysplasia in mice lacking protein tyrosine phosphatase sigma. *Nat Genet,* 21**,** 330-3.

ENCINAS, M., TANSEY, M. G., TSUI-PIERCHALA, B. A., COMELLA, J. X., MILBRANDT, J. & JOHNSON, E. M., JR. (2001) c-Src is required for glial cell line-derived neurotrophic factor (GDNF) family ligand-mediated neuronal survival via a phosphatidylinositol-3 kinase (PI-3K)-dependent pathway. *J Neurosci,* 21**,** 1464-72.

ENOKIDO, Y., WYATT, S. & DAVIES, A. M. (1999) Developmental changes in the response of trigeminal neurons to neurotrophins: influence of birthdate and the ganglion environment. *Development,* 126**,** 4365-73.

ENSSLEN, S. E., ROSDAHL, J. A. & BRADY-KALNAY, S. M. (2003) The receptor protein tyrosine phosphatase mu, PTPmu, regulates histogenesis of the chick retina. *Dev Biol,* 264**,** 106-18.

ENSSLEN-CRAIG, S. E. & BRADY-KALNAY, S. M. (2004) Receptor protein tyrosine phosphatases regulate neural development and axon guidance. *Dev Biol,* 275**,** 12-22.

ERICKSON, J. T., CONOVER, J. C., BORDAY, V., CHAMPAGNAT, J., BARBACID, M., YANCOPOULOS, G. & KATZ, D. M. (1996) Mice lacking brain-derived neurotrophic factor exhibit visceral sensory neuron losses distinct from mice lacking NT4 and display a severe developmental deficit in control of breathing. *J Neurosci,* 16**,** 5361-71.

ERNFORS, P., LEE, K. F. & JAENISCH, R. (1994a) Mice lacking brain-derived neurotrophic factor develop with sensory deficits. *Nature,* 368**,** 147-50.

ERNFORS, P., LEE, K. F., KUCERA, J. & JAENISCH, R. (1994b) Lack of neurotrophin-3 leads to deficiencies in the peripheral nervous system and loss of limb proprioceptive afferents. *Cell,* 77**,** 503-12.

ERNFORS, P. & PERSSON, H. (1991) Developmentally regulated expression of HDNF/NT-3 mRNA in rat spinal cord motoneurons and expression of BDNF mRNA in embryonic dorsal root ganglion. *European Journal of Neuroscience,* 3**,** 953-961.

ERNSBERGER, U. (2009) Role of neurotrophin signalling in the differentiation of neurons from dorsal root ganglia and sympathetic ganglia. *Cell Tissue Res,* 336**,** 349-84.

FAGAN, A. M., GARBER, M., BARBACID, M., SILOS-SANTIAGO, I. & HOLTZMAN, D. M. (1997) A role for TrkA during maturation of striatal and basal forebrain cholinergic neurons in vivo. *J Neurosci,* 17**,** 7644-54.

FAN, G., EGLES, C., SUN, Y., MINICHIELLO, L., RENGER, J. J., KLEIN, R., LIU, G. & JAENISCH, R. (2000) Knocking the NT4 gene into the BDNF locus rescues BDNF deficient mice and reveals distinct NT4 and BDNF activities. *Nat Neurosci,* 3**,** 350-7.

FANG, K. S., MARTINS GREEN, M., WILLIAMS, L. T. & HANAFUSA, H. (1996) Characterization of chicken protein tyrosine phosphatase alpha and its expression in the central nervous system. *Brain Res Mol Brain Res,* 37**,** 1-14.

FANG, K. S., SABE, H., SAITO, H. & HANAFUSA, H. (1994) Comparative study of three protein-tyrosine phosphatases. Chicken protein-tyrosine phosphatase lambda dephosphorylates c-Src tyrosine 527. *J Biol Chem,* 269**,** 20194-200.

FARINAS, I. (1999) Neurotrophin actions during the development of the peripheral nervous system. *Microsc Res Tech,* 45**,** 233-42.

FARINAS, I., JONES, K. R., BACKUS, C., WANG, X. Y. & REICHARDT, L. F. (1994) Severe sensory and sympathetic deficits in mice lacking neurotrophin-3. *Nature,* 369**,** 658-61.

FARINAS, I., WILKINSON, G. A., BACKUS, C., REICHARDT, L. F. & PATAPOUTIAN, A. (1998) Characterization of neurotrophin and Trk receptor functions in developing sensory ganglia: direct NT-3 activation of TrkB neurons in vivo. *Neuron,* 21**,** 325-34.

FARINAS, I., YOSHIDA, C. K., BACKUS, C. & REICHARDT, L. F. (1996) Lack of neurotrophin-3 results in death of spinal sensory neurons and premature differentiation of their precursors. *Neuron,* 17**,** 1065-78.

FAUX, C., HAWADLE, M., NIXON, J., WALLACE, A., LEE, S., MURRAY, S. & STOKER, A. (2007) PTPsigma binds and dephosphorylates neurotrophin receptors and can suppress NGF-dependent neurite outgrowth from sensory neurons. *Biochim Biophys Acta,* 1773**,** 1689-700.

FAUX, C., RAKIC, S., ANDREWS, W., YANAGAWA, Y., OBATA, K. & PARNAVELAS, J. G. (2010) Differential gene expression in migrating cortical interneurons during mouse forebrain development. *J Comp Neurol,* 518**,** 1232-48.

FINKBEINER, S. (2000) CREB couples neurotrophin signals to survival messages. *Neuron,* 25**,** 11-4.

FIRE, A., XU, S., MONTGOMERY, M. K., KOSTAS, S. A., DRIVER, S. E. & MELLO, C. C. (1998) Potent and specific genetic interference by double-stranded RNA in Caenorhabditis elegans. *Nature,* 391**,** 806-11.

FOROOGHIAN, F., KOJIC, L., GU, Q. & PRASAD, S. S. (2001) Identification of a novel truncated isoform of trkB in the kitten primary visual cortex. *J Mol Neurosci,* 17**,** 81-8.

FORREST, A. R., TAYLOR, D. F., CROWE, M. L., CHALK, A. M., WADDELL, N. J., KOLLE, G., FAULKNER, G. J., KODZIUS, R., KATAYAMA, S., WELLS, C., KAI, C., KAWAI, J., CARNINCI, P., HAYASHIZAKI, Y. & GRIMMOND, S. M. (2006) Genome-wide review of transcriptional complexity in mouse protein kinases and phosphatases. *Genome Biol,* 7**,** R5.

FOX, A. N. & ZINN, K. (2005) The heparan sulfate proteoglycan syndecan is an in vivo ligand for the Drosophila LAR receptor tyrosine phosphatase. *Curr Biol,* 15**,** 1701-11.

FREI, T., VON BOHLEN UND HALBACH, F., WILLE, W. & SCHACHNER, M. (1992) Different extracellular domains of the neural cell adhesion molecule (N-CAM) are involved in different functions. *J Cell Biol,* 118**,** 177-94.

FRIEDEL, R. H., SCHNURCH, H., STUBBUSCH, J. & BARDE, Y. A. (1997) Identification of genes differentially expressed by nerve growth factor- and neurotrophin-3-dependent sensory neurons. *Proc Natl Acad Sci U S A,* 94**,** 12670-5.

FUCHS, M., WANG, H., CIOSSEK, T., CHEN, Z. & ULLRICH, A. (1998) Differential expression of MAM-subfamily protein tyrosine phosphatases during mouse development. *Mech Dev,* 70**,** 91-109.

FUJIWARA, S., WATANABE, T., NAGATSU, T., GOHDA, J., IMOTO, M. & UMEZAWA, K. (1997) Enhancement or induction of neurite formation by a protein tyrosine phosphatase inhibitor, 3,4-dephostatin, in growth factor-treated PC12h cells. *Biochem Biophys Res Commun,* 238**,** 213-7.

FUNFSCHILLING, U., NG, Y. G., ZANG, K., MIYAZAKI, J., REICHARDT, L. F. & RICE, F. L. (2004) TrkC kinase expression in distinct subsets of cutaneous trigeminal innervation and nonneuronal cells. *J Comp Neurol,* 480**,** 392-414.

GAO, S. P. & BROMBERG, J. F. (2006) Touched and moved by STAT3. *Sci STKE,* 2006**,** pe30.

GAO, W. Q., ZHENG, J. L. & KARIHALOO, M. (1995) Neurotrophin-4/5 (NT-4/5) and brain-derived neurotrophic factor (BDNF) act at later stages of cerebellar granule cell differentiation. *J Neurosci,* 15**,** 2656-67.

GARRITY, P. A., LEE, C. H., SALECKER, I., ROBERTSON, H. C., DESAI, C. J., ZINN, K. & ZIPURSKY, S. L. (1999) Retinal axon target selection in Drosophila is regulated by a receptor protein tyrosine phosphatase. *Neuron,* 22**,** 707-17.

GARWOOD, J., HECK, N., REICHARDT, F. & FAISSNER, A. (2003) Phosphacan short isoform, a novel non-proteoglycan variant of phosphacan/RPTP-beta, interacts with neuronal receptors and promotes neurite outgrowth. *J Biol Chem*.

GASCON, E., GAILLARD, S., MALAPERT, P., LIU, Y., RODAT-DESPOIX, L., SAMOKHVALOV, I. M., DELMAS, P., HELMBACHER, F., MAINA, F. & MOQRICH, A. (2010) Hepatocyte growth factor-Met signaling is required for Runx1 extinction and peptidergic differentiation in primary nociceptive neurons. *J Neurosci,* 30**,** 12414-23.

GENC, B., ULUPINAR, E. & ERZURUMLU, R. S. (2005) Differential Trk expression in explant and dissociated trigeminal ganglion cell cultures. *J Neurobiol,* 64**,** 145-56.

GERLING, N., CULMSEE, C., KLUMPP, S. & KRIEGLSTEIN, J. (2004) The tyrosine phosphatase inhibitor orthovanadate mimics NGF-induced neuroprotective signaling in rat hippocampal neurons. *Neurochem Int,* 44**,** 505-20.

GERSHON, T., BAKER, M., NITABACH, M. & MACAGNO, E. (1998) The leech receptor protein tyrosine phosphatase HmLAR2 is concentrated in growth cones and is involved in process outgrowth. *Development,* 125**,** 1183-90.

GIL-HENN, H., VOLOHONSKY, G., TOLEDANO-KATCHALSKI, H., GANDRE, S. & ELSON, A. (2000) Generation of novel cytoplasmic forms of protein tyrosine phosphatase epsilon by proteolytic processing and translational control. *Oncogene,* 19**,** 4375-84.

GINSBERG, S. D., CHE, S., WUU, J., COUNTS, S. E. & MUFSON, E. J. (2006) Down regulation of trk but not p75NTR gene expression in single cholinergic basal forebrain neurons mark the progression of Alzheimer's disease. *J Neurochem,* 97**,** 475-87.

GINTY, D. D. & SEGAL, R. A. (2002) Retrograde neurotrophin signaling: Trk-ing along the axon. *Curr Opin Neurobiol,* 12**,** 268-74.

GONZALEZ-BRITO, M. R. & BIXBY, J. L. (2009) Protein tyrosine phosphatase receptor type O regulates development and function of the sensory nervous system. *Mol. Cell. Neurosci.,* 42**,** 458-65.

GOODYEAR, R. J., LEGAN, P. K., WRIGHT, M. B., MARCOTTI, W., OGANESIAN, A., COATS, S. A., BOOTH, C. J., KROS, C. J., SEIFERT, R. A., BOWEN-POPE, D. F. & RICHARDSON, G. P. (2003) A receptor-like inositol lipid phosphatase is required for the maturation of developing cochlear hair bundles. *J Neurosci,* 23**,** 9208-19.

GOTZ, R., KOSTER, R., WINKLER, C., RAULF, F., LOTTSPEICH, F., SCHARTL, M. & THOENEN, H. (1994) Neurotrophin-6 is a new member of the nerve growth factor family. *Nature,* 372**,** 266-9.

GRAHAM, F. L., SMILEY, J., RUSSELL, W. C. & NAIRN, R. (1977) Characteristics of a human cell line transformed by DNA from human adenovirus type 5. *J Gen Virol,* 36**,** 59-74.

GRANOT-ATTAS, S., KNOBLER, H. & ELSON, A. (2007) Protein tyrosine phosphatases in osteoclasts. *Crit Rev Eukaryot Gene Expr,* 17**,** 49-71.

GRAVES, D. J., FISCHER, E. H. & KREBS, E. G. (1960) Specificity studies on muscle phosphorylase phosphatase. *J Biol Chem,* 235**,** 805-9.

GRAZIA LAMPUGNANI, M., ZANETTI, A., CORADA, M., TAKAHASHI, T., BALCONI, G., BREVIARIO, F., ORSENIGO, F., CATTELINO, A., KEMLER, R., DANIEL, T. O. & DEJANA, E. (2003) Contact inhibition of VEGF-induced proliferation requires vascular endothelial cadherin, beta-catenin, and the phosphatase DEP-1/CD148. *J Cell Biol,* 161**,** 793-804.

GROSSE, S. M., TAGALAKIS, A. D., MUSTAPA, M. F., ELBS, M., MENG, Q. H., MOHAMMADI, A., TABOR, A. B., HAILES, H. C. & HART, S. L. (2010) Tumor-specific gene transfer with receptor-mediated nanocomplexes modified by polyethylene glycol shielding and endosomally cleavable lipid and peptide linkers. *Faseb J,* 24**,** 2301-13.

GRUMET, M., FRIEDLANDER, D. R. & SAKURAI, T. (1996) Functions of brain chondroitin sulfate proteoglycans during developments: interactions with adhesion molecules. *Perspect Dev Neurobiol,* 3**,** 319-30.

GUITON, M., GUNN-MOORE, F. J., GLASS, D. J., GEIS, D. R., YANCOPOULOS, G. D. & TAVARE, J. M. (1995) Naturally occurring tyrosine kinase inserts block high affinity binding of phospholipase C gamma and Shc to TrkC and neurotrophin-3 signaling. *J Biol Chem,* 270**,** 20384-90.

GUSTAFSON, A. L. & MASON, I. (2000) Expression of receptor tyrosine phosphatase gamma during early development of the chick embryo. *Mech Dev,* 98**,** 183-6.

HAAPASALO, A., KOPONEN, E., HOPPE, E., WONG, G. & CASTREN, E. (2001) Truncated trkB.T1 is dominant negative inhibitor of trkB.TK+-mediated cell survival. *Biochem Biophys Res Commun,* 280**,** 1352-8.

HALLBOOK, F., BACKSTROM, A., KULLANDER, K., KYLBERG, A., WILLIAMS, R. & EBENDAL, T. (1995) Neurotrophins and their receptors in chicken neuronal development. *Int J Dev Biol,* 39**,** 855-68.

HALLBOOK, F., IBANEZ, C. F. & PERSSON, H. (1991) Evolutionary studies of the nerve growth factor family reveal a novel member abundantly expressed in Xenopus ovary. *Neuron,* 6**,** 845-58.

HAMBURGER, V. & LEVI-MONTALCINI, R. (1949) Proliferation, differentiation and degeneration in the spinal ganglia of the chick embryo under normal and experimental conditions. *J Exp Zool,* 111**,** 457-501.

HANANI, M. (2005) Satellite glial cells in sensory ganglia: from form to function. *Brain Res Brain Res Rev,* 48**,** 457-76.

HANANI, M. (2010a) Satellite glial cells in sympathetic and parasympathetic ganglia: in search of function. *Brain Res Rev,* 64**,** 304-27.

HANANI, M. (2010b) Satellite glial cells: more than just 'rings around the neuron'. *Neuron Glia Biol,* 6**,** 1-2.

HANTMAN, A. W. & PERL, E. R. (2005) Molecular and genetic features of a labeled class of spinal substantia gelatinosa neurons in a transgenic mouse. *J Comp Neurol,* 492**,** 90-100.

HAREL, L., COSTA, B. & FAINZILBER, M. (2010) On the death Trk. *Dev Neurobiol,* 70**,** 298-303.

HARRINGTON, R. J., GUTCH, M. J., HENGARTNER, M. O., TONKS, N. K. & CHISHOLM, A. D. (2002) The C. elegans LAR-like receptor tyrosine phosphatase PTP-3 and the VAB-1 Eph receptor tyrosine kinase have partly redundant functions in morphogenesis. *Development,* 129**,** 2141-2153.

HARROCH, S., FURTADO, G. C., BRUECK, W., ROSENBLUTH, J., LAFAILLE, J., CHAO, M., BUXBAUM, J. D. & SCHLESSINGER, J. (2002) A critical role for the protein tyrosine phosphatase receptor type Z in functional recovery from demyelinating lesions. *Nat Genet,* 32**,** 411-4.

HARROCH, S., PALMERI, M., ROSENBLUTH, J., CUSTER, A., OKIGAKI, M., SHRAGER, P., BLUM, M., BUXBAUM, J. D. & SCHLESSINGER, J. (2000) No obvious abnormality in mice deficient in receptor protein tyrosine phosphatase beta [In Process Citation]. *Mol Cell Biol,* 20**,** 7706-15.

HART, S. L., ARANCIBIA-CARCAMO, C. V., WOLFERT, M. A., MAILHOS, C., O'REILLY, N. J., ALI, R. R., COUTELLE, C., GEORGE, A. J., HARBOTTLE, R. P., KNIGHT, A. M., LARKIN, D. F., LEVINSKY, R. J., SEYMOUR, L. W., THRASHER, A. J. & KINNON, C. (1998) Lipid-mediated enhancement of transfection by a nonviral integrin-targeting vector. *Hum Gene Ther,* 9**,** 575-85.

HASHEMI, H., HURLEY, M., GIBSON, A., PANOVA, V., TCHETCHELNITSKI, V., BARR, A. & STOKER, A. W. (2010) Receptor tyrosine phosphatase PTPgamma is a regulator of spinal cord neurogenesis. *Mol. Cell. Neurosci.*

HAWORTH, K., SHU, K. K., STOKES, A., MORRIS, R. & STOKER, A. (1998) The expression of receptor tyrosine phosphatases is responsive to sciatic nerve crush. *Mol. Cell. Neurosci.,* 12**,** 93-104.

HEMPSTEAD, B. L., RABIN, S. J., KAPLAN, L., REID, S., PARADA, L. F. & KAPLAN, D. R. (1992) Overexpression of the trk tyrosine kinase rapidly accelerates nerve growth factor-induced differentiation. *Neuron,* 9**,** 883-96.

HENDRIKS, W., SCHEPENS, J., BRUGMAN, C., ZEEUWEN, P. & WIERINGA, B. (1995) A novel receptor-type protein tyrosine phosphatase with a single catalytic domain is specifically expressed in mouse brain. *Biochem J,* 305 (Pt 2)**,** 499-504.

HENDRIKS, W. J., ELSON, A., HARROCH, S. & STOKER, A. W. (2008) Protein tyrosine phosphatases: functional inferences from mouse models and human diseases. *Febs J,* 275**,** 816-30.

HEPPENSTALL, P. A. & LEWIN, G. R. (2001) BDNF but not NT-4 is required for normal flexion reflex plasticity and function. *Proc Natl Acad Sci U S A,* 98**,** 8107-12.

HERMISTON, M. L., XU, Z. & WEISS, A. (2003) CD45: a critical regulator of signaling thresholds in immune cells. *Annu Rev Immunol,* 21**,** 107-37.

HILTUNEN, J. O., ARUMAE, U., MOSHNYAKOV, M. & SAARMA, M. (1996) Expression of mRNAs for neurotrophins and their receptors in developing rat heart. *Circ Res,* 79**,** 930-9.

HOFER, M., PAGLIUSI, S. R., HOHN, A., LEIBROCK, J. & BARDE, Y. A. (1990) Regional distribution of brain-derived neurotrophic factor mRNA in the adult mouse brain. *Embo J,* 9**,** 2459-64.

HOHN, A., LEIBROCK, J., BAILEY, K. & BARDE, Y. A. (1990) Identification and characterization of a novel member of the nerve growth factor/brain-derived neurotrophic factor family. *Nature,* 344**,** 339-41.

HORVAT, A., SCHWAIGER, F., HAGER, G., BROCKER, F., STREIF, R., KNYAZEV, P., ULLRICH, A. & KREUTZBERG, G. W. (2001) A novel role for protein tyrosine phosphatase shp1 in controlling glial activation in the normal and injured nervous system. *J Neurosci,* 21**,** 865-74.

HORVAT-BROCKER, A., REINHARD, J., ILLES, S., PAECH, T., ZOIDL, G., HARROCH, S., DISTLER, C., KNYAZEV, P., ULLRICH, A. & FAISSNER, A. (2008) Receptor protein tyrosine phosphatases are expressed by cycling retinal progenitor cells and involved in neuronal development of mouse retina. *Neuroscience,* 152**,** 618-45.

HOWER, A. E., BELTRAN, P. J. & BIXBY, J. L. (2009) Dimerization of tyrosine phosphatase PTPRO decreases its activity and ability to inactivate TrkC. *J Neurochem,* 110**,** 1635-47.

HU, C. D., CHINENOV, Y. & KERPPOLA, T. K. (2002) Visualization of interactions among bZIP and Rel family proteins in living cells using bimolecular fluorescence complementation. *Mol Cell,* 9**,** 789-98.

HU, C. D. & KERPPOLA, T. K. (2003) Simultaneous visualization of multiple protein interactions in living cells using multicolor fluorescence complementation analysis. *Nat Biotechnol,* 21**,** 539-45.

HUANG, E. J. & REICHARDT, L. F. (2001) Neurotrophins: roles in neuronal development and function. *Annu Rev Neurosci,* 24**,** 677-736.

HUANG, E. J. & REICHARDT, L. F. (2003) Trk receptors: roles in neuronal signal transduction. *Annu Rev Biochem,* 72**,** 609-42.

HUANG, E. J., WILKINSON, G. A., FARINAS, I., BACKUS, C., ZANG, K., WONG, S. L. & REICHARDT, L. F. (1999) Expression of Trk receptors in the developing mouse trigeminal ganglion: in vivo evidence for NT-3 activation of TrkA and TrkB in addition to TrkC. *Development,* 126**,** 2191-203.

HUNTER, T. & SEFTON, B. M. (1980) Transforming gene product of Rous sarcoma virus phosphorylates tyrosine. *Proc Natl Acad Sci U S A,* 77**,** 1311-5.

HUPPI, K., MARTIN, S. E. & CAPLEN, N. J. (2005) Defining and assaying RNAi in mammalian cells. *Mol Cell,* 17**,** 1-10.

HYMAN, C., HOFER, M., BARDE, Y. A., JUHASZ, M., YANCOPOULOS, G. D., SQUINTO, S. P. & LINDSAY, R. M. (1991) BDNF is a neurotrophic factor for dopaminergic neurons of the substantia nigra. *Nature,* 350**,** 230-2.

HYMAN, C., JUHASZ, M., JACKSON, C., WRIGHT, P., IP, N. Y. & LINDSAY, R. M. (1994) Overlapping and distinct actions of the neurotrophins BDNF, NT-3, and NT-4/5 on cultured dopaminergic and GABAergic neurons of the ventral mesencephalon. *J Neurosci,* 14**,** 335-47.

INAGAKI, N., THOENEN, H. & LINDHOLM, D. (1995) TrkA tyrosine residues involved in NGF-induced neurite outgrowth of PC12 cells. *Eur J Neurosci,* 7**,** 1125-33.

INDO, Y. (2001) Molecular basis of congenital insensitivity to pain with anhidrosis (CIPA): mutations and polymorphisms in TRKA (NTRK1) gene encoding the receptor tyrosine kinase for nerve growth factor. *Hum Mutat,* 18**,** 462-71.

INOUE, K., ITO, K., OSATO, M., LEE, B., BAE, S. C. & ITO, Y. (2007) The transcription factor Runx3 represses the neurotrophin receptor TrkB during lineage commitment of dorsal root ganglion neurons. *J Biol Chem,* 282**,** 24175-84.

INOUE, K., OZAKI, S., SHIGA, T., ITO, K., MASUDA, T., OKADO, N., ISEDA, T., KAWAGUCHI, S., OGAWA, M., BAE, S. C., YAMASHITA, N., ITOHARA, S., KUDO, N. & ITO, Y. (2002) Runx3 controls the axonal projection of proprioceptive dorsal root ganglion neurons. *Nat Neurosci,* 5**,** 946-54.

IP, N. Y., LI, Y., YANCOPOULOS, G. D. & LINDSAY, R. M. (1993) Cultured hippocampal neurons show responses to BDNF, NT-3, and NT-4, but not NGF. *J Neurosci,* 13**,** 3394-405.

IRIE-SASAKI, J., SASAKI, T., MATSUMOTO, W., OPAVSKY, A., CHENG, M., WELSTEAD, G., GRIFFITHS, E., KRAWCZYK, C., RICHARDSON, C. D., AITKEN, K., ISCOVE, N., KORETZKY, G., JOHNSON, P., LIU, P., ROTHSTEIN, D. M. & PENNINGER, J. M. (2001) CD45 is a JAK phosphatase and negatively regulates cytokine receptor signalling. *Nature,* 409**,** 349-54.

IRSHAD, S., PEDLEY, R. B., ANDERSON, J., LATCHMAN, D. S. & BUDHRAM-MAHADEO, V. (2004) The Brn-3b transcription factor regulates the growth, behavior, and invasiveness of human neuroblastoma cells in vitro and in vivo. *J Biol Chem,* 279**,** 21617-27.

JANDT, E., DENNER, K., KOVALENKO, M., OSTMAN, A. & BOHMER, F. D. (2003) The protein-tyrosine phosphatase DEP-1 modulates growth factor-stimulated cell migration and cell-matrix adhesion. *Oncogene,* 22**,** 4175-85.

JARES-ERIJMAN, E. A. & JOVIN, T. M. (2003) FRET imaging. *Nat Biotechnol,* 21**,** 1387-95.

JESSELL, T. M. (2000) Neuronal specification in the spinal cord: inductive signals and transcriptional codes. *Nat Rev Genet,* 1**,** 20-9.

JIANG, G., DEN HERTOG, J. & HUNTER, T. (2000) Receptor-like protein tyrosine phosphatase alpha homodimerizes on the cell surface. *Mol Cell Biol,* 20**,** 5917-29.

JIANG, G., DEN HERTOG, J., SU, J., NOEL, J., SAP, J. & HUNTER, T. (1999) Dimerization inhibits the activity of receptor-like protein-tyrosine phosphatase-alpha. *Nature,* 401**,** 606-10.

JIANG, S., TULLOCH, A. G., KIM, T. A., FU, Y., ROGERS, R., GASKELL, A., WHITE, R. A., AVRAHAM, H. & AVRAHAM, S. (1998) Characterization and chromosomal localization of PTP-NP-2, a new isoform of protein tyrosine phosphatase-like receptor, expressed on synaptic boutons [In Process Citation]. *Gene,* 215**,** 345-59.

JIANG, Y. P., WANG, H., DEUSTACHIO, P., MUSACCHIO, J. M., SCHLESSINGER, J. & SAP, J. (1993) Cloning and characterization of R-PTP-kappa, a new member of the receptor protein tyrosine phosphatase family with a proteolytically cleaved cellular adhesion molecule-like extracellular region. *Molecular and Cellular Biology,* 13**,** 2942-2951.

JOHNSON, D., LANAHAN, A., BUCK, C. R., SEHGAL, A., MORGAN, C., MERCER, E., BOTHWELL, M. & CHAO, M. (1986) Expression and structure of the human NGF receptor. *Cell,* 47**,** 545-54.

JOHNSON, K. G. & HOLT, C. E. (2000) Expression of CRYP-alpha, LAR, PTP-delta, and PTP-rho in the developing Xenopus visual system. *Mech Dev,* 92**,** 291-4.

JOHNSON, K. G., TENNEY, A. P., GHOSE, A., DUCKWORTH, A. M., HIGASHI, M. E., PARFITT, K., MARCU, O., HESLIP, T. R., MARSH, J. L., SCHWARZ, T. L., FLANAGAN, J. G. & VAN VACTOR, D. (2006) The HSPGs Syndecan and Dallylike bind the receptor phosphatase LAR and exert distinct effects on synaptic development. *Neuron,* 49**,** 517-31.

JOHNSON, K. G. & VAN VACTOR, D. (2003) Receptor protein tyrosine phosphatases in nervous system development. *Physiol Rev,* 83**,** 1-24.

JONES, K. R., FARINAS, I., BACKUS, C. & REICHARDT, L. F. (1994) Targeted disruption of the BDNF gene perturbs brain and sensory neuron development but not motor neuron development. *Cell,* 76**,** 989-99.

JONES, K. R. & REICHARDT, L. F. (1990) Molecular cloning of a human gene that is a member of the nerve growth factor family. *Proc Natl Acad Sci U S A,* 87**,** 8060-4.

JULLIEN, J., GUILI, V., DERRINGTON, E. A., DARLIX, J. L., REICHARDT, L. F. & RUDKIN, B. B. (2003) Trafficking of TrkA-green fluorescent protein chimerae during nerve growth factor-induced differentiation. *J Biol Chem,* 278**,** 8706-16.

JUNG, M., RAMANKULOV, A., ROIGAS, J., JOHANNSEN, M., RINGSDORF, M., KRISTIANSEN, G. & JUNG, K. (2007) In search of suitable reference genes for gene expression studies of human renal cell carcinoma by real-time PCR. *BMC Mol Biol,* 8**,** 47.

KAMINKER, J. S., CANON, J., SALECKER, I. & BANERJEE, U. (2002) Control of photoreceptor axon target choice by transcriptional repression of Runt. *Nat Neurosci,* 5**,** 746-50.

KAO, S., JAISWAL, R. K., KOLCH, W. & LANDRETH, G. E. (2001) Identification of the mechanisms regulating the differential activation of the mapk cascade by epidermal growth factor and nerve growth factor in PC12 cells. *J Biol Chem,* 276**,** 18169-77.

KAPLAN, D. & MILLER, F. (2000) Neurotrophin signal transduction in the nervous system. *Current Opinion in Neurobiology,* 10**,** 381-391.

KAPLAN, D. R., HEMPSTEAD, B. L., MARTIN-ZANCA, D., CHAO, M. V. & PARADA, L. F. (1991a) The trk proto-oncogene product: a signal transducing receptor for nerve growth factor. *Science,* 252**,** 554-8.

KAPLAN, D. R., MARTIN-ZANCA, D. & PARADA, L. F. (1991b) Tyrosine phosphorylation and tyrosine kinase activity of the trk proto-oncogene product induced by NGF. *Nature,* 350**,** 158-60.

KAPLAN, D. R. & STEPHENS, R. M. (1994) Neurotrophin signal transduction by the Trk receptor. *J Neurobiol,* 25**,** 1404-17.

KATOH-SEMBA, R., TAKEUCHI, I. K., SEMBA, R. & KATO, K. (1997) Distribution of brain-derived neurotrophic factor in rats and its changes with development in the brain. *J Neurochem,* 69**,** 34-42.

KAUFMANN, N., DEPROTO, J., RANJAN, R., WAN, H. & VAN VACTOR, D. (2002) Drosophila liprin-alpha and the receptor phosphatase Dlar control synapse morphogenesis. *Neuron,* 34**,** 27-38.

KERPPOLA, T. K. (2006) Design and implementation of bimolecular fluorescence complementation (BiFC) assays for the visualization of protein interactions in living cells. *Nat Protoc,* 1**,** 1278-86.

KERPPOLA, T. K. (2008) Bimolecular fluorescence complementation (BiFC) analysis as a probe of protein interactions in living cells. *Annu Rev Biophys,* 37**,** 465-87.

KIKAWA, K. D., VIDALE, D. R., VAN ETTEN, R. L. & KINCH, M. S. (2002) Regulation of the EphA2 kinase by the low molecular weight tyrosine phosphatase induces transformation. *J Biol Chem,* 277**,** 39274-9.

KIM, J. W., CLOSS, E. I., ALBRITTON, L. M. & CUNNINGHAM, J. M. (1991) Transport of cationic amino acids by the mouse ecotropic retrovirus receptor. *Nature,* 352**,** 725-8.

KIM, M., KIM, H. & JHO, E. H. (2010) Identification of ptpro as a novel target gene of Wnt signaling and its potential role as a receptor for Wnt. *FEBS Lett,* 584**,** 3923-8.

KITAMURA, K., MAITI, A., NG, D. H., JOHNSON, P., MAIZEL, A. L. & TAKEDA, A. (1995) Characterization of the interaction between CD45 and CD45-AP. *J Biol Chem,* 270**,** 21151-7.

KLEIN, M., HEMPSTEAD, B. L. & TENG, K. K. (2005) Activation of STAT5-dependent transcription by the neurotrophin receptor Trk. *J Neurobiol,* 63**,** 159-71.

KLEIN, R., CONWAY, D., PARADA, L. F. & BARBACID, M. (1990a) The trkB tyrosine protein kinase gene codes for a second neurogenic receptor that lacks the catalytic kinase domain. *Cell,* 61**,** 647-56.

KLEIN, R., JING, S., NANDURI, V., O'ROURKE, E. & BARBACID, M. (1991a) The trk proto-oncogene encodes a receptor for nerve growth factor. *Cell,* 65**,** 189-197.

KLEIN, R., MARTIN-ZANCA, D., BARBACID, M. & PARADA, L. F. (1990b) Expression of the tyrosine kinase receptor gene *trk*B is confined to the murine embryonic and adult nervous system. *Development,* 109**,** 845-850.

KLEIN, R., NANDURI, V., JING, S. A., LAMBALLE, F., TAPLEY, P., BRYANT, S., CORDON-CARDO, C., JONES, K. R., REICHARDT, L. F. & BARBACID, M. (1991b) The trkB tyrosine protein kinase is a receptor for brain-derived neurotrophic factor and neurotrophin-3. *Cell,* 66**,** 395-403.

KLEIN, R., PARADA, L. F., COULIER, F. & BARBACID, M. (1989) trkB, a novel tyrosine protein kinase receptor expressed during mouse neural development. *Embo J,* 8**,** 3701-9.

KLEIN, R., SILOS-SANTIAGO, I., SMEYNE, R. J., LIRA, S. A., BRAMBILLA, R., BRYANT, S., ZHANG, L., SNIDER, W. D. & BARBACID, M. (1994) Disruption of the neurotrophin-3 receptor gene trkC eliminates la muscle afferents and results in abnormal movements. *Nature,* 368**,** 249-51.

KLEIN, R., SMEYNE, R. J., WURST, W., LONG, L. K., AUERBACH, B. A., JOYNER, A. L. & BARBACID, M. (1993) Targeted disruption of the trkB neurotrophin receptor gene results in nervous system lesions and neonatal death. *Cell,* 75**,** 113-22.

KOLKMAN, M. J., STREIJGER, F., LINKELS, M., BLOEMEN, M., HEEREN, D. J., HENDRIKS, W. J. & VAN DER ZEE, C. E. (2004) Mice lacking leukocyte common antigen-related (LAR) protein tyrosine phosphatase domains demonstrate spatial learning impairment in the two-trial water maze and hyperactivity in multiple behavioural tests. *Behav Brain Res,* 154**,** 171-82.

KOMORI, T., GYOBU, H., UENO, H., KITAMURA, T., SENBA, E. & MORIKAWA, Y. (2008) Expression of kin of irregular chiasm-like 3/mKirre in proprioceptive neurons of the dorsal root ganglia and its interaction with nephrin in muscle spindles. *J Comp Neurol,* 511**,** 92-108.

KOOP, E. A., LOPES, S. M., FEIKEN, E., BLUYSSEN, H. A., VAN DER VALK, M., VOEST, E. E., MUMMERY, C. L., MOOLENAAR, W. H. & GEBBINK, M. F. (2003) Receptor protein tyrosine phosphatase mu expression as a marker for endothelial cell heterogeneity; analysis of RPTPmu gene expression using LacZ knock-in mice. *Int J Dev Biol,* 47**,** 345-54.

KOVALENKO, M., DENNER, K., SANDSTROM, J., PERSSON, C., GROSS, S., JANDT, E., VILELLA, R., BOHMER, F. & OSTMAN, A. (2000) Site-selective dephosphorylation of the platelet-derived growth factor beta-receptor by the receptor-like protein-tyrosine phosphatase DEP-1. *J Biol Chem,* 275**,** 16219-26.

KOZAK, M. (1987) An analysis of 5'-noncoding sequences from 699 vertebrate messenger RNAs. *Nucleic Acids Res,* 15**,** 8125-48.

KRAMER, I., SIGRIST, M., DE NOOIJ, J. C., TANIUCHI, I., JESSELL, T. M. & ARBER, S. (2006) A role for Runx transcription factor signaling in dorsal root ganglion sensory neuron diversification. *Neuron,* 49**,** 379-93.

KRAUSE, D. S., FACKLER, M. J., CIVIN, C. I. & MAY, W. S. (1996) CD34: structure, biology, and clinical utility. *Blood,* 87**,** 1-13.

KREBS, E. G., GRAVES, D. J. & FISCHER, E. H. (1959) Factors affecting the activity of muscle phosphorylase b kinase. *J Biol Chem,* 234**,** 2867-73.

KRUEGER, N. X., VAN VACTOR, D., WAN, H. I., GELBART, W. M., GOODMAN, C. S. & SAITO, H. (1996) The transmembrane tyrosine phosphatase DLAR controls motor axon guidance in Drosophila. *Cell,* 84**,** 611-22.

KUBOSAKI, A., GROSS, S., MIURA, J., SAEKI, K., ZHU, M., NAKAMURA, S., HENDRIKS, W. & NOTKINS, A. L. (2004) Targeted Disruption of the IA-2{beta} Gene Causes Glucose Intolerance and Impairs Insulin Secretion but Does Not Prevent the Development of Diabetes in NOD Mice. *Diabetes,* 53**,** 1684-1691.

KULAS, D. T., GOLDSTEIN, B. J. & MOONEY, R. A. (1996) The transmembrane protein-tyrosine phosphatase LAR modulates signaling by multiple receptor tyrosine kinases. *J Biol Chem,* 271**,** 748-54.

KULAS, D. T., ZHANG, W. R., GOLDSTEIN, B. J., FURLANETTO, R. W. & MOONEY, R. A. (1995) Insulin receptor signaling is augmented by antisense inhibition of the protein tyrosine phosphatase LAR. *J Biol Chem,* 270**,** 2435-8.

KUMANOGOH, H., ASAMI, J., NAKAMURA, S. & INOUE, T. (2008) Balanced expression of various TrkB receptor isoforms from the Ntrk2 gene locus in the mouse nervous system. *Mol. Cell. Neurosci.,* 39**,** 465-77.

KUTNER, R. H., ZHANG, X. Y. & REISER, J. (2009) Production, concentration and titration of pseudotyped HIV-1-based lentiviral vectors. *Nat Protoc,* 4**,** 495-505.

KWON, S. K., WOO, J., KIM, S. Y., KIM, H. & KIM, E. (2010) Trans-synaptic adhesions between netrin-G ligand-3 (NGL-3) and receptor tyrosine phosphatases LAR, protein-tyrosine phosphatase delta (PTPdelta), and PTPsigma via specific domains regulate excitatory synapse formation. *J Biol Chem,* 285**,** 13966-78.

LAFONT, D., ADAGE, T., GRECO, B. & ZARATIN, P. (2009) A novel role for receptor like protein tyrosine phosphatase zeta in modulation of sensorimotor responses to noxious stimuli: evidences from knockout mice studies. *Behav Brain Res,* 201**,** 29-40.

LAI, K. O., FU, W. Y., IP, F. C. & IP, N. Y. (1998) Cloning and expression of a novel neurotrophin, NT-7, from carp. *Mol. Cell. Neurosci.,* 11**,** 64-76.

LAKICS, V., KARRAN, E. H. & BOESS, F. G. (2010) Quantitative comparison of phosphodiesterase mRNA distribution in human brain and peripheral tissues. *Neuropharmacology*.

LAMBALLE, F., KLEIN, R. & BARBACID, M. (1991) trkC, a new member of the trk family of tyrosine protein kinases, is a receptor for neurotrophin-3. *Cell,* 66**,** 967-79.

LAMBALLE, F., SMEYNE, R. J. & BARBACID, M. (1994) Developmental expression of trkC, the neurotrophin-3 receptor, in the mammalian nervous system. *J Neurosci,* 14**,** 14-28.

LAMBALLE, F., TAPLEY, P. & BARBACID, M. (1993) trkC encodes multiple neurotrophin-3 receptors with distinct biological properties and substrate specificities. *Embo J,* 12**,** 3083-94.

LAMMERS, R., BOSSENMAIER, B., COOL, D. E., TONKS, N. K., SCHLESSINGER, J., FISCHER, E. H. & ULLRICH, A. (1993) Differential activities of protein tyrosine phosphatases in intact cells. *J Biol Chem,* 268**,** 22456-62.

LAMPRIANOU, S. & HARROCH, S. (2006) Receptor protein tyrosine phosphatase from stem cells to mature glial cells of the central nervous system. *J Mol Neurosci,* 29**,** 241-55.

LAMPRIANOU, S., VACARESSE, N., SUZUKI, Y., MEZIANE, H., BUXBAUM, J. D., SCHLESSINGER, J. & HARROCH, S. (2006) Receptor protein tyrosine phosphatase gamma is a marker for pyramidal cells and sensory neurons in the nervous system and is not necessary for normal development. *Mol Cell Biol,* 26**,** 5106-19.

LAPORTE, J., BEDEZ, F., BOLINO, A. & MANDEL, J. L. (2003) Myotubularins, a large disease-associated family of cooperating catalytically active and inactive phosphoinositides phosphatases. *Hum Mol Genet,* 12 Spec No 2**,** R285-92.

LARSEN, M., TREMBLAY, M. L. & YAMADA, K. M. (2003) Phosphatases in cell-matrix adhesion and migration. *Nat Rev Mol Cell Biol,* 4**,** 700-11.

LAWSON, S. N. & BISCOE, T. J. (1979) Development of mouse dorsal root ganglia: an autoradiographic and quantitative study. *J Neurocytol,* 8**,** 265-74.

LE DOUARIN, N. M. & KALCHEIM, C. (1999) *The Neural Crest,* Cambridge, Cambridge Univ. Press.

LEDIG, M. M., HAJ, F., BIXBY, J. L., STOKER, A. W. & MUELLER, B. K. (1999a) The receptor tyrosine phosphatase CRYPalpha promotes intraretinal axon growth. *J Cell Biol,* 147**,** 375-88.

LEDIG, M. M., MCKINNELL, I. W., MRSIC-FLOGEL, T., WANG, J., ALVARES, C., MASON, I., BIXBY, J. L., MUELLER, B. K. & STOKER, A. W. (1999b) Expression of receptor tyrosine phosphatases during development of the retinotectal projection of the chick. *J Neurobiol,* 39**,** 81-96.

LEE, F. S. & CHAO, M. V. (2001) Activation of Trk neurotrophin receptors in the absence of neurotrophins. *Proc Natl Acad Sci U S A,* 98**,** 3555-60.

LEE, K. F., DAVIES, A. M. & JAENISCH, R. (1994) p75-deficient embryonic dorsal root sensory and neonatal sympathetic neurons display a decreased sensitivity to NGF. *Development,* 120**,** 1027-33.

LEE, R., KERMANI, P., TENG, K. K. & HEMPSTEAD, B. L. (2001) Regulation of cell survival by secreted proneurotrophins. *Science,* 294**,** 1945-8.

LEE, S., FAUX, C., NIXON, J., ALETE, D., CHILTON, J., HAWADLE, M. & STOKER, A. W. (2007) Dimerization of protein tyrosine phosphatase sigma governs both ligand binding and isoform specificity. *Mol Cell Biol,* 27**,** 1795-808.

LEI, L. & PARADA, L. F. (2007) Transcriptional regulation of Trk family neurotrophin receptors. *Cell Mol Life Sci,* 64**,** 522-32.

LEIBROCK, J., LOTTSPEICH, F., HOHN, A., HOFER, M., HENGERER, B., MASIAKOWSKI, P., THOENEN, H. & BARDE, Y. A. (1989) Molecular cloning and expression of brain-derived neurotrophic factor. *Nature,* 341**,** 149-52.

LEIGHTON, P. A., MITCHELL, K. J., GOODRICH, L. V., LU, X., PINSON, K., SCHERZ, P., SKARNES, W. C. & TESSIER-LAVIGNE, M. (2001) Defining brain wiring patterns and mechanisms through gene trapping in mice. *Nature,* 410**,** 174-9.

LENNON, G., AUFFRAY, C., POLYMEROPOULOS, M. & SOARES, M. B. (1996) The I.M.A.G.E. Consortium: an integrated molecular analysis of genomes and their expression. *Genomics,* 33**,** 151-2.

LESLIE, N. R. & DOWNES, C. P. (2004) PTEN function: how normal cells control it and tumour cells lose it. *Biochem J,* 382**,** 1-11.

LESSMANN, V. (1998) Neurotrophin-dependent modulation of glutamatergic synaptic transmission in the mammalian CNS. *Gen Pharmacol,* 31**,** 667-74.

LEVANON, D., BETTOUN, D., HARRIS-CERRUTI, C., WOOLF, E., NEGREANU, V., EILAM, R., BERNSTEIN, Y., GOLDENBERG, D., XIAO, C., FLIEGAUF, M., KREMER, E., OTTO, F., BRENNER, O., LEV-TOV, A. & GRONER, Y. (2002) The Runx3 transcription factor regulates development and survival of TrkC dorsal root ganglia neurons. *Embo J,* 21**,** 3454-63.

LEVI-MONTALCINI, R. (1952) Effects of mouse tumor transplantation on the nervous system. *Ann N Y Acad Sci,* 55**,** 330-44.

LEVI-MONTALCINI, R. & COHEN, S. (1956) In Vitro and in Vivo Effects of a Nerve Growth-Stimulating Agent Isolated from Snake Venom. *Proc Natl Acad Sci U S A,* 42**,** 695-9.

LEVI-MONTALCINI, R., MEYER, H. & HAMBURGER, V. (1954) In vitro experiments on the effects of mouse sarcomas 180 and 37 on the spinal and sympathetic ganglia of the chick embryo. *Cancer Res,* 14**,** 49-57.

LI, L. & DIXON, J. E. (2000) Form, function, and regulation of protein tyrosine phosphatases and their involvement in human diseases. *Semin Immunol,* 12**,** 75-84.

LI, W., NISHIMURA, R., KASHISHIAN, A., BATZER, A. G., KIM, W. J., COOPER, J. A. & SCHLESSINGER, J. (1994) A new function for a phosphotyrosine phosphatase: linking GRB2-Sos to a receptor tyrosine kinase. *Mol Cell Biol,* 14**,** 509-17.

LIEBL, D. J., TESSAROLLO, L., PALKO, M. E. & PARADA, L. F. (1997) Absence of sensory neurons before target innervation in brain-derived neurotrophic factor-, neurotrophin 3-, and TrkC-deficient embryonic mice. *J Neurosci,* 17**,** 9113-21.

LIEPINSH, E., ILAG, L. L., OTTING, G. & IBANEZ, C. F. (1997) NMR structure of the death domain of the p75 neurotrophin receptor. *Embo J,* 16**,** 4999-5005.

LIM, S. H., KWON, S. K., LEE, M. K., MOON, J., JEONG, D. G., PARK, E., KIM, S. J., PARK, B. C., LEE, S. C., RYU, S. E., YU, D. Y., CHUNG, B. H., KIM, E., MYUNG, P. K. & LEE, J. R. (2009) Synapse formation regulated by protein tyrosine phosphatase receptor T through interaction with cell adhesion molecules and Fyn. *Embo J,* 28**,** 3564-78.

LIN, M. I., DAS, I., SCHWARTZ, G. M., TSOULFAS, P., MIKAWA, T. & HEMPSTEAD, B. L. (2000) Trk C receptor signaling regulates cardiac myocyte proliferation during early heart development in vivo. *Dev Biol,* 226**,** 180-91.

LINDSAY, R. M. (1996) Role of neurotrophins and trk receptors in the development and maintenance of sensory neurons: an overview. *Philos Trans R Soc Lond B Biol Sci,* 351**,** 365-73.

LIU, X., ERNFORS, P., WU, H. & JAENISCH, R. (1995) Sensory but not motor neuron deficits in mice lacking NT4 and BDNF. *Nature,* 375**,** 238-41.

LIU, Y. & MA, Q. (2010) Generation of somatic sensory neuron diversity and implications on sensory coding. *Curr Opin Neurobiol*.

LIVAK, K. J. & SCHMITTGEN, T. D. (2001) Analysis of relative gene expression data using real-time quantitative PCR and the 2(-Delta Delta C(T)) Method. *Methods,* 25**,** 402-8.

LO, K. Y., CHIN, W. H., NG, Y. P., CHENG, A. W., CHEUNG, Z. H. & IP, N. Y. (2005) SLAM-associated protein as a potential negative regulator in Trk signaling. *J Biol Chem,* 280**,** 41744-52.

LOEB, D. M., MARAGOS, J., MARTIN-ZANCA, D., CHAO, M. V., PARADA, L. F. & GREENE, L. A. (1991) The trk proto-oncogene rescues NGF responsiveness in mutant NGF-nonresponsive PC12 cell lines. *Cell,* 66**,** 961-6.

LONGO, F. M., MARTIGNETTI, J. A., LE BEAU, J. M., ZHANG, J. S., BARNES, J. P. & BROSIUS, J. (1993) Leukocyte common antigen-related receptor-linked tyrosine phosphatase. Regulation of mRNA expression. *J Biol Chem,* 268**,** 26503-11.

LOPEZ-GIMENEZ, J. F., CANALS, M., PEDIANI, J. D. & MILLIGAN, G. (2007) The alpha1b-adrenoceptor exists as a higher-order oligomer: effective oligomerization is required for receptor maturation, surface delivery, and function. *Mol Pharmacol,* 71**,** 1015-29.

LORBER, B., BERRY, M., HENDRIKS, W., DEN HERTOG, J., PULIDO, R. & LOGAN, A. (2004) Stimulated regeneration of the crushed adult rat optic nerve correlates with attenuated expression of the protein tyrosine phosphatases RPTPalpha, STEP, and LAR. *Mol Cell Neurosci,* 27**,** 404-16.

LORBER, B., HENDRIKS, W. J., VAN DER ZEE, C. E., BERRY, M. & LOGAN, A. (2005) Effects of LAR and PTP-BL phosphatase deficiency on adult mouse retinal cells activated by lens injury. *Eur J Neurosci,* 21**,** 2375-83.

LU, B., PANG, P. T. & WOO, N. H. (2005) The yin and yang of neurotrophin action. *Nat Rev Neurosci,* 6**,** 603-14.

LYONS, W. E., MAMOUNAS, L. A., RICAURTE, G. A., COPPOLA, V., REID, S. W., BORA, S. H., WIHLER, C., KOLIATSOS, V. E. & TESSAROLLO, L. (1999) Brain-derived neurotrophic factor-deficient mice develop aggressiveness and hyperphagia in conjunction with brain serotonergic abnormalities. *Proc Natl Acad Sci U S A,* 96**,** 15239-44.

MAEDA, N. & NODA, M. (1996) 6B4 proteoglycan/phosphacan is a repulsive substratum but promotes morphological differentiation of cortical neurons. *Development,* 122**,** 647-658.

MAEDA, N. & NODA, M. (1998) Involvement of receptor-like protein tyrosine phosphatase zeta/RPTPbeta and its ligand pleiotrophin/heparin-binding growth-associated molecule (HB-GAM) in neuronal migration. *J Cell Biol,* 142**,** 203-16.

MAGISTRELLI, G., TOMA, S. & ISACCHI, A. (1996) Substitution of two variant residues in the protein tyrosine phosphatase-like PTP35/IA-2 sequence reconstitutes catalytic activity. *Biochem Biophys Res Commun,* 227**,** 581-8.

MAINA, G., ROSSO, G., ZANARDINI, R., BOGETTO, F., GENNARELLI, M. & BOCCHIO-CHIAVETTO, L. (2010) Serum levels of brain-derived neurotrophic factor in drug-naive obsessive-compulsive patients: a case-control study. *J Affect Disord,* 122**,** 174-8.

MAISONPIERRE, P. C., BELLUSCIO, L., FRIEDMAN, B., ALDERSON, R. F., WIEGAND, S. J., FURTH, M. E., LINDSAY, R. M. & YANCOPOULOS, G. D. (1990a) NT-3, BDNF, and NGF in the developing rat nervous system: parallel as well as reciprocal patterns of expression. *Neuron,* 5**,** 501-9.

MAISONPIERRE, P. C., BELLUSCIO, L., SQUINTO, S., IP, N. Y., FURTH, M. E., LINDSAY, R. M. & YANCOPOULOS, G. D. (1990b) Neurotrophin-3: a neurotrophic factor related to NGF and BDNF. *Science,* 247**,** 1446-51.

MAJETI, R., BILWES, A. M., NOEL, J. P., HUNTER, T. & WEISS, A. (1998) Dimerization-induced inhibition of receptor protein tyrosine phosphatase function through an inhibitory wedge. *Science,* 279**,** 88-91.

MAJETI, R. & WEISS, A. (2001) Regulatory mechanisms for receptor protein tyrosine phosphatases. *Chem Rev,* 101**,** 2441-8.

MAJOR, D. L. & BRADY-KALNAY, S. M. (2007) Rho GTPases regulate PTPmu-mediated nasal neurite outgrowth and temporal repulsion of retinal ganglion cell neurons. *Mol. Cell. Neurosci.,* 34**,** 453-67.

MAKKERH, J. P., CENI, C., AULD, D. S., VAILLANCOURT, F., DORVAL, G. & BARKER, P. A. (2005) p75 neurotrophin receptor reduces ligand-induced Trk receptor ubiquitination and delays Trk receptor internalization and degradation. *EMBO Rep,* 6**,** 936-41.

MAKSUMOVA, L., WANG, Y., WONG, N. K., LE, H. T., PALLEN, C. J. & JOHNSON, P. (2007) Differential function of PTPalpha and PTPalpha Y789F in T cells and regulation of PTPalpha phosphorylation at Tyr-789 by CD45. *J Biol Chem,* 282**,** 20925-32.

MALIN, S. A., DAVIS, B. M. & MOLLIVER, D. C. (2007) Production of dissociated sensory neuron cultures and considerations for their use in studying neuronal function and plasticity. *Nat Protoc,* 2**,** 152-60.

MANDAI, K., GUO, T., ST HILLAIRE, C., MEABON, J. S., KANNING, K. C., BOTHWELL, M. & GINTY, D. D. (2009) LIG family receptor tyrosine kinase-associated proteins modulate growth factor signals during neural development. *Neuron,* 63**,** 614-27.

MARGOLIS, R. U. & MARGOLIS, R. K. (1997) Chondroitin sulfate proteoglycans as mediators of axon growth and pathfinding. *Cell Tissue Res,* 290**,** 343-8.

MARMIGERE, F. & ERNFORS, P. (2007) Specification and connectivity of neuronal subtypes in the sensory lineage. *Nat Rev Neurosci,* 8**,** 114-27.

MARMIGERE, F., MONTELIUS, A., WEGNER, M., GRONER, Y., REICHARDT, L. F. & ERNFORS, P. (2006) The Runx1/AML1 transcription factor selectively regulates development and survival of TrkA nociceptive sensory neurons. *Nat Neurosci,* 9**,** 180-7.

MARO, G. S., VERMEREN, M., VOICULESCU, O., MELTON, L., COHEN, J., CHARNAY, P. & TOPILKO, P. (2004) Neural crest boundary cap cells constitute a source of neuronal and glial cells of the PNS. *Nat Neurosci,* 7**,** 930-8.

MARSH, H. N., DUBREUIL, C. I., QUEVEDO, C., LEE, A., MAJDAN, M., WALSH, G. S., HAUSDORFF, S., SAID, F. A., ZOUEVA, O., KOZLOWSKI, M., SIMINOVITCH, K., NEEL, B. G., MILLER, F. D. & KAPLAN, D. R. (2003) SHP-1 negatively regulates neuronal survival by functioning as a TrkA phosphatase. *J Cell Biol,* 163**,** 999-1010.

MARSH, H. N., SCHOLZ, W. K., LAMBALLE, F., KLEIN, R., NANDURI, V., BARBACID, M. & PALFREY, H. C. (1993) Signal transduction events mediated by the BDNF receptor gp 145trkB in primary hippocampal pyramidal cell culture. *J Neurosci,* 13**,** 4281-92.

MARTIN-ZANCA, D., BARBACID, M. & PARADA, L. F. (1990) Expression of the trk proto-oncogene is restricted to the sensory cranial and spinal ganglia of neural crest origin in mouse development. *Genes and Development,* 4**,** 683-694.

MARTIN-ZANCA, D., HUGHES, S. H. & BARBACID, M. (1986) A human oncogene formed by the fusion of truncated tropomyosin and protein tyrosine kinase sequences. *Nature,* 319**,** 743-748.

MARTIN-ZANCA, D., OSKAM, R., MITRA, G., COPELAND, T. & BARBACID, M. (1989) Molecular and biochemical characterization of the human trk proto-oncogene. *Mol Cell Biol,* 9**,** 24-33.

MARX, J. L. (1986) The 1986 Nobel Prize for physiology or medicine. *Science,* 234**,** 543-4.

MAUREL-ZAFFRAN, C., SUZUKI, T., GAHMON, G., TREISMAN, J. E. & DICKSON, B. J. (2001) Cell-Autonomous and -Nonautonomous Functions of LAR in R7 Photoreceptor Axon Targeting. *Neuron,* 32**,** 225-35.

MCLEAN, J., BATT, J., DOERING, L. C., ROTIN, D. & BAIN, J. R. (2002) Enhanced rate of nerve regeneration and directional errors after sciatic nerve injury in receptor protein tyrosine phosphatase sigma knock-out mice. *J Neurosci,* 22**,** 5481-91.

MCMAHON, S. B., ARMANINI, M. P., LING, L. H. & PHILLIPS, H. S. (1994) Expression and coexpression of Trk receptors in subpopulations of adult primary sensory neurons projecting to identified peripheral targets. *Neuron,* 12**,** 1161-71.

MEATHREL, K., ADAMEK, T., BATT, J., ROTIN, D. & DOERING, L. C. (2002) Protein tyrosine phosphatase sigma-deficient mice show aberrant cytoarchitecture and structural abnormalities in the central nervous system. *J Neurosci Res,* 70**,** 24-35.

MEDLEY, Q. G., BUCHBINDER, E. A., TACHIBANA, K., NGO, H., SERRA-PAGES, C. & STREULI, M. (2003) Signaling between the FAK protein tyrosine kinase and Trio. *J Biol Chem*.

MENDROLA, J. M., BERGER, M. B., KING, M. C. & LEMMON, M. A. (2002) The single transmembrane domains of ErbB receptors self-associate in cell membranes. *J Biol Chem,* 277**,** 4704-12.

MENG, K., RODRIGUEZ-PENA, A., DIMITROV, T., CHEN, W., YAMIN, M., NODA, M. & DEUEL, T. F. (2000) Pleiotrophin signals increased tyrosine phosphorylation of beta beta-catenin through inactivation of the intrinsic catalytic activity of the receptor-type protein tyrosine phosphatase beta/zeta. *Proc Natl Acad Sci U S A,* 97**,** 2603-8.

MENN, B., TIMSIT, S., CALOTHY, G. & LAMBALLE, F. (1998) Differential expression of TrkC catalytic and noncatalytic isoforms suggests that they act independently or in association. *J Comp Neurol,* 401**,** 47-64.

MERLIO, J. P., ERNFORS, P., JABER, M. & PERSSON, H. (1992) Molecular cloning of rat trkC and distribution of cells expressing messenger RNAs for members of the trk family in the rat central nervous system. *Neuroscience,* 51**,** 513-32.

MIDDLEMAS, D. S., LINDBERG, R. A. & HUNTER, T. (1991) trkB, a neural receptor protein-tyrosine kinase: evidence for a full-length and two truncated receptors. *Mol Cell Biol,* 11**,** 143-53.

MILEV, P., FRIEDLANDER, D. R., SAKURAI, T., KARTHIKEYAN, L., FLAD, M., MARGOLIS, R. K., GRUMET, M. & MARGOLIS, R. U. (1994) Interactions of the chondroitin sulfate proteoglycan phosphacan, the extracellular domain of a receptor-type protein tyrosine phosphatase, with neurons, glia, and neural cell adhesion molecules. *J Cell Biol,* 127**,** 1703-15.

MILEV, P., MAUREL, P., HARING, M., MARGOLIS, R. K. & MARGOLIS, R. U. (1996) TAG-1/Axonin-1 is a high-affinity ligand of neurocan, phosphacan/protein-tyrosine phosphatase-zeta/beta, and N-CAM. *J Biol Chem,* 271**,** 15716-15723.

MINICHIELLO, L., CALELLA, A. M., MEDINA, D. L., BONHOEFFER, T., KLEIN, R. & KORTE, M. (2002) Mechanism of TrkB-mediated hippocampal long-term potentiation. *Neuron,* 36**,** 121-37.

MINICHIELLO, L., CASAGRANDA, F., TATCHE, R. S., STUCKY, C. L., POSTIGO, A., LEWIN, G. R., DAVIES, A. M. & KLEIN, R. (1998) Point mutation in trkB causes loss of NT4-dependent neurons without major effects on diverse BDNF responses. *Neuron,* 21**,** 335-45.

MINICHIELLO, L. & KLEIN, R. (1996) TrkB and TrkC neurotrophin receptors cooperate in promoting survival of hippocampal and cerebellar granule neurons. *Genes Dev,* 10**,** 2849-58.

MINICHIELLO, L., PIEHL, F., VAZQUEZ, E., SCHIMMANG, T., HOKFELT, T., REPRESA, J. & KLEIN, R. (1995) Differential effects of combined trk receptor mutations on dorsal root ganglion and inner ear sensory neurons. *Development,* 121**,** 4067-75.

MIRANDA, C., FUMAGALLI, T., ANANIA, M. C., VIZIOLI, M. G., PAGLIARDINI, S., PIEROTTI, M. A. & GRECO, A. (2010) Role of STAT3 in in vitro transformation triggered by TRK oncogenes. *PLoS One,* 5**,** e9446.

MIRSKY, R. & JESSEN, K. R. (1999) The neurobiology of Schwann cells. *Brain Pathol,* 9**,** 293-311.

MITTAL, V. (2004) Improving the efficiency of RNA interference in mammals. *Nat Rev Genet,* 5**,** 355-65.

MIZUNO, K., HASEGAWA, K., KATAGIRI, T., OGIMOTO, M., ICHIKAWA, T. & YAKURA, H. (1993) MPTPdelta, a putative murine homolog of HPTPdelta, is expressed in specialized regions of the brain and in the B-cell lineage. *Mol. Cell. Biol.,* 13**,** 5513-5523.

MOFFAT, J., GRUENEBERG, D. A., YANG, X., KIM, S. Y., KLOEPFER, A. M., HINKLE, G., PIQANI, B., EISENHAURE, T. M., LUO, B., GRENIER, J. K., CARPENTER, A. E., FOO, S. Y., STEWART, S. A., STOCKWELL, B. R., HACOHEN, N., HAHN, W. C., LANDER, E. S., SABATINI, D. M. & ROOT, D. E. (2006) A lentiviral RNAi library for human and mouse genes applied to an arrayed viral high-content screen. *Cell,* 124**,** 1283-98.

MOLLER, N. P., MOLLER, K. B., LAMMERS, R., KHARITONENKOV, A., HOPPE, E., WIBERG, F. C., SURES, I. & ULLRICH, A. (1995) Selective down-regulation of the insulin receptor signal by protein-tyrosine phosphatases alpha and epsilon. *J Biol Chem,* 270**,** 23126-31.

MOLLIVER, D. C. & SNIDER, W. D. (1997) Nerve growth factor receptor TrkA is down-regulated during postnatal development by a subset of dorsal root ganglion neurons. *J Comp Neurol,* 381**,** 428-38.

MOLLIVER, D. C., WRIGHT, D. E., LEITNER, M. L., PARSADANIAN, A. S., DOSTER, K., WEN, D., YAN, Q. & SNIDER, W. D. (1997) IB4-binding DRG neurons switch from NGF to GDNF dependence in early postnatal life. *Neuron,* 19**,** 849-61.

MONTGOMERY, A. M., BECKER, J. C., SIU, C. H., LEMMON, V. P., CHERESH, D. A., PANCOOK, J. D., ZHAO, X. & REISFELD, R. A. (1996) Human neural cell adhesion molecule L1 and rat homologue NILE are ligands for integrin alpha v beta 3. *J Cell Biol,* 132**,** 475-85.

MORELL, M., ESPARGARO, A., AVILES, F. X. & VENTURA, S. (2007) Detection of transient protein-protein interactions by bimolecular fluorescence complementation: the Abl-SH3 case. *Proteomics,* 7**,** 1023-36.

MORELL, M., VENTURA, S. & AVILES, F. X. (2009) Protein complementation assays: approaches for the in vivo analysis of protein interactions. *FEBS Lett,* 583**,** 1684-91.

MORRISON, S. J. (2001) Neuronal potential and lineage determination by neural stem cells. *Curr Opin Cell Biol,* 13**,** 666-72.

MOSHNYAKOV, M., ARUMAE, U. & SAARMA, M. (1996) mRNAS for one, two or three members of trk receptor family are expressed in single rat trigeminal ganglion neurons. *Brain Res Mol Brain Res,* 43**,** 141-8.

MU, X., SILOS-SANTIAGO, I., CARROLL, S. L. & SNIDER, W. D. (1993) Neurotrophin receptor genes are expressed in distinct patterns in developing dorsal root ganglia. *J Neurosci,* 13**,** 4029-41.

MUKOUYAMA, Y., KUROYANAGI, H., SHIRASAWA, T., TOMODA, T., SAFFEN, D., OISHI, M. & WATANABE, T. (1997) Induction of protein tyrosine phosphatase epsilon transcripts during NGF-induced neuronal differentiation of PC12D cells and during the development of the cerebellum. *Brain Res Mol Brain Res,* 50**,** 230-6.

MULLOY, J. C., JANKOVIC, V., WUNDERLICH, M., DELWEL, R., CAMMENGA, J., KREJCI, O., ZHAO, H., VALK, P. J., LOWENBERG, B. & NIMER, S. D. (2005) AML1-ETO fusion protein up-regulates TRKA mRNA expression in human CD34+ cells, allowing nerve growth factor-induced expansion. *Proc Natl Acad Sci U S A,* 102**,** 4016-21.

MURAI, K. K., MISNER, D. & RANSCHT, B. (2002) Contactin supports synaptic plasticity associated with hippocampal long-term depression but not potentiation. *Curr Biol,* 12**,** 181-90.

MURATA, Y., MORI, M., KOTANI, T., SUPRIATNA, Y., OKAZAWA, H., KUSAKARI, S., SAITO, Y., OHNISHI, H. & MATOZAKI, T. (2010) Tyrosine phosphorylation of R3 subtype receptor-type protein tyrosine phosphatases and their complex formations with Grb2 or Fyn. *Genes Cells,* 15**,** 513-24.

MUSTELIN, T., COGGESHALL, K. M. & ALTMAN, A. (1989) Rapid activation of the T-cell tyrosine protein kinase pp56^{lck} by the CD45 phosphotyrosine phosphatase. *Proc. Natl. Acad. Sci. USA,* 86**,** 6302-6306.

NAKAGAWA, Y., AOKI, N., AOYAMA, K., SHIMIZU, H., SHIMANO, H., YAMADA, N. & MIYAZAKI, H. (2005) Receptor-Type Protein Tyrosine Phosphatase epsilon (PTPepsilonM) is a Negative Regulator of Insulin Signaling in Primary Hepatocytes and Liver. *Zoolog Sci,* 22**,** 169-75.

NAKAGAWARA, A. (2001) Trk receptor tyrosine kinases: a bridge between cancer and neural development. *Cancer Lett,* 169**,** 107-14.

NAKAMURA, S., SENZAKI, K., YOSHIKAWA, M., NISHIMURA, M., INOUE, K., ITO, Y., OZAKI, S. & SHIGA, T. (2008) Dynamic regulation of the expression of neurotrophin receptors by Runx3. *Development,* 135**,** 1703-11.

NEVES-PEREIRA, M., MUNDO, E., MUGLIA, P., KING, N., MACCIARDI, F. & KENNEDY, J. L. (2002) The brain-derived neurotrophic factor gene confers susceptibility to bipolar disorder: evidence from a family-based association study. *Am J Hum Genet,* 71**,** 651-5.

NG, Y. P., CHEUNG, Z. H. & IP, N. Y. (2006) STAT3 as a downstream mediator of Trk signaling and functions. *J Biol Chem,* 281**,** 15636-44.

NIKOLETOPOULOU, V., LICKERT, H., FRADE, J. M., RENCUREL, C., GIALLONARDO, P., ZHANG, L., BIBEL, M. & BARDE, Y. A. (2010) Neurotrophin receptors TrkA and TrkC cause neuronal death whereas TrkB does not. *Nature,* 467**,** 59-63.

NINKINA, N., ADU, J., FISCHER, A., PINON, L. G., BUCHMAN, V. L. & DAVIES, A. M. (1996) Expression and function of TrkB variants in developing sensory neurons. *Embo J,* 15**,** 6385-93.

NOCKHER, W. A. & RENZ, H. (2006) Neurotrophins in allergic diseases: from neuronal growth factors to intercellular signaling molecules. *J Allergy Clin Immunol,* 117**,** 583-9.

NOORDMAN, Y. E., AUGUSTUS, E. D., SCHEPENS, J. T., CHIRIVI, R. G., RIOS, P., PULIDO, R. & HENDRIKS, W. J. (2008) Multimerisation of receptor-type protein tyrosine phosphatases PTPBR7 and PTP-SL attenuates enzymatic activity. *Biochim Biophys Acta,* 1783**,** 275-86.

O'GRADY, P., THAI, T. C. & SAITO, H. (1998) The laminin-nidogen complex is a ligand for a specific splice isoform of the transmembrane protein tyrosine phosphatase LAR. *J Cell Biol,* 141**,** 1675-84.

OBLANDER, S. A., ENSSLEN-CRAIG, S. E., LONGO, F. M. & BRADY-KALNAY, S. M. (2007) E-cadherin promotes retinal ganglion cell neurite outgrowth in a protein tyrosine phosphatase-mu-dependent manner. *Mol Cell Neurosci,* 34**,** 481-92.

OGATA, M., SAWADA, M., FUJINO, Y. & HAMAOKA, T. (1995) cDNA cloning and characterization of a novel receptor-type protein tyrosine phosphatase expressed predominantly in the brain. *J Biol Chem,* 270**,** 2337-43.

OGATA, M., SAWADA, M., KOSUGI, A. & HAMAOKA, T. (1994) Developmentally regulated expression of a murine receptor-type protein tyrosine phosphatase in the thymus. *J Immunol,* 153**,** 4478-87.

OSTMAN, A. & BOHMER, F. D. (2001) Regulation of receptor tyrosine kinase signaling by protein tyrosine phosphatases. *Trends Cell Biol,* 11**,** 258-66.

OSTMAN, A., HELLBERG, C. & BOHMER, F. D. (2006) Protein-tyrosine phosphatases and cancer. *Nat Rev Cancer,* 6**,** 307-20.

OSTMAN, A., YANG, Q. & TONKS, N. K. (1994) Expression of DEP-1, a receptor-like protein-tyrosine-phosphatase, is enhanced with increasing cell density. *Proc Natl Acad Sci U S A,* 91**,** 9680-4.

PALKA, H. L., PARK, M. & TONKS, N. K. (2003) Hepatocyte Growth Factor Receptor Tyrosine Kinase Met Is a Substrate of the Receptor Protein-tyrosine Phosphatase DEP-1. *J Biol Chem,* 278**,** 5728-5735.

PALKO, M. E., COPPOLA, V. & TESSAROLLO, L. (1999) Evidence for a role of truncated trkC receptor isoforms in mouse development. *J Neurosci,* 19**,** 775-82.

PAP, M. & COOPER, G. M. (1998) Role of glycogen synthase kinase-3 in the phosphatidylinositol 3-Kinase/Akt cell survival pathway. *J Biol Chem,* 273**,** 19929-32.

PAPIN, J. A., HUNTER, T., PALSSON, B. O. & SUBRAMANIAM, S. (2005) Reconstruction of cellular signalling networks and analysis of their properties. *Nat Rev Mol Cell Biol,* 6**,** 99-111.

PATAPOUTIAN, A. & REICHARDT, L. F. (2001) Trk receptors: mediators of neurotrophin action. *Curr Opin Neurobiol,* 11**,** 272-80.

PATTERSON, K. I., BRUMMER, T., O'BRIEN, P. M. & DALY, R. J. (2009) Dual-specificity phosphatases: critical regulators with diverse cellular targets. *Biochem J,* 418**,** 475-89.

PAUL, S. & LOMBROSO, P. J. (2003) Receptor and nonreceptor protein tyrosine phosphatases in the nervous system. *Cell Mol Life Sci,* 60**,** 2465-82.

PERETZ, A., GIL-HENN, H., SOBKO, A., SHINDER, V., ATTALI, B. & ELSON, A. (2000) Hypomyelination and increased activity of voltage-gated K(+) channels in mice lacking protein tyrosine phosphatase epsilon. *Embo J,* 19**,** 4036-45.

PEREZ-PINERA, P., ZHANG, W., CHANG, Y., VEGA, J. A. & DEUEL, T. F. (2007) Anaplastic lymphoma kinase is activated through the pleiotrophin/receptor protein-tyrosine phosphatase beta/zeta signaling pathway: an alternative mechanism of receptor tyrosine kinase activation. *J Biol Chem,* 282**,** 28683-90.

PERSSON, C., SJOBLOM, T., GROEN, A., KAPPERT, K., ENGSTROM, U., HELLMAN, U., HELDIN, C. H., DEN HERTOG, J. & OSTMAN, A. (2004) Preferential oxidation of the second phosphatase domain of receptor-like PTP-alpha revealed by an antibody against oxidized protein tyrosine phosphatases. *Proc Natl Acad Sci U S A,* 101**,** 1886-91.

PETRONE, A., BATTAGLIA, F., WANG, C., DUSA, A., SU, J., ZAGZAG, D., BIANCHI, R., CASACCIA-BONNEFIL, P., ARANCIO, O. & SAP, J. (2003) Receptor protein tyrosine phosphatase alpha is essential for hippocampal neuronal migration and long-term potentiation. *Embo J,* 22**,** 4121-31.

PHILLIPS, H. S. & ARMANINI, M. P. (1996) Expression of the trk family of neurotrophin receptors in developing and adult dorsal root ganglion neurons. *Philos Trans R Soc Lond B Biol Sci,* 351**,** 413-6.

PHILLIPS, H. S., HAINS, J. M., LARAMEE, G. R., ROSENTHAL, A. & WINSLOW, J. W. (1990) Widespread expression of BDNF but not NT3 by target areas of basal forebrain cholinergic neurons. *Science,* 250**,** 290-4.

PILLAI, A. (2008) Brain-derived neurotropic factor/TrkB signaling in the pathogenesis and novel pharmacotherapy of schizophrenia. *Neurosignals,* 16**,** 183-93.

PINTER, A. & FLEISSNER, E. (1979) Structural studies of retroviruses: characterization of oligomeric complexes of murine and feline leukemia virus envelope and core components formed upon cross-linking. *J Virol,* 30**,** 157-65.

PONNIAH, S., WANG, D. Z., LIM, K. L. & PALLEN, C. J. (1999) Targeted disruption of the tyrosine phosphatase PTPalpha leads to constitutive downregulation of the kinases Src and Fyn. *Curr Biol,* 9**,** 535-8.

PRICE, R. D., MILNE, S. A., SHARKEY, J. & MATSUOKA, N. (2007) Advances in small molecules promoting neurotrophic function. *Pharmacol Ther,* 115**,** 292-306.

PRINGLE, N. P., YU, W. P., GUTHRIE, S., ROELINK, H., LUMSDEN, A., PETERSON, A. C. & RICHARDSON, W. D. (1996) Determination of neuroepithelial cell fate: induction of the oligodendrocyte lineage by ventral midline cells and sonic hedgehog. *Dev Biol,* 177**,** 30-42.

PULIDO, R. & HOOFT VAN HUIJSDUIJNEN, R. (2008) Protein tyrosine phosphatases: dual-specificity phosphatases in health and disease. *Febs J,* 275**,** 848-66.

PULIDO, R., ZUNIGA, A. & ULLRICH, A. (1998) PTP-SL and STEP protein tyrosine phosphatases regulate the activation of the extracellular signal-regulated kinases ERK1 and ERK2 by association through a kinase interaction motif. *Embo J,* 17**,** 7337-50.

QIAO, S., IWASHITA, T., FURUKAWA, T., YAMAMOTO, M., SOBUE, G. & TAKAHASHI, M. (2001) Differential effects of leukocyte common antigen-related protein on biochemical and biological activities of RET-MEN2A and RET-MEN2B mutant proteins. *J Biol Chem,* 276**,** 9460-7.

QIU, M. S. & GREEN, S. H. (1991) NGF and EGF rapidly activate p21ras in PC12 cells by distinct, convergent pathways involving tyrosine phosphorylation. *Neuron,* 7**,** 937-46.

QUINONEZ, R. & SUTTON, R. E. (2002) Lentiviral vectors for gene delivery into cells. *DNA Cell Biol,* 21**,** 937-51.

RAFFIONI, S., BRADSHAW, R. A. & BUXSER, S. E. (1993) The receptors for nerve growth factor and other neurotrophins. *Annu Rev Biochem,* 62**,** 823-50.

RAJAGOPAL, R., CHEN, Z. Y., LEE, F. S. & CHAO, M. V. (2004) Transactivation of Trk neurotrophin receptors by G-protein-coupled receptor ligands occurs on intracellular membranes. *J Neurosci,* 24**,** 6650-8.

RASHID-DOUBELL, F., MCKINNELL, I., ARICESCU, A. R., SAJNANI, G. & STOKER, A. (2002) Chick PTPsigma regulates the targeting of retinal axons within the optic tectum. *J Neurosci,* 22**,** 5024-33.

RATCLIFFE, C. F., QU, Y., MCCORMICK, K. A., TIBBS, V. C., DIXON, J. E., SCHEUER, T. & CATTERALL, W. A. (2000) A sodium channel signaling complex: modulation by associated receptor protein tyrosine phosphatase beta. *Nat Neurosci,* 3**,** 437-44.

RAUGEI, G., RAMPONI, G. & CHIARUGI, P. (2002) Low molecular weight protein tyrosine phosphatases: small, but smart. *Cell Mol Life Sci,* 59**,** 941-9.

REF.1 http://www.sigmaaldrich.com/life-science/functional-genomics-and-rnai/shrna/library-information.html#Citing. Mission TRC shRNA constructs (Sigma).

REF.2 http://www.broadinstitute.org/genome_bio/trc/rules.html.

REF.3 http://www.broadinstitute.org/genome_bio/trc/protocols/InterferonResponse.pdf.

REICHARDT, L. F. (2006) Neurotrophin-regulated signalling pathways. *Philos Trans R Soc Lond B Biol Sci,* 361**,** 1545-64.

REINHARDT, R. R., CHIN, E., ZHANG, B., ROTH, R. A. & BONDY, C. A. (1994) Selective coexpression of insulin receptor-related receptor (IRR) and TRK in NGF-sensitive neurons. *J Neurosci,* 14**,** 4674-83.

REMY, I., WILSON, I. A. & MICHNICK, S. W. (1999) Erythropoietin receptor activation by a ligand-induced conformation change. *Science,* 283**,** 990-3.

RIBASES, M., GRATACOS, M., ARMENGOL, L., DE CID, R., BADIA, A., JIMENEZ, L., SOLANO, R., VALLEJO, J., FERNANDEZ, F. & ESTIVILL, X. (2003) Met66 in the brain-derived neurotrophic factor (BDNF) precursor is associated with anorexia nervosa restrictive type. *Mol Psychiatry,* 8**,** 745-51.

RIBASES, M., GRATACOS, M., BADIA, A., JIMENEZ, L., SOLANO, R., VALLEJO, J., FERNANDEZ-ARANDA, F. & ESTIVILL, X. (2005) Contribution of NTRK2 to the genetic susceptibility to anorexia nervosa, harm avoidance and minimum body mass index. *Mol Psychiatry,* 10**,** 851-60.

RIFKIN, J. T., TODD, V. J., ANDERSON, L. W. & LEFCORT, F. (2000) Dynamic expression of neurotrophin receptors during sensory neuron genesis and differentiation. *Dev Biol,* 227**,** 465-80.

RIOS, M., FAN, G., FEKETE, C., KELLY, J., BATES, B., KUEHN, R., LECHAN, R. M. & JAENISCH, R. (2001) Conditional deletion of brain-derived neurotrophic factor in the postnatal brain leads to obesity and hyperactivity. *Mol Endocrinol,* 15**,** 1748-57.

ROBINSON, D. R., WU, Y. M. & LIN, S. F. (2000) The protein tyrosine kinase family of the human genome. *Oncogene,* 19**,** 5548-57.

ROGERS, M. V., BUENSUCESO, C., MONTAGUE, F. & MAHADEVAN, L. (1994) Vanadate stimulates differentiation and neurite outgrowth in rat pheochromocytoma PC12 cells and neurite extension in human neuroblastoma SH-SY5Y cells. *Neuroscience,* 60**,** 479-494.

ROOSEN, A., SCHOBER, A., STRELAU, J., BOTTNER, M., FAULHABER, J., BENDNER, G., MCILWRATH, S. L., SELLER, H., EHMKE, H., LEWIN, G. R. & UNSICKER, K. (2001) Lack of neurotrophin-4 causes selective structural and chemical deficits in sympathetic ganglia and their preganglionic innervation. *J Neurosci,* 21**,** 3073-84.

ROSENTHAL, A., GOEDDEL, D. V., NGUYEN, T., LEWIS, M., SHIH, A., LARAMEE, G. R., NIKOLICS, K. & WINSLOW, J. W. (1990) Primary structure and biological activity of a novel human neurotrophic factor. *Neuron,* 4**,** 767-73.

SACCO, F., TINTI, M., PALMA, A., FERRARI, E., NARDOZZA, A. P., HOOFT VAN HUIJSDUIJNEN, R., TAKAHASHI, T., CASTAGNOLI, L. & CESARENI, G. (2009) Tumor suppressor density-enhanced phosphatase-1 (DEP-1) inhibits the RAS pathway by direct dephosphorylation of ERK1/2 kinases. *J Biol Chem,* 284**,** 22048-58.

SAEKI, K., ZHU, M., KUBOSAKI, A., XIE, J., LAN, M. S. & NOTKINS, A. L. (2002) Targeted disruption of the protein tyrosine phosphatase-like molecule IA-2 results in alterations in glucose tolerance tests and insulin secretion. *Diabetes,* 51**,** 1842-50.

SAHIN, M., DOWLING, J. J. & HOCKFIELD, S. (1995) Seven protein tyrosine phosphatases are differentially expressed in the developing rat brain. *J Comp Neurol,* 351**,** 617-31.

SAJNANI-PEREZ, G., CHILTON, J. K., ARICESCU, A. R., HAJ, F. & STOKER, A. W. (2003) Isoform-specific binding of the tyrosine phosphatase PTPsigma to a ligand in developing muscle. *Mol. Cell. Neurosci.,* 22**,** 37-48.

SALLEE, J. L., WITTCHEN, E. S. & BURRIDGE, K. (2006) Regulation of cell adhesion by protein tyrosine phosphatases 2. Cell-cell adhesion. *J Biol Chem*.

SALTER, M. W. & WANG, Y. T. (2000) Sodium channels develop a tyrosine phosphatase complex. *Nat Neurosci,* 3**,** 417-9.

SAMBROOK, J., FRITSCH, E. F. & MANIATIS, T. (1989) *Molecular cloning: a laboratory manual,* Cold Spring Harbor, NY, Cold Spring Harbor Press.

SANDY, P., VENTURA, A. & JACKS, T. (2005) Mammalian RNAi: a practical guide. *Biotechniques,* 39**,** 215-24.

SAPIEHA, P. S., DUPLAN, L., UETANI, N., JOLY, S., TREMBLAY, M. L., KENNEDY, T. E. & DI POLO, A. (2005) Receptor protein tyrosine phosphatase sigma inhibits axon regrowth in the adult injured CNS. *Mol Cell Neurosci,* 28**,** 625-35.

SCHAAPVELD, R. Q., SCHEPENS, J. T., BACHNER, D., ATTEMA, J., WIERINGA, B., JAP, P. H. & HENDRIKS, W. J. (1998) Developmental expression of the cell adhesion molecule-like protein tyrosine phosphatases LAR, RPTPdelta and RPTPsigma in the mouse. *Mech Dev,* 77**,** 59-62.

SCHAAPVELD, R. Q., VAN DEN MAAGDENBERG, A. M., SCHEPENS, J. T., WEGHUIS, D. O., GEURTS VAN KESSEL, A., WIERINGA, B. & HENDRIKS, W. J. (1995) The mouse gene Ptprf encoding the leukocyte common antigen-related molecule LAR: cloning, characterization, and chromosomal localization. *Genomics,* 27**,** 124-30.

SCHAEREN-WIEMERS, N. & GERFIN-MOSER, A. (1993) A single protocol to detect transcripts of various types and expression levels in neural tissue and cultured cells: in situ hybridization using digoxigenin-labelled cRNA probes. *Histochemistry,* 100**,** 431-40.

SCHAMBACH, A., GALLA, M., MODLICH, U., WILL, E., CHANDRA, S., REEVES, L., COLBERT, M., WILLIAMS, D. A., VON KALLE, C. & BAUM, C. (2006) Lentiviral vectors pseudotyped with murine ecotropic envelope: increased biosafety and convenience in preclinical research. *Exp Hematol,* 34**,** 588-92.

SCHLESSINGER, J. (2000) Cell signaling by receptor tyrosine kinases. *Cell,* 103**,** 211-25.

SCHLESSINGER, J. & ULLRICH, A. (1992) Growth factor signaling by receptor tyrosine kinases. *Neuron,* 9**,** 383-91.

SCHMITTGEN, T. D., LEE, E. J. & JIANG, J. (2008) High-throughput real-time PCR. *Methods Mol Biol,* 429**,** 89-98.

SCHMITTGEN, T. D. & LIVAK, K. J. (2008) Analyzing real-time PCR data by the comparative C(T) method. *Nat Protoc,* 3**,** 1101-8.

SCHMITTGEN, T. D. & ZAKRAJSEK, B. A. (2000) Effect of experimental treatment on housekeeping gene expression: validation by real-time, quantitative RT-PCR. *J Biochem Biophys Methods,* 46**,** 69-81.

SCHNEIDER, M. B., STANDOP, J., ULRICH, A., WITTEL, U., FRIESS, H., ANDREN-SANDBERG, A. & POUR, P. M. (2001) Expression of nerve growth factors in pancreatic neural tissue and pancreatic cancer. *J Histochem Cytochem,* 49**,** 1205-10.

SCHRAMM, A., SCHULTE, J. H., ASTRAHANTSEFF, K., APOSTOLOV, O., LIMPT, V., SIEVERTS, H., KUHFITTIG-KULLE, S., PFEIFFER, P., VERSTEEG, R. & EGGERT, A. (2005) Biological effects of TrkA and TrkB receptor signaling in neuroblastoma. *Cancer Lett,* 228**,** 143-53.

SCHRAVEN, B. (2000) Cd148. *J Biol Regul Homeost Agents,* 14**,** 220-2.

SCIARRETTA, C., FRITZSCH, B., BEISEL, K., ROCHA-SANCHEZ, S. M., BUNIELLO, A., HORN, J. M. & MINICHIELLO, L. (2010) PLCgamma-activated signalling is essential for TrkB mediated sensory neuron structural plasticity. *BMC Dev Biol,* 10**,** 103.

SCOTT, S. A. (1992) *Sensory Neurons: Diversity, Development and Plasticity.,* New York/Oxford, Oxford Univ. Press.

SEGAL, R. A., BHATTACHARYYA, A., RUA, L. A., ALBERTA, J. A., STEPHENS, R. M., KAPLAN, D. R. & STILES, C. D. (1996) Differential utilization of Trk autophosphorylation sites. *J Biol Chem,* 271**,** 20175-81.

SEGAL, R. A., GOUMNEROVA, L. C., KWON, Y. K., STILES, C. D. & POMEROY, S. L. (1994) Expression of the neurotrophin receptor TrkC is linked to a favorable outcome in medulloblastoma. *Proc Natl Acad Sci U S A,* 91**,** 12867-71.

SEGAL, R. A. & GREENBERG, M. E. (1996) Intracellular signaling pathways activated by neurotrophic factors. *Annu Rev Neurosci,* 19**,** 463-89.

SEKAR, R. B. & PERIASAMY, A. (2003) Fluorescence resonance energy transfer (FRET) microscopy imaging of live cell protein localizations. *J Cell Biol,* 160**,** 629-33.

SEN, S., NESSE, R. M., STOLTENBERG, S. F., LI, S., GLEIBERMAN, L., CHAKRAVARTI, A., WEDER, A. B. & BURMEISTER, M. (2003) A BDNF coding variant is associated with the NEO personality inventory domain neuroticism, a risk factor for depression. *Neuropsychopharmacology,* 28**,** 397-401.

SERRA-PAGES, C., MEDLEY, Q. G., TANG, M., HART, A. & STREULI, M. (1998) Liprins, a family of LAR transmembrane protein-tyrosine phosphatase- interacting proteins. *J Biol Chem,* 273**,** 15611-20.

SHARMA, E. & LOMBROSO, P. J. (1995) A neuronal protein tyrosine phosphatase induced by nerve growth factor. *J Biol Chem,* 270**,** 49-53.

SHELTON, D. L. & REICHARDT, L. F. (1984) Expression of the beta-nerve growth factor gene correlates with the density of sympathetic innervation in effector organs. *Proc Natl Acad Sci U S A,* 81**,** 7951-5.

SHEN, P., CANOLL, P. D., SAP, J. & MUSACCHIO, J. M. (1999) Expression of a truncated receptor protein tyrosine phosphatase kappa in the brain of an adult transgenic mouse. *Brain Res,* 826**,** 157-71.

SHEN, Y., TENNEY, A. P., BUSCH, S. A., HORN, K. P., CUASCUT, F. X., LIU, K., HE, Z., SILVER, J. & FLANAGAN, J. G. (2009) PTPsigma is a receptor for chondroitin sulfate proteoglycan, an inhibitor of neural regeneration. *Science,* 326**,** 592-6.

SHINTANI, T., IHARA, M., SAKUTA, H., TAKAHASHI, H., WATAKABE, I. & NODA, M. (2006) Eph receptors are negatively controlled by protein tyrosine phosphatase receptor type O. *Nat Neurosci,* 9**,** 761-9.

SHINTANI, T., MAEDA, N. & NODA, M. (2001) Receptor-Like Protein Tyrosine Phosphatase gamma (RPTPgamma), But Not PTPzeta/RPTPbeta, Inhibits Nerve-Growth-Factor-Induced Neurite Outgrowth in PC12D Cells. *Dev Neurosci,* 23**,** 55-69.

SHINTANI, T. & NODA, M. (2008) Protein tyrosine phosphatase receptor type Z dephosphorylates TrkA receptors and attenuates NGF-dependent neurite outgrowth of PC12 cells. *J Biochem,* 144**,** 259-66.

SHINTANI, T., WATANABE, E., MAEDA, N. & NODA, M. (1998) Neurons as well as astrocytes express proteoglycan-type protein tyrosine phosphatase zeta/RPTPbeta: analysis of mice in which the PTPzeta/RPTPbeta gene was replaced with the LacZ gene. *Neurosci Lett,* 247**,** 135-8.

SHYU, Y. J. & HU, C. D. (2008) Fluorescence complementation: an emerging tool for biological research. *Trends Biotechnol,* 26**,** 622-30.

SHYU, Y. J., LIU, H., DENG, X. & HU, C. D. (2006) Identification of new fluorescent protein fragments for bimolecular fluorescence complementation analysis under physiological conditions. *Biotechniques,* 40**,** 61-6.

SINN, P. L., SAUTER, S. L. & MCCRAY, P. B., JR. (2005) Gene therapy progress and prospects: development of improved lentiviral and retroviral vectors--design, biosafety, and production. *Gene Ther,* 12**,** 1089-98.

SIROIS, J., COTE, J. F., CHAREST, A., UETANI, N., BOURDEAU, A., DUNCAN, S. A., DANIELS, E. & TREMBLAY, M. L. (2006) Essential function of PTP-PEST during mouse embryonic vascularization, mesenchyme formation, neurogenesis and early liver development. *Mech Dev,* 123**,** 869-80.

SKAPER, S. D. (2008) The biology of neurotrophins, signalling pathways, and functional peptide mimetics of neurotrophins and their receptors. *CNS Neurol Disord Drug Targets,* 7**,** 46-62.

SKELTON, M. R., PONNIAH, S., WANG, D. Z., DOETSCHMAN, T., VORHEES, C. V. & PALLEN, C. J. (2003) Protein tyrosine phosphatase alpha (PTP alpha) knockout mice show deficits in Morris water maze learning, decreased locomotor activity, and decreases in anxiety. *Brain Res,* 984**,** 1-10.

SKLAR, P., GABRIEL, S. B., MCINNIS, M. G., BENNETT, P., LIM, Y. M., TSAN, G., SCHAFFNER, S., KIROV, G., JONES, I., OWEN, M., CRADDOCK, N., DEPAULO, J. R. & LANDER, E. S. (2002) Family-based association study of 76 candidate genes in bipolar disorder: BDNF is a potential risk locus. Brain-derived neutrophic factor. *Mol Psychiatry,* 7**,** 579-93.

SNYDER, S. E., LI, J., SCHAUWECKER, P. E., MCNEILL, T. H. & SALTON, S. R. (1996) Comparison of RPTP zeta/beta, phosphacan, and trkB mRNA expression in the developing and adult rat nervous system and induction of RPTP zeta/beta and phosphacan mRNA following brain injury. *Brain Res Mol Brain Res,* 40**,** 79-96.

SOFRONIEW, M. V., HOWE, C. L. & MOBLEY, W. C. (2001) Nerve growth factor signaling, neuroprotection, and neural repair. *Annu Rev Neurosci,* 24**,** 1217-81.

SOMIA, N. & VERMA, I. M. (2000) Gene therapy: trials and tribulations. *Nat Rev Genet,* 1**,** 91-9.

SOMMER, L., RAO, M. & ANDERSON, D. J. (1997) RPTP delta and the novel protein tyrosine phosphatase RPTP psi are expressed in restricted regions of the developing central nervous system. *Dev Dyn,* 208**,** 48-61.

SQUINTO, S. P., STITT, T. N., ALDRICH, T. H., DAVIS, S., BIANCO, S. M., RADZIEJEWSKI, C., GLASS, D. J., MASAIAKOWSKI, P., FURTH, M. E., VELENZUELA, D. M., DISTEFANO, P. S. & YANCOPOULOS, G. D. (1991) trkB encodes a functional receptor for brain-derived neurotrophic factor and neurotrophin-3 but not nerve growth factor. *Cell,* 65**,** 885-893.

STEPANEK, L., SUN, Q. L., WANG, J., WANG, C. & BIXBY, J. L. (2001) CRYP-2/cPTPRO is a neurite inhibitory repulsive guidance cue for retinal neurons in vitro. *J Cell Biol,* 154**,** 867-78.

STOILOV, P., CASTREN, E. & STAMM, S. (2002) Analysis of the human TrkB gene genomic organization reveals novel TrkB isoforms, unusual gene length, and splicing mechanism. *Biochem Biophys Res Commun,* 290**,** 1054-65.

STOKER, A. & DUTTA, R. (1998) Protein tyrosine phosphatases and neural development. *Bioessays,* 20**,** 463-72.

STOKER, A. W. (1994) Isoforms of a novel cell adhesion molecule-like protein tyrosine phosphatase are implicated in neural development. *Mech Dev,* 46**,** 201-17.

STOKER, A. W. (2005) Protein tyrosine phosphatases and signalling. *J Endocrinol,* 185**,** 19-33.

STOKER, A. W., GEHRIG, B., NEWTON, M. R. & BAY, B. H. (1995) Comparative localisation of CRYP alpha, a CAM-like tyrosine phosphatase, and NgCAM in the developing chick visual system. *Brain Res Dev Brain Res,* 90**,** 129-40.

STREULI, M., KREUGER, N. X. & SAITO, H. (1989) A family of receptor-linked protein tyrosine phosphatases in humans and Drosophila. *Proc. Natl. Acad. Sci. USA,* 86**,** 8698-8702.

STREULI, M., KREUGER, N. X., THAI, T., TANG, M. & SAITO, H. (1990) Distinct functional roles of the two intracellular phosphatase like domains of the receptor-linked protein tyrosine phosphatases LCA and LAR. *EMBO J.,* 9**,** 2399-2407.

STUDER, L., SPENGER, C., SEILER, R. W., ALTAR, C. A., LINDSAY, R. M. & HYMAN, C. (1995) Comparison of the effects of the neurotrophins on the morphological structure of dopaminergic neurons in cultures of rat substantia nigra. *Eur J Neurosci,* 7**,** 223-33.

SU, J., MURANJAN, M. & SAP, J. (1999) Receptor protein tyrosine phosphatase alpha activates Src-family kinases and controls integrin-mediated responses in fibroblasts. *Curr Biol,* 9**,** 505-11.

SUAREZ PESTANA, E., TENEV, T., GROSS, S., STOYANOV, B., OGATA, M. & BOHMER, F. D. (1999) The transmembrane protein tyrosine phosphatase RPTPsigma modulates signaling of the epidermal growth factor receptor in A431 cells. *Oncogene,* 18**,** 4069-79.

SUN, Q., BAHRI, S., SCHMID, A., CHIA, W. & ZINN, K. (2000a) Receptor tyrosine phosphatases regulate axon guidance across the midline of the Drosophila embryo. *Development,* 127**,** 801-12.

SUN, Q., SCHINDELHOLZ, B., KNIRR, M., SCHMID, A. & ZINN, K. (2001) Complex genetic interactions among four receptor tyrosine phosphatases regulate axon guidance in Drosophila. *Mol Cell Neurosci,* 17**,** 274-91.

SUN, Q. L., WANG, J., BOOKMAN, R. J. & BIXBY, J. L. (2000b) Growth cone steering by receptor tyrosine phosphatase delta defines a distinct class of guidance Cue. *Mol Cell Neurosci,* 16**,** 686-95.

SUN, Y., DYKES, I. M., LIANG, X., ENG, S. R., EVANS, S. M. & TURNER, E. E. (2008) A central role for Islet1 in sensory neuron development linking sensory and spinal gene regulatory programs. *Nat Neurosci,* 11**,** 1283-93.

TABERNERO, L., ARICESCU, A. R., JONES, E. Y. & SZEDLACSEK, S. E. (2008) Protein tyrosine phosphatases: structure-function relationships. *Febs J,* 275**,** 867-82.

TAKAHASHI, H., ARSTIKAITIS, P., PRASAD, T., BARTLETT, T. E., WANG, Y. T., MURPHY, T. H. & CRAIG, A. M. (2011) Postsynaptic TrkC and Presynaptic PTPsigma Function as a Bidirectional Excitatory Synaptic Organizing Complex. *Neuron,* 69**,** 287-303.

TAKAI, S., YAMADA, M., ARAKI, T., KOSHIMIZU, H., NAWA, H. & HATANAKA, H. (2002) Shp-2 positively regulates brain-derived neurotrophic factor-promoted survival of cultured ventral mesencephalic dopaminergic neurons through a brain immunoglobulin-like molecule with tyrosine-based activation motifs/Shp substrate-1. *J Neurochem,* 82**,** 353-64.

TARCIC, G., BOGUSLAVSKY, S. K., WAKIM, J., KIUCHI, T., LIU, A., REINITZ, F., NATHANSON, D., TAKAHASHI, T., MISCHEL, P. S., NG, T. & YARDEN, Y. (2009) An unbiased screen identifies DEP-1 tumor suppressor as a phosphatase controlling EGFR endocytosis. *Curr Biol,* 19**,** 1788-98.

TAYLOR, M. K., YEAGER, K. & MORRISON, S. J. (2007) Physiological Notch signaling promotes gliogenesis in the developing peripheral and central nervous systems. *Development,* 134**,** 2435-47.

TENG, K. K., FELICE, S., KIM, T. & HEMPSTEAD, B. L. (2010) Understanding proneurotrophin actions: Recent advances and challenges. *Dev Neurobiol,* 70**,** 350-9.

TERTOOLEN, L. G., BLANCHETOT, C., JIANG, G., OVERVOORDE, J., GADELLA, T. W., JR., HUNTER, T. & DEN HERTOG, J. (2001a) Dimerization of receptor protein-tyrosine phosphatase alpha in living cells. *BMC Cell Biol,* 2**,** 8.

TERTOOLEN, L. G., BLANCHETOT, C., JIANG, G., OVERVOORDE, J., GADELLA, T. W., JR., HUNTER, T. & HERTOG JD, J. (2001b) Dimerization of Receptor Protein-Tyrosine Phosphatase alpha in living cells. *BMC Cell Biol,* 2.

TESSAROLLO, L. (1998) Pleiotropic functions of neurotrophins in development. *Cytokine Growth Factor Rev,* 9**,** 125-37.

TESSAROLLO, L., TSOULFAS, P., DONOVAN, M. J., PALKO, M. E., BLAIR-FLYNN, J., HEMPSTEAD, B. L. & PARADA, L. F. (1997) Targeted deletion of all isoforms of the trkC gene suggests the use of alternate receptors by its ligand neurotrophin-3 in neuronal development and implicates trkC in normal cardiogenesis. *Proc Natl Acad Sci U S A,* 94**,** 14776-81.

TESSAROLLO, L., TSOULFAS, P., MARTIN-ZANCA, D., GILBERT, D. J., JENKINS, N. A., COPELAND, N. G. & PARADA, L. F. (1993) trkC, a receptor for neurotrophin-3, is widely expressed in the developing nervous system and in non-neuronal tissues. *Development,* 118**,** 463-75.

THOENEN, H. (1995) Neurotrophins and neuronal plasticity. *Science,* 270**,** 593-8.

THOENEN, H. & SENDTNER, M. (2002) Neurotrophins: from enthusiastic expectations through sobering experiences to rational therapeutic approaches. *Nat Neurosci,* 5 Suppl**,** 1046-50.

THOMPSON, K., UETANI, N., TREMBLAY, M. & KENNEDY, T. (2001) Loss of receptor protein tyrosine phosphatase sigma enhances the rate of motoneuron regeneration. *Society for Neuroscience abstracts,* 802.12.

THOMPSON, K. M., UETANI, N., MANITT, C., ELCHEBLY, M., TREMBLAY, M. L. & KENNEDY, T. E. (2003) Receptor protein tyrosine phosphatase sigma inhibits axonal regeneration and the rate of axon extension. *Mol Cell Neurosci,* 23**,** 681-92.

TIRAN, Z., PERETZ, A., SINES, T., SHINDER, V., SAP, J., ATTALI, B. & ELSON, A. (2006) Tyrosine Phosphatases Epsilon and Alpha Perform Specific and Overlapping Functions in Regulation of Voltage-gated Potassium Channels in Schwann Cells. *Mol Biol Cell*.

TISI, M. A., XIE, Y., YEO, T. T. & LONGO, F. M. (2000) Downregulation of LAR tyrosine phosphatase prevents apoptosis and augments NGF-induced neurite outgrowth. *J Neurobiol,* 42**,** 477-486.

TODARO, G. J. & GREEN, H. (1963) Quantitative studies of the growth of mouse embryo cells in culture and their development into established lines. *J Cell Biol,* 17**,** 299-313.

TOGARI, A., DICKENS, G., KUZUYA, H. & GUROFF, G. (1985) The effect of fibroblast growth factor on PC12 cells. *J Neurosci,* 5**,** 307-16.

TOLEDO-ARAL, J. J., BREHM, P., HALEGOUA, S. & MANDEL, G. (1995) A single pulse of nerve growth factor triggers long-term neuronal excitability through sodium channel gene induction. *Neuron,* 14**,** 607-11.

TOMEMORI, T., SEKI, N., SUZUKI, Y., SHIMIZU, T., NAGATA, H., KONNO, A. & SHIRASAWA, T. (2000) Isolation and characterization of murine orthologue of PTP-BK. *Biochem Biophys Res Commun,* 276**,** 974-81.

TONKS, N. K. (2006) Protein tyrosine phosphatases: from genes, to function, to disease. *Nat Rev Mol Cell Biol,* 7**,** 833-46.

TONKS, N. K., DILTZ, C. D. & FISCHER, E. H. (1990) CD45, an integral membrane protein tyrosine phosphatase. Characterization of enzyme activity. *J Biol Chem,* 265**,** 10674-80.

TRACY, S., VAN DER GEER, P. & HUNTER, T. (1995) The receptor-like protein-tyrosine phosphatase, RPTP alpha, is phosphorylated by protein kinase C on two serines close to the inner face of the plasma membrane. *J Biol Chem,* 270**,** 10587-94.

TRAVERSE, S., GOMEZ, N., PATERSON, H., MARSHALL, C. & COHEN, P. (1992) Sustained activation of the mitogen-activated protein (MAP) kinase cascade may be required for differentiation of PC12 cells. Comparison of the effects of nerve growth factor and epidermal growth factor. *Biochem J,* 288 (Pt 2)**,** 351-5.

TROWBRIDGE, I. S. & THOMAS, M. L. (1994) CD45: an emerging role as a protein tyrosine phosphatase required for lymphocyte activation and development. *Annu Rev Immunol,* 12**,** 85-116.

TSAI, W., MORIELLI, A. D., CACHERO, T. G. & PERALTA, E. G. (1999) Receptor protein tyrosine phosphatase alpha participates in the m1 muscarinic acetylcholine receptor-dependent regulation of Kv1.2 channel activity. *Embo J,* 18**,** 109-18.

TSOULFAS, P., SOPPET, D., ESCANDON, E., TESSAROLLO, L., MENDOZA-RAMIREZ, J. L., ROSENTHAL, A., NIKOLICS, K. & PARADA, L. F. (1993) The rat trkC locus encodes multiple neurogenic receptors that exhibit differential response to neurotrophin-3 in PC12 cells. *Neuron,* 10**,** 975-90.

TSUJIKAWA, K., ICHIJO, T., MORIYAMA, K., TADOTSU, N., SAKAMOTO, K., SAKANE, N., FUKADA, S., FURUKAWA, T., SAITO, H. & YAMAMOTO, H. (2002) Regulation of Lck and Fyn tyrosine kinase activities by transmembrane protein tyrosine phosphatase leukocyte common antigen-related molecule. *Mol Cancer Res,* 1**,** 155-63.

TSURUDA, A., SUZUKI, S., MAEKAWA, T. & OKA, S. (2004) Constitutively active Src facilitates NGF-induced phosphorylation of TrkA and causes enhancement of the MAPK signaling in SK-N-MC cells. *FEBS Lett,* 560**,** 215-20.

TUTTLE, R., NAKAGAWA, Y., JOHNSON, J. E. & O'LEARY, D. D. (1999) Defects in thalamocortical axon pathfinding correlate with altered cell domains in Mash-1-deficient mice. *Development,* 126**,** 1903-16.

UETANI, N., ASANO, M., MIZUNO, K., YAKURA, H. & IWAKURA, Y. (1997) Targeted disruption of the murine protein tyrosine phoshatase delta (MPTPdelta) results in grwoth retardation and behavioural abnormailites. IN YAKURA, H. (Ed.) *Kinases and phosphatases in lymphocyte and neuronal signalling.* Tokyo, Springer-Verlag.

UETANI, N., CHAGNON, M. J., KENNEDY, T. E., IWAKURA, Y. & TREMBLAY, M. L. (2006) Mammalian motoneuron axon targeting requires receptor protein tyrosine phosphatases sigma and delta. *J Neurosci,* 26**,** 5872-80.

UETANI, N., KATO, K., OGURA, H., MIZUNO, K., KAWANO, K., MIKOSHIBA, K., YAKURA, H., ASANO, M. & IWAKURA, Y. (2000) Impaired learning with enhanced hippocampal long-term potentiation in PTPdelta-deficient mice. *Embo J,* 19**,** 2775-2785.

ULLRICH, A. & SCHLESSINGER, J. (1990) Signal Transduction by receptors with tyrosine kinase activity. *Cell,* 61**,** 203-212.

URFER, R., TSOULFAS, P., O'CONNELL, L., SHELTON, D. L., PARADA, L. F. & PRESTA, L. G. (1995) An immunoglobulin-like domain determines the specificity of neurotrophin receptors. *Embo J,* 14**,** 2795-805.

USHIRO, H. & COHEN, S. (1980) Identification of phosphotyrosine as a product of epidermal growth factor-activated protein kinase in A-431 cell membranes. *J Biol Chem,* 255**,** 8363-5.

VAEGTER, C. B., JANSEN, P., FJORBACK, A. W., GLERUP, S., SKELDAL, S., KJOLBY, M., RICHNER, M., ERDMANN, B., NYENGAARD, J. R., TESSAROLLO, L., LEWIN, G. R., WILLNOW, T. E., CHAO, M. V. & NYKJAER, A. (2011) Sortilin associates with Trk receptors to enhance anterograde transport and neurotrophin signaling. *Nat Neurosci,* 14**,** 54-61.

VALENZUELA, D. M., MAISONPIERRE, P. C., GLASS, D. J., ROJAS, E., NUNEZ, L., KONG, Y., GIES, D. R., STITT, T. N., IP, N. Y. & YANCOPOULOS, G. D. (1993) Alternative forms of rat TrkC with different functional capabilities. *Neuron,* 10**,** 963-74.

VAN DEN MAAGDENBERG, A. M., BACHNER, D., SCHEPENS, J. T., PETERS, W., FRANSEN, J. A., WIERINGA, B. & HENDRIKS, W. J. (1999) The mouse Ptprr gene encodes two protein tyrosine phosphatases, PTP-SL and PTPBR7, that display distinct patterns of expression during neural development. *Eur J Neurosci,* 11**,** 3832-44.

VAN DER SAR, A. M., ZIVKOVIC, D. & DEN HERTOG, J. (2002) Eye defects in receptor protein-tyrosine phosphatase alpha knock-down zebrafish. *Dev Dyn,* 223**,** 292-7.

VAN DER WIJK, T., BLANCHETOT, C. & DEN HERTOG, J. (2005) Regulation of receptor protein-tyrosine phosphatase dimerization. *Methods,* 35**,** 73-9.

VAN DER ZEE, C. E., MAN, T. Y., VAN LIESHOUT, E. M., VAN DER HEIJDEN, I., VAN BREE, M. & HENDRIKS, W. J. (2003) Delayed peripheral nerve regeneration and central nervous system collateral sprouting in leucocyte common antigen-related protein tyrosine phosphatase-deficient mice. *Eur J Neurosci,* 17**,** 991-1005.

VAN DER ZEE, C. E. E. M., MAN, T. Y., VAN DER HEIJDEN, I., LIESHOUT, E. M. M. & HENDRIKS, W. J. A. J. (2000) LAR protein tyrosine phosphatase deficient mice show a delay in PNS sensorty nerve regeneration and CNA cholinergic collateral sprouting. *Eur J Neurobiol,* 12**,** 290.

VAN EEKELEN, M., RUNTUWENE, V., OVERVOORDE, J. & DEN HERTOG, J. (2010) RPTPalpha and PTPepsilon signaling via Fyn/Yes and RhoA is essential for zebrafish convergence and extension cell movements during gastrulation. *Dev Biol,* 340**,** 626-39.

VAN LIESHOUT, E. M., VAN DER HEIJDEN, I., HENDRIKS, W. J. & VAN DER ZEE, C. E. (2001) A decrease in size and number of basal forebrain cholinergic neurons is paralleled by diminished hippocampal cholinergic innervation in mice lacking leukocyte common antigen-related protein tyrosine phosphatase activity. *Neuroscience,* 102**,** 833-841.

VAN VACTOR, D. (1998) Protein tyrosine phosphatases in the developing nervous system. *Curr Opin Cell Biol,* 10**,** 174-81.

VANDESOMPELE, J., DE PRETER, K., PATTYN, F., POPPE, B., VAN ROY, N., DE PAEPE, A. & SPELEMAN, F. (2002) Accurate normalization of real-time quantitative RT-PCR data by geometric averaging of multiple internal control genes. *Genome Biol,* 3**,** RESEARCH0034.

VANDESOMPELE, J., DE PRETER, K., PATTYN, F., POPPE, B., VAN ROY, N., DE PAEPE, A. & SPELEMAN, F. (2007) GeNorm software manual.

http://medgen.ugent.be/~jvdesomp/genorm/geNorm_manual.pdf.

VEGA, J. A., GARCIA-SUAREZ, O., HANNESTAD, J., PEREZ-PEREZ, M. & GERMANA, A. (2003) Neurotrophins and the immune system. *J Anat,* 203**,** 1-19.

VEZZALINI, M., MOMBELLO, A., MENESTRINA, F., MAFFICINI, A., DELLA PERUTA, M., VAN NIEKERK, C., BARBARESCHI, M., SCARPA, A. & SORIO, C. (2007) Expression of transmembrane protein tyrosine phosphatase gamma (PTPgamma) in normal and neoplastic human tissues. *Histopathology,* 50**,** 615-28.

VIDI, P. A., CHEMEL, B. R., HU, C. D. & WATTS, V. J. (2008) Ligand-dependent oligomerization of dopamine D(2) and adenosine A(2A) receptors in living neuronal cells. *Mol Pharmacol,* 74**,** 544-51.

VIDI, P. A. & WATTS, V. J. (2009) Fluorescent and bioluminescent protein-fragment complementation assays in the study of G protein-coupled receptor oligomerization and signaling. *Mol Pharmacol,* 75**,** 733-9.

VISEL, A., THALLER, C. & EICHELE, G. (2004) GenePaint.org: an atlas of gene expression patterns in the mouse embryo. *Nucleic Acids Res,* 32**,** D552-6.

WAKAMATSU, Y. (2004) Understanding glial differentiation in vertebrate nervous system development. *Tohoku J Exp Med,* 203**,** 233-40.

WALLACE, M. J., BATT, J., FLADD, C. A., HENDERSON, J. T., SKARNES, W. & ROTIN, D. (1999) Neuronal defects and posterior pituitary hypoplasia in mice lacking the receptor tyrosine phosphatase PTPsigma. *Nat Genet,* 21**,** 334-8.

WANG, H., YAN, H., CANOLL, P. D., SILVENNOINEN, O., SCHLESSINGER, J. & MUSACCHIO, J. M. (1995) Expression of receptor protein tyrosine phosphatase-sigma (RPTP-sigma) in the nervous system of the developing and adult rat. *J Neurosci Res,* 41**,** 297-310.

WANG, J. & BIXBY, J. L. (1999) Receptor Tyrosine Phosphatase-delta Is a Homophilic, Neurite-Promoting Cell Adhesion Molecule for CNS Neurons. *Mol Cell Neurosci,* 14**,** 370-384.

WANG, X., WENG, L. P. & YU, Q. (2000) Specific inhibition of FGF-induced MAPK activation by the receptor-like protein tyrosine phosphatase LAR. *Oncogene,* 19**,** 2346-53.

WATSON, F. L., HEERSSEN, H. M., BHATTACHARYYA, A., KLESSE, L., LIN, M. Z. & SEGAL, R. A. (2001) Neurotrophins use the Erk5 pathway to mediate a retrograde survival response. *Nat Neurosci,* 4**,** 981-8.

WATSON, F. L., PORCIONATTO, M. A., BHATTACHARYYA, A., STILES, C. D. & SEGAL, R. A. (1999) TrkA glycosylation regulates receptor localization and activity. *J Neurobiol,* 39**,** 323-36.

WAY, B. A. & MOONEY, R. A. (1994) Differential effects of phosphotyrosine phosphatase expression on hormone-dependent and independent pp60c-src activity. *Mol Cell Biochem,* 139**,** 167-75.

WETMORE, C. & OLSON, L. (1995) Neuronal and nonneuronal expression of neurotrophins and their receptors in sensory and sympathetic ganglia suggest new intercellular trophic interactions. *J Comp Neurol,* 353**,** 143-59.

WHITE, F. A., SILOS-SANTIAGO, I., MOLLIVER, D. C., NISHIMURA, M., PHILLIPS, H., BARBACID, M. & SNIDER, W. D. (1996) Synchronous onset of NGF and TrkA survival dependence in developing dorsal root ganglia. *J Neurosci,* 16**,** 4662-72.

WILKINSON, D. G. & NIETO, M. A. (1993) Detection of messenger RNA by in situ hybridization to tissue sections and whole mounts. *Methods Enzymol,* 225**,** 361-73.

WILKINSON, G. A., FARINAS, I., BACKUS, C., YOSHIDA, C. K. & REICHARDT, L. F. (1996) Neurotrophin-3 is a survival factor in vivo for early mouse trigeminal neurons. *J Neurosci,* 16**,** 7661-9.

WOO, J., KWON, S. K., CHOI, S., KIM, S., LEE, J. R., DUNAH, A. W., SHENG, M. & KIM, E. (2009) Trans-synaptic adhesion between NGL-3 and LAR regulates the formation of excitatory synapses. *Nat Neurosci,* 12**,** 428-37.

WRIGHT, D. E. & SNIDER, W. D. (1995) Neurotrophin receptor mRNA expression defines distinct populations of neurons in rat dorsal root ganglia. *J Comp Neurol,* 351**,** 329-38.

WU, H. H., BELLMUNT, E., SCHEIB, J. L., VENEGAS, V., BURKERT, C., REICHARDT, L. F., ZHOU, Z., FARINAS, I. & CARTER, B. D. (2009) Glial precursors clear sensory neuron corpses during development via Jedi-1, an engulfment receptor. *Nat Neurosci,* 12**,** 1534-41.

XIE, Y., MASSA, S. M., ENSSLEN-CRAIG, S. E., MAJOR, D. L., YANG, T., TISI, M. A., DEREVYANNY, V. D., RUNGE, W. O., MEHTA, B. P., MOORE, L. A., BRADY-KALNAY, S. M. & LONGO, F. M. (2006) Protein-tyrosine phosphatase (PTP) wedge domain peptides: a novel approach for inhibition of PTP function and augmentation of protein-tyrosine kinase function. *J Biol Chem,* 281**,** 16482-92.

XIE, Y., YEO, T. T., ZHANG, C., YANG, T., TISI, M. A., MASSA, S. M. & LONGO, F. M. (2001) The leukocyte common antigen-related protein tyrosine phosphatase receptor regulates regenerative neurite outgrowth in vivo. *J Neurosci,* 21**,** 5130-8.

XIU, M. H., HUI, L., DANG, Y. F., HOU, T. D., ZHANG, C. X., ZHENG, Y. L., CHEN DA, C., KOSTEN, T. R. & ZHANG, X. Y. (2009) Decreased serum BDNF levels in chronic institutionalized schizophrenia on long-term treatment with typical and atypical antipsychotics. *Prog Neuropsychopharmacol Biol Psychiatry,* 33**,** 1508-12.

YAKA, R., GAMLIEL, A., GURWITZ, D. & STEIN, R. (1998) NGF induces transient but not sustained activation of ERK in PC12 mutant cells incapable of differentiating. *J Cell Biochem,* 70**,** 425-32.

YAMADA, M., OHNISHI, H., SANO, S., ARAKI, T., NAKATANI, A., IKEUCHI, T. & HATANAKA, H. (1999) Brain-derived neurotrophic factor stimulates interactions of Shp2 with phosphatidylinositol 3-kinase and Grb2 in cultured cerebral cortical neurons. *J Neurochem,* 73**,** 41-9.

YAMAMOTO, M., SOBUE, G., YAMAMOTO, K., TERAO, S. & MITSUMA, T. (1996) Expression of mRNAs for neurotrophic factors (NGF, BDNF, NT-3, and GDNF) and their receptors (p75NGFR, trkA, trkB, and trkC) in the adult human peripheral nervous system and nonneural tissues. *Neurochem Res,* 21**,** 929-38.

YAN, H., GROSSMAN, A., WANG, H., D'EUSTACHIO, P., MOSSIE, K., MUSACCHIO, J. M., SILVENNOINEN, O. & SCHLESSINGER, J. (1993) A novel receptor tyrosine phosphatase-sigma that is highly expressed in the nervous system. *J Biol Chem,* 268**,** 24880-6.

YANG, T., BERNABEU, R., XIE, Y., ZHANG, J. S., MASSA, S. M., REMPEL, H. C. & LONGO, F. M. (2003) Leukocyte antigen-related protein tyrosine phosphatase receptor: a small ectodomain isoform functions as a homophilic ligand and promotes neurite outgrowth. *J Neurosci,* 23**,** 3353-63.

YANG, T., MASSA, S. M. & LONGO, F. M. (2006) LAR protein tyrosine phosphatase receptor associates with TrkB and modulates neurotrophic signaling pathways. *J Neurobiol,* 66**,** 1420-36.

YANG, T., YIN, W., DEREVYANNY, V. D., MOORE, L. A. & LONGO, F. M. (2005a) Identification of an ectodomain within the LAR protein tyrosine phosphatase receptor that binds homophilically and activates signalling pathways promoting neurite outgrowth. *Eur J Neurosci,* 22**,** 2159-70.

YANG, X., LI, J., ZHOU, Y., SHEN, Q. & CHEN, J. (2005b) Discovery of novel inhibitor of human leukocyte common antigen-related phosphatase. *Biochim Biophys Acta,* 1726**,** 34-41.

YANO, H., CONG, F., BIRGE, R. B., GOFF, S. P. & CHAO, M. V. (2000) Association of the Abl tyrosine kinase with the Trk nerve growth factor receptor. *J Neurosci Res,* 59**,** 356-64.

YEO, G. S., CONNIE HUNG, C. C., ROCHFORD, J., KEOGH, J., GRAY, J., SIVARAMAKRISHNAN, S., O'RAHILLY, S. & FAROOQI, I. S. (2004) A de novo mutation affecting human TrkB associated with severe obesity and developmental delay. *Nat Neurosci,* 7**,** 1187-9.

YEO, T. T., YANG, T., MASSA, S. M., ZHANG, J. S., HONKANIEMI, J., BUTCHER, L. L. & LONGO, F. M. (1997) Deficient LAR expression decreases basal forebrain cholinergic neuronal size and hippocampal cholinergic innervation. *J Neurosci Res,* 47**,** 348-60.

YOSHIKAWA, M., SENZAKI, K., YOKOMIZO, T., TAKAHASHI, S., OZAKI, S. & SHIGA, T. (2007) Runx1 selectively regulates cell fate specification and axonal projections of dorsal root ganglion neurons. *Dev Biol,* 303**,** 663-74.

YUAN, X. B., JIN, M., XU, X., SONG, Y. Q., WU, C. P., POO, M. M. & DUAN, S. (2003) Signalling and crosstalk of Rho GTPases in mediating axon guidance. *Nat Cell Biol,* 5**,** 38-45.

ZAVADA, J. (1972) VSV pseudotype particles with the coat of avian myeloblastosis virus. *Nat New Biol,* 240**,** 122-4.

ZHANG, B., METHAROM, P., JULLIE, H., ELLEM, K. A., CLEGHORN, G., WEST, M. J. & WEI, M. Q. (2004) The significance of controlled conditions in lentiviral vector titration and in the use of multiplicity of infection (MOI) for predicting gene transfer events. *Genet Vaccines Ther,* 2**,** 6.

ZHANG, H. T., LI, L. Y., ZOU, X. L., SONG, X. B., HU, Y. L., FENG, Z. T. & WANG, T. T. (2007a) Immunohistochemical distribution of NGF, BDNF, NT-3, and NT-4 in adult rhesus monkey brains. *J Histochem Cytochem,* 55**,** 1-19.

ZHANG, J. S., HONKANIEMI, J., YANG, T., YEO, T. T. & LONGO, F. M. (1998) LAR tyrosine phosphatase receptor: a developmental isoform is present in neurites and growth cones and its expression is regional- and cell-specific. *Mol. Cell. Neurosci.,* 10**,** 271-86.

ZHANG, X., GUO, A., YU, J., POSSEMATO, A., CHEN, Y., ZHENG, W., POLAKIEWICZ, R. D., KINZLER, K. W., VOGELSTEIN, B., VELCULESCU, V. E. & WANG, Z. J. (2007b) Identification of STAT3 as a substrate of receptor protein tyrosine phosphatase T. *Proc Natl Acad Sci U S A,* 104**,** 4060-4.

ZHANG, Y., LI, Z. X., LI, H., PENG, L., LUO, H. J., LI, W. Q. & LUO, W. H. (2010) [Determination of serum copper and zinc in different chemical forms by graphite furnace atomic absorption spectrometry with ethanol-EDTA precipitation method]. *Guang Pu Xue Yu Guang Pu Fen Xi,* 30**,** 816-9.

ZHENG, X. M., RESNICK, R. J. & SHALLOWAY, D. (2000) A phosphotyrosine displacement mechanism for activation of Src by PTPalpha. *Embo J,* 19**,** 964-78.

ZHENG, X. M., RESNICK, R. J. & SHALLOWAY, D. (2002) Mitotic activation of protein-tyrosine phosphatase alpha and regulation of its Src-mediated transforming activity by its sites of protein kinase C phosphorylation. *J Biol Chem,* 277**,** 21922-9.

ZHENG, X. M., WANG, Y. & PALLEN, C. J. (1992) Cell transformation and activation of pp60c-src by overexpression of a protein tyrosine phosphatase. *Nature,* 359**,** 336-9.

ZWEIFEL, L. S., KURUVILLA, R. & GINTY, D. D. (2005) Functions and mechanisms of retrograde neurotrophin signalling. *Nat Rev Neurosci,* 6**,** 615-25.